THE IDENTIFICATION AND CHARACTERIZATION OF ARTISTS' DYES AND PIGMENTS USING LASER DESORPTION/IONIZATION MASS SPECTROMETRY

By

Donna M. Grim

A DISSERTATION

Submitted to
Michigan State University
in partial fulfillment of the requirement
for the degree of

Doctor of Philosophy

Department of Chemistry

2003

ABSTRACT

THE IDENTIFICATION AND CHARACTERIZATION OF ARTISTS' DYES AND PIGMENTS USING LASER DESORPTION/IONIZATION MASS SPECTROMETRY

By

Donna M. Grim

Laser desorption mass spectrometry (LDMS) was evaluated as an analytical tool for the characterization of dyes and pigments found in ink and in artists' paints. Experimentation revealed that colorants can be easily detected on a variety of surfaces. Samples included ink from modern ballpoint pens, and ink found on stamps and on newspapers. However, the primary focus of this work rested in the LD mass spectrometric analysis of standard watercolor and oil paints.

Artists' paints are typically three component systems that include a colorant, vehicle, and resin. Currently, there are numerous analytical techniques available and used by art conservators to analyze these components individually, and a limited number are available for their analysis as mixtures. In the specific area of the identification and characterization of colorants, scientists have cited significant weaknesses in these methods. Consequently, there is a need for the development of new methods having the ability to identify more than one colorant in an impure mixture, and to provide molecular level information on both organic and inorganic colorants, simultaneously. Laser desorption mass spectrometry (LDMS) is an ideal candidate.

The LD mass spectra of numerous colorants will be presented, which demonstrate the potential for the development of LDMS as a sensitive analytical technique to be used

in art conservation laboratories. The molecular level information generated in LD mass spectra can lead to the unambiguous identification of specific colorants present in an impure paint mixture. For example, the LD mass spectra of colorants used to create an illuminated page of the Koran from the 17^{th} century, were obtained and the identified colorants offer insight into the authenticity of the document. Furthermore, sample size considerations and challenges typically encountered in the analysis of whole documents and paintings were identified and addressed. Proposed solutions were tested and the results suggest that the sampling challenges will not limit the use of LDMS as a tool in the field of art conservation.

To my husband, Mike, for his patience, understanding, and relentless love and support.

ACKNOWLEDGEMENTS

I would like to thank my advisor, Dr. John Allison, for all of his guidance and support throughout my graduate school career. You are a wonderful mentor and a positive influence on all of your students. Thank you for everything!

I would like to thank my committee members, Dr. Jay Siegel, Dr. Simon Garrett, Dr. James Jackson, and Dr. Gary Blanchard for helping my project along the way.

I would also like to thank Dr. Karen Trentelman and Valerie Baas, from the Detroit Institute of Arts, for their insightful conversations and sample donations.

I would like to thank Dr. Susan J. Masten, from the Environmental Engineering Department, Michigan State University, for the use of her facilities to perform ozone experiments.

On a personal note, I would like to thank Mike, Jasminka, Richie, Eric, Nicole, and Paul for their friendship and helping to make my short stay in Michigan a little bit brighter. Also, thank you to my family for always believing in me.

TABLE OF CONTENTS

List of Tables

Chapter One: Introduction

Chapter Two: Water Colors

Chapter Three: Lake Pigments

Chapter Four: Inorganic Pigments

Chapter Five: Stamps

Appendix

List of Figures

Chapter One: Introduction

Chapter Two: Watercolors

Chapter Three: Lake Pigments

Chapter Four: Inorganic Pigments

Chapter Five: Stamps

Chapter Six: Studies of the Interactions of H_2S with Colorants

Chapter Seven: Newspaper Ink

Chapter Eight: Practical Experimental Aspects

Chapter One: Introduction

In 2001, the art community received a shock, when the Smithsonian Institute's art conservation laboratory (Washington, D.C.), one of the most well-known and productive art conservation laboratories in the nation, was in danger of being shut down, as a result of governmental funding cutbacks. The chemistry community responded immediately, and the chemistry of art became a common theme in journal articles and at conferences. For instance the July 31, 2001 issue of *Chemical and Engineering News* featured a cover story entitled, "Chemistry and Art: Helping to Conserve Our Nation's Treasures" (1). The article highlighted the achievements of art conservators at the National Gallery of Art, also located in Washington, D.C. As a result of the overwhelming support from both the art and chemistry communities, as well as the general public, the Smithsonian Institute's art conservation laboratory is still active today. Even though the chemistry of art is a narrow component of the field of chemistry, the research is still valued and serves a significant role in preserving and maintaining the history and cultures of the world.

Project Overview

A paint is a complex system, which can be broken down into three components: the colorant (dyes or pigments), the vehicle (solvent system), and the resin (binder). Once the paint is applied to a substrate, a varnish layer (thin, protective coating) may be added. Scientists work to explain the role of each component in the mixture and how they interact with each other to create what our eyes perceive as art. This work draws the attention of art historians, art conservators, and forensic scientists. To narrow the field,

let us consider the chemistry of the colorant. One job of art historians is to decipher the artist's ever-changing palette, not only to gain a clear understanding of the artist's intent with the colors he selected, but also to learn the provenance of colorants, which provides information on pigment trade routes and availability. For example, during the High Renaissance period (1600s) in Venice, the political climate influenced the way in which Venetian artists portrayed religious figures. Traditionally, artists placed religious subjects such as the Madonna in the center of the painting. During this time period, artists began focusing on landscape details; however, at this time and place, artists were forbidden from choosing landscapes as the primary focus of their paintings. One may wonder why artists from this period consistently selected autumnal colors for landscape features in their paintings. The golden features are considered to be almost exaggerated – what were the artists trying to convey by this consistent choice? The answer to the question is chemical in nature, since the pigment commonly used throughout Italy to paint green trees, copper resinate, darkened and turned golden as time passed (2). This leads into the area of art conservation.

Art conservators are more interested in learning the mechanisms behind colorant reactions with their environment, including gases in the atmosphere and the paint mixture itself. Once the mechanism has been confirmed, art conservators can focus on developing preventative measures, such as paint additives or protective coatings. They can also work on finding methods to reverse a damaging chemical reaction, or at least make the color change less apparent.

In an unrelated field, forensic scientists are interested in the chemistry of art, in regards to the determination of the authenticity of art objects. Simply identifying the

colorants used to create a work of art can sometimes prove that it is a forgery. For example, the controversial Vinland Map was allegedly created in the early 15th century. Predating Christopher Columbus' discovery of America (1492), the map depicted regions of the "New World". Carbon dating of the parchment was consistent with the alleged time of creation, however the chemical analysis of the colorants used to create the map indicated the presence of anastase TiO_2, which had not been discovered until the early 20th century (3,4). The Vinland Map was obviously a modern day forgery.

Here we demonstrate the technique of laser desorption/ionization mass spectrometry (LDMS) as a versatile tool for the analysis of colorants. Colorants encountered in works of art and items of historical interest are most often organic dyes, inorganic pigments, or lakes (organic dyes on an inorganic support). Based on the interests in art chemistry, there were two general directions in which the project could proceed. The first and more basic, is the development of LDMS as a useful analytical tool for the identification of artists' colorants. Table 1.1 lists all of the analytical instrumentation available to art conservators at the Getty Conservation Institute (Los Angeles, CA). It is important to note that this is an extreme example, considering that the majority of art conservation laboratories are significantly smaller, and may be limited to only a few and in some cases, none of these techniques. Considering the list in Table 1.1, it appears as though artists are currently well-equipped for the identification of colorants. Therefore, the second and more promising direction was the development of LDMS for the characterization of the chemical reactions of colorants in response to their environment. For example, as its name implies, ultramarine blue is a greenish/blue pigment, which is known to change into a blotchy-grayish color over time. This transformation is well-

known and is called "Ultramarine Sickness", however the mechanism behind the reaction is poorly understood (5)

Chemical Analysis	Microscopy
UV/vis Spectroscopy	Electron Microprobe
X-ray Fluorescence	Environmental scanning electron microscopy
X-ray Diffraction	Polarizing light microscopy
Infrared Spectroscopy	
GC/MS	
LC/MS	

Table 1.1: Summary of analytical instrumentation available at the Getty Conservation Institute, Los Angeles, CA

On February 1, 1995, the Netherlands Organization for Scientific Research funded an intense five year research project entitled MOLART (Molecular Aspects of Aging in Painted Works of Art). The primary goal of MOLART was to contribute to the development of a scientific framework for the conservation of painted art on the molecular level. Numerous graduate students participated in the project, and earned their doctoral degrees by researching a specific area of art conservation. The project focused on molecular level studies of specific artist materials, falling into three broad categories: resins and varnishes, polymer networks, and pigments. A detailed description of the research projects initiated, as well as progress reports for each of the studies, including listings of presentations and publications, is available (6).

Project Title	Primary Researcher(s)
Copper green glazes	Klaas Jan van den Berg
Indigo used in easel paintings	Margriet van Eikema Hommes & Ella Hendriks
LD-ITMS in the analysis of natural organic pigments	N. Wyplosz
Orpiment, deterioration of arsenic sulfide pigments	Arie Wallert
Smalt	J. R. J. van Asperen de Boer & A. Wallert
Cadmium pigments	J. R. J. van Asperen de Boer
Secondary Ion Mass Spectromery on paint cross sections	Klaas Jan van den Berg & Ron Heeren

Table 1.2: Summary of MOLART molecular level studies of artists' pigments.

Considering that the focus of our project is the analysis of artists' pigments, the projects falling under MOLART's broad category of the molecular analysis of pigments will be highlighted. Table 1.2 summarizes the title of each project with the names of the scientists conducting the research. Each of the colorants listed in Table 1.2 share a common trait. They all eventually change color, either by reacting with pollutants in the atmosphere, the vehicle, or with other colorants present in the paint mixture. For instance, copper resinate is known to change from a green color to a brown color. Each group proposed a series of questions to be answered. For example, the research team involved in the indigo project sought to answer the following questions.

1) What are the physical and chemical changes that take place as indigo paint discolors?

2) What are the causes of discoloration?

3) At what rate does this change occur and is it a linear or exponential process?

4) Can the results of aging tests be used to estimate the original appearance of indigo paint areas that have discolored on paintings?

Several different mass spectrometric techniques were commonly employed to answer these questions along with many others in additional projects. For example, as the title of the project indicates, laser desorption ion trap mass spectrometry (LD-ITMS) was used to characterize natural organic pigments. Pure reference chemicals, including flavonoids, anthraquinones, and indigo, as well as the extract of plants (specifically weld, dyer's broom, and madder) were analyzed. This project was of particular interest to us, since these natural organic colorants have historically been used to prepare lake pigments, which are known to be extremely light fugitive. Direct LDMS, LD followed by post electron ionization, and traditional MALDI (Nd:YAG laser, 335 nm) were used to analyze the colorants. Notably, indigo was detected on the surface of a wool fiber using a nitrogen laser (337 nm).

The diversity and success of the MOLART project in the field of art conservation, helped to formulate our project. Furthermore, their initiative to gain a molecular level understanding of the numerous chemical changes which occur in paintings over time, and their frequent decision to use mass spectrometry to achieve this goal, was inspiring. However, a discussion with local art conservators at the Detroit Institute of Arts, helped to finalize the direction of our project.

During a discussion with art conservators, *they* surprisingly expressed dissatisfaction with the methods listed in Table 1.1. For example, x-ray fluorescence provides elemental information, as opposed to more informative molecular level information. Suppose a paint mixture is composed of ultramarine blue and red ochre (Fe_2O_3). Ultramarine blue does not contain iron, but physically resembles Prussian blue [$Fe_4(Fe_3CN_6)$], which does. Complications may arise if the paint mixture is analyzed

using a technique, such as XRF. Iron will be detected due to the presence of the red ochre, but due to the similar appearance of the two blue pigments, a false positive identification for Prussian blue may result (7). Additionally, other techniques, such as infrared spectroscopy, require a pure sample for analysis. The numerous components of a paint mixture make it difficult to obtain a pure sample from a painting.

Another weakness involves the characterization of lakes. Many of the techniques available to art conservatorss require the separation of the organic dye from the inorganic support, which are then analyzed separately. Consequently, art conservators are seeking the development of new analytical techniques which would allow them to analyze a lake pigment as a unit. While both project directions were pursued, the primary focus of the project became to develop LDMS to a point at which it could be a useful analytical technique in art conservation laboratories for the identification of artists' colorants.

The Analyte: Dyes and Pigments

Color is the result of molecules absorbing light from the visible region of the electromagnetic spectrum (450 – 625 nm wavelength). Light consists of oscillating electric and magnetic fields. The energy of the photon (light) is indirectly proportional to the wavelength (λ) of the photon, by the relationship, $E = hc/\lambda$, where h = Planck's constant and c = the speed of light in a vacuum. When the frequency of the light oscillation and the frequency of the electron or molecular "transition motion" are the same, an atom or molecule can absorb energy. Consequently, an electron may be promoted to a higher energy antibonding orbital by the absorption of light. A transition is possible for all valence electrons in a molecule. Table 1.3 summarizes the allowed

transition states for sigma (σ), pi (π), and nonbonding (n) electron pairs. The UV laser used in the LDMS experiments here, emits pulses of light at 337 nm wavelength, thus we are interested in the n $\rightarrow \pi^*$ and $\pi \rightarrow \pi^*$ transitions. Molar absorptivity (ε) reflects the efficiency of light absorption. Thus, a large ε indicates a high efficiency of light absorption, which increases the probability of the electronic transition occurring. Typical molar absorptivity ranges for the n $\rightarrow \pi^*$ and $\pi \rightarrow \pi^*$ transitions are 10 – 100 L/cm•mol and 1000 – 10,000 L/cm•mol, respectively (8).

Colorant molecules are generally termed dyes and pigments. Dyes are typically organic aromatic compounds and are known to be partially or completely soluble in their "vehicle" (solvent system). The presence of multiple chromophores in a colorant results in an increased molar absorptivity value, but does not affect λ_{max}. An increase in conjugation also increases ε, resulting from the additive effect of conjugated double bonds, but also shifts λ_{max} to a longer wavelength (9).

Electronic Transition	Wavelength
$\sigma \rightarrow \sigma^*$	$\lambda < 185$ nm (vacuum UV)
n $\rightarrow \sigma^*$	$150 < \lambda < 250$ nm
n $\rightarrow \pi^*$, $\pi \rightarrow \pi^*$	$200 < \lambda < 700$ nm

Table 1.3: Summary of allowed transition states.

Inorganic colorants typically fall into the category of pigments. The color of inorganic pigments may arise from ligand field transitions, charge transfer transitions, intervalence charge transfer transitions, or metal reflectance (in the case of Au or Ag). The attachment of specific ligands to metals greatly influences the wavelength of

maximum absorbance. Many transition metal ions are colored in solution due to their incomplete d-orbitals. The absorption of relatively low energy visible light will promote an electron to an excited state. Since the d-orbital is the outermost shell, d-electron excitations are highly influenced by external forces. Consequently, solvent and ligand effects are significant. 4f and 5f metals (lanthinides and actinides) absorb light because of f electron excitation. Ligand and solvent effects are minor considering that the f electrons are not the outermost electron, and are thus shielded. Charge transfer absorption involves a complex, consisting of an electron donor and an electron acceptor (a metal and a complex anion). Absorption of light causes the transfer of an electron from the donor orbital to the acceptor orbital, resulting in an excited state where an oxidation/reduction reaction has occurred. The metal ion in the complex serves as the electron acceptor (10).

Between an organic dye and an inorganic pigment is a "lake". A lake is a unique type of pigment having both organic and inorganic components, since it is prepared by precipitating an organic dye onto an inorganic substrate. By doing so, a dye is given pigment properties. It is unclear whether or not a lake should be considered as a separate compound or simply a dye which is chemically adsorbed onto the inorganic surface. In either case, the color of lakes originates from the adsorbed organic dye absorbing light.

The Technique: Laser Desorption/Ionization Mass Spectrometry

Overview of Mass Spectrometric Techniques

A mass spectrometer is a very powerful detector following separation by gas chromatography (GC). In the GCMS experiment, volatile components of a mixture, such

as ink, are separated, then ionized using electron impact ionization (EI) and subsequently analyzed by the mass spectrometer. Desorption/ionization (DI) methods that are used with mass spectrometry have the advantage of generating ions for MS analysis from nonvolatile/thermally labile analytes. Currently there are a number of DI methods available. These are summarized in Table 1.4. For example, field desorption (FD) can be used to generate ions from analyte molecules with molecular weights greater than 1,000 (11). In this method, analyte molecules are deposited onto a FD "emitter", which employs a carbon surface. When the surface is heated in the presence of a high electric field, ions can be generated from the analyte. FD has been used recently for the analysis of ballpoint pen inks (12). Secondary ion mass spectrometry (SIMS) and FAB are two very similar techniques (13). In a SIMS experiment, the analyte is deposited onto a metal surface, which is inserted into the ion source of the mass spectrometer. This target is continuously bombarded with ions having several keV of kinetic energy. Secondary ions representative of species on the target surface are generated and analyzed. In the FAB experiment, the analyte is dissolved in a liquid matrix such as glycerol. This viscous solution is deposited on a metal surface, and inserted into the ion source of the mass spectrometer. This target is continuously bombarded using fast (keV) Xe atoms, typically. Both are used with magnetic sector mass analyzers. We note that both FAB and SIMS have been used to obtain spectra of nonvolatile organic dyes (14-16), and there has been one report of using SIMS to analyze colorants on paper (17).

Matrix-assisted laser desorption/ionization (MALDI) (18) and LD (19) are very similar experiments differing only in the presence of a crystalline matrix used to absorb

the laser radiation in MALDI. In both techniques, a pulsed laser ionizes a solid analyte. The ions generated are separated using time-of-flight mass spectrometry (TOF-MS).

Very recently, the characterization of colorants in ballpoint pen inks was accomplished using electrospray ionization mass spectrometry (ESIMS), which is another desorption/ionization method (20). In this experiment, a liquid sample is forced through a needle held at a high potential, resulting in the formation of multiply-charged droplets. In the vacuum system, solvent evaporates from the droplets and a point is reached when a "coulombic explosion" occurs. The original droplet explodes into numerous smaller droplets, carrying multiple charges. ESI is considered a soft ionization method. Consequently, ions of characteristic m/z values will appear in the mass spectrum, with minimal or no fragmentation (21). Negative ion ESI MS has also been used for the analysis of sulfonated azo dyes (22).

Method	Analyte Form	Mechanisms	Mass Analyzer	Ionization Method
Field Desorption (FD)	Adsorbed on a carbon surface	Thermal excitation & electric-field induced emission	Magnetic sector	Continuous
Secondary Ion Mass Spectrometry (SIMS)	Adsorbed on a metal surface	Fast ions collide with the surface and deposit energy	Magnetic sector	Continuous
Fast Atom Bombardment (FAB)	Dissolved in a liquid matrix	Fast atoms collide with the surface and deposit energy	Magnetic sector	Continuous
Matrix Assisted Laser Desorption/Ionization (MALDI)	Embedded in matrix crystals	Absorb laser light from a pulsed laser	Time-of-Flight MS	Pulsed
Laser Desorption (LD)	Adsorbed on a metal surface	Absorb laser light from a pulsed laser	Time-of-Flight MS	Pulsed

Table 1.4: Desorption/ionization methods used in mass spectrometry

Development of LDMS

In 1970, Vastola, Mumma, and Pirone performed what is considered to be one of the first successful laser desorption/ionization mass spectrometric experiments (23). In their historic experiment, they were able to produce molecular ion species of several alkali hexylsulfonate salts, which were known to decompose under analysis using typical gas phase ionization techniques (EI, CI). Specifically, they observed peaks in their mass spectrum representing cationized salts and dimers. No fragmentation was noted, classifying the technique as a "soft ionization" method. In the early developmental stages

of LDMS, a variety of lasers were employed, having wavelengths ranging in the IR region to the far UV (24).

Initially, LDMS was well-suited for the analysis of relatively small (< m/z 1000), nonvolatile, thermally labile, polar molecules. This was in contrast to existing gas phase ionization techniques, such as EI or CI, which required the derivatization of polar groups prior to analysis, to create a volatile compound. LDMS was further developed and applied to the analysis of larger, nonvolatile bio-organic molecules. In 1978, Kistemaker and coworkers experimented with a continuous-wave (cw) CO_2 laser (10.6 μm), as well as a Nd-YAG laser (265 nm) and were able to generate pseudomolecular ions originating from several oligosaccharides, glycosides, and oligopeptides, by alkali attachment (25). Considering that LDMS is a pulsed experiment, a time-of-flight (TOF) mass spectrometer is commonly employed, since it has the ability to generate a complete mass spectrum from a single laser pulse. However, Stoll and Röllgen used a cw-CO_2 laser ion source, coupled with a quadrupole mass spectrometer to produce molecular ions of carboxylic acids and tetra-n-butylammonium salts (26).

There have been several proposed mechanisms describing the desorption and ionization processes (27-31). Evidence has been presented suggesting a thermal process. In general, absorption of the laser light results in a rapid increase in temperature over a broad, unfocused area of the substrate, followed by exponential decay of the temperature over several μs. Vastola and Pirone have reported continued emission of ions for several hundred μs following the duration of the laser pulse (30). This results in both a spatial distribution and a kinetic energy distribution of ions, which have detrimental effects on resolution in a TOF experiment. Ions of the same m/z value desorbed at different times

will have different starting points (spatial distribution). Contrary to laser microprobe experiments, "unfocused" lasers are typically employed in laser desorption experiments. The result is the formation of "hot spots". Consequently, ions of the same m/z value may be desorbed with different kinetic energies. To increase resolution in a TOF experiment, a delay time (~ 100-250 ns) between each laser pulse and the application of an ion-extraction potential is used (32). This allows time for all of the ions to reach the "starting point" and reduces the energy spread of desorbed ions to thermal values. Thus, all ions are theoretically accelerated to the same kinetic energy.

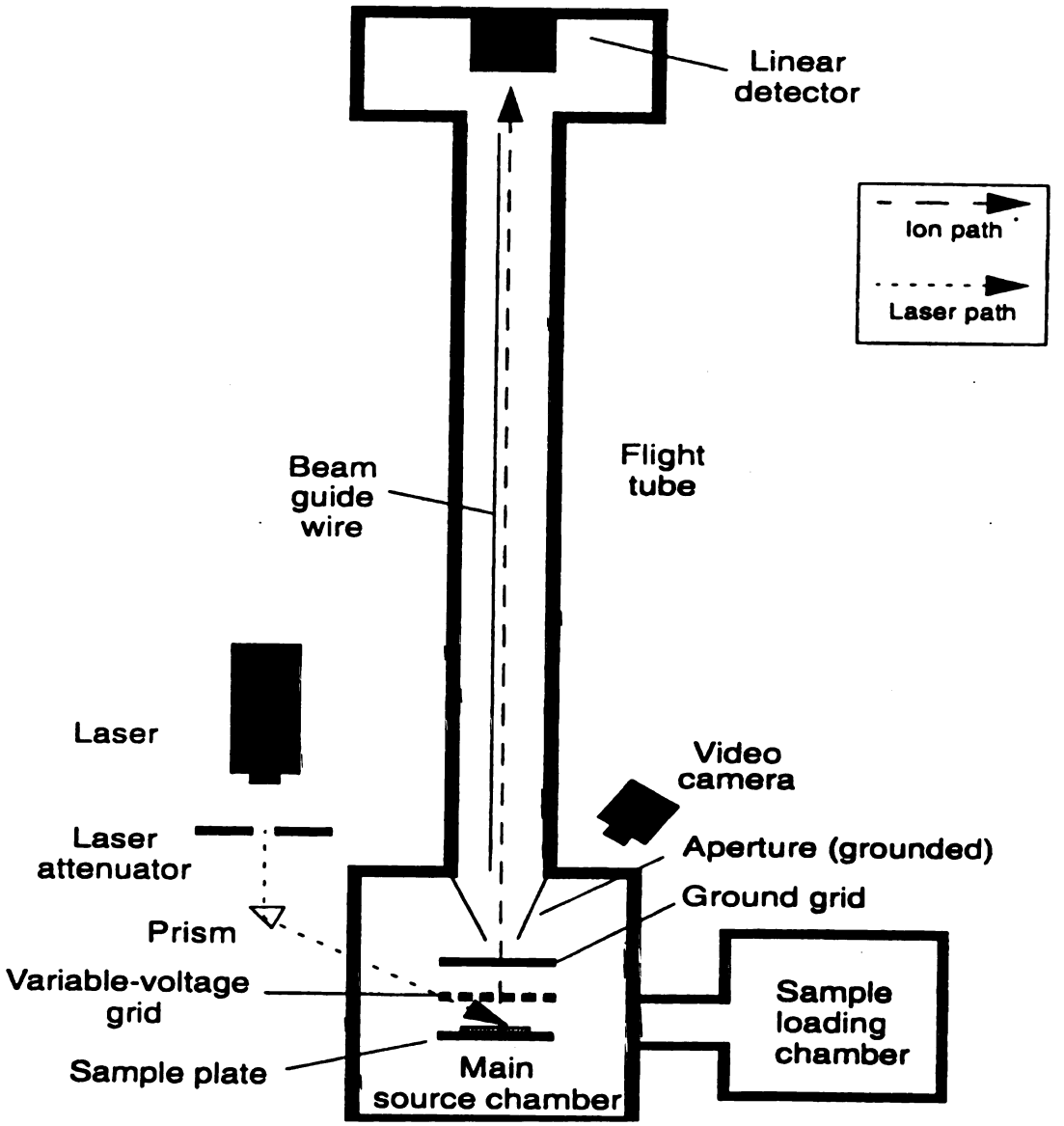

Figure 1.1: Matrix-assisted laser desorption time-of-flight mass spectrometer (Voyager-DE mass spectrometer)

Instrumentation

Positive and negative ion mass spectra of ink and paint samples were obtained using a Perseptive Biosystems Voyager delayed extraction time-of-flight (TOF) mass spectrometer (Framingham, MA). This instrument, illustrated in Figure 1.1, is typically designed to perform matrix-assisted laser desorption ionization (MALDI) experiments, however direct LDMS experiments were performed in this work. In the current MALDI technology, sample plates containing 100-400 "wells" are introduced into the instrument. One microliter of a sample solution can be placed in a well. The solvent evaporates, leaving a solid sample target in the well for analysis. The planar target is moved, using mechanical X-Y devices, so that light from a pulsed laser can be focused onto various positions. For our purposes, this plate can be easily modified such that a piece of paper containing ink or paint is introduced, and the paper is moved so that the laser irradiates one or more locations where ink is present, generating ions for subsequent MS analysis.

Once the sample is introduced into the ion source, the instrument utilizes a pulsed nitrogen laser (337 nm, 3 ns, 3 Hz) to desorb and ionize the sample. The ionized molecules are accelerated and analyzed using a linear time-of-flight (TOF) mass spectrometer. The guide wire located in the TOF tube attracts the ions to keep them on a focused route to the detector. In the TOF tube, ions of different masses accelerated to the same kinetic energy will travel at different velocities. As a result, ions with different m/z values will reach the detector at different times. This allows for separation of the ions according to velocity. An electron multiplier is employed as the detector.

The electron multiplier is made of a copper-beryllium alloy, which has the ability to sputter electrons when bombarded with ions. For example, if one fast ion collides with

the copper-beryllium surface, 10 electrons may be sputtered off. The 10 ejected electrons are then accelerated to another copper-beryllium surface, which is held at a slightly larger potential, where each one of the 10 electrons sputters off 10 more electrons. The process continues, until the signal is amplified 10^5-10^6 times (33).

The following user-selected parameters were employed: for analysis of positive (negative) ions formed by LD, the sample plate was held at a voltage of 20,000 V (-15,000 V), an intermediate acceleration grid was held at 94.5% (94.5%) of the plate voltage, and a delay time ranging between 100 – 250 ns (dependent on the sample) was used between laser irradiation and ion acceleration. The manufacturer supplies several different sample plates, which were employed in these experiments. For example, one type of sample plate does not contain wells, but is machined such that a polyacrylamide gel can be attached. When paper is taped onto this metal sample plate, and spectra are generated at a rate of 3 Hz, full resolution of the instrument is realized using the conditions cited here. Care must be taken to maintain a flat target.

Calibration

For TOF MS experiments, ion flight times are measured, and m/z values must be computed. To calibrate LD spectra, a spectrum containing peaks with known m/z values is first obtained. In most experiments, a saturated solution of CsI (99.9%; Aldrich, Milwaukee, WI) was pipetted onto paper and allowed to dry. Laser irradiation of this target yields positive ions including Cs^+, and ions with the formula $Cs_{(n+1)}I_n^+$, such as Cs_2I^+. These were used for calibrating the instrument, so that flight times for other ions could be converted into m/z values in the mass spectra generated. Similarly, for neat ink

analysis, 2μL of the same CsI solution were pipetted onto a gold plate containing 100 wells, allowed to dry, and used for generating spectra for calibration.

Sample Analysis

As a result of the different types of samples analyzed in this work, including paint and ink on paper, stamps, currency, coins, medallions, etc., a variety of different sample preparation procedures were employed. Consequently, each method will be discussed when appropriate.

The Experiment: LDMS of Colorants

Why does this experiment work? In theory, it is a relatively easy task to predetermine if one can obtain a UV- laser desorption mass spectrum of an organic compound. One simply needs to prepare a dilute solution of the organic compound and obtain a UV/vis spectrum to see if the compound absorbs strongly at 337 nm. If so, one can expect to see a peak in the mass spectrum representing molecular ions, or either protonated or deprotonated molecules. If not, one can simply employ an organic matrix. Inorganic compounds are not as simple, since it is much more difficult to determine whether or not the solid material is going to absorb energy from the UV laser. Additionally, inorganic compounds exist as crystal lattices, and it is even more difficult to predict how they will form ions if they are able to absorb the energy from the laser. In order to try to predict, we need to consider the energy involved for each of the three steps in the LDMS experiment: 1) absorption, 2) desorption, 3) ionization.

Consider the generic crystal lattice shown in figure 1.2. M represents the metal, and X indicates the ligand. The initial step in the LDMS experiment is irradiation of the sample using a pulsed N_2 laser. If the sample can not absorb photons at 337 nm, the experiment has ended. Limited absorbance data is available for inorganic compounds in the solid state. Assuming that the compound absorbs energy, the question becomes how much energy has been absorbed? The efficiency of light absorption is reflected in the molar absorptivity of the analyte under the specified conditions. Again, without UV/vis data, these values are usually difficult to obtain and/or not available. Assuming that the compound absorbs at this wavelength, the crystal lattice heats up rapidly, rupturing bonds in the lattice. But which bonds? This remains unknown until the mass spectrum is obtained. Assuming that a M_aX_b fragment breaks loose from the lattice, will it form an ion?

Desorption/Ionization

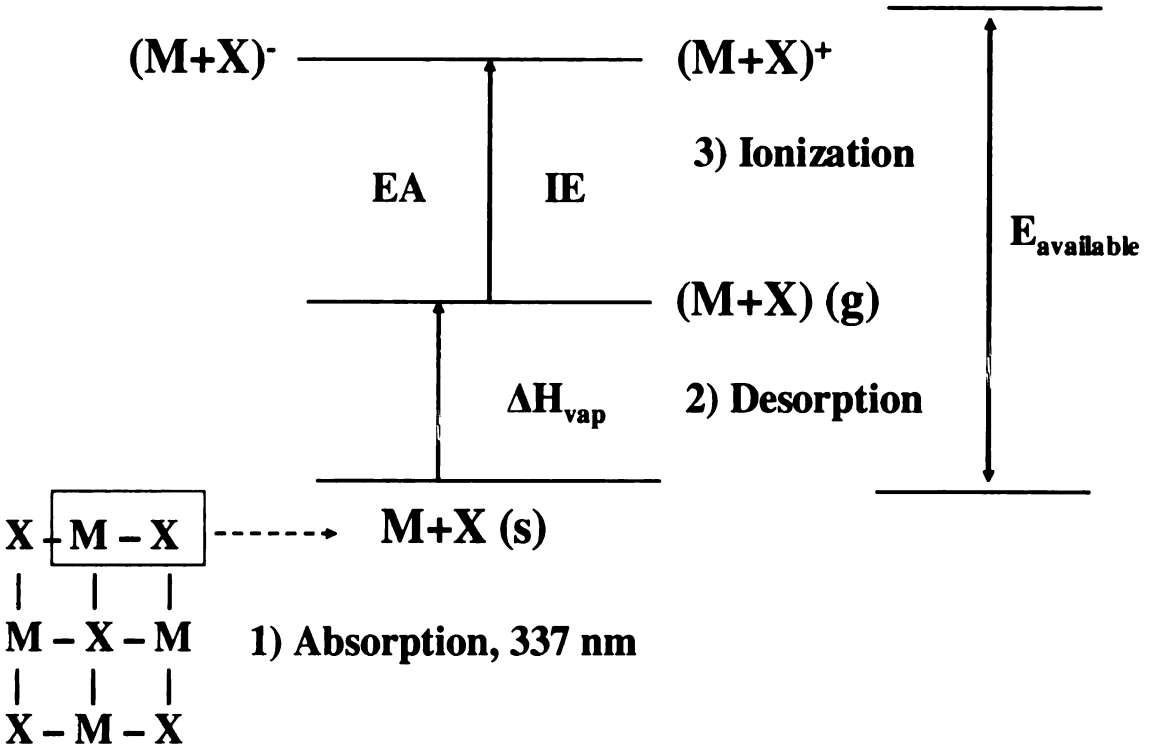

Figure 1.2: Summary of the steps involved in the desorption/ionization of an inorganic compound.

The first step is a deposition of energy, since the following steps require energy. The next step is desorption, which involves the sublimation of the analyte in a condensed phase to the gas phase. Typically, heat of vaporation values may be available for the pure metal, however the data are not available for fragments of a particular inorganic lattice.

The final step is ionization, which can be a competing process between the formation of positive and negative ions. In the formation of positive ions, ionization potentials and proton affinity values of gas phase molecules are considered. In the formation of negative ions, electron affinities of gas phase molecules are considered.

Obviously, ions observed in a mass spectrum are determined by the polarity of the experiment performed. If sufficient energy is absorbed in the initial step of the experiment, for both the desorption and ionization steps to occur, ions are observed. Though we can not predict if and how a particular pigment will generate ions in a LDMS experiment, we know that the experiment frequently works, because we can obtain spectra of numerous organic and inorganic pigments.

What to Expect

In regards to mass spectrometric analysis, dyes may be broken down into two broad classes: ionic and neutral. If the dye is ionic, it is in the form of a salt (C^+A^-), containing a cationic portion (C^+) and an anionic portion (A^-). Methyl violet is an example of a cationic dye and its structure is shown in Figure 1.3a. The dye molecule is a triphenyl methane dye, with five methyl groups attached to three nitrogen atoms (358 Da). A Cl^- serves as its counterion. Solvent black 29, shown in Figure 1.3b, is an example of an anionic dye. The structure consists of a Cr^{3+} center with two identical ligands, each carrying a 2- charge attached to it, giving the overall structure a 1- charge. The dye has a metal cation as its counterion. Since these two examples already exist as ions, they only require enough energy to be desorbed in a LDMS experiment. Consequently, a peak at m/z 358 representing the intact C^+ ion would be expected in the positive ion mass spectrum of methyl violet, and a peak at m/z 666 representing the intact A^- ion would be expected in the negative ion mass spectrum of Solvent black 29.

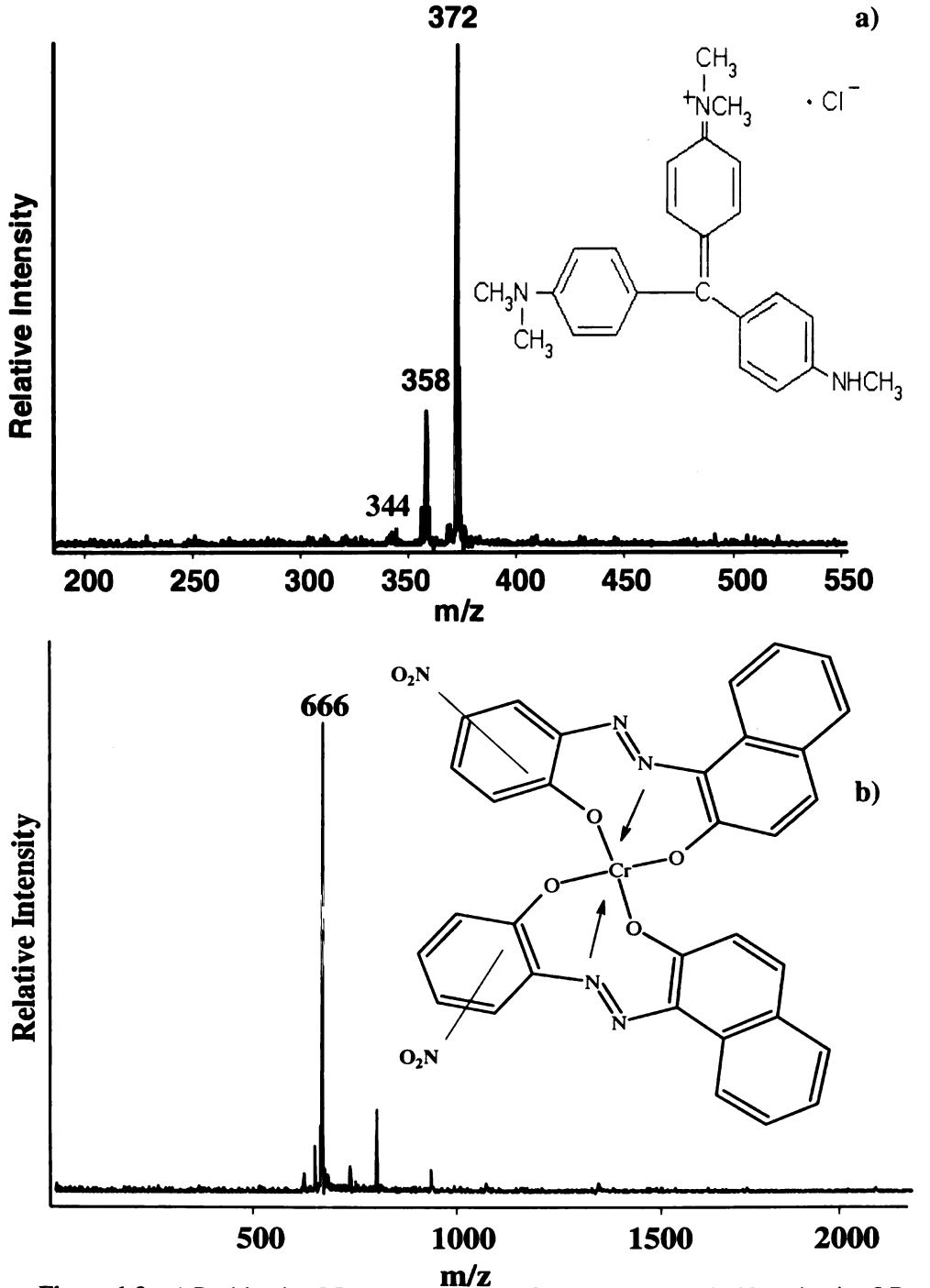

Figure 1.3: a) Positive ion LD mass spectrum of Ink A on paper; b) Negative ion LD mass spectrum of Ink B on paper.

Two industrial ink jet inks were provided to us, with known compositions. Ink A contains the cationic dye methyl violet and its positive ion LD mass spectrum is shown in Figure 1.3a (35). Dyes are frequently sold as impure mixtures. In the case of methyl violet, the hexamethylated form (m/z 372) is more abundant than the pentamethylated form (m/z 358). This becomes evident when examining the ink's positive ion LD mass spectrum (Figure 1.3a). The base peak (largest peak) is seen at m/z 372, which corresponds to the hexamethylated structure (crystal violet), whereas the peak at m/z 358 represents methyl violet. Note, the manufacturer used methyl violet, but the mass spectrum shows it was really crystal violet.

Ink B contains the anionic dye Solvent Black 29. The negative ion LD mass spectrum of Ink B on paper is shown in Figure 1.3b (35). As expected, a peak is present at m/z 666 representing the intact anionic portion of the dye salt. The structure of Solvent Black 29 is very stable, and therefore no degradation products were observed in LD mass spectra.

Neutral dyes are very different than ionic dyes in that they must be desorbed and ionized to be detected in a LDMS experiment, resulting in a few different expectations in the mass spectrum. In a positive ion LD mass spectrum of a neutral dye such as copper phthalocyanine (structure shown in Figure 1.4a), a peak representing the molecular ion is observed and a peak representing the deprotonated molecule is seen in negative ion mode (1.4b) (36). In other instances (discussed in Chapter 2) peaks representing both the molecular ion (M^+) and protonated molecule [$(M + H)^+$] are observed simultaneously in positive ion mode. Likewise, in the negative ion mass spectrum, peaks representing both the molecular ion (M^-) and deprotonated molecule [$(M - H)^-$] were present. The LD mass

spectra of these examples will be shown and discussed in more detail in later chapters, however at this point the dyes are presented to gain an understanding of what to expect in a mass spectrum of similar dye compounds.

Inorganic pigments exist as crystal lattices, and it is therefore much harder to predict what ions will be observed in a mass spectrum. Therefore, much of our work involving the LDMS analysis of inorganic pigments has been a learning process, in discovering how the colorants form ions in this experiment. The analysis of numerous inorganic pigments containing metals such as Fe, Pb, Cr, As, and Hg will be presented. Unlike organic dyes, inorganic pigments possess metals having unique isotopic patterns, making their appearance in a mass spectrum very obvious. Generally, these patterns allow for an easy, positive identification of a compound. However, there are times when the patterns become quite complex, requiring skill and knowledge of how the patterns change with the addition of different elements. The following is an explanation of how isotopic pattern analysis is performed.

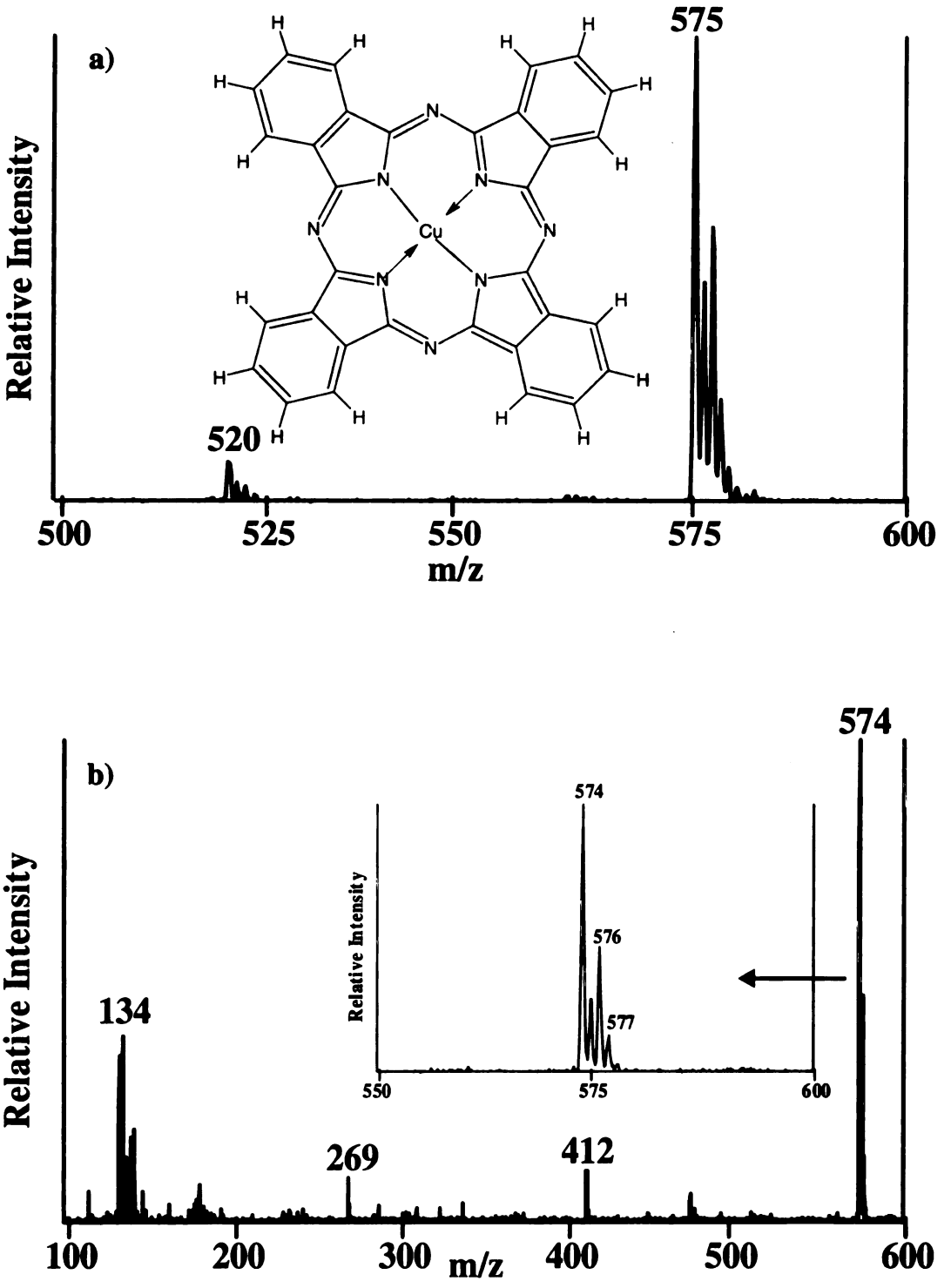

Figure 1.4: a) Positive ion LD mass spectrum of copper phthalocyanine (Aldrich) on paper; b) Negative ion LD mass spectrum of copper pthalocyanine on paper.

Isotopic Profiling

Certain elements exist in nature in more than one isotopic form. Isotopes are stable atoms having the same number of protons, but differing in the number of neutrons present in the nucleus. Isotopes occur naturally in different abundances. The most abundant is designated as the "A" form. The atomic weights of the elements listed on the Periodic Table are the average masses. The average mass is a weighted sum of all of the isotopes of a specific element. In a negative ion mass spectrum of chlorine, a single peak at m/z 35 representing Cl^- ions will not be observed. Rather, a pattern resembling that of Figure 1.5a will be present. Figure 1.5a represents the theoretical isotopic distribution for Cl. Cl^{35} occurs much more commonly in nature than Cl^{37} ("A+2"). The ratio is roughly 3:1. This pattern is unique only to Cl, and therefore may be used to confirm the presence of an ion containing Cl in a mass spectrum. Considering that the relative abundances for most isotopes are relatively constant, the isotopic pattern for samples containing more than one element having distinct isotopes can be predicted.

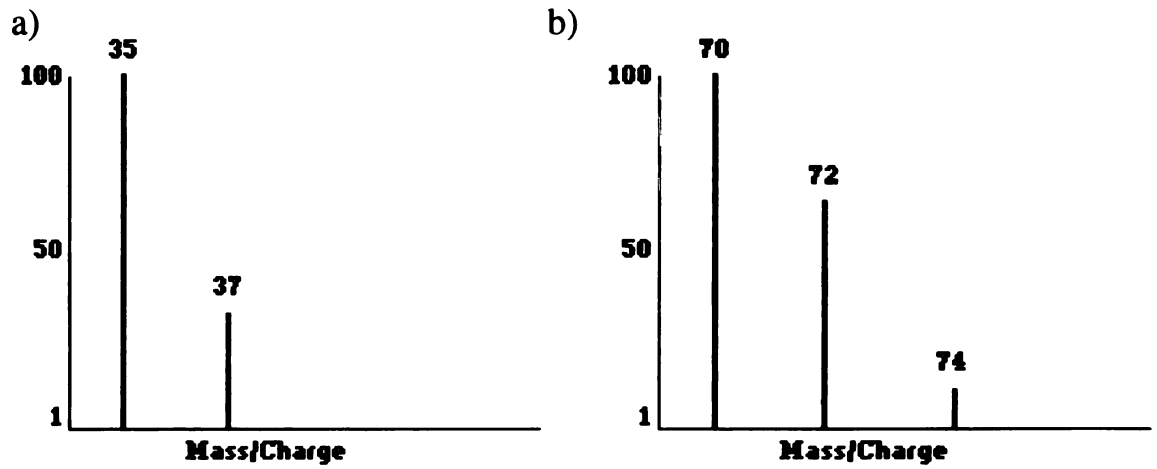

Figure 1.5: Theoretical isotopic pattern for a) Cl; b) Cl_2.

What does the isotopic pattern for Cl_2 look like? Consider a container containing hundreds of chlorine atoms. The exact number of atoms present in the container is of no importance, since it is already known that the relative amounts of the atoms are in a 3:1 ratio. Thus, the probability of choosing a Cl^{35} from the container will always be 66.67% and 33.33% for Cl^{37}. Table 1.5 lists all of the possible combinations in which the Cl atoms could be chosen, with their corresponding probabilities. The peak appearing at m/z 72 has two combinations with equal probabilities. These values are summed, yielding a final ratio of 9:6:1 for the peaks at m/z 70, 72, and 74, respectively. This corresponds with Figure 1.5b, representing the theoretical isotopic distribution for two Cl atoms. While this calculation was relatively simple and not very time consuming, the situation becomes much more complicated when compounds containing multiple elements with distinctive isotopic patterns are analyzed, as in the case of artists' pigments.

Cl_1	Cl_2	Molecular Weight	Probability
35	35	70	3 x 3 = 9
35	37	72	1 x 3 = 3
37	35	72	3 x 1 = 3
37	37	74	1 x 1 = 1

Table 1.5: Manual calculation for the isotopic distribution of Cl_2.

References

1) Ember LR. Chemistry and art: helping to conserve the nation's treasure. Chemical and Engineering News 2001; July 31: 51-59.

2) Howarth E. Crash course in art. New York: Barnes & Noble, 1994.

3) Brown KL, Clark RJH. Analysis of pigmentary materials on the Vinland Map and Tartar Relation by Raman microprobe spectroscopy. Anal Chem 2002;74:3658-3661.

4) McCrone WC. The Vinland Map. Anal Chem 1988;60:1009-1018.

5) Plesters J. Ultramarine blue, natural and artificial. In: Roy A, editor. Artists' pigments: a handbook of their history and characteristics, vol. 2. New York: Oxford University Press, 1993;37-65.

6) http://www.amolf.nl/research/biomacromolecular_mass_spectrometry/molart/molart.html

7) Berrie BH. Prussian blue. In: Fitzhugh EW, editor. Artists' pigments: a handbook of their history and characteristics, vol. 3. New York: Oxford University Press,1997; 191-217.

8) Skoog DA, Holler FJ, Nieman TA. Principles of instrumental analysis, 5th ed.. USA: Brooks/Cole, 1997.

9) Zollinger H. Color chemistry: syntheses, properties and applications of organic pigments, 2nd ed. USA: John Wiley & Sons, 1991.

10) Schenk GH. Inorganic and organic charge transfer spectra in solution and their analytical implications. Record of Chemical Progress 1967;28:135-148.

11) Giessman U, Rollgen FW. Electrodynamic effects in field desorption mass-spectrometry. Int J Mass Spectrom Ion Phys 1981;38:267-79.

12) Sakayanagi M, Komuro J, Konda Y, Watanabe K, Harigaya Y. Analysis of ballpoint pen inks by field desorption mass spectrometry. J Forensic Sci 1999;44:1204-1214.

13) Lyon PA, editor. Desorption mass spectrometry – are SIMS and FAB the same? Washington, DC: American Chemical Society, 1985.

14) Monaghan JJ, Barber M, Bordoli RS, Sedgewick RD, Tyler AN. Fast atom bombardment mass spectra of involatile sulphonated azo dyestuffs. Org Mass Spectrom 1982;17:569-74.

15) Scheifers SM, Verma S, Cooks RG. Characterization of organic dyes by secondary ion mass spectrometry. Anal Chem 1983;55:2260-5.

16) Detter-Hoskin LD, Busch KL. SIMS: secondary ion mass spectrometry. In: Conners TE, Banerjee, editors. Surface analysis of paper. New York: CRC Press, 1995;206-34.

17) Pachuta SJ, Staral JS. Nondestructive analysis of colorants on paper by time-of-flight secondary ion mass spectrometry. Anal Chem 1994;66:276-84.

18) Kara M, Bachman D, Hillenkamp F. Influence of the wavelength in high-irradiance ultraviolet-laser desorption mass-spectrometry of organic molecules. Anal Chem 1985;57:2935-9.

19) Denoyer E, Van Grieken R, Adams F, Natusch DFS. Laser microprobe mass spectrometry 1: Basic principles and performance characteristics. Anal Chem 1982;54:26-41.

20) Ng L-K, Lafontaine P, Brazeau L. Ballpoint pen inks: characterization by positive and negative ion-electrospray ionization mass spectrometry for the forensic examination of writing inks. J Forensic Sci 2002;47:1-10.

21) McCloskey JA, editor. Methods in enzymology, vol. 193. New York: Academic Press, 1990.

22) Lee ED, Muck W,Henion JD. Determination of sulfonated azo dyes by liquid chromatography/atmospheric pressure ionization mass spectrometry. Anal Chem 1987;59:2647-52.

23) Vastola FJ, Mumma RO, Pirone AJ. Organic Mass Spectrometry 1970;3:101.

24) Conzemius RJ, Capellen JM. A review of the applications to solids of the laser ion source in mass spectrometry. Int J Mass Spectrom Ion Physics 1980;34:197-271.

25) Posthumus MA, Kistmaker PG, Meuzelaar HLC. Laser desorption mass spectrometry of polar nonvolatile bio-organic molecules. Anal Chem 1978;50:985-991.

26) Stoll R, Rollgen FW. Laser desorption mass spectrometry of thermally labile compounds using a continuous wave CO_2 laser. Organic Mass Spectrometry 1979;14:642-645.

27) Cotter RJ, Yugey AL. Thermally produced ions in desorption mass spectrometry. Anal Chem 1981;53:1306-1307.

28) Benzazouz M, Hakim B, Debrum JL, Strivay D, Weber G. Study of the mechanism of direct laser desorption/ionization for some small organic molecules (m < 400 Daltons). Rapid Commun Mass Spectrom 1999;13:2302-2304.

29) Hillenkamp F. Laser desorption techniques of nonvolatile organic substances. Int J Mass Spectrom Ion Physics. 1982;45:305-313.

30) Cotter RJ, Tabet J-C. Laser desorption ms for nonvolatile organic molecules. American Laboratory 1984;16:86-99.

31) Tabet J-C, Cotter RJ. Laser desorption time-of-flight mass spectrometry of high mass molecules. Anal Chem 194;56:1662-1667.

32) van Breeman RB, Snow M, Cotter RJ. Time-resolved laser desorption mass spectrometry. 1. Desorption of preformed ions. Int J Mass Spectrom Ion Physics 1983;49:35-50.

33) Watson JT. Introduction to mass spectrometry. Philadelphia: Lippincott-Raven, 1997.

34) Lias S, Bartmess JE, Liebman JF, Holmes JL, Levin RD, Mallard G. Gas-phase ion and neutral thermochemistry. J Physical and Chemical Reference Data 1988;17:649,794-95.

35) Grim DM, Siegel J, Allison J. Evaluation of desorption/ionization mass spectrometric methods in the forensic applications of the analysis of inks on paper. J Forensic Sci 2001;46:1411-20.

36) Grim DM, Allison J. Identification of colorants used in watercolor and oil paintings by UV laser desorption mass spectrometry. International J Mass Spectrometry 2003;222:85-99.

Chapter Two: Water Colors

Introduction

Art conservators devote much time and effort to preserving our artistic heritage. Museums frequently lack open windows, to keep out the sun's damaging UV-rays. Art objects may only be displayed for limited time periods, under minimal lighting (1). Typical air pollution concentrations in museums have also been determined (2-6). Preventative measures have been employed in museums, which include the use of activated carbon air-filtration or alternative absorption or washing systems, use of reduced ventilation rates (to hinder the circulation of harmful gases), enclosure of art objects within display cases, and protection behind glass or varnish layers (7-9). The job of art conservators is made much more difficult by the fugitive and unstable nature of artist's colorants. Watercolor paints are infamous for fading and/or shifting hue, as a response to environmental conditions (ie. light, pollutant gases) (10,11). In particular, azo dyes have been reported to be extremely susceptible to light (12,13). Consequently, several kinetic studies have been performed to characterize the degradation process (14,15). The effects of air pollutants which have been detected in museums, specifically O_3 (16-23), NO_2 (24), HNO_3 (25,26), peroxyacetyl nitate (PAN) (27), and carbonyls such as formaldehyde (28), on organic colorants have been well researched. The Cass research group, at the California Institute of Technology, has performed extensive studies in this area over the past decade. A summary of their work follows.

Ozone is a highly oxidizing air pollutant present in relatively low concentrations, however in regions of high concentration of photochemical smog, the concentration can reach between 0.3 and 0.4 ppm (18). In their experiments, modern watercolors (i.e.

triphenylmethanes, acridones, and alizarins) and natural organic colorants (i.e. indigo and curcumin) were subjected to ozone exposure, equivalent to the accumulated dose during less than ten years in a typical air conditioned museum. They concluded that the ozone-induced fading of natural colorants typically proceeds via destruction of the chromophore, yielding colorless reaction products and hence a faded sample of the same hue (16,18,20,22).

Nitrogen oxides are formed in the atmosphere from the nitric oxide emissions of fuel combustion sources. These include NO_2, HNO_3 and PAN. Studies completed at the California Institute of Technology indicated that the nitrogen oxides were not as damaging as ozone (required longer exposure times to induce fading or color shifts) (24-28), however they noted that specific chemical classes of dyes were more susceptible to particular gases than others. For instance, lakes are more susceptible to NO_2, whereas triphenylmethane dyes were more susceptible to HNO_3 than to O_3 (24). Whitmore and Cass have concluded that unsaturated organic compounds are particularly vulnerable to oxidation reactions, resulting in the discoloration of the colorant. They also noted that NO_2 can result in the addition of nitro ($-NO_2$) or nitroso ($-ONO_2$) groups to organic molecules, which then tend to yellow due to the NO_2 chromophore (24).

The Cass group employed a Diano Match Scan II spectrophotometer to measure the diffuse reflectance spectra of colorants before and after exposure to different pollutant gases. From the spectral reflectance data, tristimulus values (X, Y, Z) and color differences (ΔE, from the CIE 1976 L*a*b formula) were calculated for CIE Illuminated C (24,29). Munsell notatations, which break down the color change into changes in the visual perception of hue, value (lightness), and chroma (saturation), were subsequently

computed from these tristimulus values. ΔE gives the magnitude of the color change and provides a basis for comparing the effect of gaseous pollutant exposure on the colorant systems. Consequently, the results of their experiments are reported in the form of a measure of the color change, as opposed to actual chemical information describing the degradation mechanisms. One study is noted (exposure to atmospheric nitric acid) in which, Grossjean, Salmon, and Cass employed chemical ionization mass spectrometry (CIMS) to identify some (but not all) of the degradation products (25). The following reasons were provided to explain why not all of the products were detected: 1) formation of volatile products that were no longer present on the Teflon filter at the completion of nitric acid exposure experiment, 2) products formed in low yields of <1%, since the mass spectrometer's data acquisition systems did not record mass fragments whose abundances were less than 1% of the base peak, and 3) products of very low vapor pressure, of which no detectable amount could be introduced into the reaction chamber of the instrument's ion source even at high probe temperature. From this study, Grossjean *et al.* were able to propose degradation pathways for alizarin, acridone, quinacridone, and indigo (25).

The Cass research group has touched upon the potential of mass spectrometry for the characterization of dye degradation mechanisms. Here, laser desorption mass spectrometry is being explored as a potential analytical technique for the detection of organic watercolor dye degradation products. Potential obstacles are acknowledged, including the formation of small, volatile, non-absorbing degradation products, which are non-ideal analytes for the LDMS experiment. In a previous project, briefly discussed in the next section, we were able to effectively characterize the degradation process for methyl violet, a common organic toner used in modern ink formulations. Demethylated

degradation products were easily detected (30-32). Preliminary experiments were designed and performed based on the results of the LDMS analysis of methyl violet.

The goals of the current project were to 1) obtain positive and negative ion LD mass spectra of commonly used watercolor paints; 2) identify the colorants in the mass spectra; 3) artificially age the samples using a variety of light sources and expose the colorants to different environmental pollutants (O_3, NO_3, etc.); 4) identify and quantify degradation/reaction products; 5) determine if there is a relation between the age of the paint and the extent of degradation/reaction products present in the mass spectra. Preliminary data suggested that goals 1 and 2 were obtainable. Many of the dyes found in the watercolor paints selected produced very intense, well-resolved peaks representative of the intact dye molecule, indicating that the dye molecules are readily desorbed and ionized when irradiated with a 337 nm laser. Additionally, specific dye information was frequently provided on the labels of the watercolor tubes, making the identification process relatively easy. However, a lack of dye information on the watercolor tubes was not a deterrent. Identification of unknown samples was completed using mass spectral interpretation and the information readily available in the literature. Problems were encountered when trying to "age" and react the watercolors.

A box of Niji watercolors (Yasutomo & Co., San Francisco, CA) was purchased containing the colorants labeled carmine, vermilion, lemon yellow, chrome green, viridian, cobalt blue, Prussian blue, yellow ochre, burnt sienna, burnt umber, and ivory black. The names of the colorants drew interest, since several of them are typically associated with inorganic compounds. However, their LD mass spectra prove different. Positive and negative ion LD mass spectra were obtained for all of the samples, dissolved

in water and applied to paper. Following long exposure to various light sources, including a UV-lamp, a Hg-arc lamp, and natural sun light, only a few of the colors had faded to a noticeable extent.

Additional artist grade pigments were obtained (Cadmium Red Hue 095 and Cadmium Orange Hue, Winsor & Newton), which listed the dye compositions on their labels. Mass spectra of these colorants confirmed the information provided on the label, however these paints also failed to change color following long exposure to light. Consulting the literature, it was found that the structures of contemporary organic watercolor dyes have been modified, significantly improving their resistance to light and environmental pollutants. While this is wonderful for contemporary watercolor artists, artists 100 years ago did not have access to the new and improved watercolors. Consequently, their masterpieces were created with colorants known to disappear over time, if not protected properly. The challenge became to find a supply of the older "bad" watercolors, since they are no longer manufactured. The search was unsuccessful, therefore we resorted to choosing the least stable pigments available based on ASTM (American Standards for Testing Materials) light-fastness ratings. A detailed analysis of these colorants follows.

Watercolor paints are composed of one or more organic dyes, which are known to be fugitive (fade easily on exposure to light) and reactive with gases in their environment. Lightfastness is a term generally used to describe the ability of a colorant to resist fading on exposure to light. However, lightfastness also encompasses a colorant's impermanence to additional damaging environmental factors, including weak acids, alkalis and impurities in the atmosphere. The ASTM has established a well-defined

testing procedure to which each colorant is subjected (33-35). They have developed a scale (ASTM I-V), rating each colorant according to its lightfastness. A summary of the ASTM scale is provided in Table 2.1.

Rating	Meaning
ASTM I	Excellent lightfastness.
ASTM II	Very good lightfastness.
ASTM III	Not sufficiently lightfast to be used in paints conforming to the specification. Such colors can fade rather badly, particularly the tints.
ASTM IV	Pigments falling into this category will fade rapidly.
ASTM V	Pigments will bleach very quickly.

Table 2.1. A summary of the ASTM lightfastness scale.

Colorants have been named and categorized based on the Color Index. Throughout this chapter, the common and color index names will be given for each colorant discussed, and the names may be used interchangeably. The chemical class of each colorant will also be provided. Generally, the common name gives some kind of indication of the chemical class, but not always.

Experimental

A box of Niji watercolors (Yasutomo & Co., San Francisco, CA) was purchased containing colorants labeled carmine, vermilion, lemon yellow, chrome green, viridian, cobalt blue, Prussian blue, yellow ochre, burnt sienna, burnt umber, and ivory black. Additional colorants listed in Table 2.2 were purchased from a local artist's supply store. All of the samples were dissolved in water and applied to paper (Hammermill Fore MP). After the samples were dry, they were subjected to positive and negative ion LDMS analysis, as described in Chapter 1.

UV-accelerating aging studies were performed on dye-on-paper samples using a UV-lamp (254 nm, 760 microwatts/cm^2, UVP Inc., San Gabriel, CA model UVGL-58), as well as a Hg-arc lamp (Oriel, Stratford, CT), and analyzed at various intervals. Controlled ozone exposure experiments were performed in a reaction chamber (0.308 L) at the Environmental Engineering Department (Michigan State University, East Lansing, MI). Samples were exposed to 375 ppm O_3, at a flow rate of 2.57 mL/min, for 12.5 minutes. Exposure to concentrated HNO_3 vapors, was accomplished by suspending the sample (dye-on-paper) over a HNO_3 bath in a covered beaker. Exposure times varied.

Colorant (Brand)	Dye Composition	Vehicle
Cadmium Orange Hue 090 (Winsor & Newton)	Diarylide yellow (PY 83) Perinone orange (PO43)	Gum Arabic/dextrin
Cadmium Red Hue 095 (Winsor & Newton)	Perylene (PR 149) Pyrrole (PR 255)	Gum Arabic/dextrin
Purple Lake 544 (Winsor & Newton)	Cu-phthalocyanine (PB 15) Rhodamine/PMTA (PV 2)	Gum Arabic/dextrin
Mauve 398 (Winsor & Newton)	Quinacridone (PR 122) Carbazole dioxazine (PV 23)	Gum Arabic/dextrin
Alizarin Crimson Hue 003 (Winsor & Newton)	Quinaccridene-pyrrolidone, Quinacridone (PR 206)	Gum Arabic/dextrin
Rose Madder 580 (Winsor & Newton)	1,2 dihydroxyanthraquinone lake (PR 83)	Gum Arabic/dextrin
Hooker's Green Dark 312 (Winsor & Newton)	Chlorinated cu-phthalocyanine (PG7) Quinacridone (PO 49) Cu-phthalocyanine (PB 15)	Gum Arabic/dextrin
Indigo 322 (Winsor & Newton)	Amorphous carbon (PBk 7) Complex silicate of Na & Al with S (PB 29) Cu-phthalocyanine (PB 15)	Gum Arabic/dextrin
Opera (Holbein Artist's Watercolor)	PR 122, BV 10	(not provided)

Table 2.2. Artist-grade watercolors subjected to LDMS analysis.

Summary of Methyl Violet Degradation Study

As mentioned previously, methyl violet and its degradation mechanism was studied extensively, as part of a separate ink dating project (30-32). Important concepts were learned in regards to the ability to detect organic colorants off of paper (a nontraditional surface for an LDMS experiment). Additionally, a method for artificially accelerating the age of organic colorants using UV light was developed. This project served as a "springboard" to a much more extensive project involving the LDMS analysis of several organic watercolor dyes. The results of the methyl violet study relevant to this project are summarized in this section. Furthermore, it will become necessary to recognize the difference between the mass spectra of new and degraded methyl violet, in order to appreciate the LDMS analysis of an illuminated manuscript discussed in a later chapter.

Methyl violet is known to be extremely light fugitive, and fades very easily when exposed to natural and artificial light sources. The structure of methyl violet is shown in Figure 2.1. It is a pentamethylated triphenyl methane cationic dye. The structure, as shown in Figure 2.1, has a molecular weight of 358 Da. As was discussed in Chapter 1, dyes are typically sold as impure mixtures and in the case of methyl violet, the hexamethylated homolog (crystal violet) is the most abundant component in the mixture. As an ink containing methyl violet ages, the dye structure degrades via an oxidative demethylation process (35), which is evident in mass spectra of aged ink (Figure 2.2).

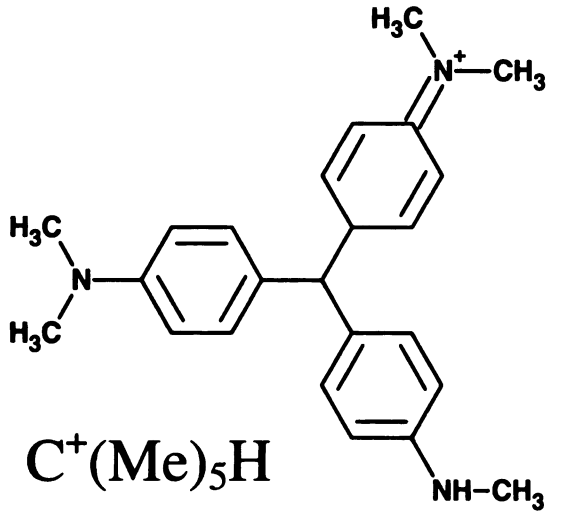

m/z	Structure
372	$C^+(Me)_6$
358	$C^+(Me)_5H$
344	$C^+(Me)_4H_2$
330	$C^+(Me)_3H_3$
316	$C^+(Me)_2H_4$
302	$C^+(Me)_1H_5$
288	C^+H_0

Figure 2.1. The structure of methyl violet and designations for its degradation products.

Figure 2.2 shows the positive ion LD mass spectra of a preliminary accelerated aging study performed on black Bic ballpoint pen ink-on-paper. The ink was applied uniformly to a piece of 4 in^2 paper. An initial positive ion LD mass spectrum was obtained. Approximately one third of the sample was covered and the entire sample was irradiated using a UV lamp (760 microwatts/cm^2) , placed directly on top of the sample for 12 hours. Another third of the sample was masked off and the sample was irradiated for another 12 hours. This experiment demonstrated that significant fading was noted following 12 or more hours of intense UV irradiation. Also, it showed that by using masks, an array of UV aged ink on a single piece of paper could be easily generated, introduced as a single sample into the mass spectrometer, and spectra for each region

obtained. We acknowledge that there is currently no accepted irradiation/age correlation for this experiment.

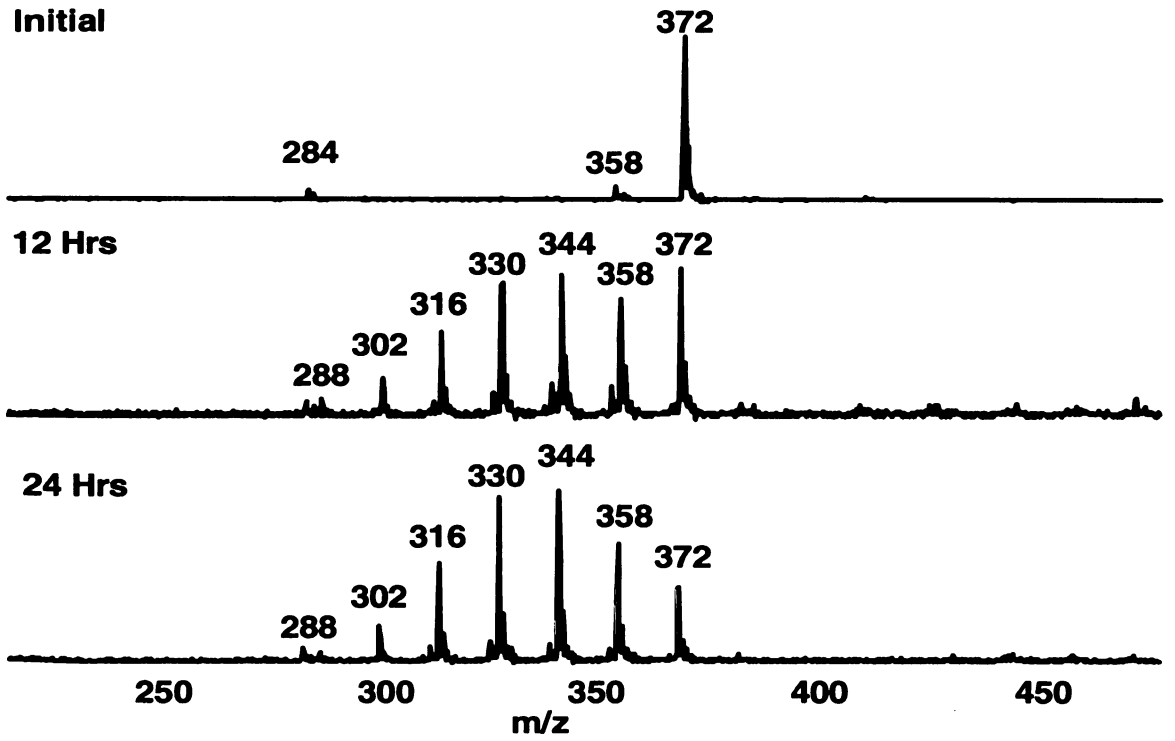

Figure 2.2. Preliminary UV-accelerated aging study: Bic ballpoint pen ink on paper.

The preliminary UV accelerated aging data are presented in Figure 2.2. Positive ion LD mass spectra are shown of methyl violet dye as originally deposited by the ballpoint pen onto paper, and the same portion of the mass spectrum is shown following 12 and 24 hours of UV irradiation. After irradiating the sample for 12 hours, degradation products (summarized in Figure 2.1) are clearly present – a series of peaks separated by 14 amu. Each methyl group (15 amu) is replaced with a H atom (1 amu), accounting for the 14 mass unit difference. The m/z 372 peak remains the most intense peak. The

spectrum shows that six new compounds, lower-mass forms of methyl violet, are now in abundance. Irradiating the sample for another 12 hours causes the initial base peak to further decrease in intensity, such that the degradation product peaks dominate. Andrasko noted similar results using high performance liquid chromatography (HPLC) to study ballpoint pen inks stored under various light conditions (36).

When comparing these results to naturally aged samples (Figure 2.3b), the same degradation products were generated. However, we realized that we had artificially aged the samples past that which we had observed in naturally aged samples. Aginsky stated the importance of ensuring that the accelerated aging method mimics natural aging as closely as possible, meaning that the technique should not induce any chemical changes that would not occur naturally (37). Consequently, the experimental design was adjusted by elevating the UV lamp 6 cm above the sample, and by monitoring the irradiated sample at much shorter time intervals (every 15 minutes). This allowed for us to visualize the dye degradation process more clearly, as well as to mimic the rate of the natural aging process more effectively. The developed method was applied to UV-accelerated aging experiments performed on watercolors.

UV-accelerated aging mimics natural aging from a dye perspective, and can be characterized by LDMS. Figure 2.3a represents a portion of the positive ion LD mass spectrum of new black Bic ballpoint pen in on paper. New ink is characterized by a large peak at m/z 372, representing the non-degraded dye molecule ($C^{+}Me_6$), with a very small peak at m/z 358 ($C^{+}Me_5H_1$). Figure 2.3b is the positive ion LD mass spectrum of a 38-month old naturally aged Bic black ballpoint pen ink on printer paper. As an ink ages, lower mass peaks appear in the spectrum representing the molecules that are referred to

as degradation products, accompanied by a decrease in the relative intensity of the original m/z 372 base peak, representing the original intact dye molecule. The number and amount of degradation products present is a function of the age of the ink, but if this was ink on a questioned document, how could the age be determined from the spectrum? As in other ink dating methods, there must either be spectra from naturally aged samples for comparison purposes, or there must be a calibrated methods for accelerating the aging of a new sample of similar ink that can be use to create a sample that yields the same spectrum. Irradiating Bic black ballpoint pen ink-on-paper, for 6.25 hours with UV light, produces a very similar mass spectrum (Figure 2.3c) as that of the naturally aged 38-month old document (aged in the dark). Based on this data alone, a calibration for the UV method can be estimated. Irradiation for 6.25 hours produces the same extent of degradation as what occurs naturally over a period of 38 months. Thus, every hour of UV irradiation accelerates the aging by approximately 182 days. If a different sample was in question, the ink could be irradiated until the same extent of degradation was observed, and from the irradiation time required, the corresponding natural age could be calculated. This approach, along with other insights into the variables that influence the rates of dye degradation, were studied in this work.

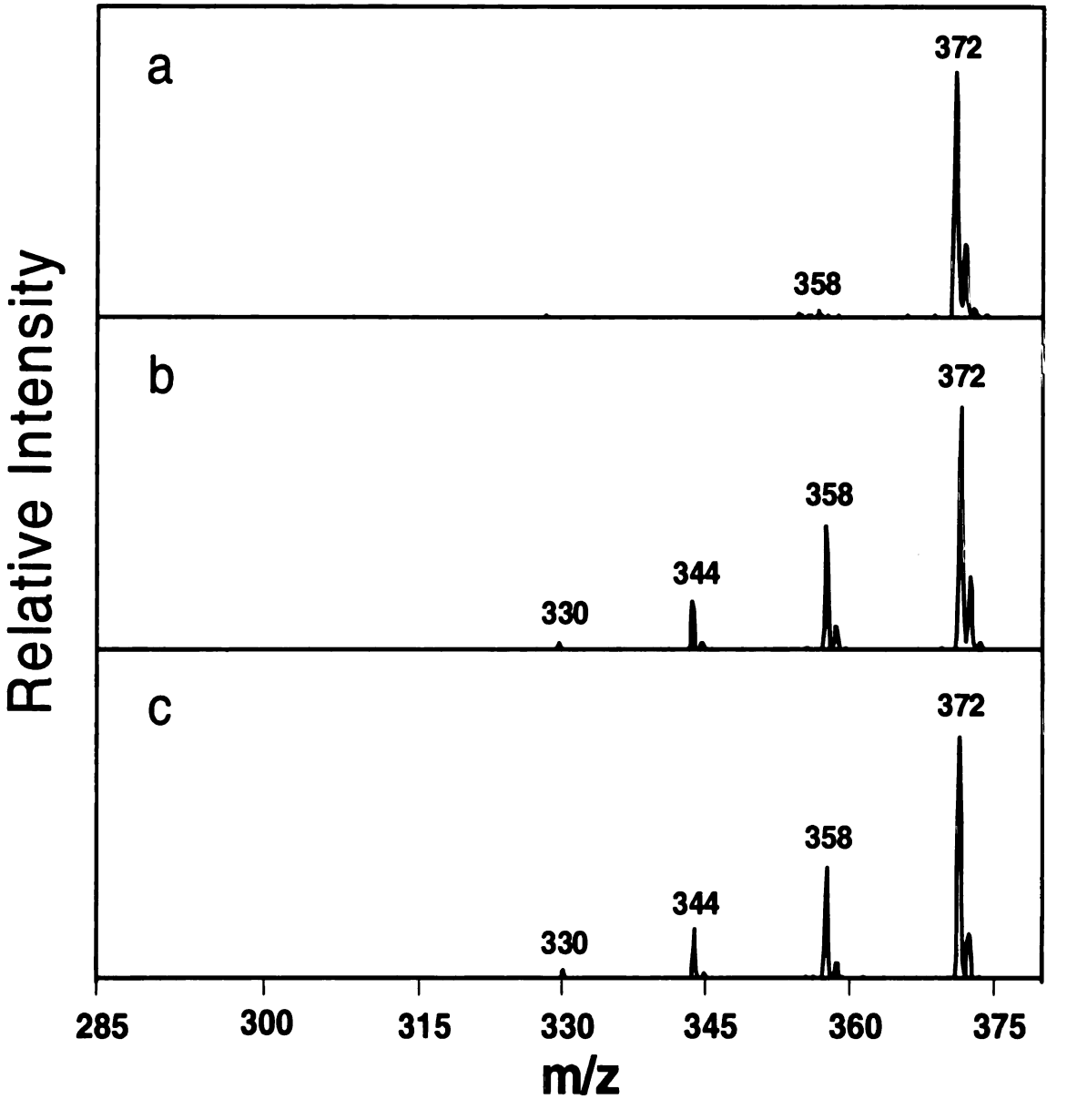

Figure 2.3. A portion of the positive ion LD mass spectrum of Bic black ballpoint pen ink-on-paper: a) ink from a new document; b) a 38-month old controlled, naturally aged document; c) ink from a document irradiated for 6.25 hours with UV light

Methyl violet can be efficiently degraded on paper with UV irradiation. Ink samples on paper were subjected to UV radiation, followed by LDMS analysis, for periods of up to 8 hours. In these time periods, more than 50% of the dye molecules can be converted into degradation products. Figure 2.4 is a plot of the normalized relative intensities for each of the three mass spectral peaks representing the dye or degradation product as a function of time for the UV accelerated aging study of Bic black ballpoint pen ink-on-paper. The relative intensity is a measure of the concentration of a particular species in comparison to the other components detected in the sample mixture. In Figure 2.4, the relative abundance of the intact dye molecule (m/z 372) decreases as the relative abundances of the degradation products (m/z 358, 344) increase with irradiation time, which is an indication of the dye degrading. How can the data be used to develop a determination of an ink's age? There are many options. For instance, the age correlation may involve the relative intensity of the m/z 372 peak, revealing the amount of dye remaining in its original form. Another possibility would be to take a ratio of two peaks that are always present, and seem to experience the most significant changes as the ink ages. Ideally, a function would be identified, in which a single value could be computed that incorporates information on all of the degradation products present. One way to accomplish this is to compute the average molecular weight for the dye at each time interval. Figure 2.5 shows the plot of the average molecular weight versus the time the document was irradiated in the UV accelerated aging study of Bic black ballpoint pen ink on paper. The average molecular weight (MW_{avg}) was calculated by multiplying the normalized intensity of each peak by the nominal mass of that peak, summing all of the products, and dividing by the sum of the relative intensities of all of the peaks:

$$MW_{avg} = \frac{[RI(m/z\ 372) \times 372] + [RI(m/z\ 358) \times 358] + [RI(m/z\ 344) \times 344] + \ldots}{RI(m/z\ 372) + RI(m/z\ 358) + RI(m/z\ 344) + \ldots.}$$

This value was computed for each of the five spectra acquired per sample, and the five molecular weights were averaged. Scatter in the data is noted, however a distinct trend is established in which an increase in the degradation of the dye, i.e., a decrease in the average molecular weight, occurs over time. The use of MW_{avg} lends some physical meaning to the experiment. For instance, when the dye is initially deposited on paper, its average molecular weight would be nearly 372 Daltons, since it is essentially only crystal violet. If a sample is analyzed that shows an average molecular weight of 364 Daltons, it is understood that the degradation products are dominating the spectrum, indicating that the dye has degraded. The lower MW_{avg} limit for this experiment is 288 Daltons, which would occur if all of the C^+Me_6 were converted to C^+H_6. We have not yet found any naturally aged samples in which degradation has been this extensive. Figure 2.5 shows that the average molecular weight falls to 361 Daltons following 450 minutes of UV irradiation.

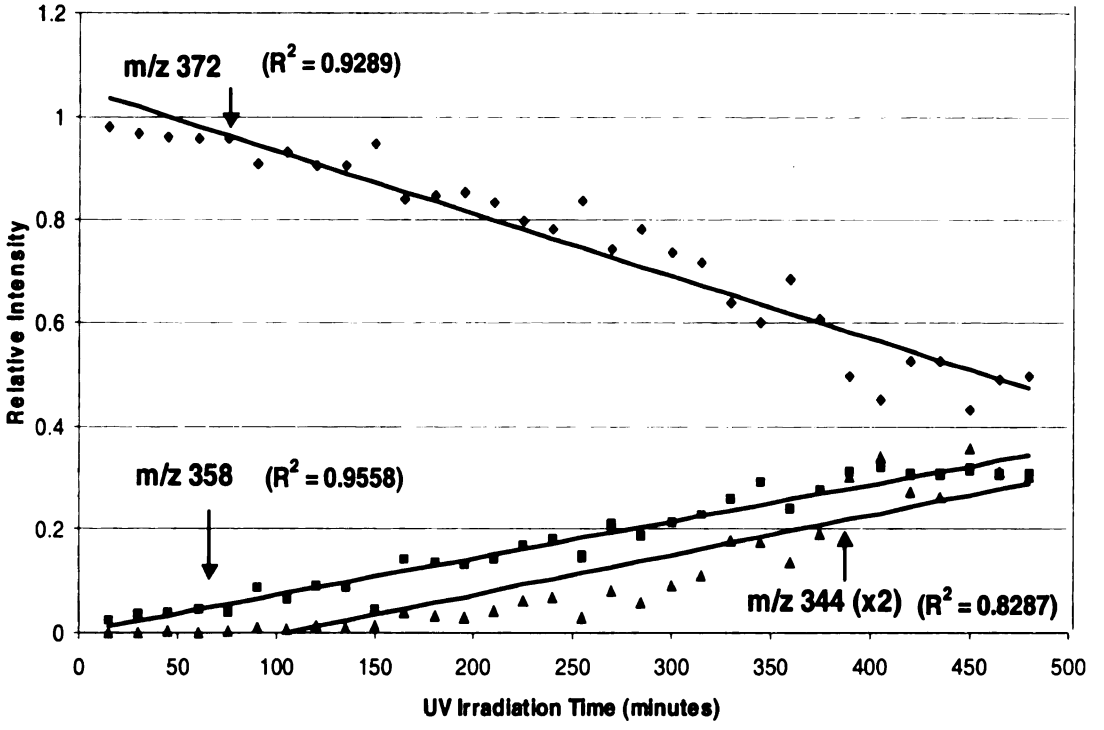

Figure 2.4. UV accelerated aging study data for new Bic black ballpoint pen ink on printer paper: a plot of the relative intensity of the m/z 372, 358, and 344 (x2) peaks versus irradiation time

Similar dye degradations occur naturally. In order to relate the UV accelerated aging curve in Figure 2.5 to aging which occurs naturally, a natural ink aging curve (Figure 2.6) was constructed using a set of controlled ink library samples from Speckin Forensic Laboratories, Okemos, MI. The samples were written with the same pen, on the same paper, and stored under the same conditions, in the dark. Again, from the LDMS spectra, the average molecular weights were computed. According to the UV accelerated aging curve prepared under the outlined experimental conditions, 500 minutes (8.3 hrs) of UV irradiation degraded methyl violet to an average molecular weight of approximately 360 Daltons. Referring to the straight line fit of the controlled natural aging data (Figure 2.6), an average molecular weight of 360 Daltons is equivalent to 52 months of natural

aging for this particular ink and paper. By combining this information in Figures 2.5 and 2.6, it appears that 500 minutes of UV irradiation (at the conditions used here) would age a document by approximately 52 months (~1560 days). Therefore, in this particular study, for every hour of UV irradiation, the document was aged roughly 187 days. This compares favorably with the initial estimate of 182 days per hour determined from the initial data shown in Figure 2.3.

A comment should be made concerning the linearity of the two best fit lines in Figures 2.5 and 2.6. The linear least squares fit to the data in Figure 2.5 has an R^2 value of 0.8845. The R^2 value is a measure of the strength of the linear relationship. The closer the R^2 value is to unity, the stronger the relation. The linear regression line or the data in Figure 2.6 has an R^2 value of 0.6331, indicating that the data generated during the UV accelerated aging study correlated better to a straight line fit than the data accumulated from the controlled natural aging study. This is not unexpected considering the time frame of the experiments. The UV accelerated aging study was completed in the matter of hours, whereas the controlled natural aging study occurred over ten years. During the UV accelerated aging study, variables affecting the aging process, such as temperature, lighting, and humidity fluctuations, were minimal, resulting in a more constant rate of aging.

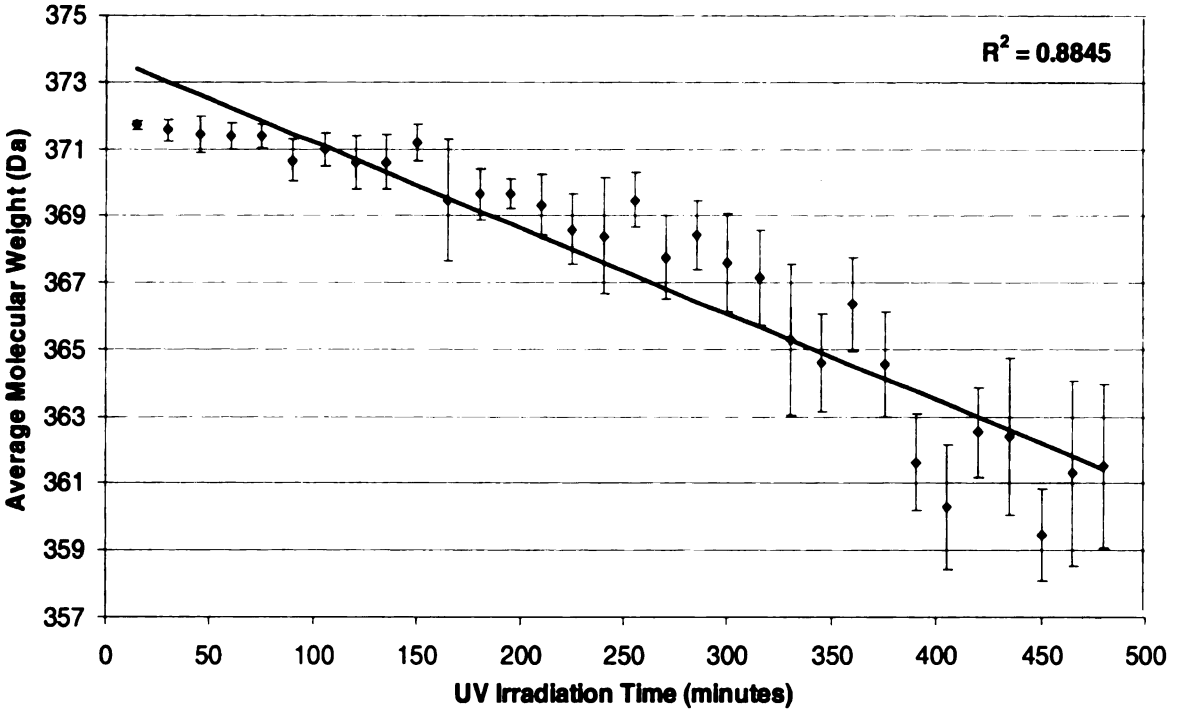

Figure 2.5: UV accelerated aging study data for new Bic black ballpoint pen ink on printer paper: a plot of the average molecular weight of the dye, methyl violet, versus minutes of UV irradiation (32).

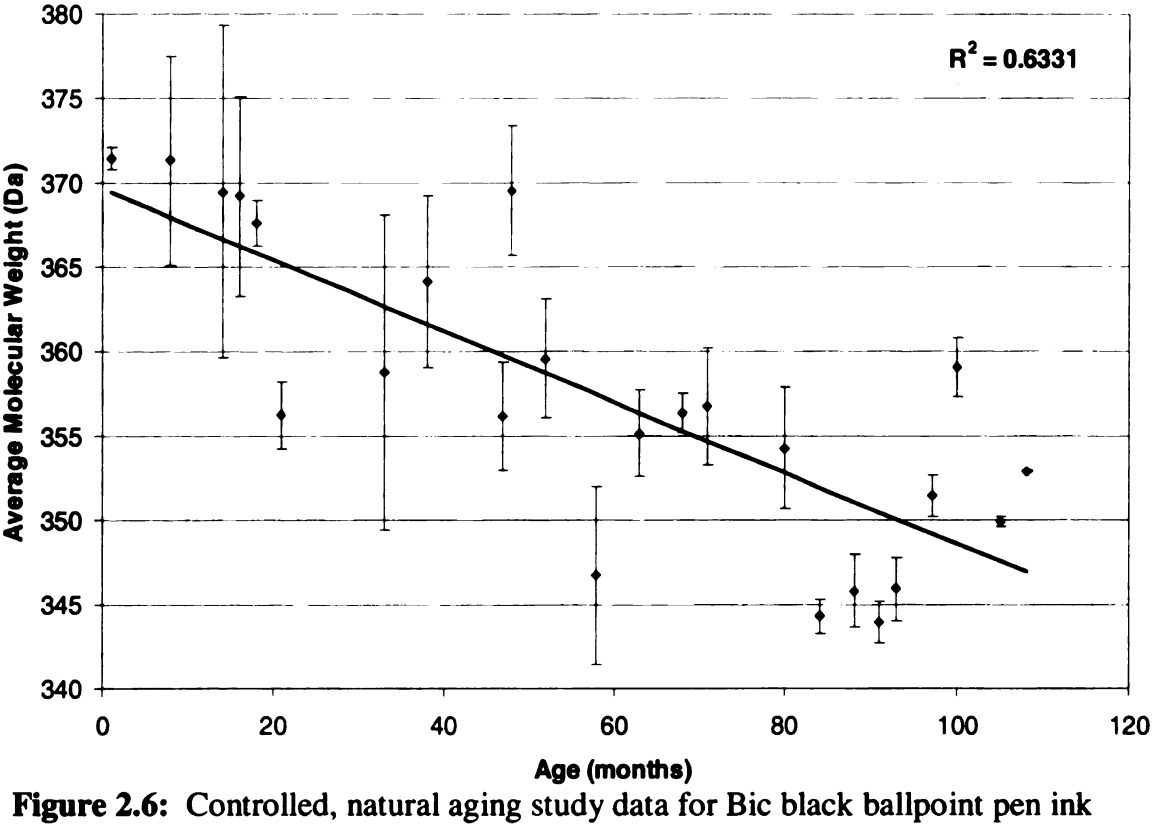

Figure 2.6: Controlled, natural aging study data for Bic black ballpoint pen ink on printer paper: a plot of the average molecular weight of the dye, methyl violet, versus the age of the document (32).

Identification of Watercolor Dyes (Unknown Dye Composition)

Artists' watercolor paints are historically known to fade, which is an indication of dyes degrading. Consequently, we had hoped to be able to apply the experimental methods developed in the analysis of methyl violet in ink, to the analysis of organic dyes in paint. A box of Niji watercolors (Yasutomo & Co., San Francisco, CA) was purchased containing the colorants labeled white, carmine, vermilion, lemon yellow, chrome green, viridian, cobalt blue, Prussian blue, yellow ochre, burnt sienna, burnt umber, and ivory black. The laser desorption mass spectra of a select number of these colorants (lemon yellow, viridian, chrome green, Prussian blue, carmine, and vermilion) will be shown and discussed. The dye compositions of these colorants were unknown. The results of accelerated aging and environmental studies performed on each colorant will also be discussed.

Cobalt Blue

The positive and negative ion mass spectra of cobalt blue are shown in Figure 2.7. The peak at m/z 575 in the positive ion mass spectrum represents the molecular ion, M^+, for copper phthalocyanine (pigment blue 15 – PB 15). Valued by artists for its bright blue-green color, copper phthalocyanine has a relatively high ASTM rating of II. Shankai *et al.* have previously reported the use of MALDI to analyze metal phthalocyanines, and do show that M^+ ions can be formed (38). Furthermore, Conneely *et al.* employed MALDI MS and ESI MS to analyze sulfonated copper phthalocyanine dyes in negative ion mode (39). The isotopic distribution is consistent with the formula $C_{32}N_8H_{16}Cu$, and is dominated by the presence of a copper atom, which has abundant

^{63}Cu (100%) and ^{65}Cu (44.57%) isotopes. In our experience with organic dyes used in ballpoint pen inks, cationic dyes such as methyl violet are detected in positive ion mode and anionic dyes, such as solvent black 29, are detected in negative ion mode (30). A response in both positive and negative ion modes indicates the presence of a neutral dye, of which copper phthalocyanine is an example. It forms an M^+ peak in positive ion mode (m/z 575), and an $[M-H]^-$ peak in negative ion mode (m/z 574).

Figure 2.8 shows positive and negative ion spectra of an aqueous solution of copper phthalocyanine (Aldrich), applied to paper. The spectra confirm the assignments in Figure 2.7.

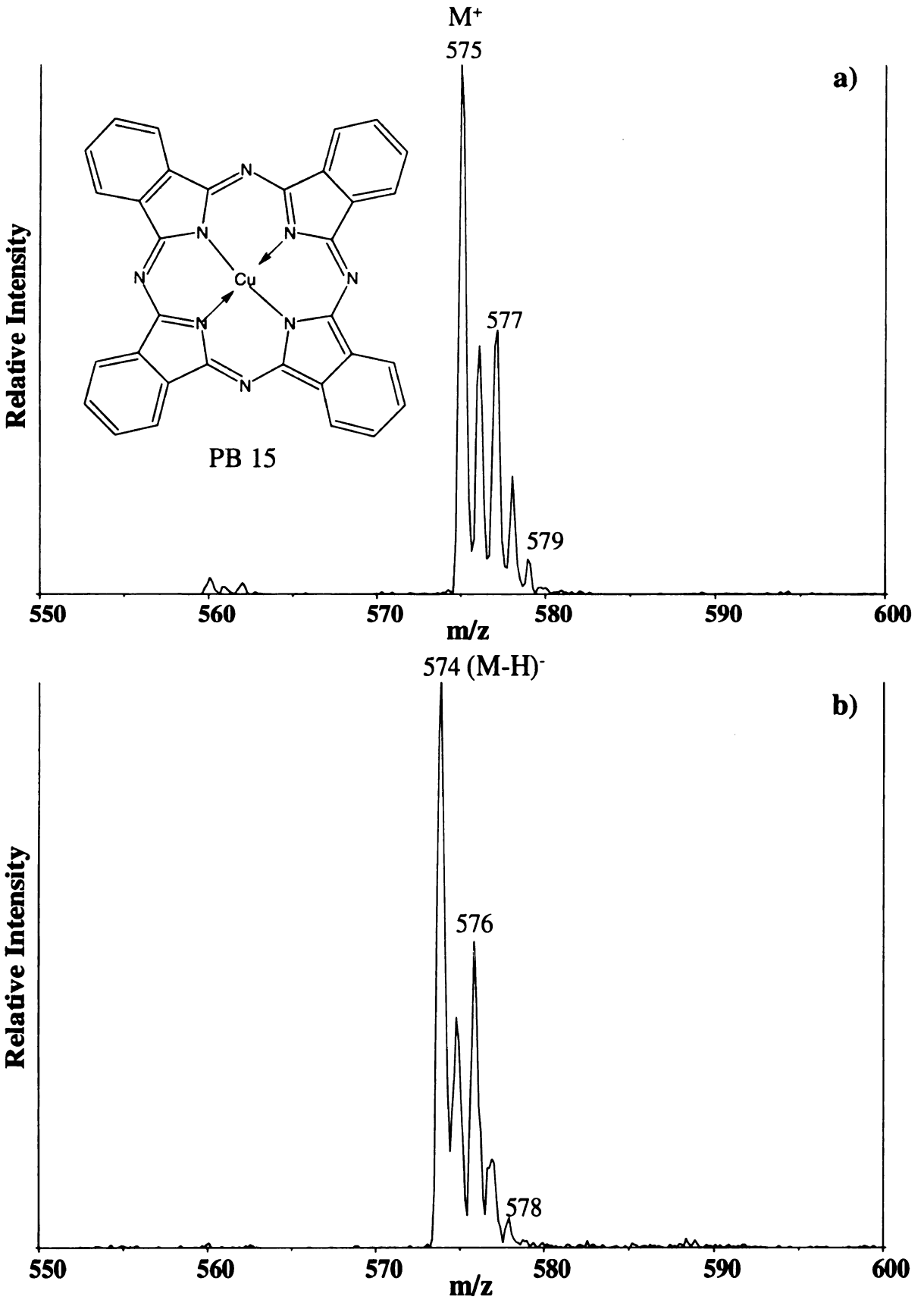

Figure 2.7: Cobalt Blue (Niji Watercolors): a) the partial positive ion LD mass spectrum; b) the partial negative ion LD mass spectrum

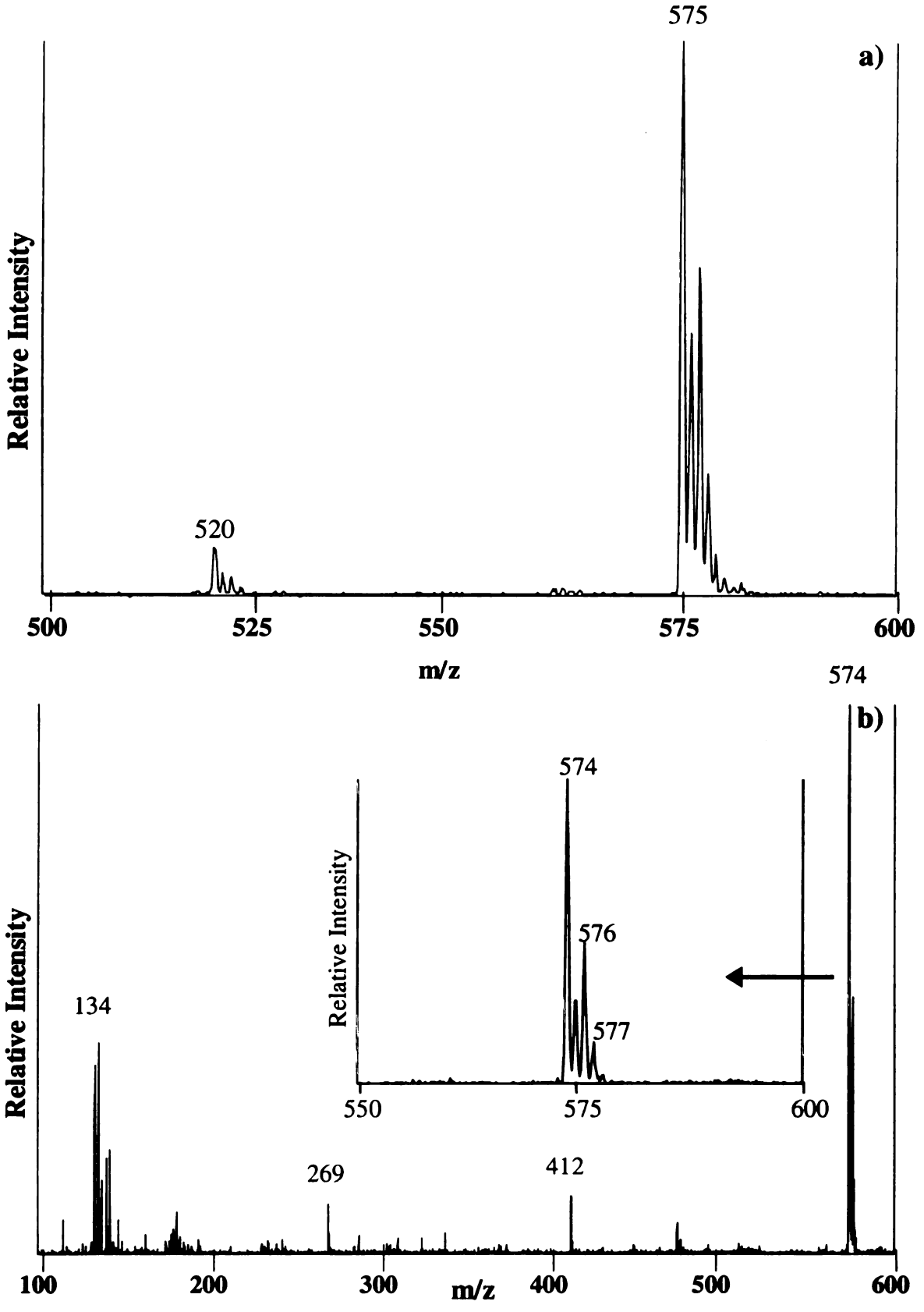

Figure 2.8: Copper phthalocyanine (Aldrich): a) the partial positive ion LD mass spectrum; b) the partial negative ion LD mass spectrum

Prussian

H

While ir

phthalo

mass sp

in the p

ion ma

respect

positiv

sugge

reache

the pr

is kn

be ad

the c

Prussian Blue

Historically, Prussian blue refers to the inorganic colorant ferric ferrocyanide. While iron blues were used since the early 1700s, until about 1970, copper phthalocyanine blue is now often used in their place (40). The positive and negative ion mass spectra of Prussian blue (Niji) are shown in Figure 2.9. Evidence of PB 15 appears in the positive ion mass spectrum at m/z 575 (Figure 2.9a) and at m/z 574 in the negative ion mass spectrum (Figure 2.9b). The cluster of peaks represent the M^+ and $[M-H]^-$ ions, respectively. The additional higher mass peaks in Figure 2.9 are noteworthy. In the positive ion mass spectrum, the peak at m/z 609 is 34 mass units higher than m/z 575, suggesting that a H atom has been replaced by a Cl atom. The same conclusion is reached for the next cluster. Negative ion m/z values and isotopic distributions confirm the presence of a mixture of copper phthalocyanine and copper chlorophthalocyanines. It is known that such compounds can be modified in a number of ways. Sulfate groups can be added to change the color (41). Additionally, chlorination of the compound will vary the color (produce a greener shade), as well as increase the dye's solubility (41).

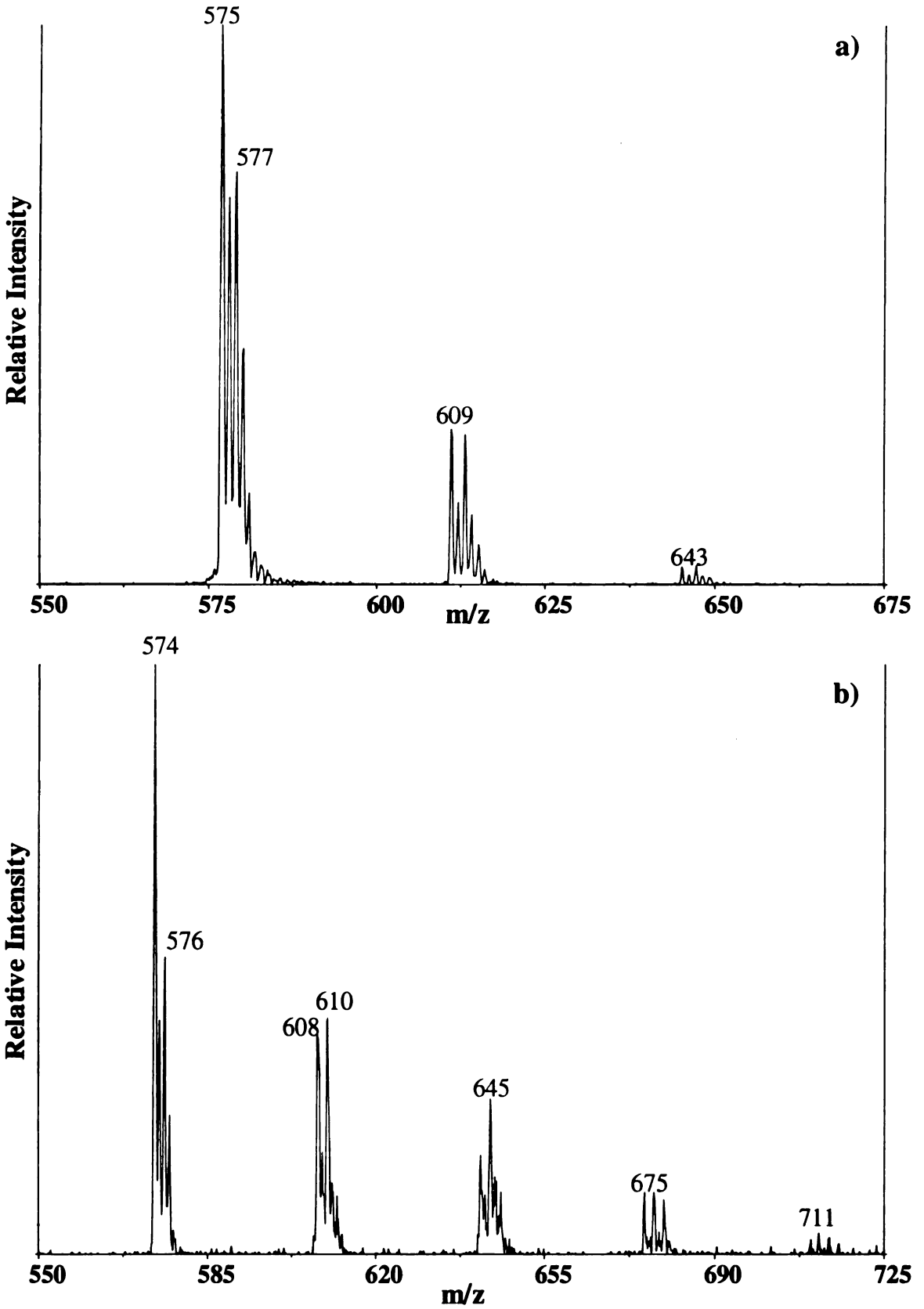

Figure 2.9: Prussian Blue (Niji Watercolors): a) the partial positive ion LD mass spectrum; b) the partial negative ion LD mass spectrum

Lemon Yellow

If an artist, a century ago, had selected a lemon yellow colorant, he/she would have chosen either a barium or strontium chromate pigment. Both Ba and Sr have unique isotopic patterns, which do not appear in the positive or negative ion LD mass spectra of this lemon yellow (Figure 2.10). Many more peaks are observed in the mass spectra, when compared to the spectra of Cobalt blue and Prussian blue. This may indicate the presence of multiple colorants in the paint mixture, or perhaps the presence of fragment ions. Fortunately, there are clues present in both the positive (Figure 2.10a) and negative ion (Figure 2.10b) mass spectra, which help to narrow down the large number of yellow dye possibilities.

In mass spectrometry, there are a few general steps to follow when interpreting a mass spectrum. For example, the peak with the largest m/z value is typically the molecular ion (or protonated molecule), unless isotopic peaks are present. Thus, in the positive ion mass spectrum (Figure 2.10a), the cluster of peaks around m/z 395 may possibly be representing the intact dye molecule. The next step is to analyze the pattern, to determine if it is consistent with any known isotopic patterns. The cluster of peaks at m/z 395 is not completely resolved, however there appears to be three peaks present, each separated by two mass units, in a 9:6:1 ratio. As was discussed in the Isotopic Pattern Analysis section in Chapter One, this pattern is characteristic of a molecule containing two Cl atoms. Additionally, there are numerous lower mass peak clusters which have two peaks present, separated by two mass units, in a 3:1 ratio, indicating the presence of only one Cl atom. Therefore, the lower mass peaks potentially represent fragment ions.

What is known thus far about the yellow dye? If the dye has a molecular weight of approximately 395 mass units, it must contain a few aromatic rings, in order to absorb UV light. The dye molecule has two Cl atoms present (70 mass units). It is also noted that the peaks at m/z 395 are not the most intense peaks in the mass spectrum. Consequently, if the lower mass peaks are indeed fragments ions, the structure of this dye molecule is not very stable (in contrast to copper phthalocyanine). Therefore, unstable functional groups, such as azo linkages (N=N), may be present. At this point, it is difficult to derive the exact dye structure from the information available in the mass spectrum. However, all of these clues can be used to perform a more efficient literature search for the dye's structure.

In the positive ion mass spectrum (Figure 2.10a), the cluster of peaks at m/z 395 have been identified as representing pigment yellow 3 (PY 3). The structure for PY 3 is shown in the inset of Figure 2.10b. It is commonly known as arylide yellow 10G, but may also be found listed as Hansa Yellow Light. It has been assigned an ASTM rating of II, and is included on the ASTM approved pigments for watercolors (42).

Like copper phthalocyanine, PY 3 is a neutral dye and has a molecular weight of 394 Da. However, a different trend is observed in the mass spectra, meaning that we do not observe simply the M^+ and $[M-H]^-$ ions in positive and negative ion modes, respectively. Instead, there is an overlap of peaks representing the M^+ (m/z 394) and $[M+H]^+$ (m/z 395) ions in positive ion mode. The presence of sodium and potassium adduct ions at m/z 417 $[M+Na]^+$ and 433 $[M+K]^+$, lend support to these assignments. Likewise, in the negative ion mass spectrum (Figure 2.10b), an overlap of peaks is observed representing M^- (m/z 394) and $[M-H]^-$ (m/z 393) ions. Returning to the positive

ion mass spectrum (Figure 2.10a), a number of the remaining peaks have been identified as fragment ions, suggesting the presence of only one dye. The positive fragment ion peak assignments are listed in Table 2.3. Only one fragment ion (m/z 171) is present in the negative ion mass spectrum. The peaks have a pattern consistent with the analyte containing one Cl atom. At this point it is unclear whether it is related to the fragment ion at m/z 170 in the positive ion mass spectrum. The remaining, unidentified peaks in the positive ion mass spectrum may possibly be products of rearrangement reactions or they may simply be due to impurities (such as reactants in the synthesis of PY 3) in the mixture. Considering the structure of the dye, the appearance of several fragment ions is not surprising. Unlike copper phthalocyanine, PY 3 is not composed primarily of fixed aromatic rings. Instead, it has a number of single bonds, which could be easily broken. Additionally, PY 3 is a different kind of molecule than methyl violet, and is expected to be less stable.

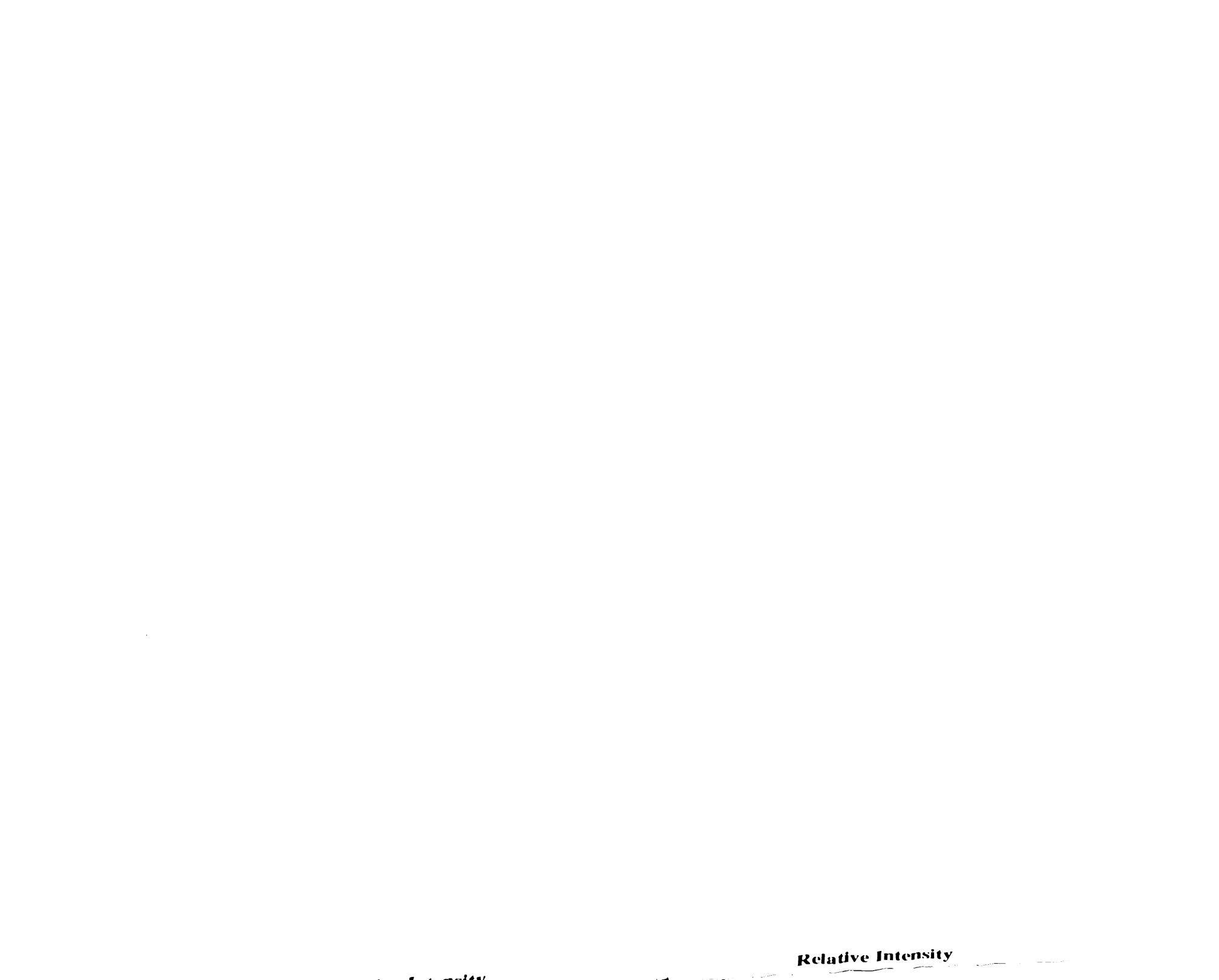
Relative Intensity

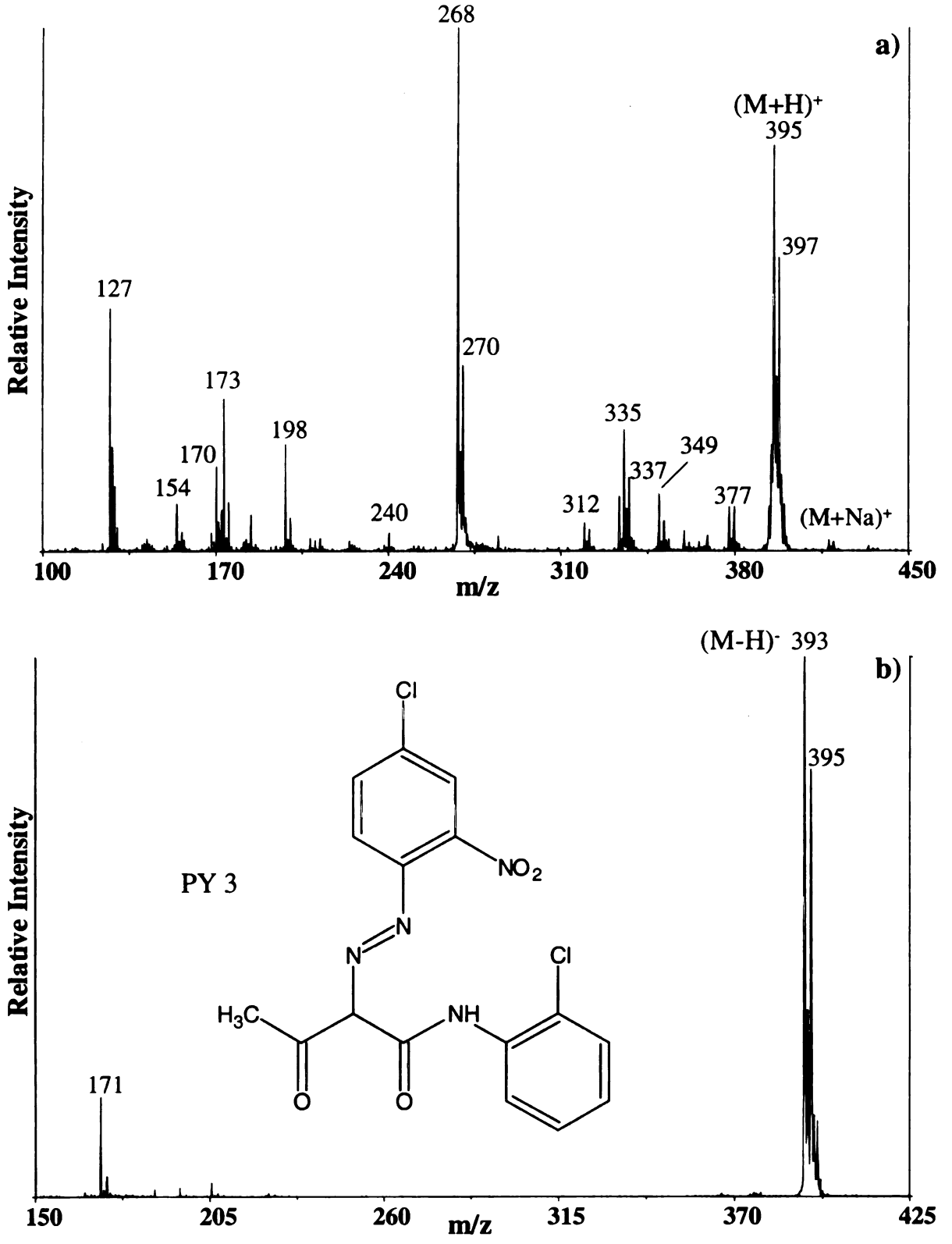

Figure 2.10: Lemon Yellow (Niji Watercolors): a) the partial positive ion LD mass spectrum; b) the partial negative ion LD mass spectrum

Fragment Ion	m/z
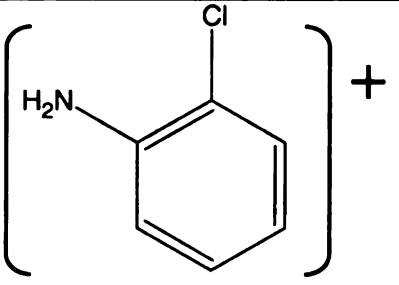	127
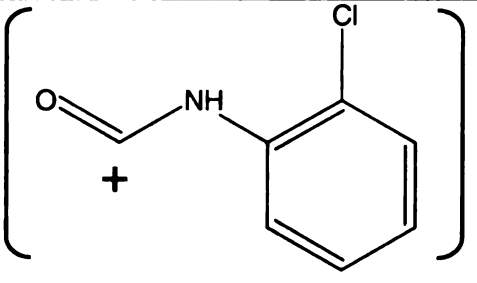	154
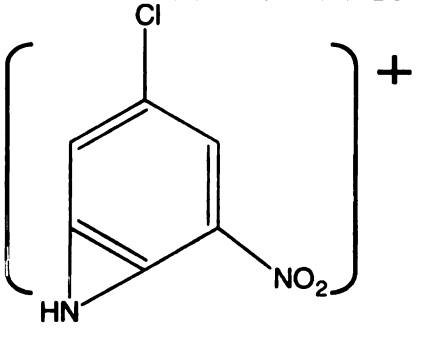	170
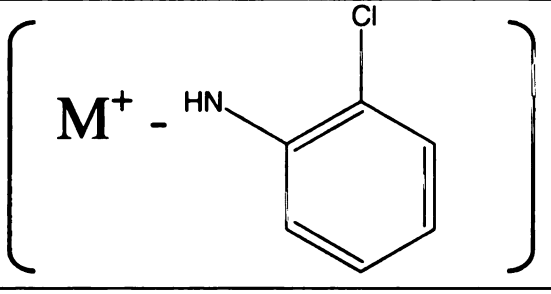	268
$[M - NO_2 - CH_3 + H]H^+$	335
$[M - NO_2]H^+$	349

Table 2.3: PY 3 positive fragment ions.

Viridian (Green)

Viridian is a green colored pigment, historically identified as a hydrated oxide of chromium ($Cr_2O_3 \cdot 2H_2O$) (43). However, the positive and negative ion LD mass spectra of this viridian, shown in Figure 2.11, suggest the presence of organic colorants. Clusters of peaks in the positive ion mass spectrum (Figure 2.11a) at m/z 395, 268, 154, etc. and at m/z 393 and 171 in the negative ion mass spectrum (Figure 2.11b), confirm the presence of PY 3 in the mixture. Green colorants may either be a pure green compound or a mixture of blue and yellow colorants. Since there is a yellow dye present, there may be evidence of a blue pigment somewhere in the mass spectra. Additional peaks are noted in the positive ion mass spectrum at m/z 1129, 1092, and 1059, which did not appear in the lemon yellow spectra. These peaks are separated by 34 mass units, suggesting that a series of Cl atoms are being replaced by H atoms. The dye has been identified as phthalocyanine green (pigment green 7 - PG 7) and the structure is shown in the inset of Figure 2.11a. PG 7 has the same base structure as PB 15, however it is completely chlorinated, resulting in the green color. Both e^- donating and e^- withdrawing groups can be added to Cu-phthalocyanine to shift the color to either the red or the blue. The structure is stable and fragment ions are not expected. The dye is known for its high tinting strength, meaning that only a small quantity of the colorant is required to produce a bright green shade, and has earned an ASTM rating of I (42).

Peaks representative of deprotonated PG 7 molecules are noted in the negative ion mass spectrum. There was no evidence of a blue dye in the paint mixture, suggesting that PY 3 was included to alter the green shade of PG 7. However, it is important to note that $(Cu_xCl_y)^-$ ions were identified in negative ion mode, based on their isotopic patterns. An

aqueous solution of $[Cu(H_2O)_4]^{2+}$ ions (blue) and $[CuCl_4]^{2-}$ ions (yellow) are green (44). However, this combination is not typically classified as an artist's water colorant.

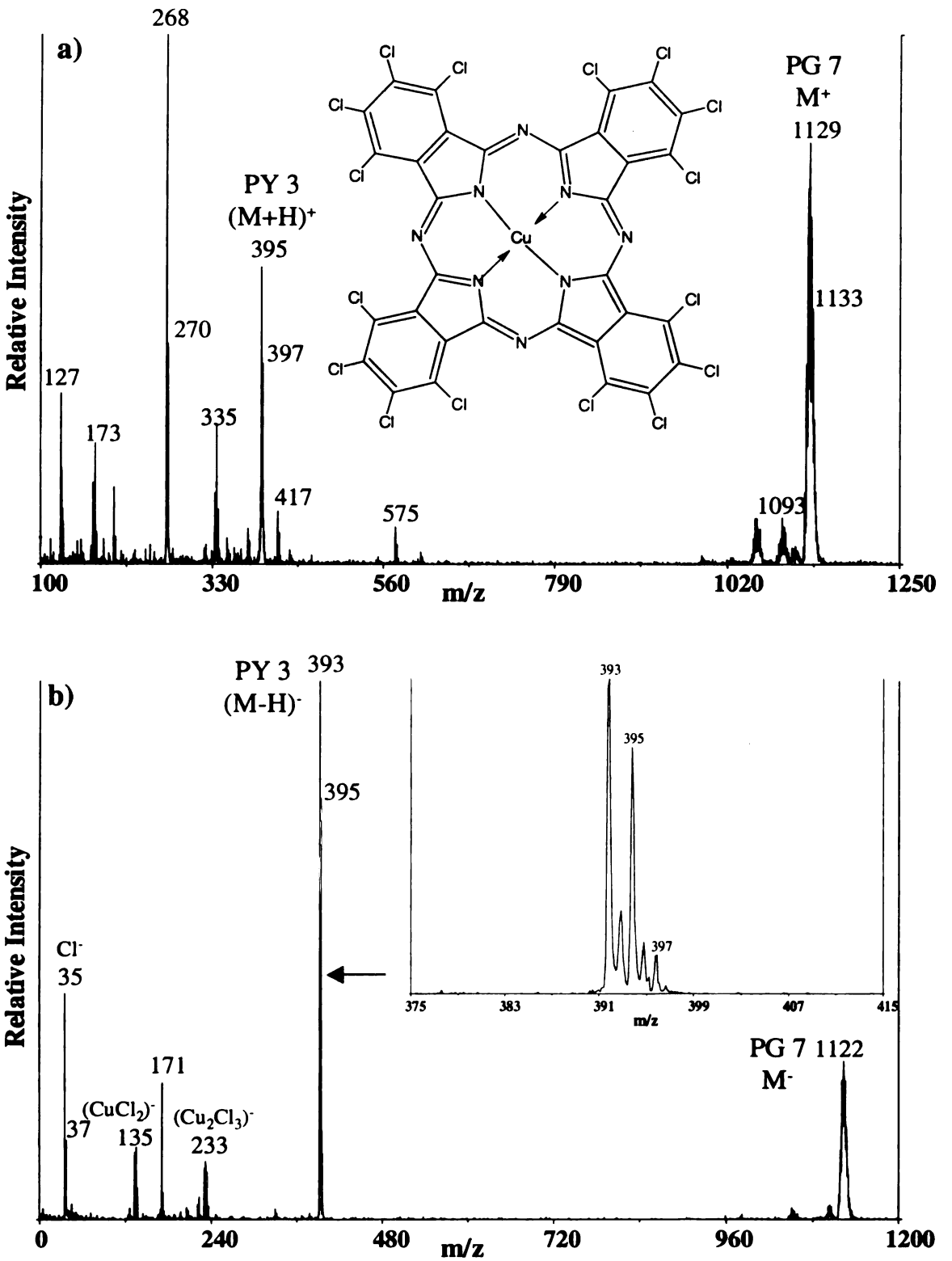

Figure 2.11: Viridian (Niji Watercolors): a) the partial positive ion LD mass spectrum; b) the negative ion LD mass spectrum

Carmine (Red)

True carmine is associated with a lake pigment. As described earlier, a lake is a colorant prepared by precipitating a transparent organic dye onto an inorganic support (45). In the case of carmine lake (Chapter 3), the dye is carminic acid, and the inorganic base is typically alumina (Al_2O_3). The positive and negative ion LD mass spectra of carmine (Niji) are shown in Figure 2.12 and are not suggestive of real carmine. Thus far, the exact dye composition of this carmine (Niji) has not been determined. Fortunately, the mass spectra provide interesting clues, which help to characterize the dyes.

In the positive ion mass spectrum (Figure 2.12a), there are peaks present in the higher mass region (~ m/z 1129) indicative of PG 7. The assignment is confirmed with the presence of complimentary peaks in the negative ion mass spectrum (Figure 2.12b). The presence of PG 7 in the paint mixture was somewhat unexpected. The Wilcox Guide to the Best Watercolor Paints is a comprehensive source which characterizes and rates a large number of modern day watercolors produced by thirty different domestic and foreign colorant manufacturers (42). The book is divided into chapters based on color (i.e. red, yellow, blue, etc.). Each chapter is broken down into sections based on the generic name of the colorant (i.e. carmine, vermilion, etc.). The dye compositions of the watercolor paints were provided, when available. Although Niji Watercolors were not included in the text, we were able to develop an idea of which colorants were more commonly used in the paint formulations. In the specific case of carmine, only red dyes were employed. Occasionally, pigment violet 19 (PV 19) was included in a paint mixture to give the paint a more pinkish tone. Of the 28 different brands of carmine included in

the Wilcox Guide, not one was created using a green colorant, which is why the presence of PG 7 was unexpected.

Based on a literature search, we were looking for evidence in the mass spectra of any of the following pigment red colorants: PR 5, 9, 48:4, 83, 88, 112, 146, 170, 176, 178, and 264. The structures of a select number of these colorants are shown in Table 4, which illustrate the different classes of these dyes. Several of the PR dyes listed have the same basic structure, but differ in their substituents. Therefore, if we can determine how certain classes of dyes "behave" in the LDMS experiment, meaning whether they form molecular ions or fragment ions, we can establish patterns that will ultimately make the mass spectral interpretation process much easier. Unfortunately, none of the peaks in both positive and negative ion modes appear to have originated from any of the expected red dyes. However, the mass spectra are still informative.

The isotopic patterns of the peaks in the positive ion mass spectrum (Figure 2.12a) are not consistent with the analyte containing Cl, whereas some of the peaks in the negative ion mass spectrum are. In the positive ion mass spectrum, there are intense peaks present at m/z 284 and 368. It is unclear whether or not these peaks are representative of a colorant, or a component of either the colorant's vehicle or the paper. The peaks appear consistently in the spectra of carmine, however they have been noted sporadically in the spectra of other Niji watercolors (ie. Prussian blue). As will be discussed shortly, the peaks at m/z 284 and 368 become more apparent in the spectra of faded colorants. This may suggest that they are originating from the paper. Positive and negative ion mass spectra were obtained of the paper by itself (spectra not shown) (46), and do not contain peaks at m/z 284 or 368. However, a peak at m/z 284 was noted in the

positive ion mass spectrum of a different paper sample from a previous study (30). Consequently, the results of the paper study suggest that the peaks at m/z 284 and 368 may be originating from a vehicle component common to other Niji water colorants. Additionally, the peaks at m/z 284 and 368 appear to be the beginning and the end of a series of peaks separated by 28 mass units. The mass difference may be the result of the loss of consecutive C_2H_4 groups.


Relative Intensity

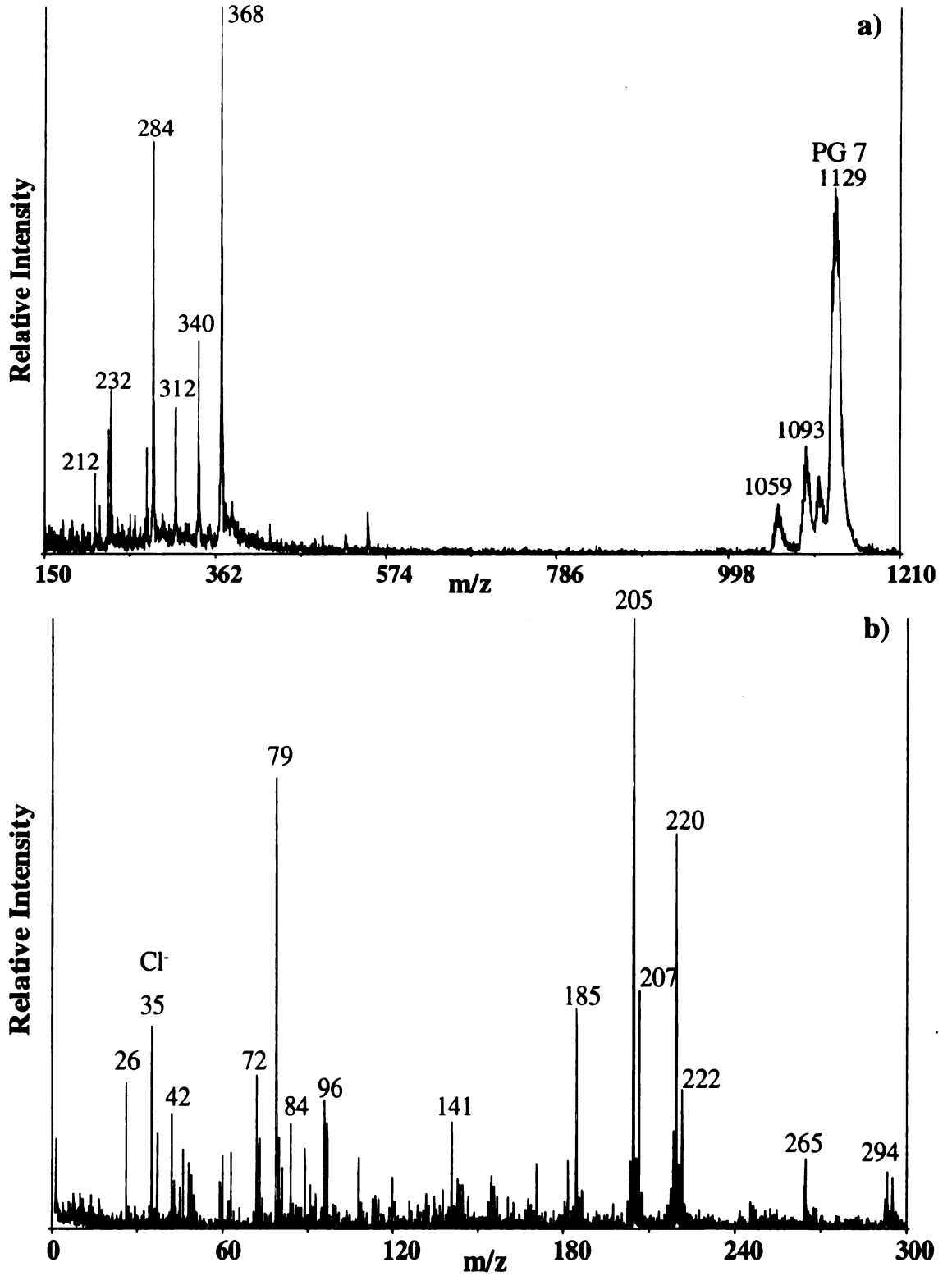

Figure 2.12: Carmine (Niji Watercolors): a) the partial positive ion LD mass spectrum; b) the negative ion LD mass spectrum

Structure	Name (MW)
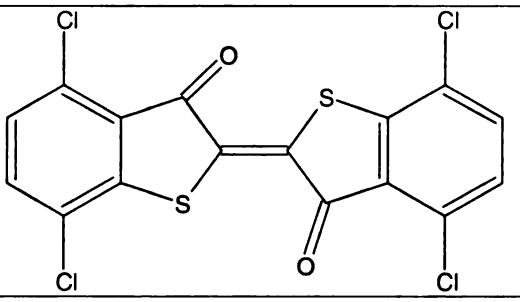	**PR 88 (434)**
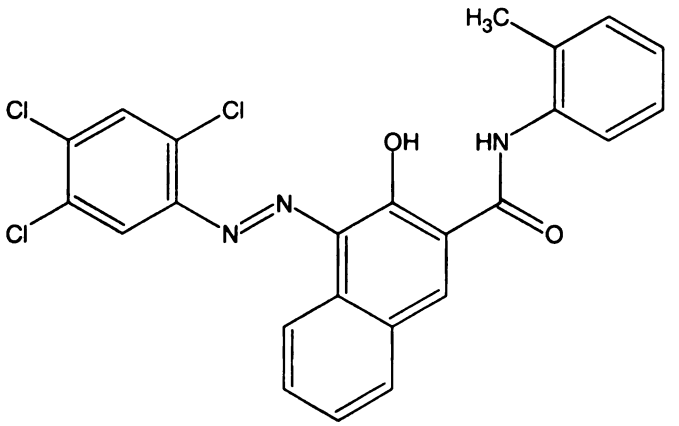	**PR 112 (484)**
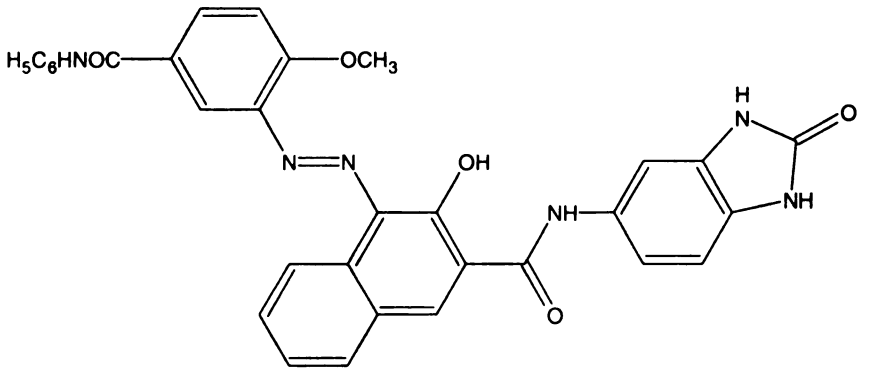	**PR 176 (573)**
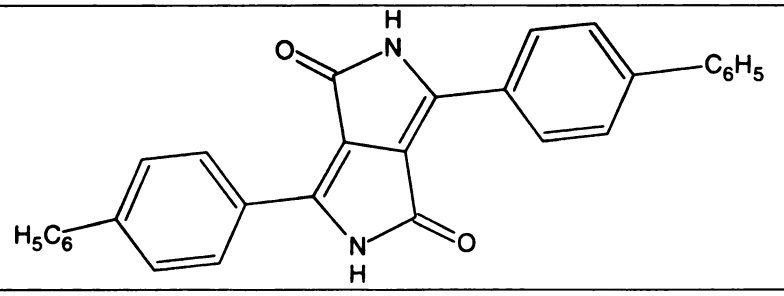	**PR 264 (440)**

Table 2.4: Structures of Pigment Red colorants typically found in carmine watercolors.

The clusters of peaks at m/z 205 and 220 in the negative ion mass spectrum (Figure 2.12b), have patterns consistent with a molecule containing one Cl atom, whereas the peaks at m/z 294 are characteristic of a molecule containing two Cl atoms. The peak at m/z 185 may be related to the ions represented at m/z 220. The peak is 35 mass units less than m/z 220, indicating the loss of a Cl atom, and lacks an isotopic pattern characteristic of Cl, which supports this claim. A cluster of peaks at m/z 463 (not shown) may represent ions containing 3 Cl atoms, however the pattern is not exact. The pattern may be affected by noise, considering the peaks are of such low intensity (~ 400 counts). Peaks representing Cl^- ions are noted at m/z 35 and 37.

Due to the noncomplimentary positive and negative ion mass spectra of carmine, there maybe more than one dye present in the carmine paint mixture, besides PG 7. The positive ion mass spectrum possibly suggests the presence of a non-chlorinated cationic dye, whereas the negative ion mass spectrum clearly shows evidence of a Cl-containing compound. Certainly, not all of the PR colorants were considered in this example, which may explain our inability to identify all of the dyes present. As will be explained in the case of vermilion, yellow and orange pigments were frequently used in combination with the red pigments. Consequently, the dye possibilities are numerous, and it was not our intention to devote the entire project to colorant identification, but to complete a survey at this point.

Vermilion (Red)

True vermilion will be discussed in detail in Chapter 4, however at this point it is important to know that the name refers to the compound mercuric sulfide (HgS). The positive and negative ion LD mass spectra of vermilion (Niji) are shown in Figure 2.13, and certainly do not show any evidence for the presence of Hg. Referring to the Wilcox Guide, the organic watercolor vermilion is typically composed of a mixture of red, orange, and yellow dyes. Both spectra are rich with information, but as in the case of carmine, the dyes remain unidentified. Complimentary peaks in both positive and negative ion modes are noted, indicating the presence of at least one (M_1) or two (M_1,M_2) neutral dyes. For instance a peak at m/z 620 appears in Figure 2.13a and a peak at m/z 619 is present in Figure 2.13b. The peaks may be representing M^+ and $[M-H]^-$ ions, respectively. The same is noted for m/z 431 (+) / m/z 430 (-), which indicates the presence of a second neutral dye (M_2). Additionally, due to the lack of Cl^- ions (m/z 35 and 37) in the negative ion mass spectrum, the dyes are apparently non-chlorinated, which significantly decreases the number of colorant possibilities.

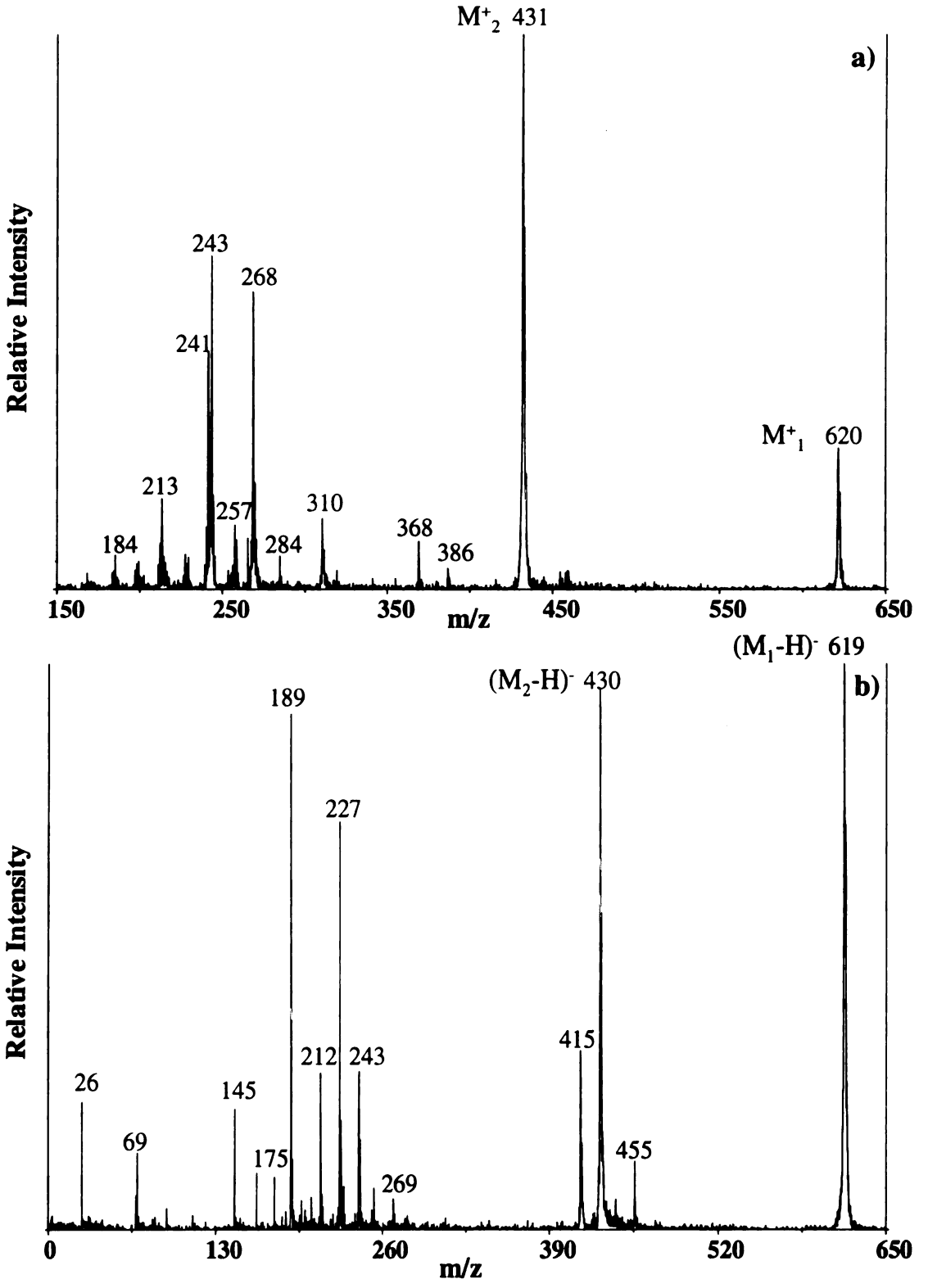

Figure 2.13: Vermilion (Niji Watercolors): a) the partial positive ion LD mass spectrum; b) the negative ion LD mass spectrum

Identification of Watercolor Dyes (Known Dye Composition)

Fortunately, many modern day artists' watercolor paints are sold in tubes with the dye composition provided on the label. The majority of the structures of these dyes can be found in Herbst and Hunger's Industrial Organic Pigments: Production, Properties, Applications (41). Consequently, the mass spectral interpretation process, in most cases, becomes much easier. As will be demonstrated in the following examples, the laser desorption mass spectra of colorants does not always correlate with the chemical composition found on the labels. In some instances only one of two components is detected. This does not necessarily mean that the second component is not present, it might simply mean that it is not detectable (does not absorb light efficiently at 337 nm) in the LDMS experiment, or it is present at a very low level. Other times, unexplainable peaks are generated which strongly suggest the presence of additional colorants not listed on the label. This may be an intentional omission to protect trade secrets.

The spectra of several of the colorants in Table 2.3 will be presented and discussed in this section. As stated in the introduction, these colorants were chosen, since they were known to be unstable and fade easily overtime. The colorants which will be discussed illustrate key points. Additionally, a few of the colorants not presented here, such as Hooker's Green and indigo, contained pigments such as PB 15 and PG 7, which were already presented and discussed in detail in the Niji watercolor examples. Rose madder lake will be presented in the following chapter on lakes, since the mass spectra of the colorant parallels the spectra of some of the lakes presented in the chapter.

Cadmium Red Hue 095

Cadmium Red Hue 095 (Winsor & Newton) is a mixture of PR 149 (Figure 2.14a) and PR 255 (Figure 2.14b). Perylene Red BL (PR 149) is an anthraquinone dye having a molecular weight of 598 Da, whereas Pyrrole Scarlet (PR 255) is categorized as an aminoketone diketopypyrolopyrrole, having a molecular weight of 288 Da. PR 149 has not been subjected to the ASTM lighfastness test, however PR 255 earned an excellent ASTM rating of I (42). The positive and negative ion LD mass spectra of Cadmium Red Hue 095 are shown in Figure 2.15. Theoretically, the mass spectral interpretation process should be easy, since the colorants are already known.

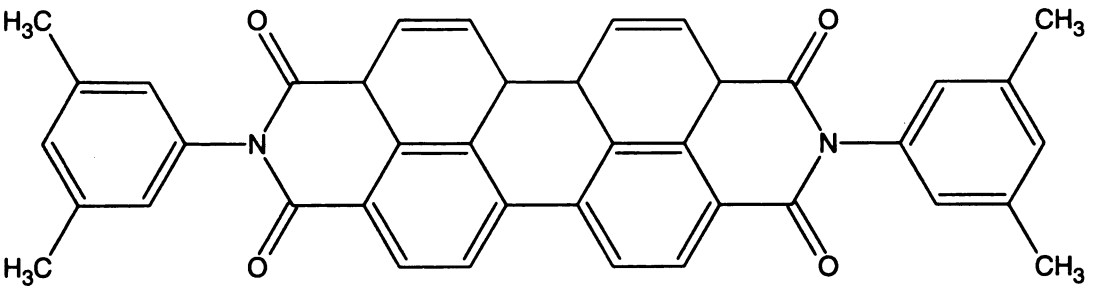

PR 149
(598 Da)

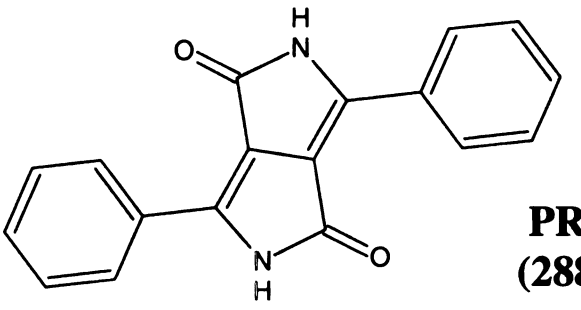

PR 255
(288 Da)

Figure 2.14: Structures of: a) PR 149; b) PR 255.

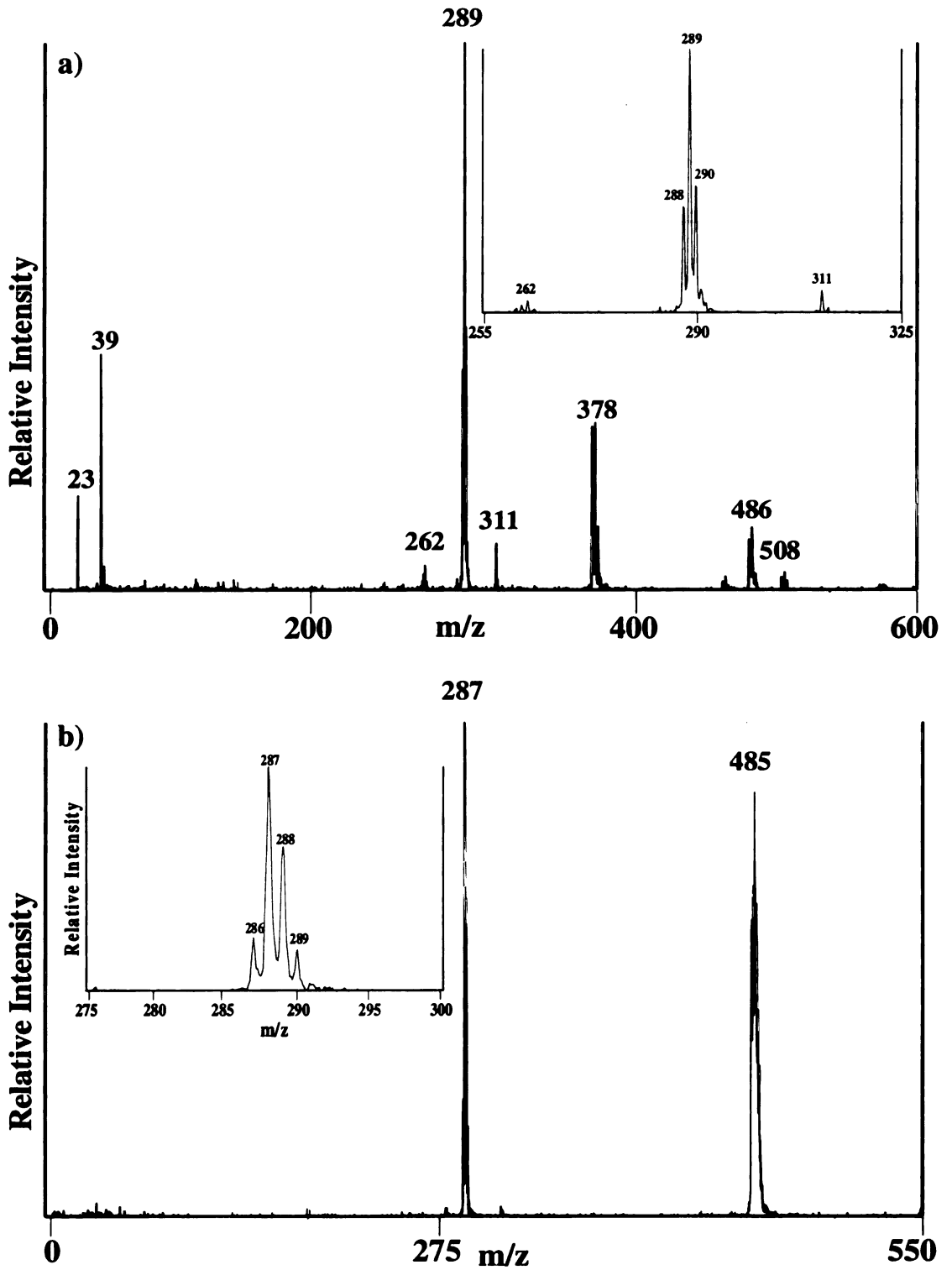

Figure 2.15: Cadmium Red Hue 095 (Winsor & Newton): a) the positive ion LD mass spectrum; b) the negative ion LD mass spectrum

In the positive ion mass spectrum, peaks are present in the m/z 288 region, representing the characteristic neutral dye overlap of the M^+ (m/z 288) and $[M+H]^+$ (m/z 289) peaks, for PR 255. The same is noted in the negative ion mass spectrum at m/z 287 $([M-H])^-$ and m/z 288 (M^-), also representing PR 255. The peaks are enlarged in the insets of the spectra, to observe the characteristic overlap. Intense clusters of peaks are noted at m/z 378 and 486 in the positive ion mass spectrum (Figures 2.16a, b) and at m/z 485 in the negative ion mass spectrum (Figures 2.16c). The isotopic patterns of these clusters suggest the presence of halogenated compounds, which neither PR 149 nor PR 255 are. Additionally, PR 149 has a molecular weight of 598 Da, and there are no peaks representing the intact dye molecule in either positive or negative ion modes. Considering the stable anthraquinone structure of PR 149, fragment ions are also not expected. Therefore, this is a specific example in which the mass spectra of a colorant does not coincide with the dye information provided on the label. There appears to be no evidence of PR 149 present in the mass spectra, however there are peaks possibly representing a second colorant not listed on the label.

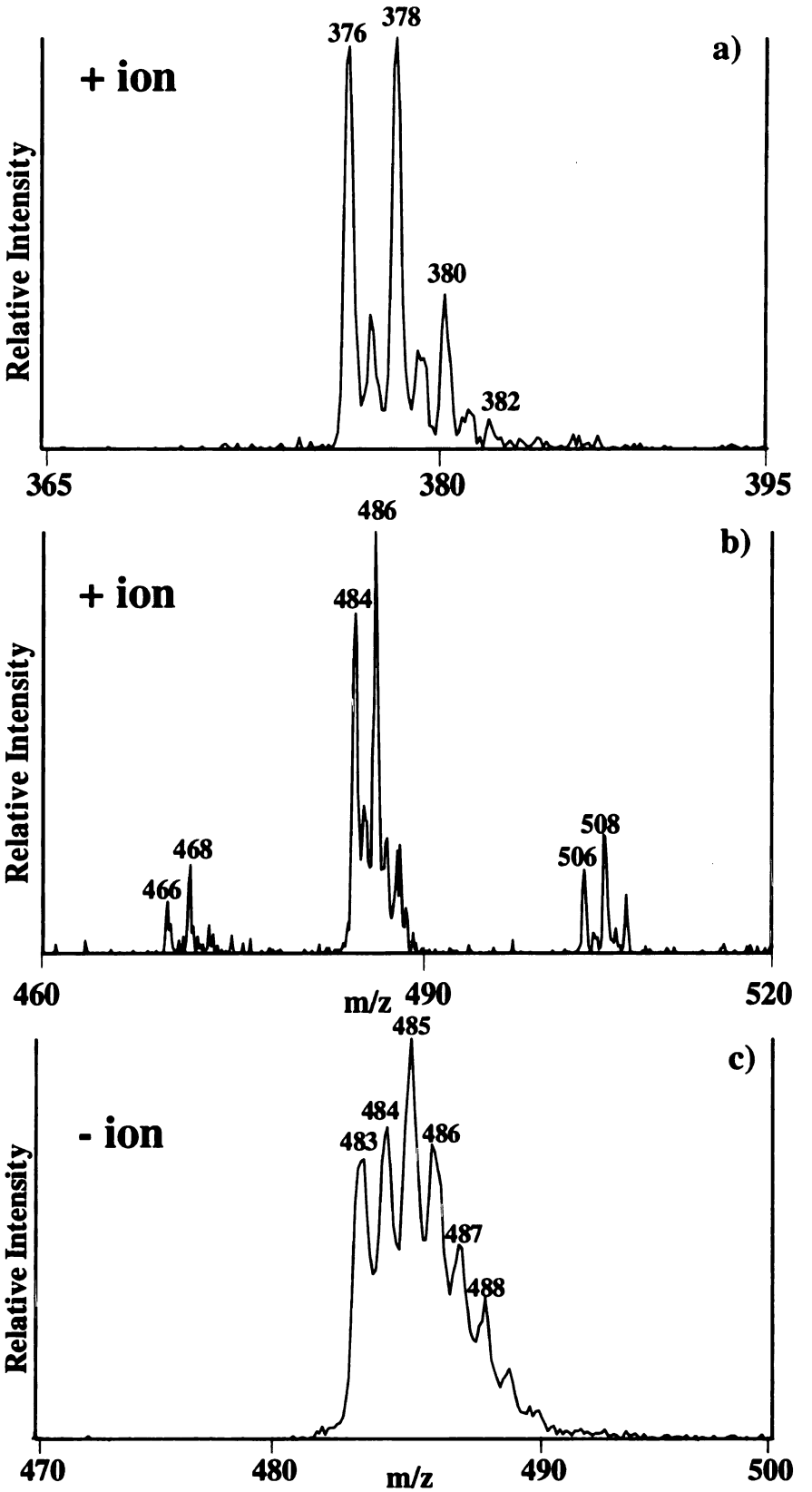

Figure 2.16: Enlarged regions of the Cadmium Red Hue 095 LD mass spectra: a) + ion, m/z 365-395; b) + ion, m/z 460-520; c) – ion, m/z 470-500).

Mauve (Dark Red)

Winsor & Newton's Mauve 398 contains the colorants PR 122 and PV 23RS, the structures of which are shown in Figure 2.17. PR 122 goes by the common name quinacridone magenta and is known to be initially resistant to light exposure. However, PR 122 is known to eventually fade, and has therefore earned an ASTM lightfastness rating of only III. Dioxazine purple (PV 23) is a carbazole dioxazine dye, and may take on either a blue (BS) or red shade (RS). The chemical distinction between the two foams is not apparent, however they have distinctly different ASTM lightfastness ratings. For instance, PV 23RS earns an ASTM rating of I, II, and III, when in a vehicle of oil, acrylic, and water, respectively. However, PV 23BS has been rated a IV, as a watercolor (42). The red shade is observed here.

Both of the colorants are represented in the positive (Figure 2.18a) and negative ion (Figure 2.18b) LD mass spectra of Mauve 398. PR 122 (340 Da – M_1) demonstrates the classic trend of the neutral dye, generating molecular ions, as well as protonated and deprotonated molecules in both the positive and negative ion mass spectra. Peaks representing the neutral losses of one and two methyl groups are noted at m/z 326 $[M\text{-}CH_3]^+$ and 311 $[M\text{-}2CH_3]^+$ are formed in both positive and negative ion mode. PV 23RS (M_2) behaves a little differently, though.

Peaks of relatively low intensity are present in the positive ion mass spectrum representing the molecular ions of PV 23RS (m/z 588). The PV 23RS dye molecule contains two chlorine atoms, which is reflected in the isotopic pattern observed at m/z 588 (enlarged in the inset of Figure 2.18a). The ratio is not exactly 9:6:1, however the presence of multiple elements skews the pattern. Additionally, the peaks are at such low

intensity, that noise may also be affecting the pattern. In the negative ion mass spectrum, peaks representing the loss of one (m/z 559) and two ethyl groups (m/z 530) are noted. These peaks maintain the 9:6:1 ratio, indicating that there was no loss of the Cl atoms. There is no evidence of the intact molecule.

The higher mass peaks at m/z 663 and 661 in the positive and negative ion mass spectra, respectively, are a mystery. Tentative assignments have been made. The isotopic patterns of these peaks do not indicate the presence of Cl, therefore it was assumed that they were due to some sort of polymerization, or reaction products involving PR 122. Possibly, two PR 122 molecules joined via an O bridge, accompanied by the loss of water. The resulting neutral species formed makes its presence known in a LDMS experiment by becoming protonated (+ ion mode) or deprotonated (- ion mode). If these assignments are incorrect, then there may simply be an additional colorant present in the paint mixture with a molecular weight of approximately 660 Da. The compound makes it presence known in both positive and negative ion modes, suggesting that it is a neutral species.

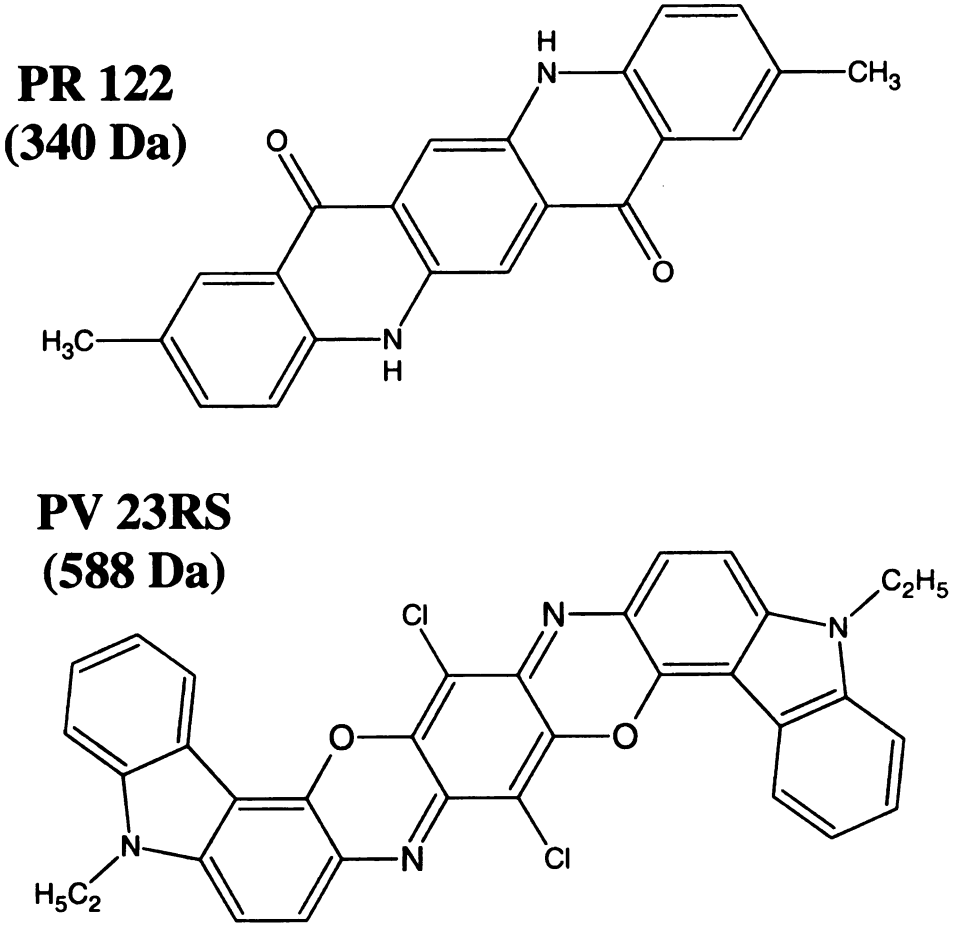

Figure 2.17: Structures of: a) PR 122; b) PV23RS.

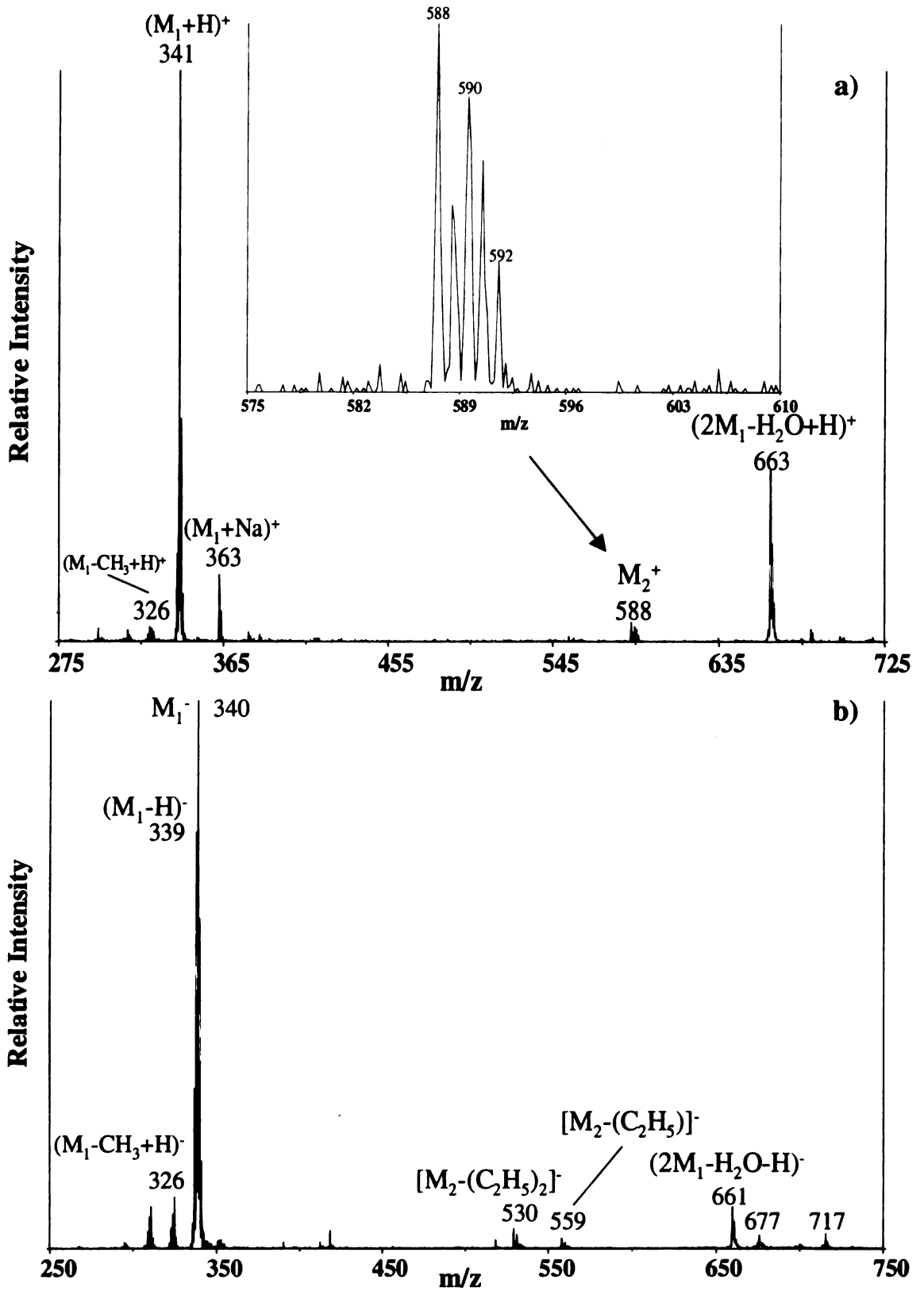

Figure 2.18: Mauve 398 (Winsor & Newton): a) the partial positive ion LD mass spectrum; b) the partial negative ion LD mass spectrum

Preliminary Light and Environmental Studies

The Niji watercolors were exposed to a variety of natural and artificial light conditions to induce fading. These included natural sunlight, UV light (254 nm), and light from a Hg lamp. In general, the colorants required longer exposure times to the light sources, as compared to those used to degrade methyl violet, before fading was evident. This indicated a higher degree of stability of the watercolor dyes. In most cases, such as Prussian blue, cobalt blue, lemon yellow, and viridian, the spectra obtained of the samples following light exposure (not shown) were the same as the initial spectra. Occasionally, low intensity, lower mass peaks appeared, but not consistently to suggest the presence of degradation products. Thus, they were assumed to be impurities in the sample. The most significant changes involved the red colorants. The vermilion watercolor will be discussed in detail.

The positive ion mass spectra of UV - aged vermilion 24 hours (Figure 2.19a) and aged with the Hg-lamp 10 hours (Figure 2.20a) appear to be relatively unaffected. One might question whether or not the peaks at m/z 310 and 368 are becoming more intense relative to the other peaks in the mass spectrum, however this was not a consistent observation when compared to other spectra obtained from the same sample. These peaks were also present in the positive ion mass spectrum of carmine. If they are truly becoming more intense in the mass spectrum as the colorant fades, it may suggest that the peaks are originating from the transparent vehicle, and are therefore not affected by light.

The positive ion mass spectrum of the sample that was faded naturally with sunlight (Figure 2.21a) is significantly different than the initial spectrum. Peaks representing the initial colorant have disappeared almost completely and the spectrum is

populated with peaks that seem to be unrelated to the dye. The peak at m/z 575 represents copper phthalocyanine, which is a component of the paper itself (explained in more detail in a later chapter). More work would need to be devoted to determining the degradation mechanism to identify these new peaks.

More changes are observed in the negative ion mass spectra. In both of the UV-exposed (Figure 2.19b) and Hg-lamp exposed (Figure 2.20b) samples, all but the peak at m/z 188 noticeably decreased in intensity, but relative to each other. The spectra are also noisier. The sample exposed to natural sunlight produced a negative ion mass spectrum in which the peaks in the m/z 430 and 619 regions decreased significantly, however the remainder of the peaks remained intense. The spectrum contains more noise, since the laser power needed to be increased significantly to obtain the spectrum.

From performing these fading experiments on the organic watercolor dyes, it seemed as though, as a dye fades (degrades), its degradation products are either too small and volatile, that they are simply removed by the vacuum system, or they are not able to absorb the energy of the laser (337 nm). The fact that some of the peaks decreased in intensity is an indication of the dye degrading. But what is happening to the dye? The chemistry of these reactions is poorly understood and the lack of identified degradation products confuses the issue. Based on these results, we decided to try different environmental conditions. Here we subjected the Winsor & Newton watercolors to pollutant gases, which included ozone, NO_2 and SO_2.


Relative Intensity

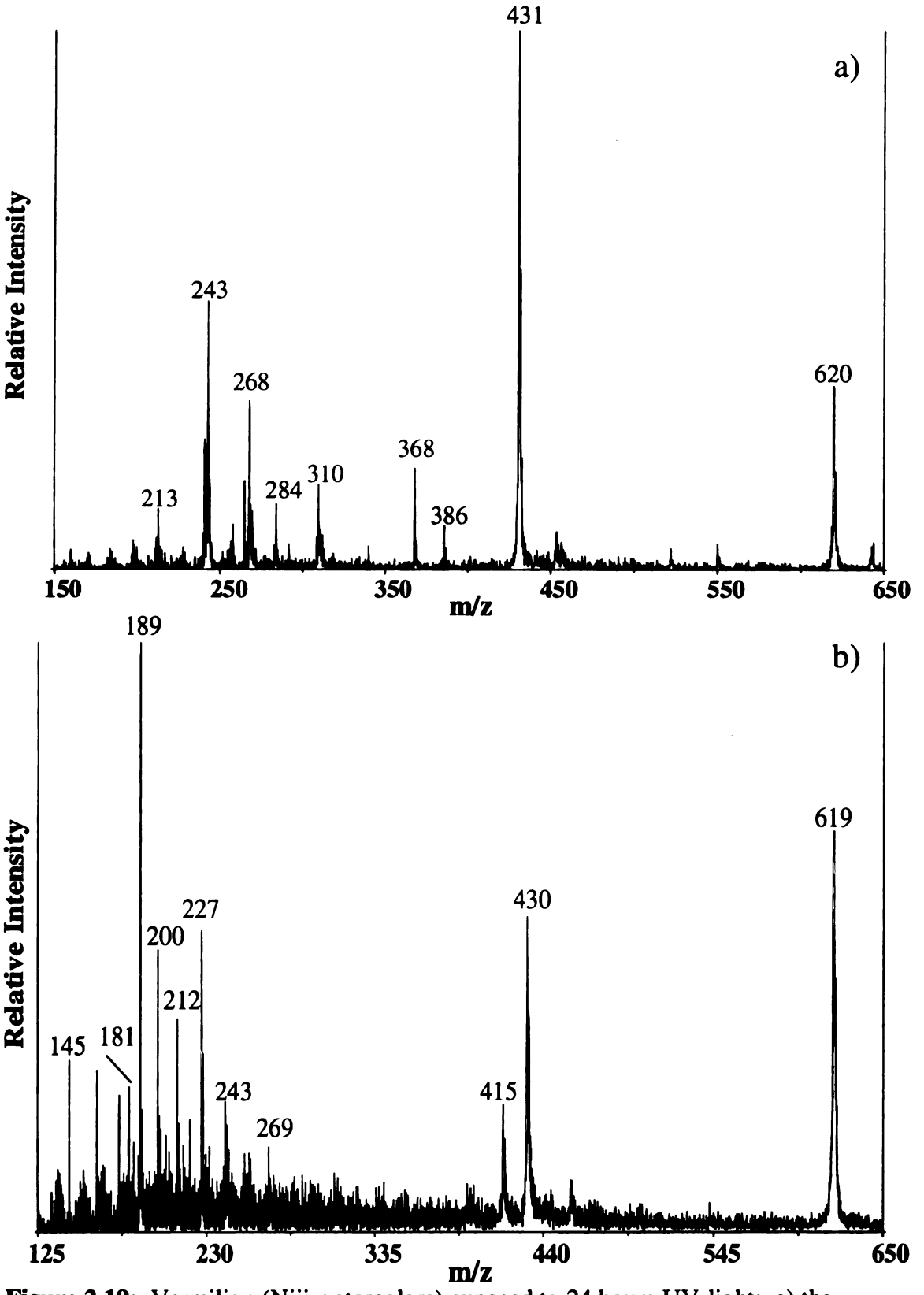

Figure 2.19: Vermilion (Niji watercolors) exposed to 24 hours UV-light: a) the partial positive ion LD mass spectrum; b) the partial negative ion LD mass spectrum

Figu

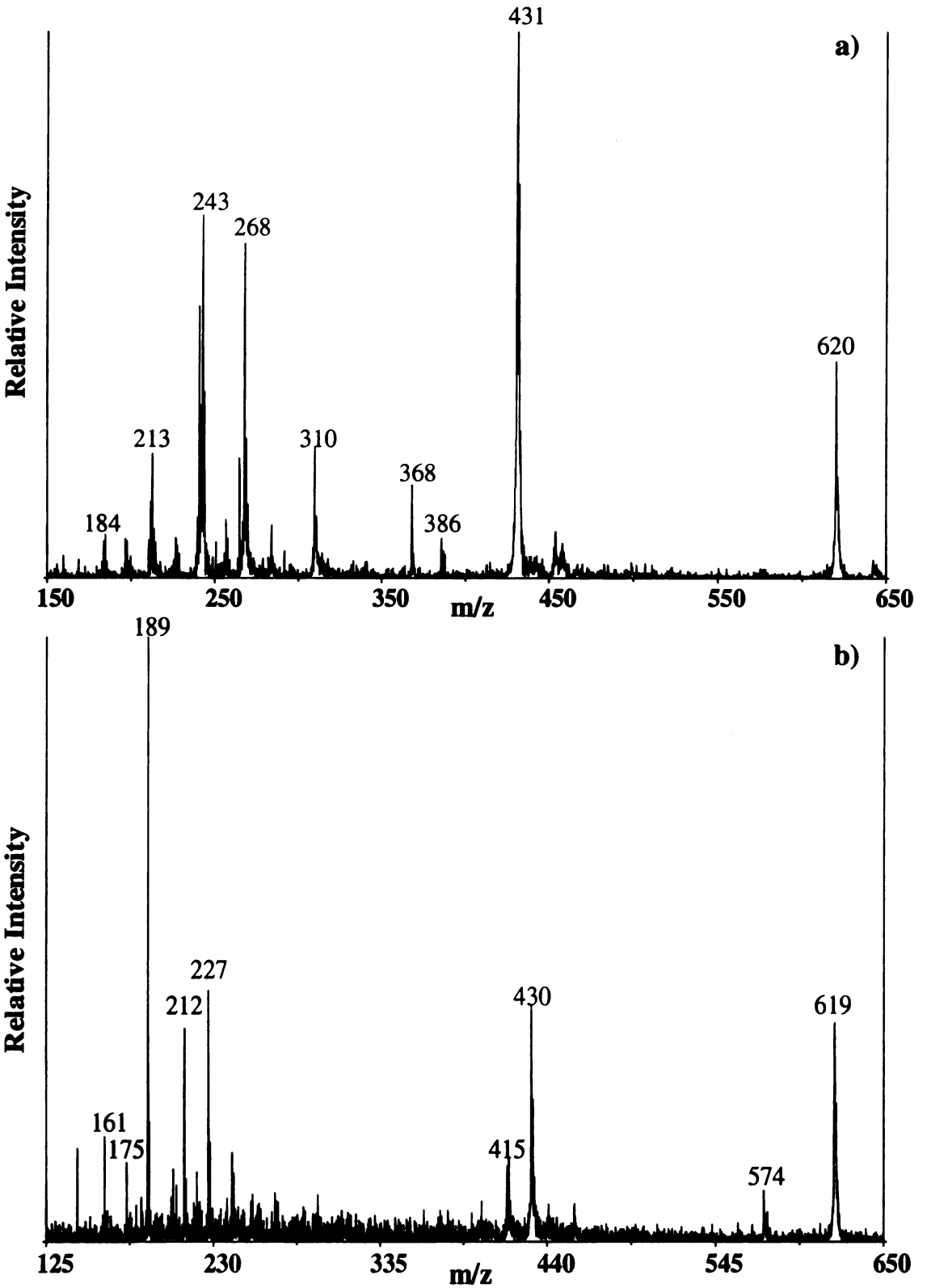

Figure 2.20: Vermilion (Niji watercolors) exposed to 10 hours light from a Hg-arc lamp: a) the partial positive ion LD mass spectrum; b) the partial negative ion LD mass spectrum

Figure

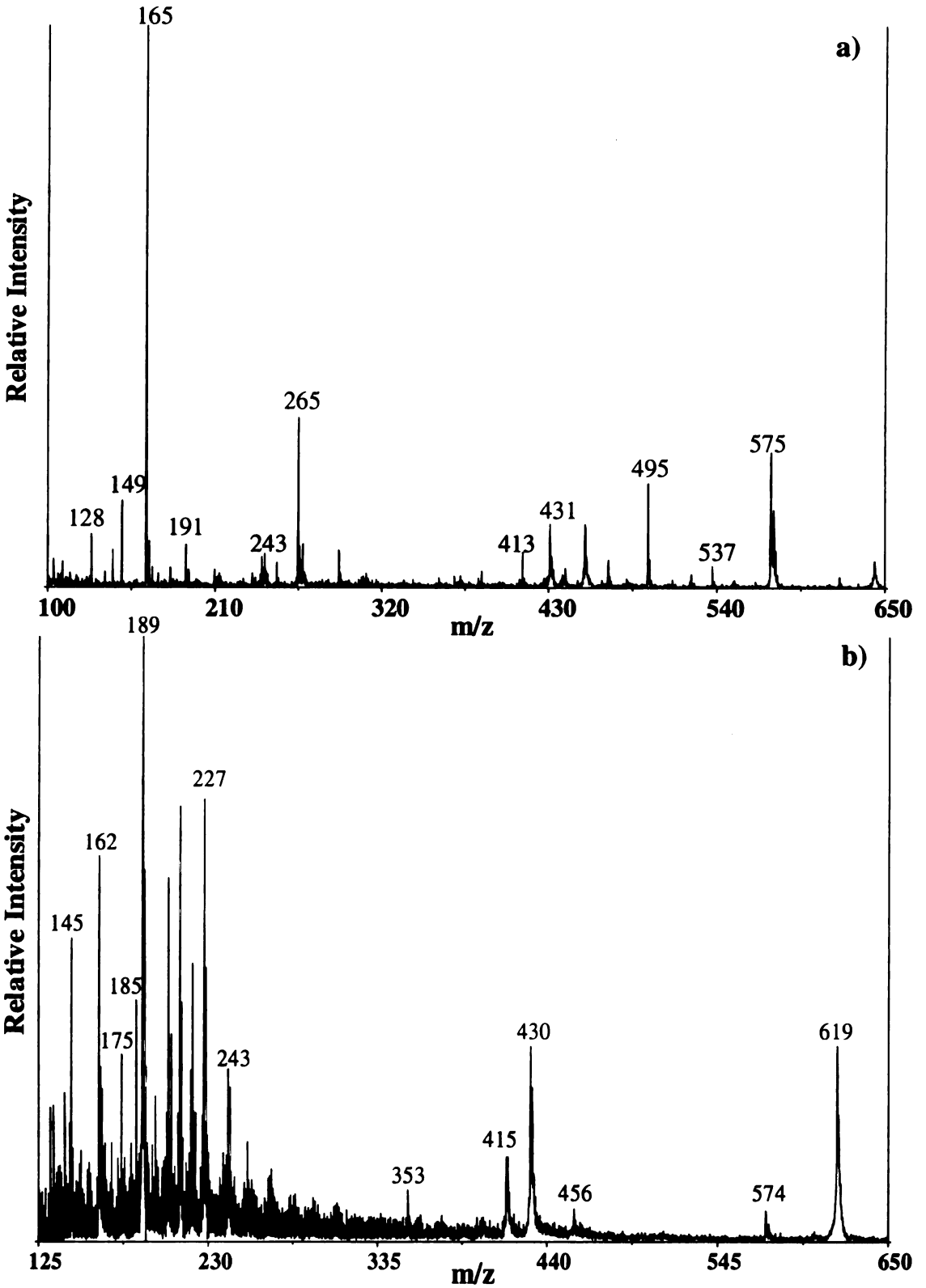

Figure 2.21: Vermilion (Niji watercolors) exposed 3 months to natural sunlight lamp: a) the partial positive ion LD mass spectrum; b) the partial negative ion LD mass spectrum

majority

environ

Mauve

ozone

paper

(Figu

repre

disap

decr

23R

Hov

con

ref

Co

str

ob

s

As in the case of the light experiments concerning the Niji watercolors, the majority of the colorants remained unaffected when exposed to the different environmental conditions. Some colorants faded, but their spectra remained the same. Mauve 398 is an example which the spectra did not, and the results of the controlled ozone exposure study will be summarized here.

Following exposure for 12.5 minutes to O_3 (375 ppm), the Mauve 398 colorant on paper faded, but did not appear to change color. In the positive ion mass spectrum (Figure 2.22a), there was only evidence of the intact PR 122 colorant (m/z 340). Peaks representing PV 23RS and the tentatively identified compound at m/z 663 have disappeared. In the negative ion mass spectrum (Figure 2.22b), the peak at m/z 661 decreased significantly and it is questionable whether PV 23RS is still present. If PV 23RS degraded completely, one would expect a color change along with the fading. However, returning to the initial LD mass spectra of mauve (Figure 2.18), the concentration of PV 23RS is minimal relative to the concentration of PR 122, as is reflected in the relative intensities of the peaks representing the intact dye molecules. Consequently, the presence of PV 23RS may have had more of an impact on the full-strength color, however the absence of PV 23RS in the faded colorant did produce an obvious shift in hue.

As with the light studies, either degradation or reaction products formed did not seem to be easily detectable. Preliminary experiments exposing the samples to SO_2 and NO_2 were inconclusive (spectra not shown) and the experiments were difficult to control with the equipment available in the lab. Consequently, we decided to change research directions.

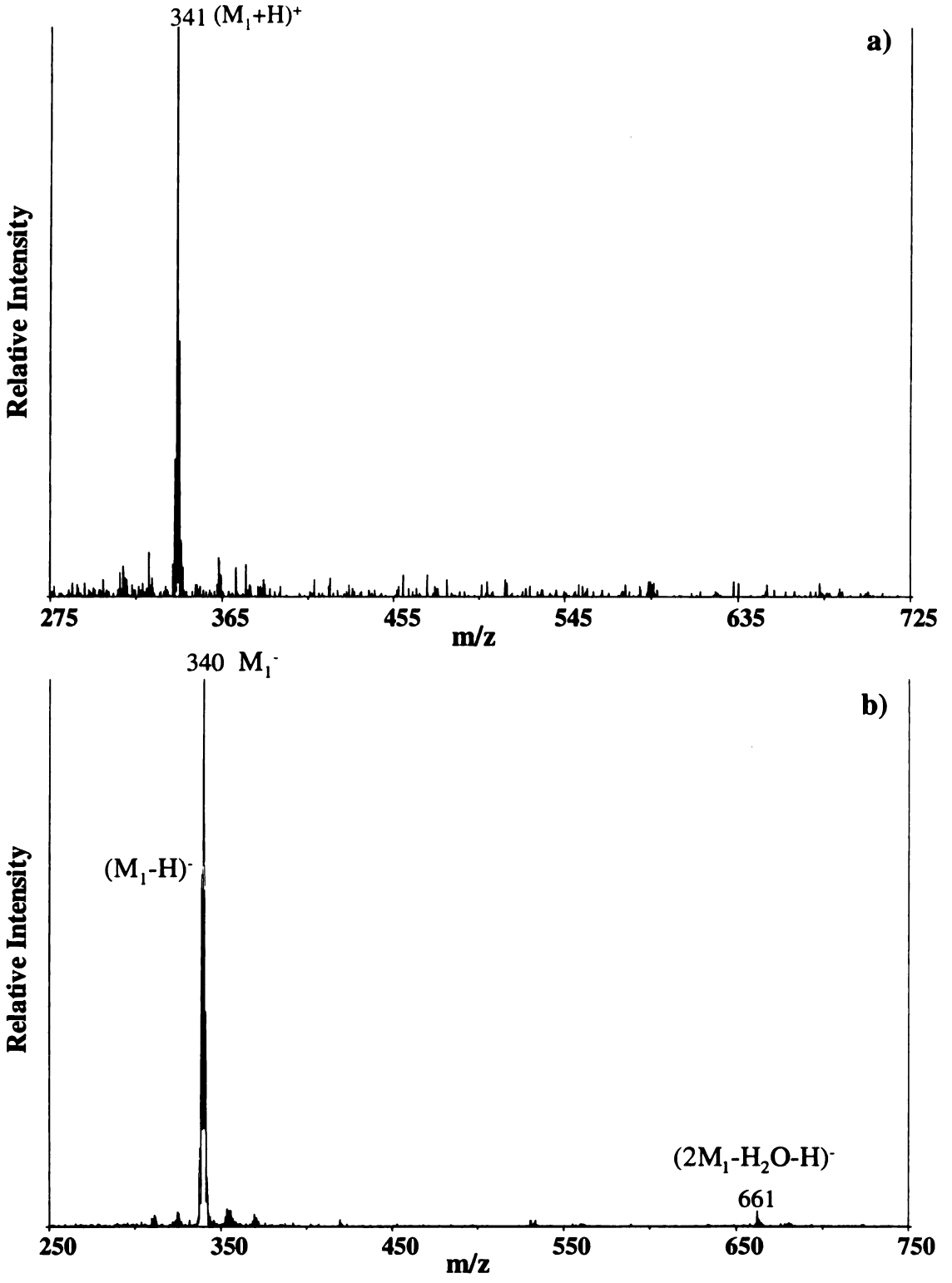

Figure 2.22: Mauve 398 (Winsor & Newton) exposed 12.5 minutes to O3 (375 ppm): a) the partial positive ion LD mass spectrum; b) the partial negative ion LD mass spectrum.

Summary

The preliminary experiments performed concerning the LDMS analysis of water colorants suggest that LDMS may be used to generate "fingerprint" spectra of organic watercolor dyes, but may not be suitable for the analysis of their degradation products. If the degradation products formed are volatile, they may not be detected in this experiment. In the case that the products are nonabsorbing at 337 nm, traditional MALDI could be employed. Considering that standard MALDI matrices are also of low molecular weight, analyte peaks may get "lost" in matrix background peaks. Based on these experiments, we decided to change research directions and look for colorants that were known to react and change color over time in response to their environment, as opposed to fading. Numerous inorganic artist pigments were known to do so. Consequently, the direction of the project changed to the analysis of inorganic colorants.

References:

1) Museum Lighting Protocol, http://www.ncptt.nps.gov/notes/32/2.stm.

2) Brimblecombe P. The composition of museum atmospheres. Atmospheric Environment 1990;25B:1-8.

3) Hackney S. The distribution of gaseous air pollution within museums. Studies in Conservation 1984;29:105-116.

4) Thompson G. The Museum Environment. London: Butterworths, 1978.

5) Hisham MWM, Grosjean D. Air pollution in southern California museums: indoor and outdoor levels of nitrogen dioxide, peroxyacetyl nitrate, nitric acid, and chlorinated hydrocarbons. Environmental Science and Technology 1991;25:857-862.

6) Hisham MWM, Grosjean D. Sulfur dioxide, hydrogen sulfide, total reduced sulfur, chlorinated hydrocarbons, and photochemical oxidants in southern California museums. Atmospheric Environment 1991;25A:1497-1505.

7) Eastlake CT, Faraday M, Russel W. Report on protection by glass of the pictures in the National Gallery. London: House of Commons, 1850.

8) Grosjean D, Parmar SS. Removal of air pollutant mixtures from museum display cases. Studies in Conservation 1991;36:129-141.

9) Parmar SS, Grosjean D. Sorbent removal of air pollutants from museum display cases. Environment International 1991;7:39-50.

10) Hemphill JE, Norton JE, Ofjor OA, Stone RL. Color fastness to light and atmospheric contaminants. Textile Chemist and Colorist 1976;8:60-62.

11) Williams EL, II, Grosjean E, Grosjean D. Exposure of artists' colorants to air pollutants: reflectance spectra of exposed and unexposed samples. Final Report to the Getty Conservation Institute, DGA, Inc., CA, 1991.

12) Csepregi Zs, Aranyosi P, Rusznák I, Töke L, Vig A. The light stability of azo dyes and azo dyeings II. Perspiration – light stability of dyeings with reactive and non-reactive derivatives, respectively, of two selected azochromophores. Dyes and Pigments 1998;37:15-31.

13) Aranyosi P, Csepregi Zs, Rusznák I, Töke L, Vig A. The light stability of azo dyes and azo dyeings III. The effect of artificial perspiration on the light stability of creactive and non-reactive derivatives of two selected azo chromophores in aqueous solution. Dyes and Pigments 1998;37:33-45.

14) Sirbiladze KJ, Vig A, Anyisimov M, Anyisimova OM, Krichevskiy GE, Rusznák I. Determination of the lightfastness of dyestuffs by kinetic characteristics. Dyes and Pigments 1990;14:23-34.

15) Aranyosi P, Czilik M, Rémi E, Parlagh G, Vig A, Rusznák I. The light stability of azo dyes and azo dyeings IV. Kinetic studies of the role of dissolved oxygen in the photofading of two heterobifunctional azo reactive dyes in aqueous solution. Dyes and Pigments 1999;43:173-182.

16) Grosjean D, Whitmore PM, Cass GR, Druzik JR. Ozone fading of natural organic colorants: mechanisms and products of the reaction of ozone with indigos. Environmental Science and Technology 1988;22:292-298.

17) Grosjean D, Whitmore PM, Cass GR, Druzik JR. Ozone fading of triphenylmethane colorants: reaction products and mechanisms. Environmental Science and Technology 1989;23:1164-1167.

18) Grosjean D, Whitmore PM, DeMoor CP, Cass GR, Druzik JR. Fading of alizarin and related artists' pigments by atmospheric ozone: reaction products and mechanisms. Environmental Science and Technology 1987;21:635-643.

19) Grosjean D, Whitmore PM, DeMoor CP, Cass GR, Druzik JR. Ozone fading of organic colorants: products and mechanisms of the reaction of ozone with curcumin. Environmental Science and Technology 1988;22:1357-1361.

20) Shaver CL, Cass GR, Druzik JR. Ozone and the deterioration of works of art. Environmental Science and Technology 1983;17:748-752.

21) Whitmore PM, Cass GR. The ozone fading of traditional Japanese colorants. Studies in Conservation 1988;33:29-40.

22) Whitmore PM, Cass GR, Druzik JR. The ozone fading of traditional natural organic colorants on paper. Journal of the American Institute for Conservation 1987;26:45-58.

23) Salvin VS. Ozone fading of dyes. American Association of Textile Chemists and Colorists 1969;1:22-28.

24) Whitmore PM, Cass GR. The fading of artists' colorants by exposure to atmospheric nitrogen dioxide. Studies in Conservation 1989;34:85-97.

25) Grosjean D, Salmon L, Cass GR. Fading of artists' colorants by atmospheric nitric acid: reaction products and mechanisms. Environmental Science and Technology 1992;26:952-959.

26) Salmon LG, Cass GR. The fading of artists' colorants by exposure to atmospheric nitric acid. Studies in Conservation 1993;38:73-91.

3.

33)

34)
A

35) P
M

36) Ad
For

37) Agi
chro

38) Shan
Phtha

39) Conne
behavi
assiste
2084.

27) Williams EL, II, Grosjean E, Groshean D. Exposure of artists' colorants to peroxyacetyl nitrate. Journal of the American Institute for Conservation 1993;32:59-79.

28) Williams EL, II, Grosjean E, Grosjean D. Exposure of artists' colorants to airborne formaldehyde. Studies in Conservation 1992;37:201-210.

29) ASTM Method D 2244-93 Standard test method for calculation of color difference from instrumentally measured color coordinates. American Society for Testing and Materials. West Conshocken, PA, 2001.

30) Grim DM, Siegel J, Allison J. Evaluation of desorption/ionization mass spectrometric methods in the forensic applications of the analysis of inks on paper. J Forensic Sci 2001;46:1411-1419.

31) Grim DM, Siegel J, Allison J. Does ink age inside of a pen cartridge? J Forensic Sci 2002;47:1294-1297.

32) Grim DM, Siegel J, Allison J. Evaluation of laser desorption mass spectrometry and UV accelerated aging of dyes on paper as tools for the evaluation of a questioned document. J Forensic Sci 2002;47:1265-1273.

33) ASTM Method D 4303-99 Standard test methods for lighfastness of pigments used in artists' paints, May 10, 1999. American Society for Testing and Materials. West Conshocken, PA, 2001.

34) ASTM Specification D 5067-99 Standard specification for artists; watercolor paints. American Society for Testing and Materials. West Conshocken, PA, 2001.

35) Personal communication with Dr. James N. Jackson, Chemistry Department, Michigan State University, East Lansing, MI.

36) Adrasko J. HPLC analysis of ballpoint pen inks stored at different light conditions. J Forensic Sci 2001;46:21-30.

37) Aginsky VN. Dating and characterizing writing, stamp pad and jet printer inks by gas chromatography/mass spectrometry. Int J Forensic Doc Examiners 1996;2:103-116.

38) Shankai Z, Feng Z, Weide H, Zhongping Y, Zhang W, Chait T. J Porphyrins Phthalocyanines 1995;9:230.

39) Conneely S, McClean S, Smyth F, McMullan G. Study of the mass spectrometric behaviour of phthalocyanine and azo dyes using electrospray ionisation and matrix-assisted laser desorption/ionisation. Rapid Commun Mass Spectrom 2001;15:2076-2084.

40) Berrie BH. Prussian blue. In: Fitzhugh EW, editor. Artists' pigments: a handbook of their history and characteristics, vol. 3. New York: Oxford University Press,1997; 191-217.

41) Herbst W, Hunger K. Industrial Organic Pigments. Production, Properties, Applications, 2nd ed. Weinheim: VCH, 1997.

42) Wilcox M. The Wilcox guide to the best watercolor paints, 2001-2 ed. USA: School of Colour Publications, 2001.

43) Kühn H. Verdigris and copper resinate. In: Roy A, editor. Artists' pigments: a handbook of their history and characteristics, vol. 2. New York: Oxford University Press, 1993;131-158.

44) Douglas B, McDaniel D, Alexander J. Concepts and models of inorganic chemistry, 3rd ed. New York: John Wiley & Sons, 1994.

45) Delamare F, Guineau B. Colors. The Story of Dyes and Pigments. New York: Harry N. Abrams, 2000.

46) Grim DM, Allison J. Identification of colorants used in watercolor and oil paintings by UV laser desorption mass spectrometry. International J Mass Spectrometry 2003;222:85-99.

Chapter Three: Lake Pigments

Introduction:

A unique class of colorants used in art is the class known as lakes. Such dye-based paints have been used since ancient times. Medieval painters mostly used mineral pigments. Dyes were also available for dyeing fabrics. These dyes were attractive but were chemically inappropriate for painting. The solution was to chemically bind the dyes to mineral substances to make the colors insoluble. The resulting pigment was a called a lake. A true lake is defined as a transparent color precipitated on a transparent base (1). A lake is prepared by dissolving the organic colorant in water and then precipitating the colorant on a base by introducing a solution of an appropriate metal salt or oxide. The introduction of lakes greatly increased the range of pigment colors available. In 1809, some pigments were discovered in a shop in the excavations at Pompeii. Following the analysis of the pigments, Chaptal determined that a particular pink pigment was a madder alumina lake (2). Madder lakes use coloring substances extracted from madder roots. If a museum laboratory is fortunate to have XRF available as a tool, they may be able to determine that an inorganic material such as alumina (Al_2O_3), tin oxide, or zinc oxide is present as the support, but they could not detect the organic dye.

As discussed in the introductory chapter, art conservators are in need of new analytical techniques to help them identify and characterize lake pigments. As a result of their unique composition, lakes require a minimum of two analytical techniques to be characterized. One method is used to identify the organic portion, and the second is used to characterize the inorganic portion. Before this is done, a separation of the two components is required, which is not an easy task. Laser desorption mass spectrometry is

a versatile tool, which is able to provide molecular information on both organic and inorganic compounds. LDMS was investigated to determine if it would be a beneficial addition to the analytical techniques currently available to art conservators. The results of the analyses of a few lakes will be presented and discussed.

Carmine Lake

Carminic acid has been used as a colorant since the 1500s. The natural organic dye is made from the dried bodies of female beetles, *coccus cacti*, that live on cactus plants in Mexico and in Central and South America. They were brought to Europe soon after the discovery of these countries. The scarlet red colorant immediately gained popularity, and was commonly used to dye fabric and cosmetics. However, the origin of the dye was a well-kept secret, simply because the ladies of this time period would have been horrified to discover that a component of their lipstick originated from a beetle. Eventually, the secret was revealed, and controversy ensued. Animal rights groups of this time period objected to the use of the colorant, because they believed that fashion was an inexcusable reason to sacrifice the lives of millions of beetles. The use of carminic acid subsequently tapered off, however it is still commonly used today. The colorant is identified as Natural Red No. 4 by the color index, and is still used to dye cosmetics (lipstick, blush, and eyeshadow) and even Cherry Coke (2,3).

Carminic acid and carmine lake are violet-red colorants that continue to be sold as oil paints, even though they are considered to be fugitive, meaning that extended exposure to sunlight can lead to bleaching of the lake. Carmine lakes are known to lose their color when mixed with specific pigments, as well. Consequently, the lake is

freque

natura

carmir

alum l

shown

alumin

indicat

the ger

domina

precipi

organic

frequently considered to be unsuitable for most artistic use. Unlike madder lakes, most natural organic lakes will change over time when exposed to light. In many uses, carmine lake is being replaced by the more stable alizarin lake (4).

Positive and negative ion LD mass spectra (Figure 3.1) were obtained for carmine alum lake suspended in linseed oil and applied to paper. The structure of carmine lake is shown in the inset of Figure 3.1a. As the name implies, the inorganic substrate is alumina (Al_2O_3). In the positive ion LD mass spectrum (Figure 3.1a), the major ions are indicative of the aluminum oxide support. These ions are listed in Table 3.1, and have the general formula $Al_xO_yH_z^+$. The negative ion spectrum (Figure 3.1b) appears to be dominated by peaks representing an organic compound. A lake is prepared by precipitating an organic dye onto an inorganic substrate. In the case of carmine lake, the organic dye is carminic acid.

Carmine Lake: Positive Ions

m/z	*Assignment*
60	AlO_2H^+
74	Al_2O^+
104	$Al_2O_3H^+$
131	$Al_3O_3H_2^+$
236	$Al_5O_6H_5^+$
365	$Al_8O_9H_5^+$

Table 3.1: A list of the identified positive ions for carmine lake.

Figure

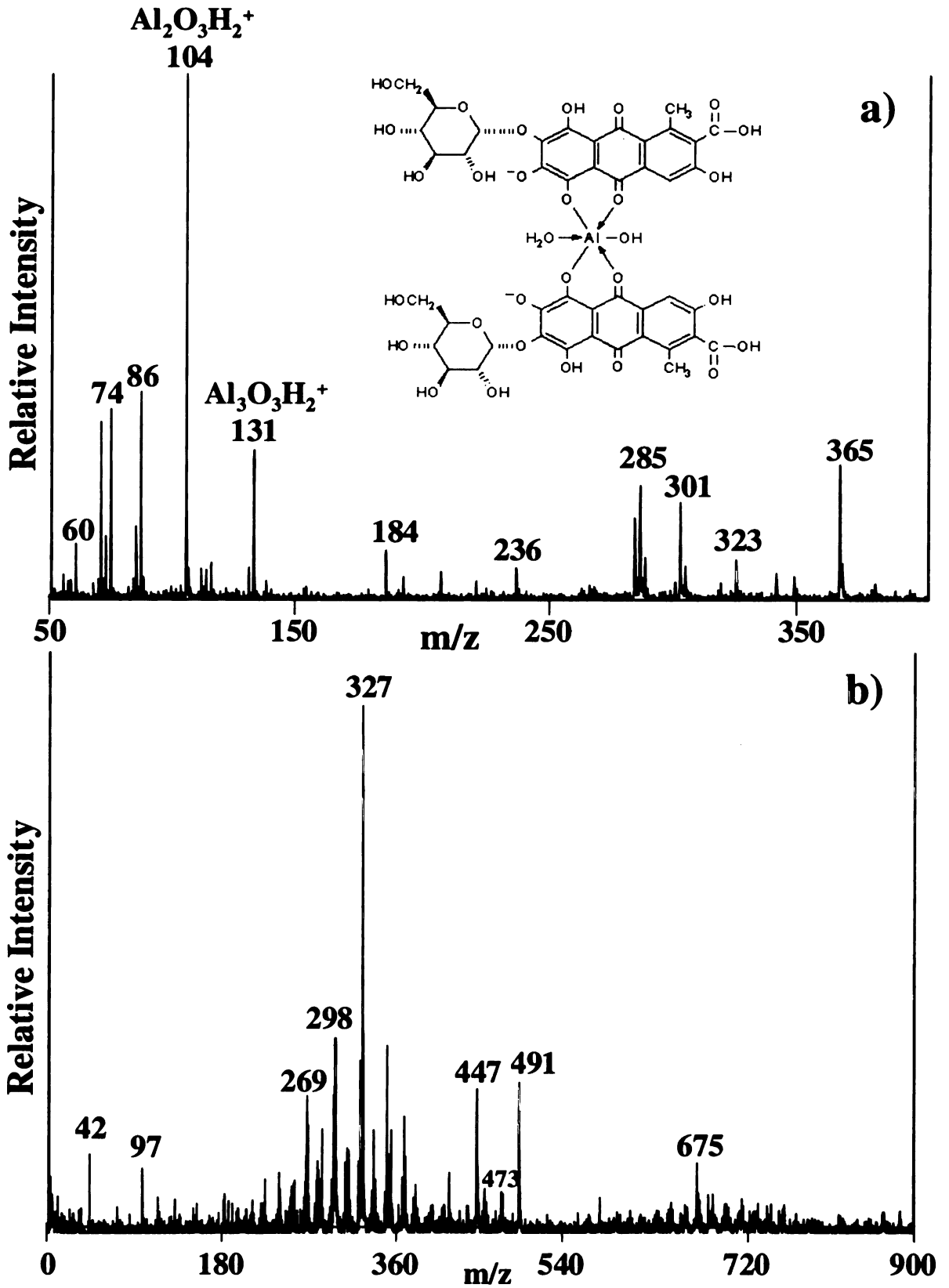

Figure 3.1: The LD mass spectra of carmine alum lake in linseed oil on paper; a) the partial positive ion mass spectrum and structure of carmine alum lake; b) the negative ion mass spectrum.

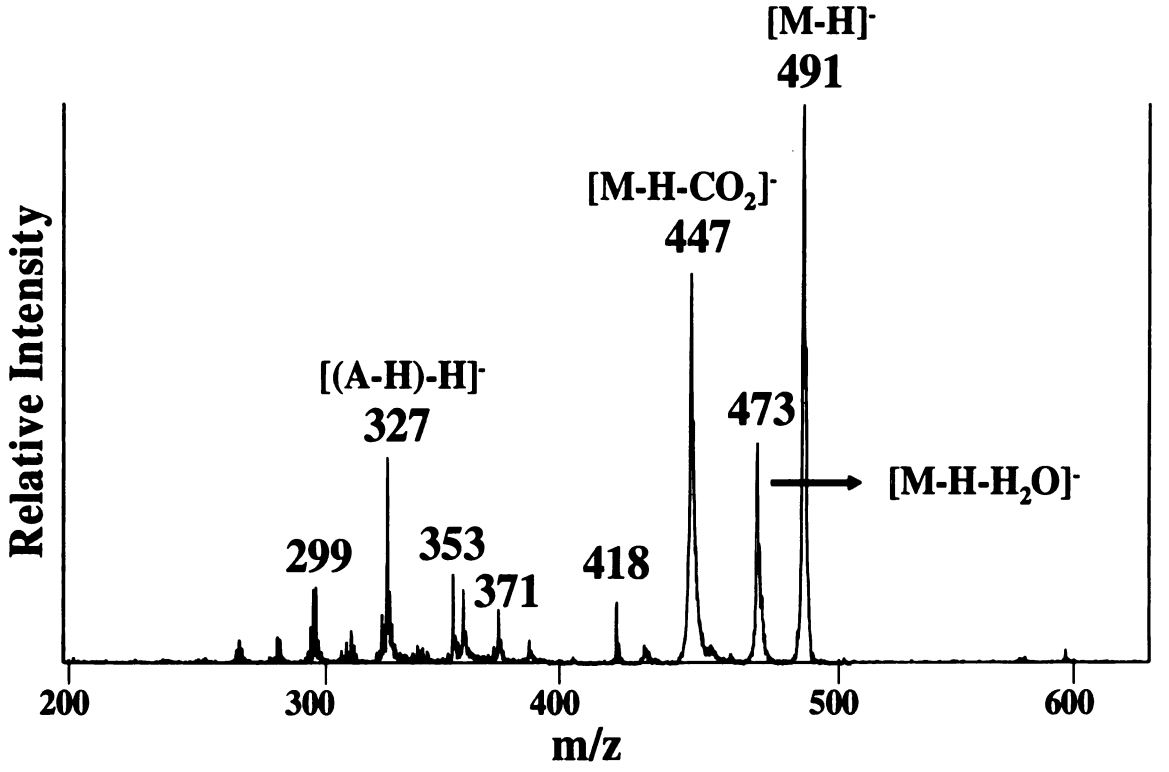

Figure 3.2: The partial negative ion LD mass spectrum of carminic acid in linseed oil on paper.

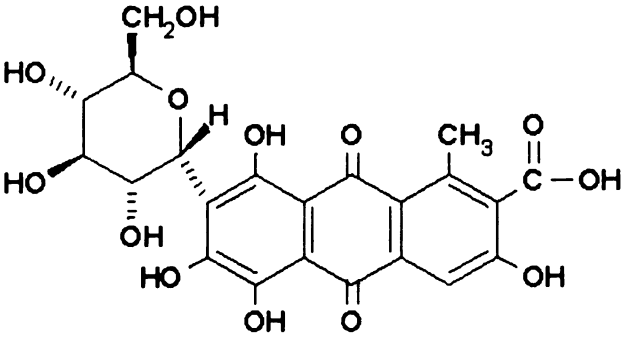

Figure 3.3: The structure of carminic acid.

To further investigate the ions observed from the lake in linseed oil, positive and negative ion LD mass spectra were obtained of carminic acid suspended in linseed oil and applied to paper. The negative ion spectrum of carminic acid in linseed oil is shown in Figure 3.2. Several peaks were identified in the negative ion spectrum derived from the organic dye. Neutral carminic acid weighs 492 Da (M) (Figure 3.3). The peak at m/z 491 represents the pseudomolecular $[M-H]^-$ ions. Peaks at m/z 473 and 447 represent the neutral losses of H_2O and CO_2 from the deprotonated molecule, respectively. Carminic acid is composed of an anthraquinone base (A), with a glucopyranosyl sugar group (G). Designating the compound as G-A, a reaction occurs in which the sugar group is lost, accompanied by a H shift, reaction:

$$G\text{-}A \rightarrow (G+H) + (A-H)$$

This leads to the $[(A-H)-H]^-$ ions at m/z 327. This could be either a fragment ion peak or the pseudomolecular ion of an anthraquinone impurity. The same peaks are observed in the negative ion mass spectrum of carmine lake (Figure 3.1b), but with varying intensities. This is not unexpected since in the lake, carminic acid is present as a dianion. Additionally, when the alumina support is taken away, all of the peaks listed in Table 3.1 disappear, which is evident in the positive ion mass spectrum of carminic acid in linseed oil on paper (not shown). Thus, the presence of both the organic and inorganic components of the lake could be detected using both positive and negative ion modes.

As a side note, when carminic acid is applied to paper from an aqueous solution, the sample instantly turns from red to black. Positive and negative ion LD mass spectra (spectra not shown) were obtained of the black sample. Few peaks were observed in the

positive ion spectrum and the negative ion spectrum is dominated by C_n^- clusters (n = 2-13). Formation of the lake clearly stabilizes the molecule so it can be used as a colorant.

In the carmine lake example, the positive ion mass spectrum provided information on the inorganic support (alumina) and the negative ion mass spectrum provided structural information on the organic dye (carminic acid). Ideally, we had hoped to identify peaks in either mass spectrum representing carminic acid-alumina complex ions. There is one peak at m/z 675 in the negative ion mass spectrum of carmine lake (Figure 3.1a), which is not present in the negative ion mass spectrum of carminic acid. This peak has been tentatively assigned as $[M+Al_5O_3]^-$. To confirm this assignment, one could perform a post source decay (PSD) LDMS experiment, to gain structural information on the ion. However, a potential problem could be that an insufficient number of ions at m/z 675 are initially formed. On average, an ion count of at least 10,000 is needed in a standard LD or MALDI experiment to perform a PSD analysis. Another option is to switch instruments. When available, a FTMS can be used to perform extreme high resolution experiments, which can be used to confirm the exact mass of an ion. If the assignment is correct, it is one piece of evidence of the organic dye and the inorganic support intact, which would be unique only to carmine lake.

Rose Madder

Historically, madder lake was manufactured using the dyestuffs found in madder roots. These coloring substances include alizarin (1,2 dihydroxyanthraquinone, Figure 3.4a), purpurin (1,2,4-trihydroxyanthraquinone, Figure 3.4b), and pseudopurpurin (1,2,4-trihydroxyanthraquinone-3-carboxylic acid, Figure 3.4c). The color of madder lake

depe

supp

conc

Onc

synt

a

depends on the concentrations of the organic colorants present, as well as the inorganic support the colorant is precipitated on. For example, a madder lake with a high concentration of purpurin will have more of a pinkish tone rather than a scarlet tone. Once alizarin was synthesized, natural madder lakes were replaced by the less costly, synthetic alizarin lakes (5).

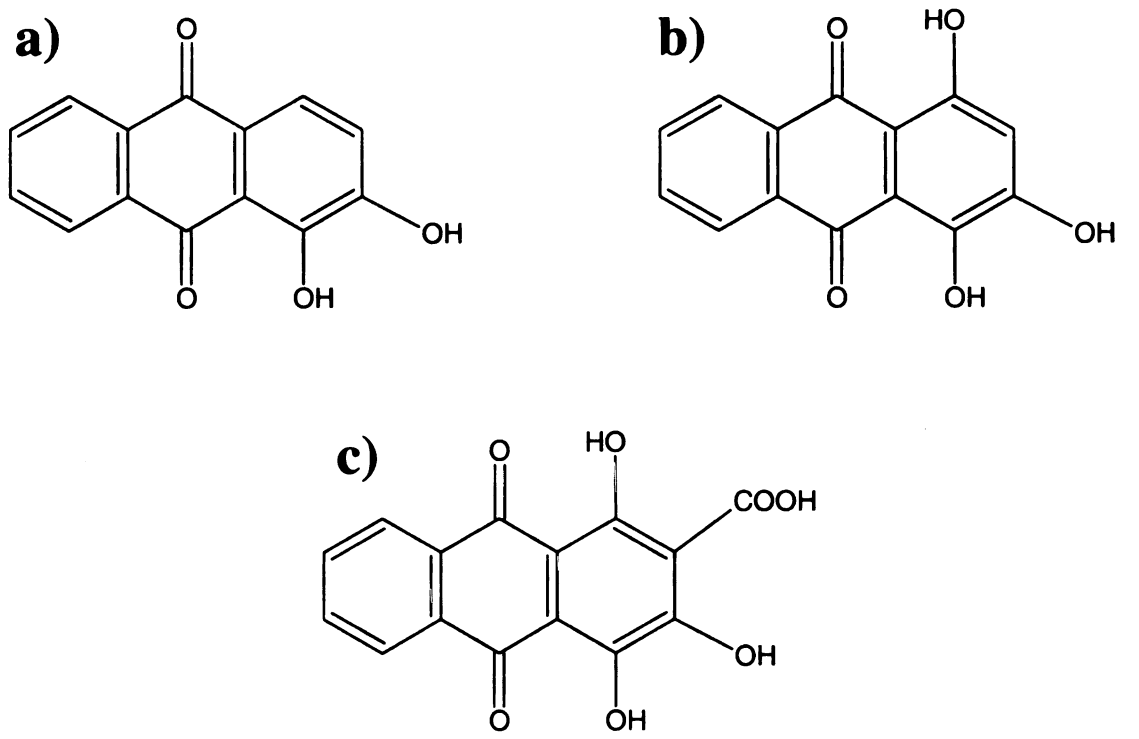

Figure 3.4: Structures of a) alizarin; b) purpurin; and c) pseudopurpurin.

Rose Madder 035 (Winsor & Newton), mentioned in Chapter Two, was analyzed. According to the label on the watercolor tube, 1,2 dihydroxyanthraquinone lake (PR 83) was the only dye used. The structure of PR 83 is shown in Figure 3.5. Like carmine lake, the organic component PR 83 is a dianion. The watercolor was dissolved in water and applied to paper. Positive and negative ion LD mass spectra were obtained and are shown in Figures 3.6a and 3.7a, respectively. The lake (dianionic) portion of PR 83 (M_1) has a molecular weight of 520 amu. The second most abundant peak in the positive ion mass spectrum occurs at m/z 543. This peak has been tentatively assigned as $(M_1\text{-}OH+Ca)^+$. M_1 carries a -2 charge. When the hydroxyl group is removed from the Al atom, the Al atom is left with a +1 charge, yielding a net -1 charge for (M_1-OH). A peak representing this species (m/z 503) is noted in the negative ion mass spectrum of Rose Madder (Figure 3.7a). When a Ca^{2+} ion attaches to the lake, the species now carries a net +1 charge.

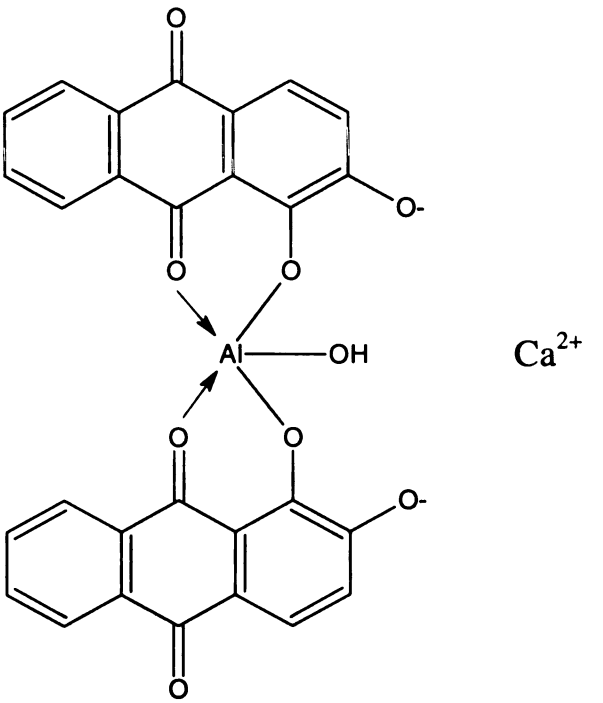

Figure 3.5: Structure of alizarin lake, PR 83.

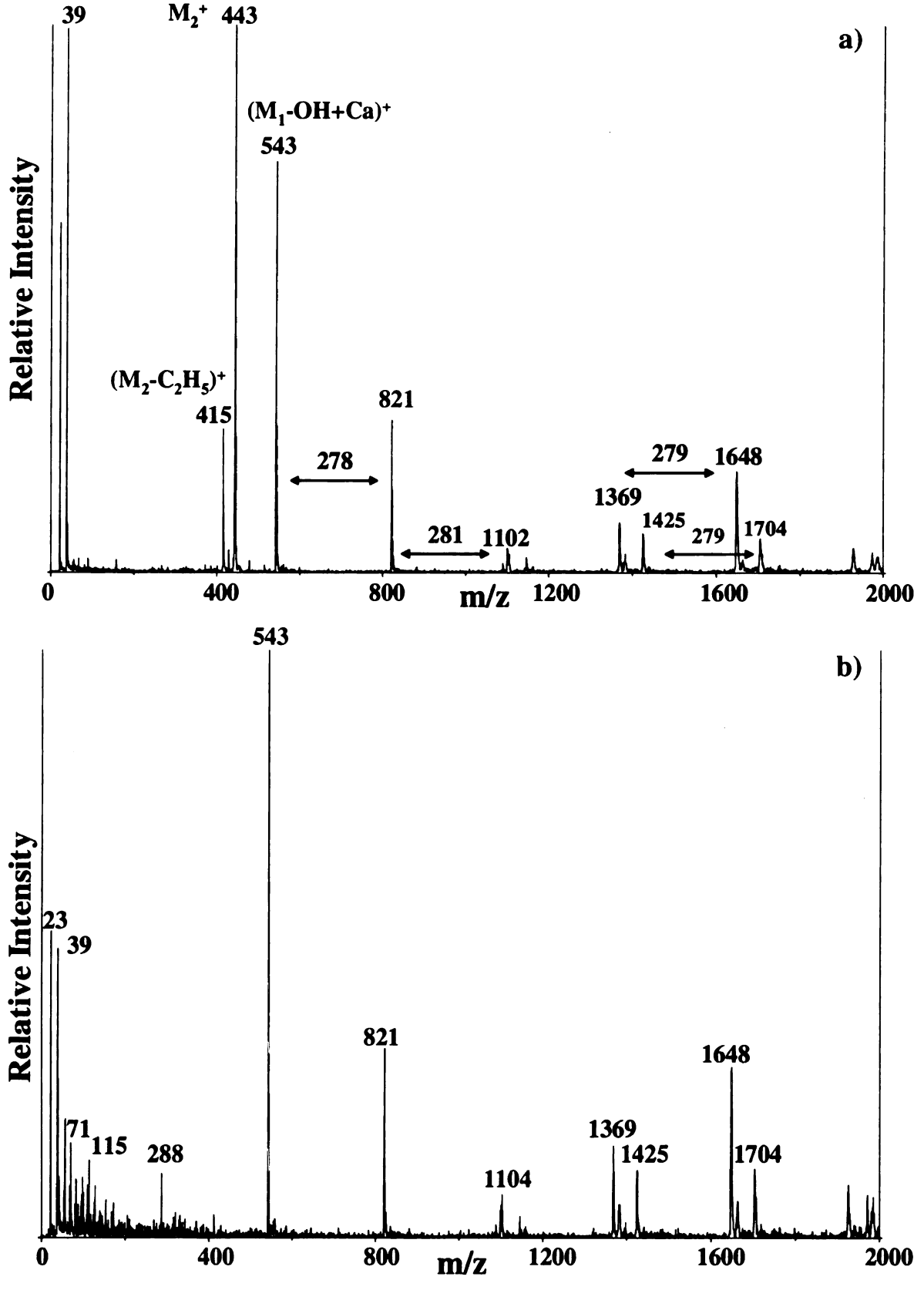

Figure 3.6: The positive ion LD mass spectra of lake pigments in water on paper; a) Rose Madder and b) R37.

Relative Intensity

0

Figure

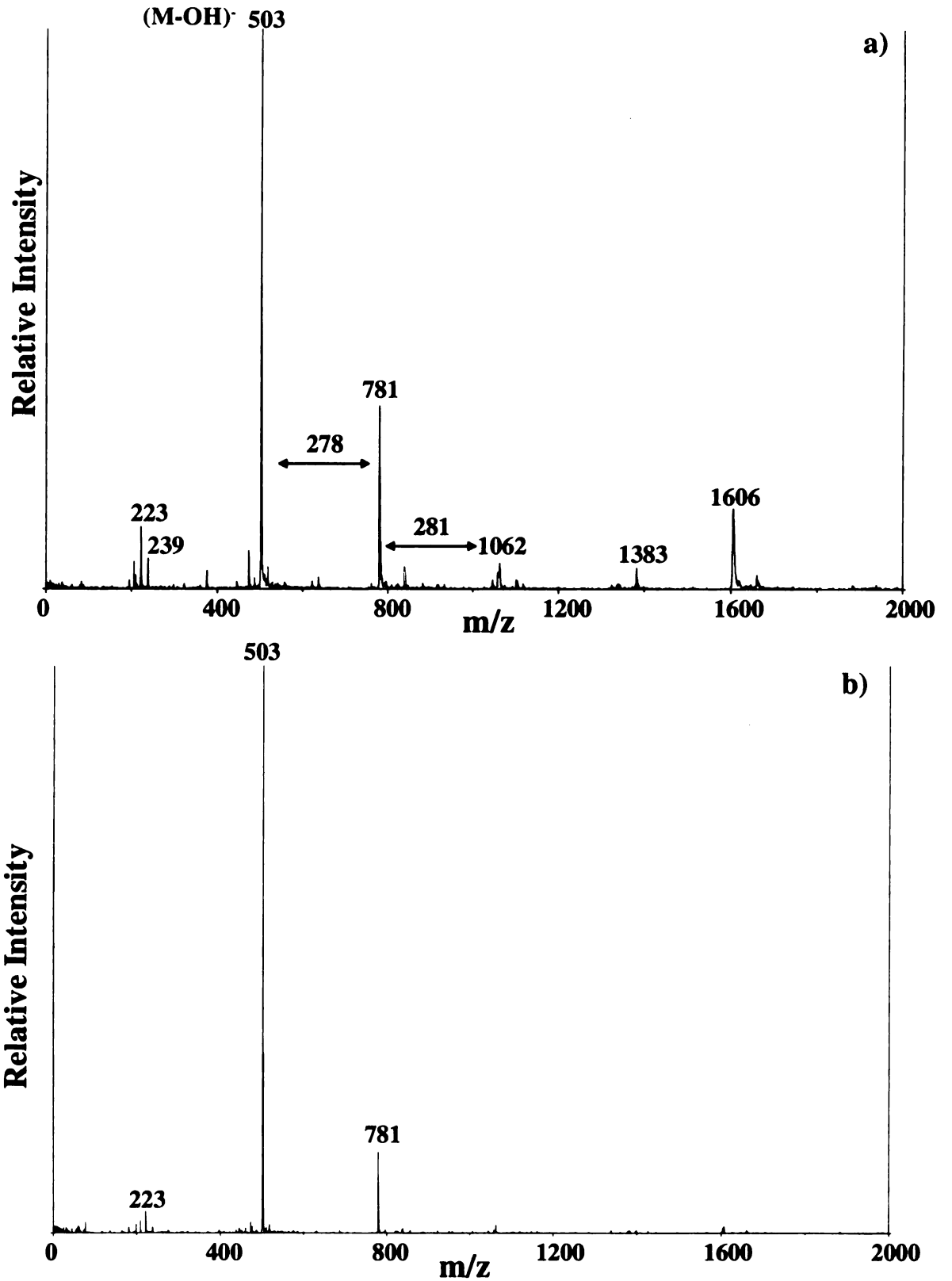

Figure 3.7: The negative ion LD mass spectra of lake pigments in water on paper; a) Rose Madder and b) R37.

The most intense peak in the positive ion mass spectrum occurs 100 mass units lower at m/z 443. From experience, the peak was easily identified as the cationic red dye, Rhodamine 6G (M_2). The structure of the dye is shown in Figure 3.8. Rhodamine 6G is a commonly used dye in modern red ballpoint ink formulas and is discussed in more detail in the following chapter. This dye was not listed in the chemical composition of the watercolor Rose Madder.

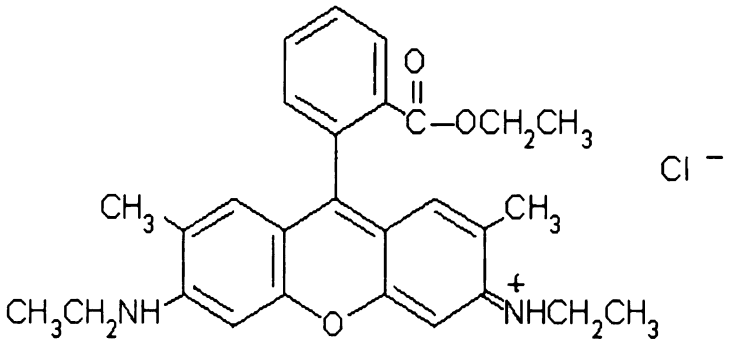

Figure 3.8: The structure of Rhodamine 6G.

The higher mass regions of both the positive (Figure 3.6a) and negative (Figure 3.7a) ion mass spectra are not as easily explained. In both spectra, there are a series of peaks separated by approximately 280 mass units. In the m/z 1300-1700 range of the positive ion mass spectrum, there even appears to be a second series occurring, 56 mass units higher than the first set. To help determine what these peaks are representing, we considered a second lake pigment, which generated very similar LD mass spectra.

The second lake pigment was labeled "R37" (Tuscan red). The pigment has a unique origin, which will be addressed in Chapter 4 ("G13"). R37 has a chemical composition of 45% ferric oxide, 17% alizarin lake, and 38% calcium carbonate. The

positive and negative ion LD mass spectra of R37 suspended in water and applied to paper are shown in Figures 3.6b and 3.7b, respectively. Neglecting the peaks representing Rhodamine 6G in the positive ion mass spectrum, the spectra are nearly identical. Originally, the mass difference (~ 280 mass units) was thought to be caused by the attachment of linseed oil molecules (discussed in greater detail in Chapter 4). The reasoning behind this explanation was based on the fact that linseed oil is commonly ground in with pigments during their manufacture. Considering what both lakes have in common (alizarin lake), a second explanation might be the adduct of a 1,2-dihydroxyanthraquinone molecule and a Ca atom.

Summary

From these few examples, we have learned that not all lakes generate the same type of ions in the LDMS experiment. For example, carmine lake generated ions indicative of the organic dye and inorganic support as separate entities. There was no evidence in either mass spectrum of the intact lake molecule as shown in Figure 3.1a. The Rose Madder watercolor was different. Peaks were identified in both the positive and negative ion mass spectra representing the intact lake molecule (with the exception of a hydroxyl group). The results of the Rose Madder experiment are ideal, simply because the peaks are unique only to alizarin lake. The results of the carmine lake are also quite useful, considering that carminic acid is not typically used alone as a pigment. Therefore, if the dye is present, the pigment is most likely carmine lake. More lakes would need to be analyzed to fully realize the potential of LDMS in this area. The results of these experiments, suggest that it has considerable potential.

References

1) Delamare F, Guineau B. Colors. The story of dyes and pigments. New York: Harry N. Abrams, Inc., 2000.

2) Schweppe H, Winter J. Madder and Alizarin. In: Fitzhugh EW, editor. Artists' pigments: a handbook of their history and characteristics, vol. 3. New York: Oxford University Press, 1997; 109-142.

3) Finlay V. Color: a natural history of the palette. New York: Ballantine Books, 2002.

4) Weber FW, Artists' pigments: their chemical and physical properties. New York: D. Van Nostrand Company, 1923.

5) Schweppe H, Roosen-Runge H. Carmine – cochineal carmine and kermes carmine. In: Feller RL, editor. Artists' pigments: a handbook of their history and characteristics, vol. 1. New York: Cambridge University Press, 1986; 255-283.

Chapter Four: Inorganic pigments

Introduction

Nearly fifty years ago, Rutherford J. Gettens of the Freer Gallery of Art had a vision of a comprehensive source on artists' materials. His project began after realizing that limited information was available on pigments in the literature. In 1961, with the support of the International Institute for Conservation (IIC) of Historic Artistic Works, Gettens proposed an international effort to accumulate a series of pigment monographs of the highest quality, each becoming its own chapter in the completed handbook. The goal was to provide artists, conservators, scientists, and art historians with an up-to-date reference on the history of pigments' manufacture and occurrence in paintings, as well as on the detailed results from the analytical techniques that have been used to characterize and identify them. Much to Gettens' dismay, only nine monographs were completed and ready for publication between the years 1966 and 1974. Limited funding and slow output prompted Gettens to appeal to the National Gallery of Art to take over the project. The absence of a formal publication agreement between Gettens and J. Carter Brown, the director of the Gallery at that time, and the death of Gettens in 1974, resulted in a standstill for the project.

The project was soon revitalized by the new director of the National Gallery of Art, Robert L. Feller. Ten more pigment monographs were produced, and were published as Volume I of Artists' Pigments: A Handbook of Their History and Characteristics (1). By this time, the original nine monographs previously published in Studies in Conservation, the journal for the IIC, were outdated. As a tribute to Gettens' vision, these monographs were revised to include more recent historical and scientific

developments, and republished in Volume II of the Artists' Pigments Handbook, edited by Ashok Roy (2). Notably, x-ray crystallographic and scanning electron microscopic (SEM) data were now available and included. Historical aspects and notable occurrences were also researched more thoroughly and expanded upon. Volume III (3) has since been published, edited by Elisabeth West Fitzhugh, discussing an additional ten pigments. Unfortunately, these three volumes present only 29 out of the 50 to 75 pigments Gettens' had originally hoped to discuss. Additionally, the authors of the monographs were thorough not only in providing information on what is known about the pigments, but what still remains unknown, such as determining the detailed mechanisms for specific color changes that occur over time. These two factors indicate that there is still much research to be done.

Table 4.1 lists the pigments covered in Volumes I-III of the Artists' Pigment handbooks (1-3). Based on the history of the handbook, we believe that the individual chapters cite and discuss all of the analytical chemistry and spectroscopy that has been used to characterize and identify the pigments. While numerous analytical techniques have been employed by art experts and conservators to characterize pigments, including microchemical spot tests, microscopy, X-ray fluorescence (XRF) and infrared, RAMAN, and UV spectroscopies, each method has its limitations. It is rare that the analytical laboratory in a museum, if present at all, would have an extensive arsenal of tools for the analysis of colorants. XRF is a popular tool when available and provides useful atomic information. It may be used to determine that a pigment contains metals such as Pb and Cr, however this is insufficient to identify a compound. Also, XRF cannot be used to detect elements lighter than F (4), an obvious limitation when the colorant is organic. In

such cases, the absence of a metal may be the most useful clue. Other methods, such as IR spectroscopy, produce a fingerprint spectrum of the pigment, which can be matched with a standard spectrum. However, the presence of binding media and other pigments can complicate interpretation. Frequently, spot tests are the most direct way to determine the presence of specific chemical species, but such methods are ultimately destructive.

Volume I	Volume II	Volume III
Indian Yellow	Azurite and Blue Verditer	Egyptian Blue
Cobalt Yellow (Aureolin)	Ultramarine Blue, Natural and Artificial	Orpiment and Realgar
Barium Sulfate, Natural and Synthetic	Lead White	Indigo and Woad
Cadmium Yellows, Oranges, and Reds	Lead-Tin Yellow	Madder and Alizarin
Red Lead and Minium	Smalt	Gamboge
Green Earth	Verdigris and Copper Resinate	Vandyke Brown
Zinc White	Vermilion and Cinnabar	Prussian Blue
Chrome Yellow and Other Chromate Pigments	Malachite and Green Verditer	Emerald Green and Scheele's Green
Lead Antimonate Yellow	Calcium Carbonate Whites	Chromium Oxide Greens
Carmine		Titanium Dioxide Whites

Table 4.1: Summary of the pigments discussed in the three volume series Artists' Pigments: A History of Their Manufacture and Characteristics.

We have investigated laser desorption/ionization mass spectrometry (LDMS) as a minimally invasive method for confirming the presence of a specific pigment. Preliminary work has shown that both positive and negative ion LDMS spectra of inorganic pigments suspended in linseed oil may be easily obtained. The spectra contain molecular level information, which could allow for the distinction between two pigments

of similar composition. Once fully developed, we believe that this method will be a significant contribution to Gettens' work, as a means to identify pigments.

As discussed in Chapter One, the primary deficiencies of current analytical instrumentation used to identify and characterize artists' pigments include:

1) the inability to detect organic and inorganic components simultaneously
2) the inability to generate molecular information concerning a colorant
3) the inability to detect multiple colorants in a paint mixture

LDMS excels in all of these areas. The ability of LDMS to generate positive and negative ions indicative of both the organic colorant and inorganic support, in the specific case of lake pigments, was demonstrated in the previous chapter. In this chapter, the results of the LDMS analysis of two additional pigments (Prussian blue and "G13"), will be presented and discussed. These examples illustrate how LDMS can be used to solve problems 2 and 3, listed above.

Once the usefulness of LDMS in the identification and characterization of inorganic pigments has been established, a specific application will be presented. Two old illuminated (decorated) manuscripts were analyzed using LDMS. The first document is purportedly a page of a Koran from the 17^{th} century. The primary source of the second document is unknown, however it is allegedly created in the 1800's, and is written in Hebrew. LD mass spectra of the colorants were obtained and analyzed to help determine the authenticity of the documents.

The Case of the Two Prussian Blues:

Prussian blue is an inorganic pigment, introduced in the early 1700s. It is considered the first of the modern pigments. Prussian blue is a hydrated iron hexacyanoferrate complex, and the generic term "iron blue" refers to both ferric ferrocyanide, $Fe_4[Fe(CN)_6]_3 \cdot xH_2O$, and the more soluble $KFe[Fe(CN)_6] \cdot xH_2O$ ("alkali ferric ferrocyanide"). Ammonium and sodium salts are also used, with x = 14-16 (5). The pigment became instantly popular worldwide for artists' palettes, interior painting, wallpapers, as well as for dying fabrics such as silk (6-8). The structure of ferric ferrocyanide is shown in Figure 4.1. Prussian blue was a key material used for making cyanotypes, a primitive photograph and precursor to the blueprint (9,10). It has also been incorporated into ink, cosmetics, and automotive paint formulations (5). Artists have used Prussian blue as both a watercolor and an oil paint pigment. When the medium is water-based, alcohol is frequently added, improving the pigment's solubility and preventing flocculation. It was popular, not only as a blue colorant with extremely high "tinting strength" (11), but also as a compatible pigment to be used in mixtures with pigments such as lead chromate, to produce the chrome green pigment (5,12).

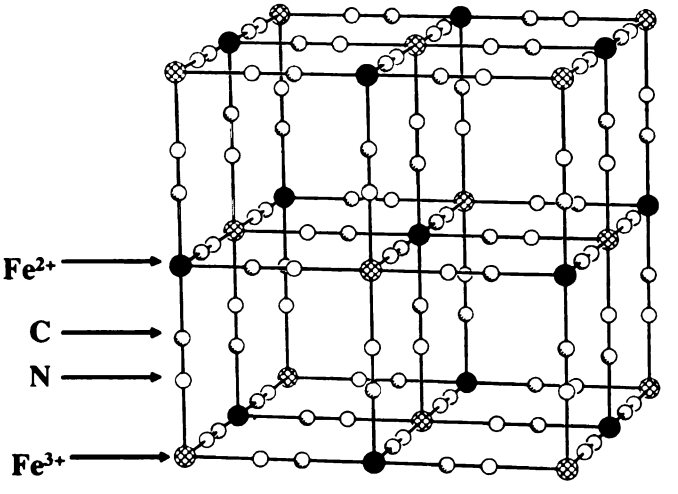

Figure 4.1: The structure of ferric ferrocyanide.

Studies of Prussian blue by Mössbauer spectroscopy (13), photoelectron spectroscopy (16), IR (17-19), neutron activation (20), Raman spectroscopy (21), and scanning electron microscopy (5) have been reported. In powder form, Prussian blue is of fine particle size, typically 0.01 to 0.2 microns in diameter. Dispersed Prussian blue is transparent under optical microscopy, and may appear as a blue streak. Aggregates are opaque, resembling indigo. Complications in identifying Prussian blue using optical microscopy have been discussed (5,22,23). As a result of its high tinting strength, Prussian blue is frequently present in only small amounts in oil paints, where impurities, bulking agents and extenders can further confuse identification. Consequently, it is often not detectable using methods such as X-ray powder diffraction analysis (5). Another problem in identifying Prussian blue involves confirming its presence in a mixture of pigments. For instance, ultramarine blue is an inorganic pigment physically resembling Prussian blue in a painting. Ultramarine blue does not contain Fe; however when the pigment is in a mixture of other pigments that do, a false positive identification for Prussian blue may result (5).

Consider the situation in which two watercolor artists have painted with a color in their palette specifically identified as Prussian blue. Figure 4.2 shows the positive and negative ion laser desorption mass spectra of Prussian blue (from the supplier Sinopia, San Francisco, CA) of the first artist, directly from paper. The positive ion spectrum, Figure 4.2a, is relatively uninformative, with the exception of the interesting peak at m/z 575, which will be discussed shortly. Some peaks are present, but do not appear to be related to the known structure of Prussian blue. The negative ion spectrum, Figure 4.2b, contains a number of peaks that can be rationalized as evolving from an iron cyanide.

Assignments were made by considering the masses of Fe (56 amu) and cyanide (CN, 26 amu), and by taking advantage of the characteristic isotopic profile of Fe which, notably, has an (A-2) isotope at m/z 54 (6.43%). Table 1 lists all of the peaks in the negative ion mass spectrum that have been identified thus far. The most intense peak is identified as $Fe(CN)_3^-$ at m/z 134. All of the peaks listed in Table 4.2 had isotopic satellites consistent with the presence of one or more iron atoms. For the majority of the ions listed in Table 1, the metals are in the +1 or +2 oxidation states. For example, m/z 134 has an isotopic signature consistent with the presence of one Fe atom, which would be in a formal oxidation state of +2, complexed with three anionic ligands, to yield a singly charged anion. A number of peaks 16 mass units above $Fe_x(CN)_y^-$ peaks were observed, suggesting the incorporation of oxygen. These could be incorporated into the ligands. Consider m/z 166, corresponding to $[Fe(CN)_3 + 2O]^-$. If both oxygen atoms were directly attached to the metal, it would be in, formally, a +8 oxidation state. Consequently, we tentatively assign it as $[Fe(OCN)_2(CN)]^-$. Also, when oxygen is present in these ions, there are always fewer O atoms present than CN groups, so direct Fe-O bonding need not be invoked.

Prussian Blue: Negative Ions

m/z	Assignment	Fe-Oxidation States
108	$Fe(CN)_2^-$	+1
124	$Fe(OCN)(CN)^-$	+1
134	$Fe(CN)_3^-$	+2
150	$Fe(OCN)(CN)_2^-$	+2
166	$Fe(OCN)_2(CN)^-$	+2
182	$Fe(OCN)_3^-$	+2
190	$Fe_2(CN)_3^-$	(+1,+1) or (0, +2)
206	$Fe_2(OCN)(CN)_2^-$	(+1,+1) or (0, +2)
216	$Fe_2(CN)_4^-$	(+1,+2) or (0, +3)
222	$Fe_2(OCN)_2(CN)^-$	(+1,+1) or (0, +2)
242	$Fe_2(CN)_5^-$	(+2,+2) or (+1,+3)
258	$Fe_2(OCN)(CN)_4^-$	(+2,+2) or (+1,+3)
274	$Fe_2(OCN)_2(CN)_3^-$	(+2,+2) or (+1,+3)

Table 4.2: A list of the identified negative ions formed by laser desorption from Prussian blue (aqueous) on paper, and the corresponding oxidation states of Fe .

Evaluation of the ions presented in Table 4.2 offers insight into the types of ions to expect, and just as importantly, into the ions which would not be found in a LD mass spectrum of similar materials. For example, it appears as though Fe prefers lower oxidation states, despite the fact that there are both Fe^{2+} and Fe^{3+} in the original crystal structure (Figure 4.1). In the negative ion mass spectrum, there are signals at m/z 108 and 134, representing the $Fe(CN)_2^-$ and $Fe(CN)_3^-$ ions, requiring Fe to be in the +1 and +2 oxidation states, respectively. However, the absence of a signal at m/z 160 representing $Fe(CN)_4^-$ is noted, which would require Fe to be in the +3 oxidation state. Furthermore, the most dominant peaks in the mass spectrum, occurring at m/z 134, 150, and 166, all represent ions in which Fe would have to be in the Fe^{2+} state. Additionally, there are

peaks representing $Fe(OCN)_3^-$, but not $Fe(OCN)_4^-$, and peaks representing $Fe_2(CN)_3^-$, $Fe_2(CN)_4^-$, and $Fe_2(CN)_5^-$, but not $Fe_2(CN)_6^-$. For ions such as $Fe(OCN)_4^-$ and $Fe_2(CN)_6^-$, at least one Fe would have to be in the +3 oxidation state. In a case such as $Fe_2(CN)_4^-$, in which mixed oxidation states are possible, the presence of Fe^{3+} need not be invoked.

Relative Intensit

Figure 4.

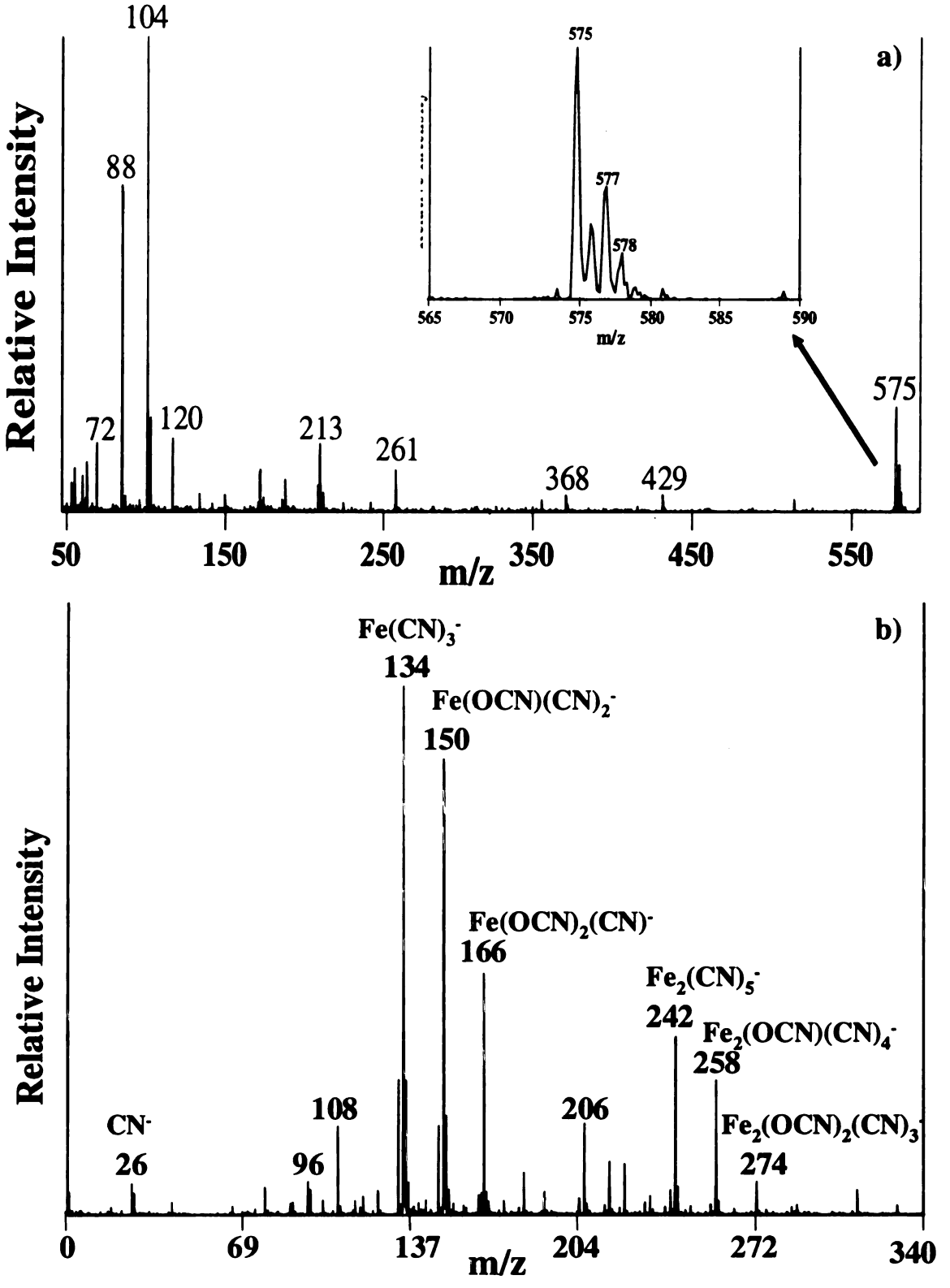

Figure 4.2: The LD mass spectra of Prussian blue (Sinopia) from an aqueous solution on paper; a) the partial positive ion mass spectrum; b) the negative ion mass spectrum.

In these spectra, there are certainly peaks that remain unassigned. However, during the manufacturing of artist's pigments, extenders and bulking agents such as alum, $CaCO_3$, $CaSO_4$, starch, alumina, magnesia, and clay are often added to provide the pigment with specific properties or to reduce the cost of production. As a result, what might be reported to be ferric ferrocyanide may in fact be a complex mixture. In summary, the negative ion spectrum provides ample evidence that the pigment is an iron compound, and that it is specifically an iron cyanide. The molecular information is certainly superior to what would be determined by a method such as XRF, which would only indicate the presence of iron. Clearly, mass spectral peaks containing both Fe and CN are present, which could be used to differentiate Prussian blue from other blue or iron-containing pigments.

Figure 4.3 shows the positive and negative ion LD mass spectra of authentic ferric ferrocyanide that was purchased from Aldrich, suspended in water and applied to HammerMill Fore MP paper. Characteristic peaks which may be indicative of the compound in some way, but do not contain iron, are again observed at m/z 72, 88, and 104 in the positive ion mass spectrum. Again, note the presence of the relatively high mass peak at m/z 575. Negative ion LDMS is clearly the method for determining the presence of Prussian blue, with the same ions observed as in Figure 4.2b.

Figure 4.

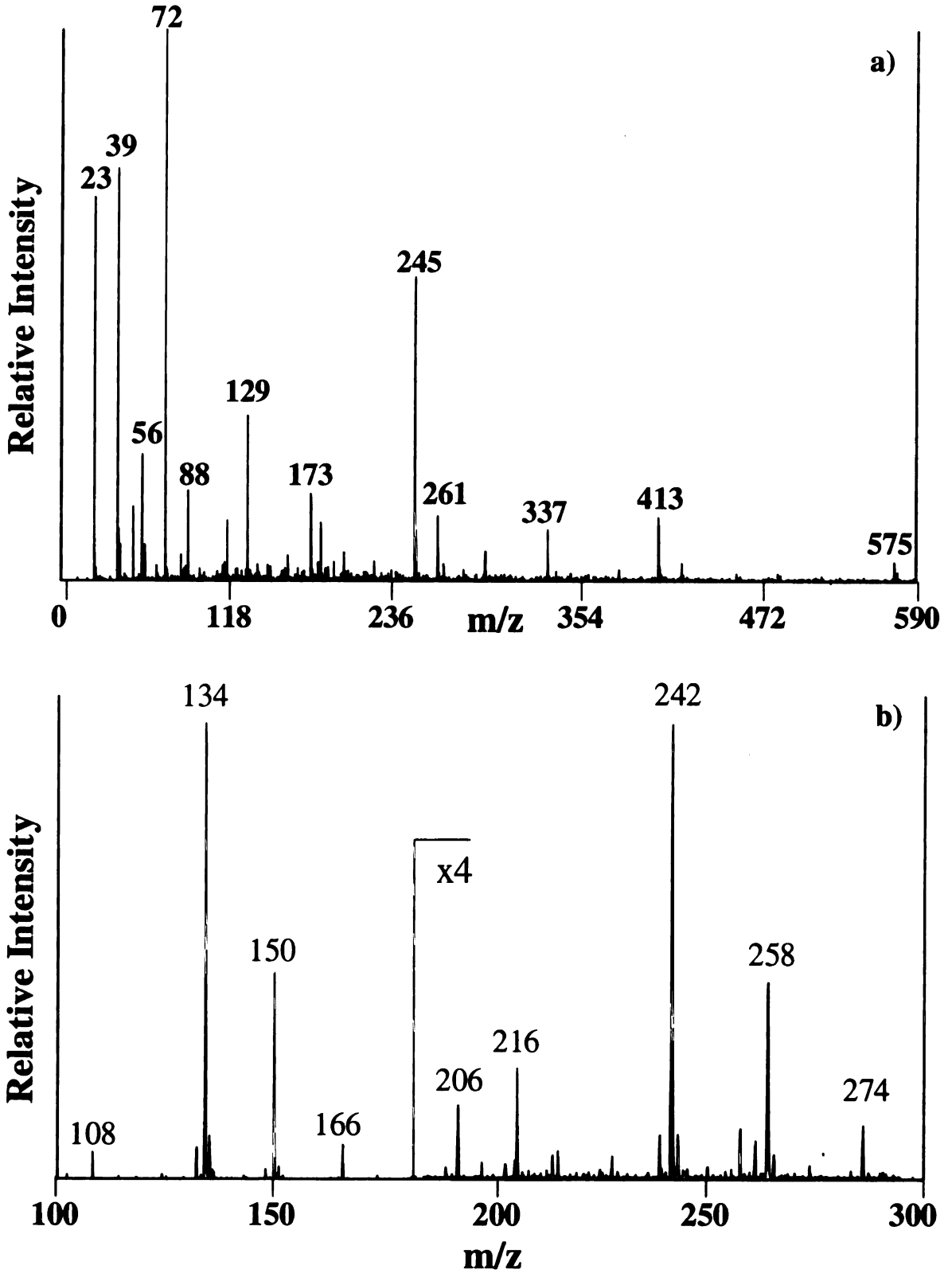

Figure 4.3: The LD mass spectra of ferric ferrocyanide (Aldrich) from an aqueous solution on paper; a) the positive ion mass spectrum; b) the partial negative ion mass spectrum.

Relative Intensity

Relative Intensity

Fig

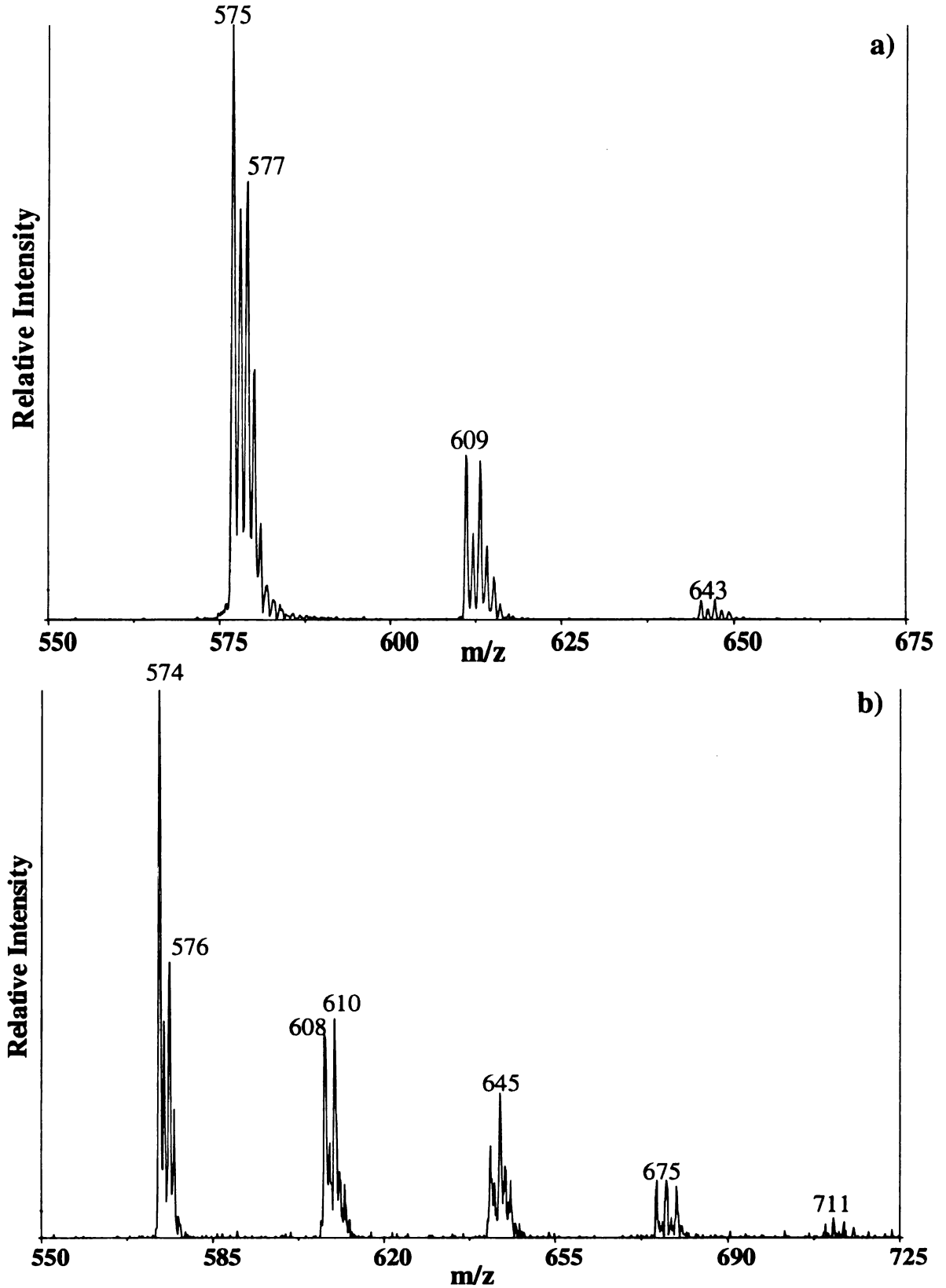

Figure 4.4: The LD mass spectra of Prussian blue (Niji) from an aqueous solution on paper; a) the partial positive ion mass spectrum; b) the partial negative ion mass spectrum.

Wat

disc

The

copp

C_{32}

of a

posit

spect

deso

for d

Pruss

ident

of fer

some

one w

spectr

the an

LD m

have s

phthal

The second artist also employed Prussian blue, but a different brand (Niji Watercolors). The positive and negative ion spectra are shown in Figure 4.4 and were discussed in detail in Chapter two. Obviously the spectrum is not of ferric ferrocyanide. The peak at m/z 575 in the positive ion spectrum represents the molecular ion, $M^{+\cdot}$, for copper phthalocyanine. The isotope distribution is consistent with the formula $C_{32}N_8H_{16}Cu$. A response in both positive and negative ion modes indicates the presence of a neutral dye, of which copper phthalocyanine is an example. It forms an $M^{+\cdot}$ peak in positive ion mode, and an $[M-H]^-$ peak in negative ion mode (m/z 574).

Again, if a laboratory was equipped with only the capability of atomic spectroscopy, identification of copper phthalocyanine would have been difficult. The desorption and ionization of the intact dye provides the required molecular information for distinguishing these two watercolors that were both sold under the same name, Prussian blue.

Now that the peak at m/z 575 in Figures 4.2a and 4.3a has been positively identified as copper phthalocyanine, one must question its presence in the mass spectrum of ferric ferrocyanide. While it is plausible that artist pigment manufacturers might blend some copper phthalocyanine with ferric ferrocyanide to alter the pigment's appearance, one would not expect a chemical company to do so. Positive and negative ion mass spectra of the paper (Figures 4.5a and 4.5b), reveal that the cationic peak at m/z 575 and the anion species at m/z 574 originate from the paper and not from the sample. The paper LD mass spectra were more complex than initially anticipated, however experiments have shown that all of the peaks, excluding the peaks representing copper phthalocyanine, are usually masked by the paint sample covering the paper. The m/z 574

pea

the

emp

been

pulp

samp

that th

sampl

This is

detecti

an oil p

using ar

the Mic

approxir

the vials

box appe

unknown

peak in negative ion mode was masked by the sample in Figures 4.2b and 4.3b, however the peak was observed in other spectra not presented here. The paper industry commonly employs copper phthalocyanine in the paper manufacturing process. The pigment has been used in paper mass coloration, paper surface treatment, and as an additive to paper pulp (23). Thus, the appearance of the peaks representing copper phthalocyanine in the sample of pigments on paper, is not unexpected.

An extremely dilute aqueous solution of copper phthalocyanine was prepared, so that the solution was visually clear. The spectra (not shown) obtained from 1μL of this sample, dried on a gold plate, revealed that the pigment was still detectable using LDMS. This is encouraging, since it demonstrates that the sensitivity of LDMS allows for the detection of the pigment, even when its presence is not apparent.

When questions arise concerning colorant composition, the subject is more likely an oil painting than a watercolor painting. In the next example, an oil paint was prepared using an "old pigment" and linseed oil. The pigment was found in a box of pigments in the Michigan State University Chemistry Department archives. The box consisted of approximately 100 vials of old inorganic pigments, in a dry powder form. Examples of the vials are shown in Figure 4.6. Images in this dissertation are presented in color. The box appears to be a pigment distributor's product case. The age of the pigments remains unknown, however there were clues indicating that the box is from the early 1900s.

Relative Intensity

Relative Intensity

0

Figur

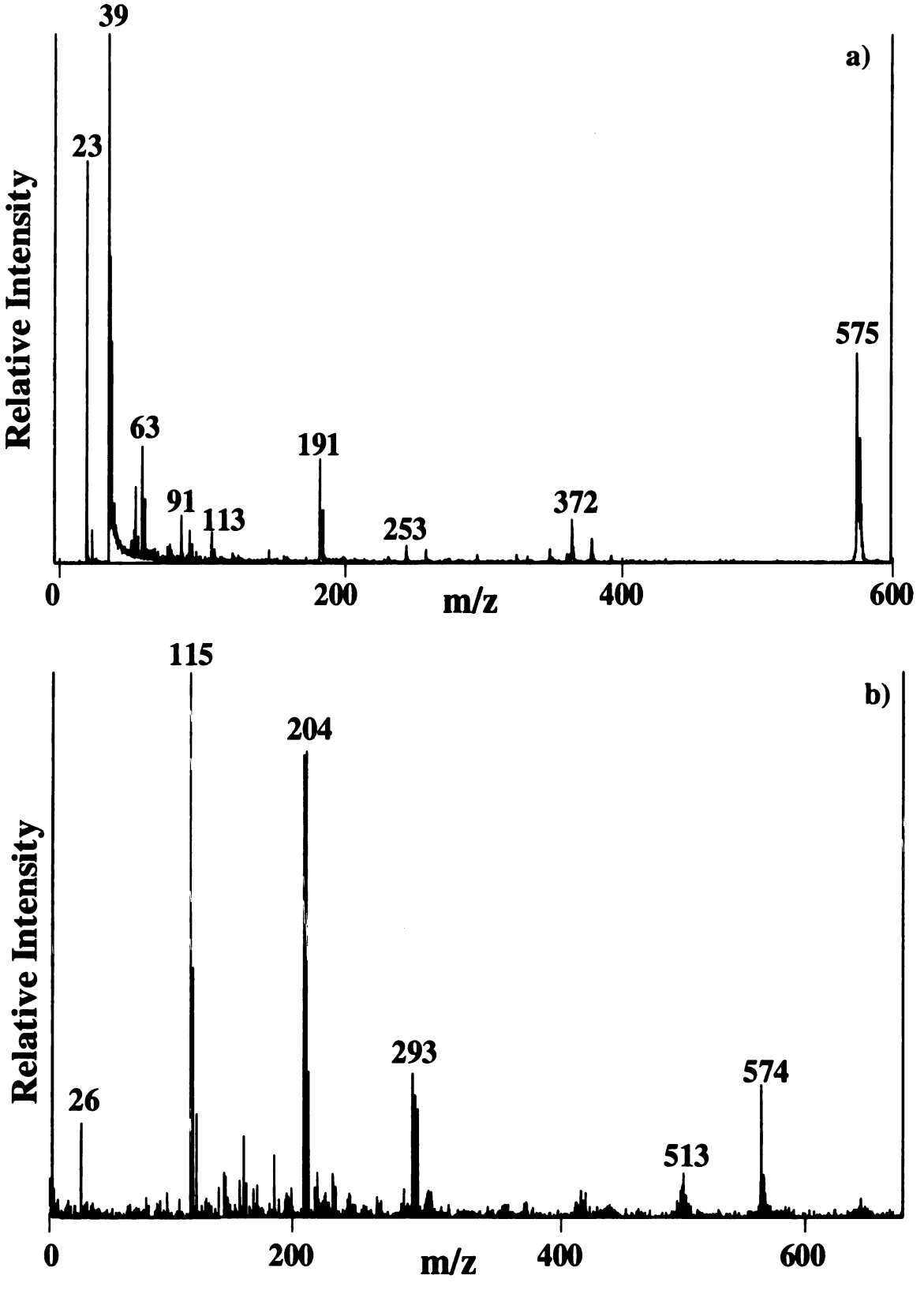

Figure 4.5: The LD mass spectra of paper (HammerMill Fore MP); a) the positive ion mass spectrum; b) the negative ion mass spectrum.

green p

to dry.

these a

suspen

support

(Figure

iron. T

ferrocy

that the

numero

are rela

Fig

"G13"

A green pigment, designated "G13", was selected for LDMS analyses. The dark green powder was suspended in linseed oil, spotted on a gold sample plate, and allowed to dry. Very informative positive and negative ion spectra of G13 were obtained and these are shown in Figure 4.7. Similar spectra were obtained from the pigment suspended in linseed oil and applied to paper. Linseed oil alone, on both paper and metal supports, does not yield ions in the UV LDMS experiment. In the negative ion spectrum (Figure 4.7b), a group of familiar peaks are noted at m/z 134, 150, and 166, containing iron. The isotopic distributions are consistent with our previous assignments for ferric ferrocyanide. Considering that ferric ferrocyanide is a blue pigment, one might presume that there is also a yellow pigment present in the mixture. Fortunately, there are numerous other peaks with characteristic isotopic patterns present in the spectra, which are related to a yellow pigment.

Figure 4.6: Examples of pigment vial from the case of pigments found in the Michigan State University's archives.

Figure

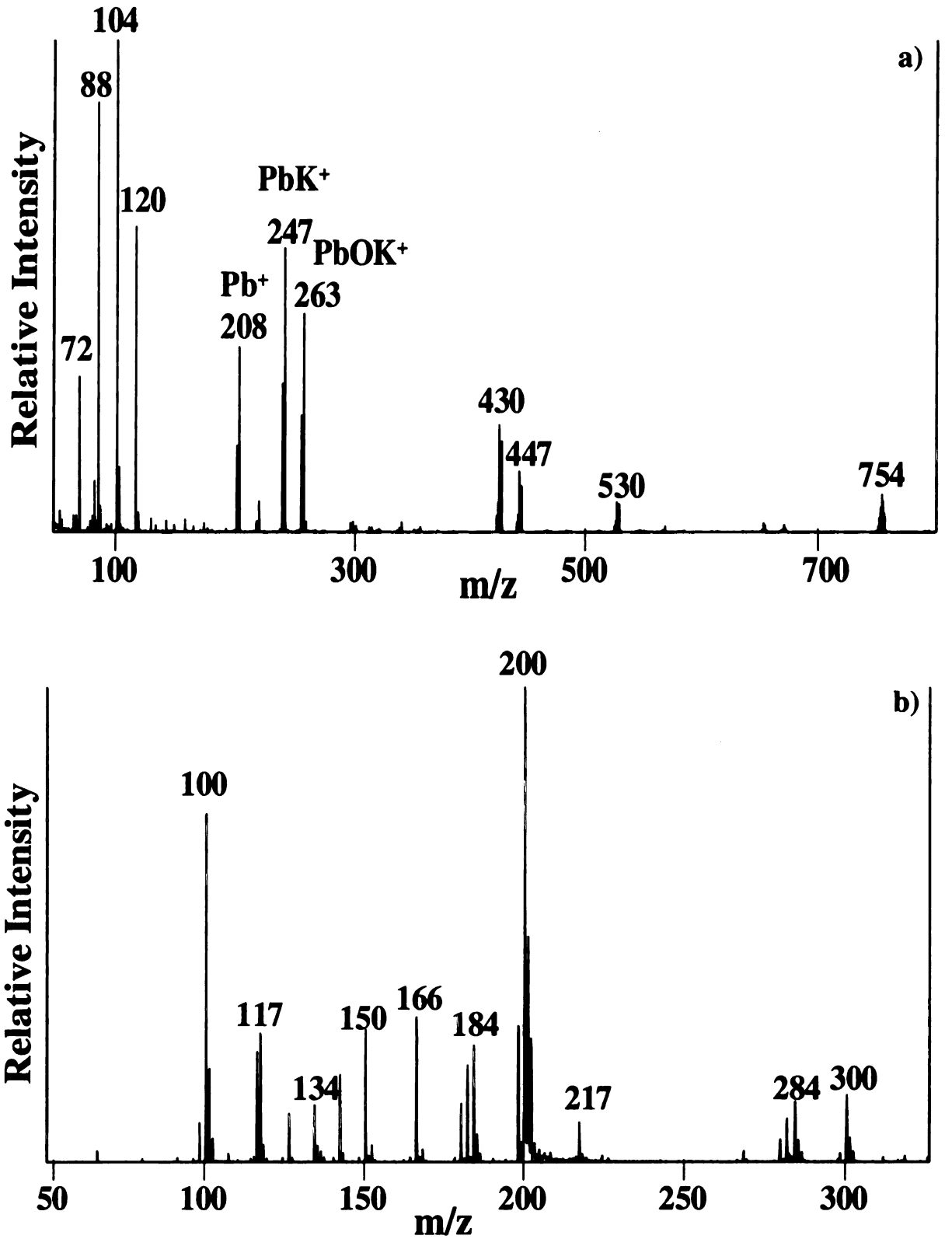

Figure 4.7: The LD mass spectra of G13 in linseed oil on a gold sample plate; a) the partial positive ion mass spectrum; b) the partial negative ion mass spectrum.

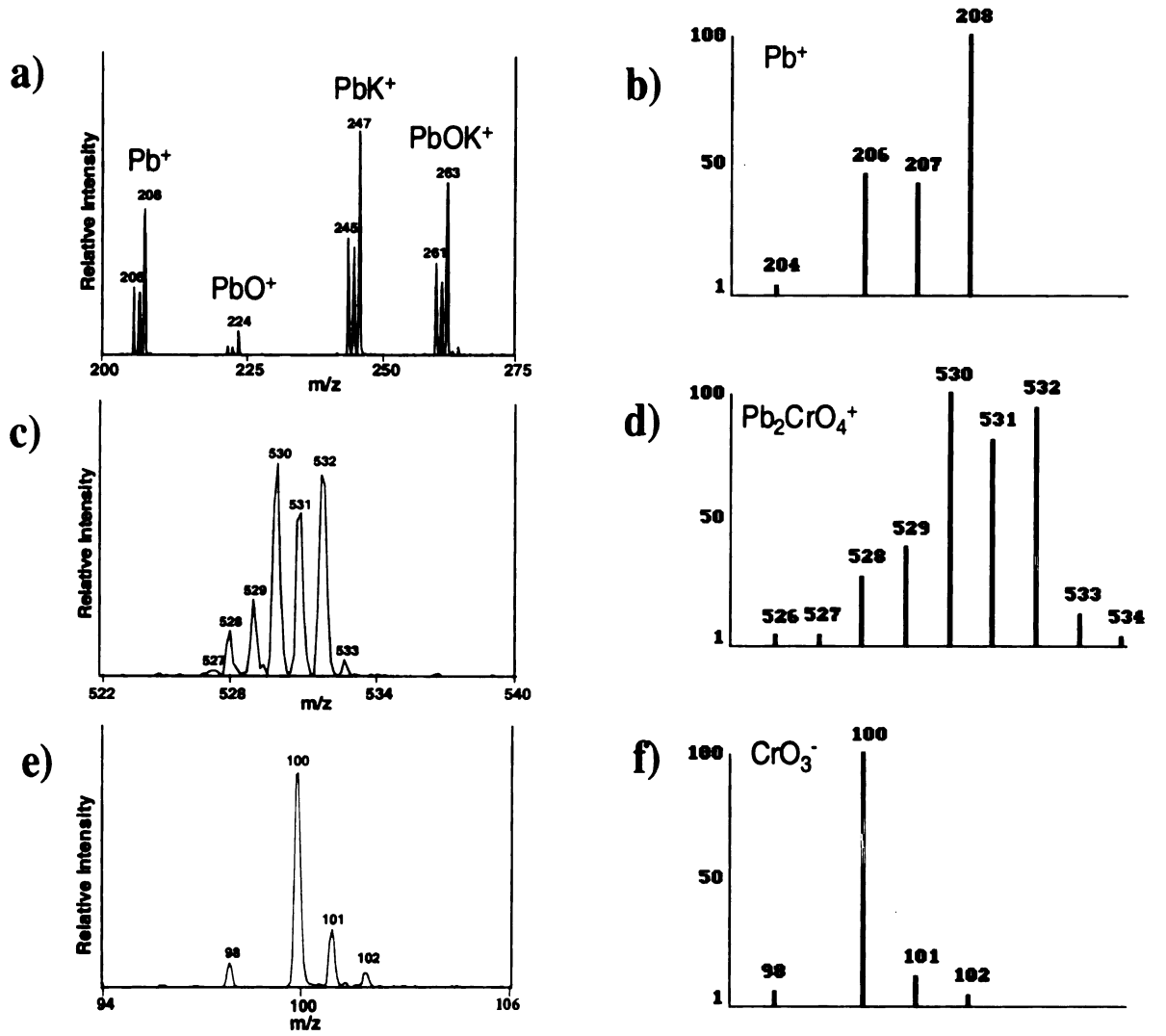

Figure 4.8: Enlarged portions of the positive and negative ion LD mass spectra of G13 in linseed oil on a gold plate; (a, c, e) experimental data; (b, d, f) theoretical mass spectra.

In the positive ion spectrum, Figure 4.7a, there are numerous isotopic patterns consistent with the presence of lead. An enlarged portion of the spectrum is shown in Figure 4.8a. The series begins at m/z 298, representing Pb^+ ions. The isotopic pattern compares well with the theoretical distribution of Pb isotopes (Figure 4.8b). The clusters of peaks 16 and 39 mass units higher are the result of additions of an O atom and a K atom, respectively. The additions do not appreciably alter the isotopic patterns. Lead

chromate is a very popular yellow pigment. Analysis of higher mass peaks reveals the presence of ions containing both lead and chromate. The peaks at m/z 530 represent $Pb_2CrO_4^+$ ions (Figure 4.8c). The additional Pb atom, as well as the presence of a Cr atom, produces a predictable and characteristic isotopic pattern for this ion (Figure 4.8d). The identification of these peaks, along with those at m/z 754 representing $Pb_3CrO_5^+$ ions, were confirmed by comparison with theoretical isotopic patterns. This allows for a confident identification of the ions formed. The remaining peak identifications are listed in Table 4.3. Additionally, confirmatory ions for the presence of the chromate salt can be found mixed in with the ferric ferrocyanide negative ions (Figure 4.7b). In fact, chromium oxide ions appear as the most intense peaks in the mass spectrum, with peaks at m/z 100, 200, and 300 representing CrO_3^-, $Cr_2O_6^-$, and $Cr_3O_9^-$, respectively. An enlarged portion of the mass spectrum displaying the CrO_3^- isotopic peaks is shown in Figure 4.8e. The pattern compares well with the theoretical isotopic pattern in Figure 4.8f. An itemized list (author unknown, shown in Figure 4.9) and a description of the contents of the vials (Figure 4.10) accompanied the box, in which this pigment was found. The contents of G13 were listed as 66.7% $PbCrO_4$ and 33.3% $Fe_4[Fe_3(CN_6)]$. The mass spectra obtained were consistent with the information provided, that the pigment was a blend of two pigments.

G13: Positive and Negative Ions

*m/z	*Assignment*
208	Pb^+
224	PbO^+
247	PbK^+
263	$PbOK^+$
308	$PbCrO_3^+$
347	$PbCrO_3K^+$
363	$PbCrO_4K^+$
430	Pb_2O^+
447	$Pb_2O_2H^+$
530	$Pb_2CrO_4^+$
754	$Pb_3CrO_5^+$
100	CrO_3^-
134	$Fe(CN)_3^-$
150	$Fe(OCN)(CN)_2^-$
166	$Fe(OCN)_2(CN)^-$
182	$Fe(OCN)_3^-$
184	$Cr_2O_5^-$
200	$Cr_2O_6^-$
284	$Cr_3O_8^-$
300	$Cr_3O_9^-$

* m/z value of most abundant isotopic form

Table 4.3: A list of the identified positive and negative ions for G13 in linseed oil.

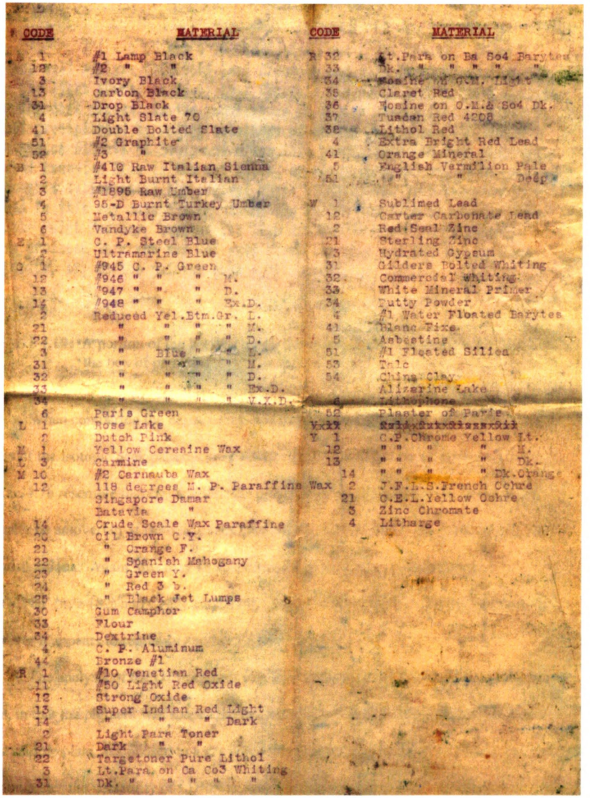

CODE	MATERIAL
1	#1 Lamp Black
13	#2 " "
3	Ivory Black
13	Carbon Black
34	Drop Black
4	Light Slate 70
41	Double Bolted Slate
51	#2 Graphite
59	73 "
1	#410 Raw Italian Sienna
2	Light Burnt Italian
3	#1895 Raw Umber
4	95-D Burnt Turkey Umber
5	Metallic Brown
6	Vandyke Brown
1	C. P. Steel Blue
2	Ultramarine Blue
1	#945 C. P. Green
12	#946 " " " M.
13	#947 " " " D.
14	#948 " " " Ex.D.
	Reduced Yel.Etm.Gr. L.
21	" " " M.
22	" " " D.
3	" Blue " " M.
31	" " " " M.
32	" " " " D.
33	" " " " Ex.D.
34	" " " " Ex.Dk.
6	Paris Green
1	Rose Lake
2	Dutch Pink
1	Yellow Cerenine Wax
3	Carmine
10	#2 Carnauba Wax
12	118 degrees M. P. Paraffine Wax
	Singapore Damar
	Batavia "
14	Crude Scale Wax Paraffine
21	Oil Brown C.Y.
21	" Orange F.
22	" Spanish Mahogany
23	" Green Y.
24	" Red 3 Y.
25	" Black Jet Lumps
30	Gum Camphor
33	Flour
34	Dextrine
4	C. P. Aluminum
44	Bronze #1
1	#10 Venetian Red
11	#50 Light Red Oxide
12	Strong Oxide
13	Super Indian Red Light
14	" " Dark
2	Light Para Toner
21	Dark " "
22	Targetoner Pure Lithol
3	Lt.Para on Ca Co3 Whiting
31	Dk. " " " "

CODE	MATERIAL
32	Lt.Para on Ba So4 Barytes
33	Dk. " " " "
34	Tonine on Ba So4 Dk.
35	Claret Red
36	Tonine on C.P.Ba So4 Dk.
37	Tuscan Red 4608
38	Lithol Red
4	Extra Bright Red Lead
41	Orange Mineral
5	English Vermilion Pale
51	" " Deep
1	Sublimed Lead
12	Carter Carbonate Lead
2	Red Seal Zinc
21	Sterling Zinc
3	Hydrated Gypsum
31	Gilders Bolted Whiting
32	Commercial whiting
33	White Mineral Primer
34	Putty Powder
4	#1 Water Floated Barytes
43	Mono Zinc
5	Asbestine
51	#1 Floated Silica
53	Talc
54	China Clay
	Alizarine Lake
	Blanc Fixe
62	Plaster of Paris
XXX	[illegible]
1	C.P.Chrome Yellow Lt.
12	" " " M.
13	" " " Dk.
14	" " " Dk.Orang
2	J.P.L.S.French Ochre
21	C.P.L.Yellow Ochre
3	Zinc Chromate
4	Litharge

Figure 4.9: An itemized list of the contents of the box.

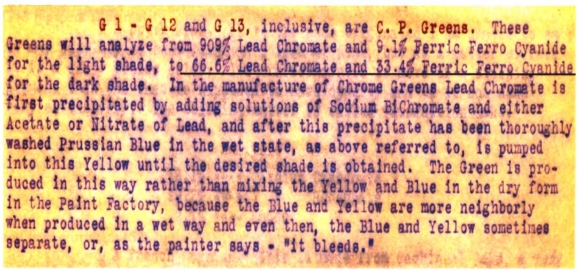
G 1 - G 12 and G 13, inclusive, are C. P. Greens. These Greens will analyze from 90% Lead Chromate and 9.1% Ferric Ferro Cyanide for the light shade, to 66.6% Lead Chromate and 33.4% Ferric Ferro Cyanide for the dark shade. In the manufacture of Chrome Greens Lead Chromate is first precipitated by adding solutions of Sodium BiChromate and either Acetate or Nitrate of Lead, and after this precipitate has been thoroughly washed Prussian Blue in the wet state, as above referred to, is pumped into this Yellow until the desired shade is obtained. The Green is produced in this way rather than mixing the Yellow and Blue in the dry form in the Paint Factory, because the Blue and Yellow are more neighborly when produced in a wet way and even then, the Blue and Yellow sometimes separate, or, as the painter says - "it bleeds."

Figure 4.10: A portion of the list describing the contents of the pigment vials found in the box of pigments.

When comparing the negative ion spectra of Prussian blue and G13, differences in a few of the isotopic peak patterns are evident. For instance, the peaks at m/z 134 in Figure 4.7b resemble that expected for the presence of two Cr atoms. The peaks could actually be an overlap of isotopic peaks for $Fe(CN)_3^-$ and Cr_2NO^-. The peaks at m/z 184 are also unique. Again, this may be an overlap of isotopic peaks for two ions: $Fe(OCN)_3^-$ (m/z 182) and $Cr_2O_5^-$ (m/z 184). The peak at m/z 180 is still unidentified, however it appears to represent another Fe-containing ion.

The analysis of the G13 pigment was very different from the analysis of Prussian blue, in that the pigment was suspended in a transparent medium (dried linseed oil) on a gold sample plate, as opposed to a dry watercolor paint sample on paper. This demonstrates the versatility of LDMS to detect different types of paint samples on a variety of surfaces, and in a complex matrix. Additionally, the Prussian blue pigment

was a single component, whereas G13 was a mixture of two pigments. Even though the G13 pigment is primarily composed of lead chromate, which would be expected due to the high tinting strength of Prussian blue, both components are still easily detected. This demonstrates that LDMS may be used to detect the presence of multiple pigments in a mixture, which as stated earlier, can be a limitation for other analytical methods in the analysis of a complex paint. For example, Figure 4.11 shows the energy dispersive x-ray (EDX) spectra of Prussian blue and chrome green, which is a mixture of Prussian blue and lead chromate (5). In the EDX spectrum of Prussian blue (Figure 4.11a), there are peaks present representative of Fe, however there is no evidence that it is an iron cyanide pigment. In the EDX spectrum of chrome green (Figure 11.b) peaks representative of Pb and Cr are noted, with some Ti and Si impurities. However, the absence of Fe is noted. This is a specific example which illustrates a case in which the concentration of Prussian blue was so low, that it did not meet the detection limit of this instrument.

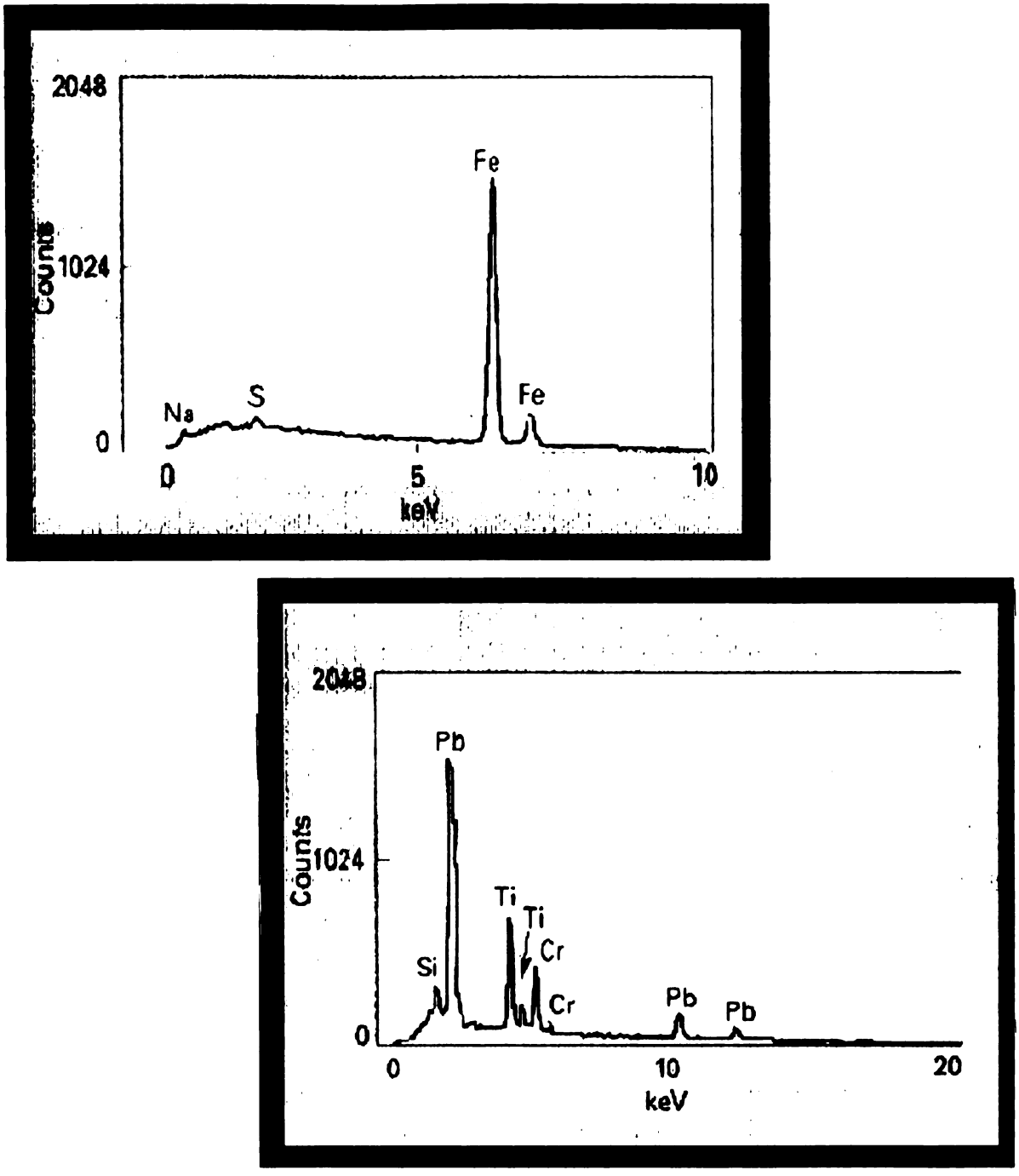

Figure 4.11: Energy dispersive x-ray spectra; a) Prussian blue; b) chrome green.

is use

ident

an il

4.12

4.13

Yo

ma

Yo

ap

sa

ic

e

The LDMS analysis of two illuminated manuscripts

LDMS is introduced here as a potential tool for the detection of art forgeries, and is used to determine if the two documents in question could be authentic, based on the identification of the colorants present. Samples analyzed using this technique included an illuminated page of the Koran, reported to be approximately 400 years old (Figure 4.12), and a decorated page of a Hebrew manuscript allegedly from the 1800s (Figure 4.13). Both were obtained from the Sadigh Gallery (303 Fifth Avenue, Suite 1603, New York, NY). Pigment standards that were analyzed in this work included vermilion, malachite, verdigris (Sinopia, San Francisco, CA), and orpiment (Kremer Pigments, New York). The vermilion sample was suspended in a 50/50 solution of water/gum Arabic, applied to standard printer paper, and dried. The malachite, verdigris, and orpiment samples were suspended in linseed oil, applied to paper, and dried. Positive and negative ion mass spectra were also obtained of the standard gold 100-well plate to serve as an example of authentic gold.

Figure 4.12: A page of the Koran, allegedly from the 17th century.

Figure 4.13: A page from a Hebrew manuscript, allegedly from the 1800s.

Example 1

A pen stroke from a red Bic® pen, on paper, was introduced into the instrument and irradiated by the nitrogen laser. The mass spectrum shown in Figure 4.14 was obtained. This represents the positive ions formed by laser irradiation. The peak at m/z 443 represents the intact dye molecule Rhodamine 6G. This is a positively-charged (cationic) dye molecule with the formula $C_{28}H_{31}N_2O_3^+$. With each C weighing 12 atomic mass units (amu), H weighing 1 amu, etc., Rhodamine 6G molecular ions weigh 443 amu. This is a very commonly-encountered red dye. Since it is naturally positively-charged, a strong peak representing the intact molecule is detected in positive ion LDMS. In the negative ion LDMS spectrum, no peak is present representing the dye (spectrum not shown). In our experience, we have seen that negatively-charged dyes only yield negative ions, and neutral dye molecules yield both positively and negatively charged forms of the intact dye (24,25). In Figure 4.14, the peak at m/z 23 represents Na^+ ions and that at m/z 39 represents K^+ ions, commonly found in most samples.

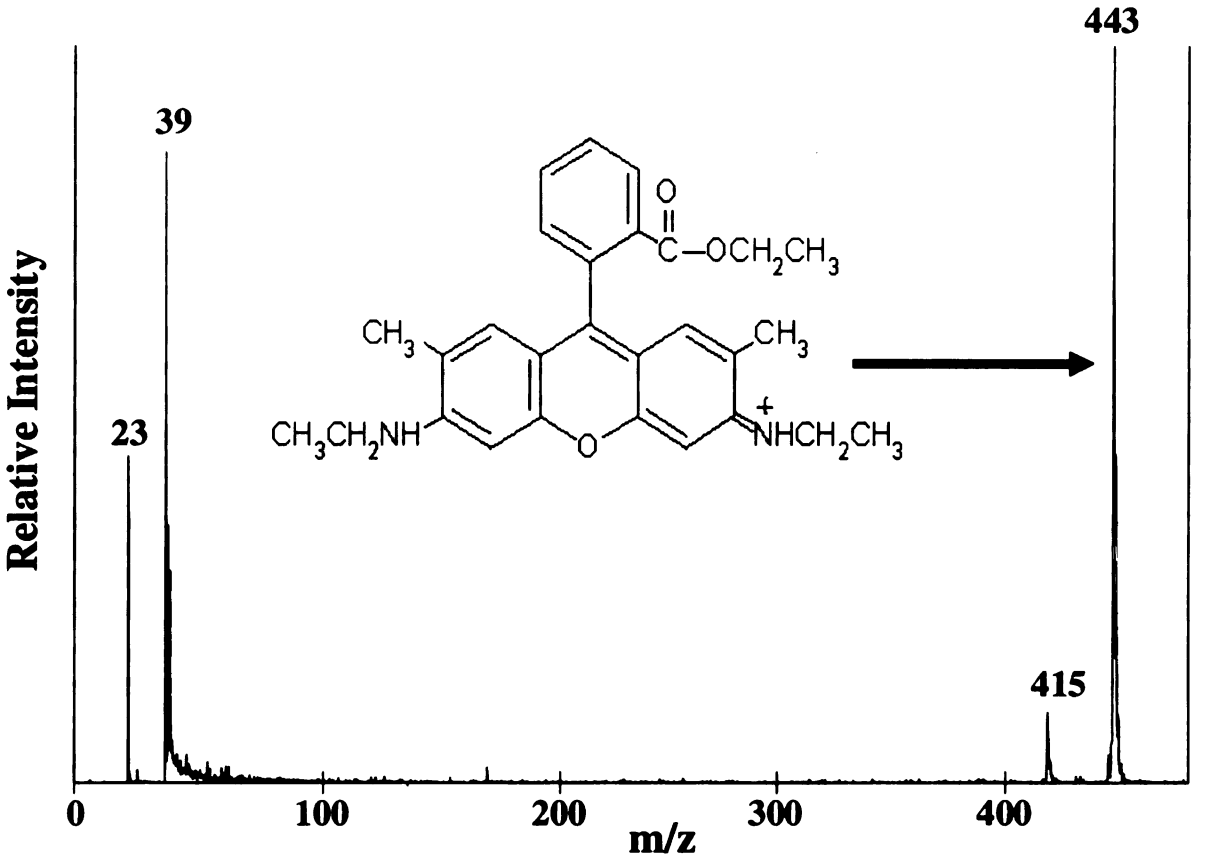

Figure 4.14: The positive ion LDMS spectrum of rhodamine 6G. The structure of the dye is shown. The singly charged dye molecule has a monoisotopic molecular mass of 443.

Example 2

In contrast, if a metallic gold (Au) surface, an inorganic sample, is irradiated with the UV laser, both positive and negative ions are formed. The positive and negative ion LDMS spectra for gold are shown in Figures 4.15a and b, respectively. In Figure 4.15a, there is a peak at m/z 197, which corresponds to the m/z value for a singly charged gold atom. Peaks representing clusters of two and three gold atoms, as singly-charged chemical species, are also observed at twice and three times the mass of atomic gold. Similar ions are observed in the negative ion spectrum (Au^- through Au_3^-). Unlike an

orga

repr

proc

met

gol

2.3

suc

rea

(S

st

p

li

i

organic dye, which exists as a collection of individual, discrete molecules, a gold surface represents a three-dimensional array of atoms. Apparently during the laser desorption process, not only atomic ions but small ionic clusters can easily be formed. Not all metals can form stable negative ions. Chemists are more familiar with positively-charged gold atoms than negatively charged gold atoms. Gold atoms have an electron affinity of 2.3 eV, indicating that they can stabilize a negative charge (extra electron). Some metals, such as titanium, have much larger electron affinities (7.9 eV), and therefore may more readily form negative ions. This is not the case with all metals. For example, scandium (Sc) has an electron affinity close to zero (0.18 eV) indicating that Sc^- may not be a stable species in the gas phase (26). Using such considerations, LDMS spectra can provide information on species present in any type of target which can 1) absorb the UV light from the laser and 2) be desorbed and ionized, to yield singly-charged gas phase ions for subsequent MS analysis, in this case, by a time-of-flight mass spectrometer.

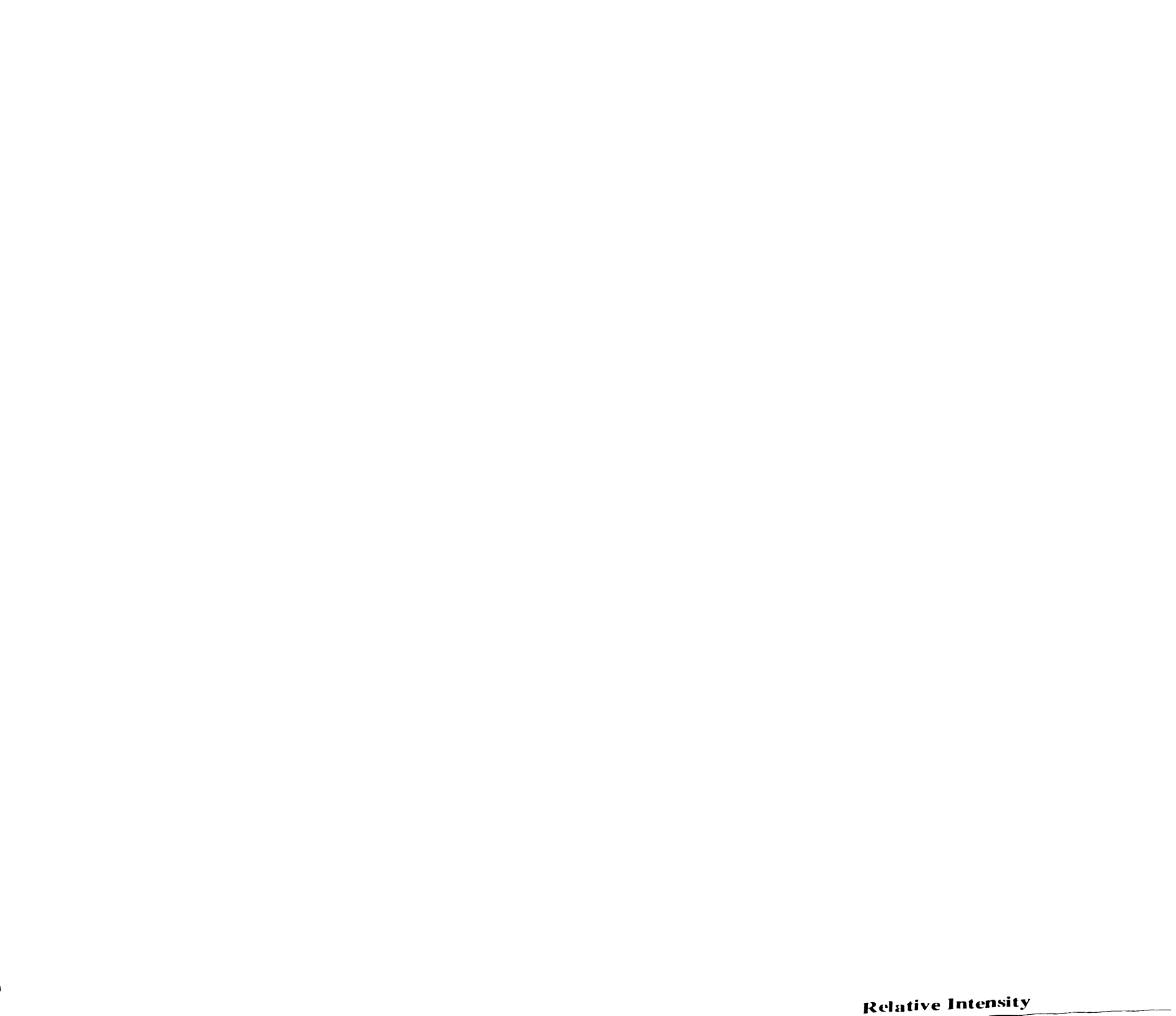
Relative Intensity

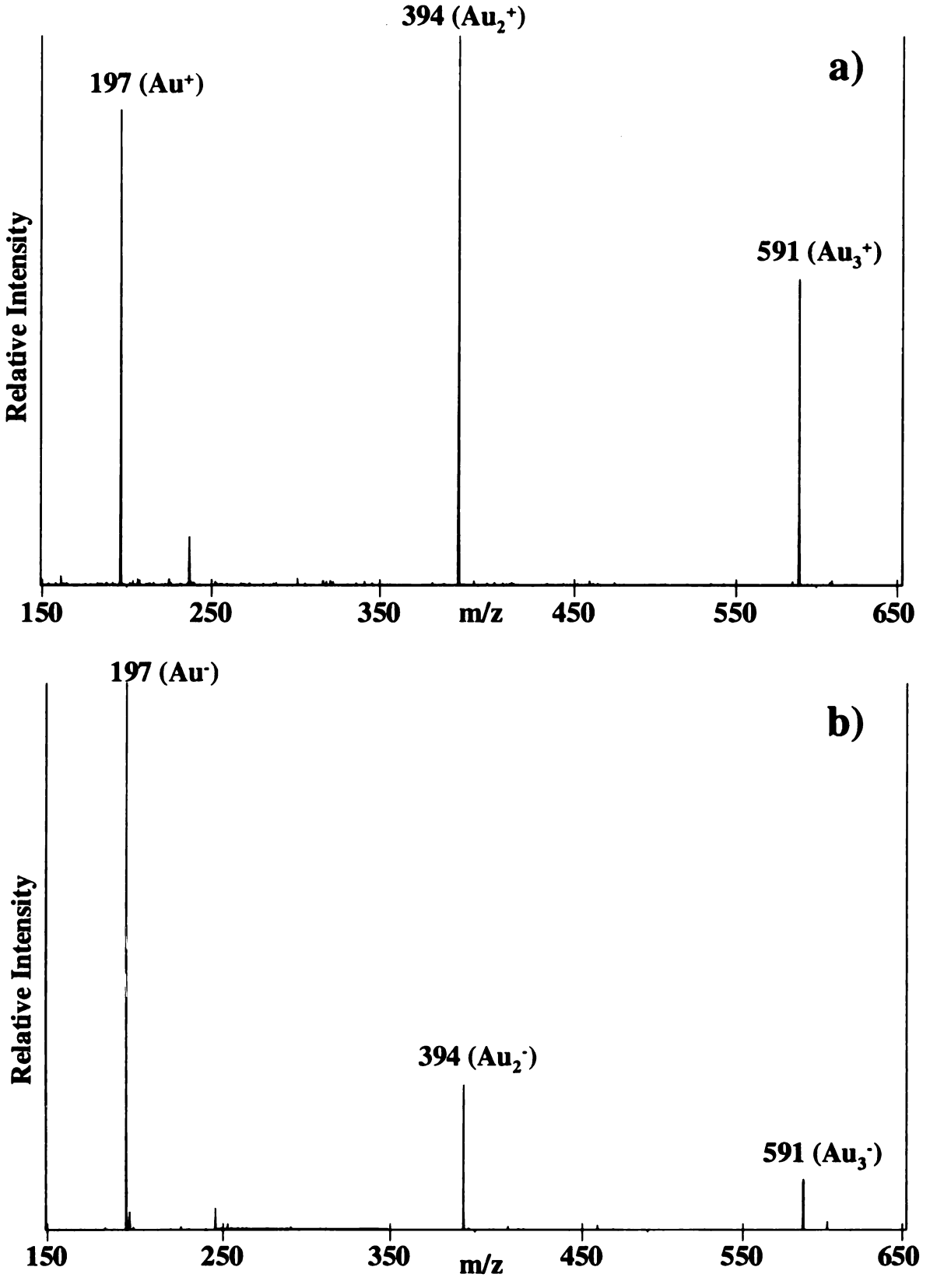

Figure 4.15: LDMS spectra of the ions formed by UV laser irradiation of a gold surface. a) positive ion LDMS spectrum; b) negative ion LDMS spectrum.

Figure 4.16 shows a portion of the illuminated page of the Koran from the 1600s that was analyzed. The text is written in black ink with red diacritical marks, and the page is illuminated using gold, red, and black inks. For the analysis, both positive and negative ion LDMS spectra were obtained for each of the colors used in the document.

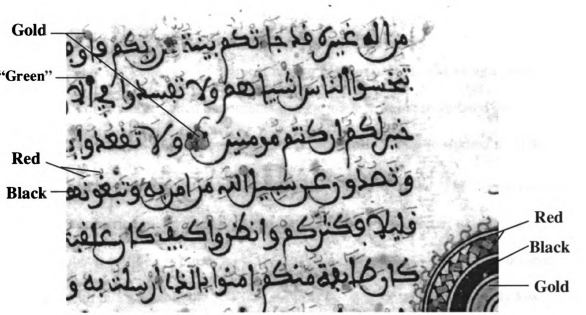

Figure 4.16: A portion of the page of the Koran used in this study.

Red

The first color on the Koran sample analyzed was the red pigment. Information sufficient to establish its identity was present in the negative ion spectrum (Figure 4.17a), so that will be the focus of this discussion. A series of peaks separated by 32 mass units (m/z 32, 64, 96, 128, 160, 192) dominate the spectrum. In mass spectrometry, a mass of 32 amu most likely represents two oxygen atoms (16 amu each) or one sulfur atom. The latter is more likely, thus the ions from m/z 32 to 192 represent sulfur cluster ions from S^-

through S_6^-. Sulfur does not suffice as a colorant alone, however its dominance in the spectrum indicates that it is a major elemental component of the pigment. Seventeenth century artists used a variety of red pigments, including red lead, several red lakes, and vermilion (HgS) (27). We have previously analyzed lead-containing pigments such as $PbCrO_4$; lead and lead-containing ions are commonly formed from such salts (25). None are observed here.

Lakes are a special type of pigment having both an organic and an inorganic component. For example, when the organic dye carminic acid is precipitated onto alumina, Al_2O_3, the red pigment carmine lake is produced. We have studied this lake previously, and its laser desorption mass spectrum has been reported (25). Vermilion, or the naturally occurring mineral analog, cinnabar, is a natural possibility to investigate, since it is a metal sulfide. A closer look at Figure 4.17a reveals a number of peaks that are formed with m/z values in the 300-600 range of the spectrum, with relatively low intensities. This region of the spectrum, in expanded form, is shown in Figure 4.17b. The clusters of peaks are very important, because they represent isotopic variants of the ionic species formed.

Fig

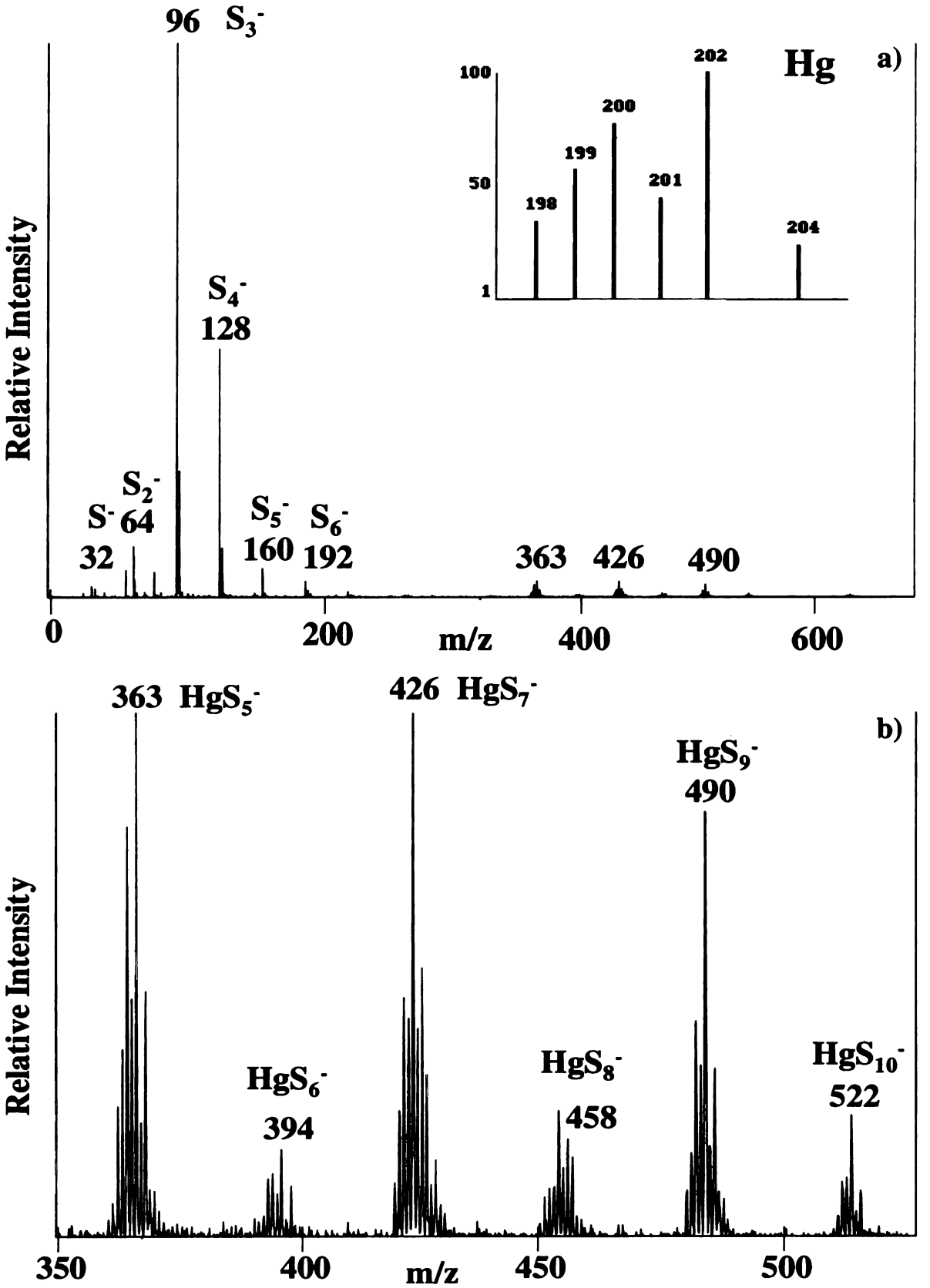

Figure 4.17: a) Negative ion LD mass spectrum of the red ink/dye region of the Koran sample. b) Expanded view of the higher m/z portion of the spectrum.

In mass spectrometry, all of the isotopic forms that exist in nature for each element are realized. For example, in Figure 4.17a, all of the S_n^- ion peaks have an additional peak 2 atomic mass units higher. These are due to the fact that, while most sulfur atoms exist with atomic masses of 32 amu, 5.4% of all sulfur atoms exist as ^{34}S, weighing 2 amu more than the most abundant isotope, ^{32}S. This is seen in the mass spectrum. The distribution of isotopes for mercury is much more complex - 6 isotopic forms, from ^{198}Hg through ^{204}Hg, are found in nature. The theoretical distribution is shown in the inset in Figure 4.17a for one mercury atom. The number and pattern of the relative abundances of the isotopes clearly indicate that the peak at m/z 363 contains a mercury atom. The m/z value is consistent with the peaks around m/z 363 representing the ionic species HgS_5^-. Ionic species representing HgS_5^- through HgS_{10}^- are observed in this spectrum. In some cases, the clusters of peaks do not exactly match up with ionic formula of the type $Hg_xS_y^-$. The probable cause is the fact that there are also species with very similar mass being formed, containing a single hydrogen atom. For example, the set of peaks around m/z 426 probably represent HgS_7^- and a small amount of HgS_7H^-. This is not unexpected. Burnin and BelBruno (28) reported similar observations in the formation of $Zn_xS_yH_z^+$ clusters from laser ablation of ZnS. The key point is that the dominant ions in the negative ion LDMS spectrum of the red ink indicated that the pigment present is a sulfide. Less intense peaks clearly indicate that it is mercury sulfide. While it was not anticipated that the compound would form species

such as HgS_7^-, this is part of what is learned in LDMS experiments - how components of a pigment combine to form stable gas phase ions that can be detected.

In addition to the information that the mass spectrum provides, a vermilion sample was obtained from an artist pigment distributor, Sinopia. The vermilion was suspended in a solution containing water and gum arabic, "painted" onto paper, and analyzed. The same mass spectrum was obtained (not shown), confirming the assignment.

Current methods for the identification of vermilion in art work include microchemical tests (29-32), x-ray diffraction (33,34), emission spectroscopy (35), infrared spectrophotometry (36-38), x-ray fluorescence (31), electron probe microanalysis (31), and x-radiography (39). While microchemical tests are ideal for indicating the presence of Hg and S, they are destructive. Additionally, x-ray diffraction analysis can lead to a positive identification for HgS, however the sample must be pure, as in many of the other techniques. Here, LDMS excels in that it is well-suited for the analysis of mixtures, such as those found on a painting. Similar spectra (not shown) of the naturally occurring HgS pigment (cinnabar, Sinopia) were also obtained. It does not appear that LDMS can distinguish between the cinnabar and the synthetically manufactured vermilion.

In summary, the major ions of the spectrum shown in Figure 4.17a indicate that the red colorant is a sulfide, less intense peaks clearly indicate that it is a mercury sulfide. Comparison of the spectrum with that of a known mercury sulfide sample identifies the colorant as HgS, vermilion. This colorant has a long and extensive history, and its presence is not unexpected for a manuscript from the 1600s. Figure 4.17a clearly shows

that the red colorant is not a modern organic dye such as a red Rhodamine dye (Figure 4.14).

Gold

If the laser is moved to irradiate a gold portion of the manuscript page, the spectrum changes. The positive and negative ion mass spectra obtained from this region are shown in Figures 4.18a and 4.18b. Clearly, the spectra do not suggest the presence of elemental gold (Figure 4.15). This is not unexpected since chrysography (painting in gold) was largely phased out in the 15^{th} century, due to the high cost of gold in any form (27). Thus, some other pigment or dye is present to give a golden, metallic color.

The positive ion LD mass spectrum, Figure 4.18a, shows four peaks separated by 32 mass units, again suggesting the presence of a sulfide. In the negative ion mass spectrum, differences of 32 (e.g., m/z 138 to 170) and 75 (e.g., m/z 170 to 245) are noted. An atomic mass of 75 corresponds to the element arsenic, As. In the 1600s a variety of yellow pigments were being used as a cheap alternative to gold. These include lead tin yellow, lead antimonate, and a variety of yellow lake pigments such as saffron lake (27). The pigment orpiment has been cited as a popular choice of artists to serve as a substitute for real gold (27). The name orpiment is derived from the latin *auripigmentum*, meaning the color of gold. Alchemists described the pigment as a "handsome yellow more closely resembling gold than any other color", and at one time it was believed to contain gold (27,40,41). Orpiment is arsenic trisulfide, As_2S_3.

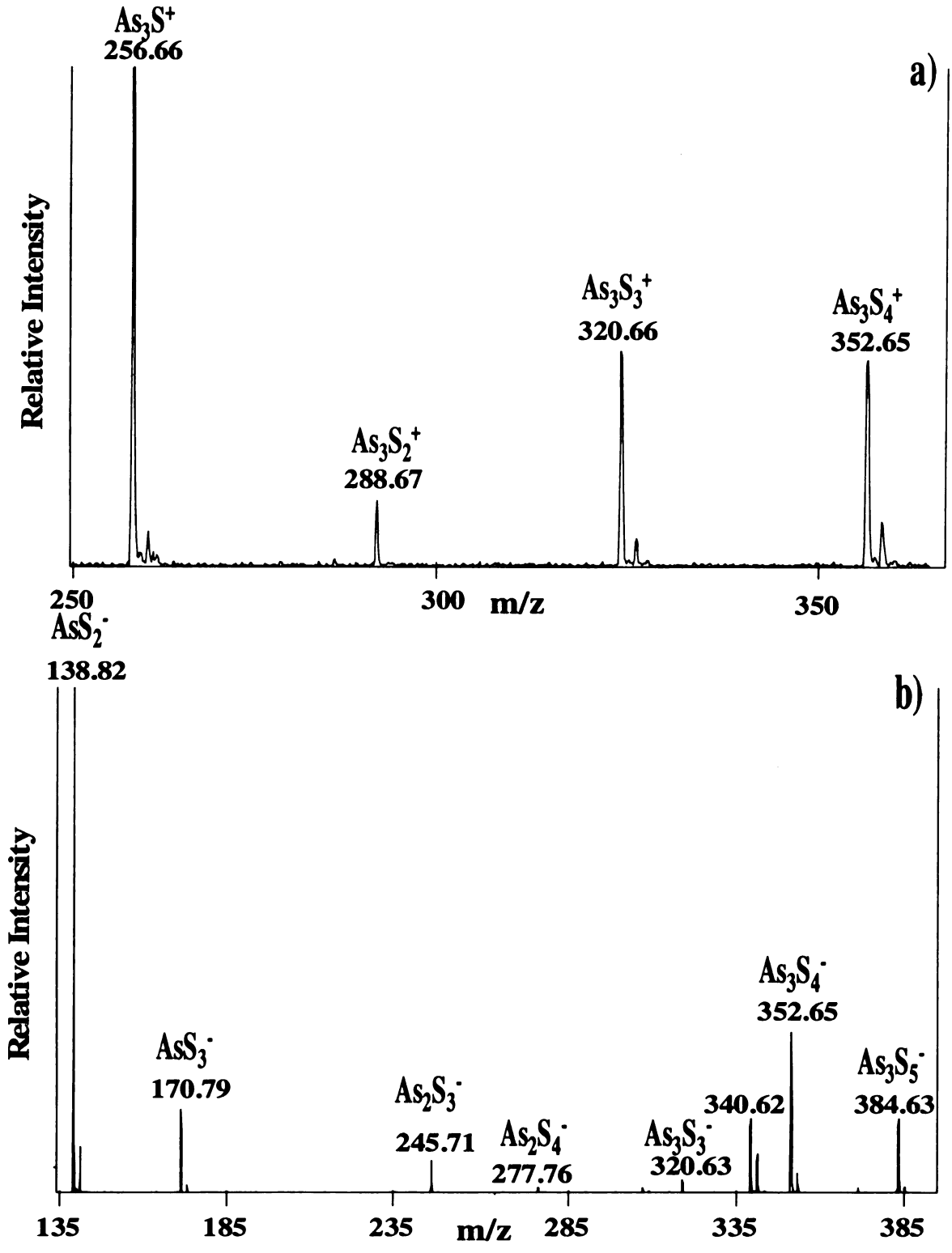

Figure 4.18: a) The partial positive ion and b) the partial negative ion LD mass spectra of the gold region of the Koran sample.

In mass spectrometry, identifications are made based on the isotopic composition of gas phase ions as determined by 1) the m/z value of the ions, 2) the isotopic variants of that ion, and occasionally 3) the accurate mass of the peaks. For many kinds of mass spectrometry, the m/z value can only be determined to the nearest m/z value ("unit mass resolution"). Both As and S atoms contain negative mass defects. That is, while the nominal mass of an As atom is 75, the exact mass is 74.9216 amu – a difference of -0.0784 amu. A similar situation exists for S. The ^{32}S atom has an atomic mass of 31.9721 mass units – a difference of -0.0279 amu. When several of these atoms are combined, the deviation from the calculated nominal mass becomes significant. For example, consider the ion As_3S^+. Using the nominal masses of As and S, its molecular mass is 257 amu. In the accurately calibrated mass spectrum (Figure 4.18a), there is a peak at m/z 256.66 (theoretical, m/z 256.74) representing these ions. The difference between the nominal and experimental values (-0.3 amu) can be accounted for when the exact masses of As and S are considered.

In both the positive and negative ion mass spectra, the m/z values are consistent with the presence of As and S. In the positive ion spectrum, ions with the general formula $As_3S_n^+$ (n = 1-4) are generated. In the negative ion spectrum, ions with the general formula $As_mS_n^-$ are detected. To confirm that the pigment used here is actually orpiment, positive and negative ion LD mass spectra were taken of the actual pigment obtained from Kremer Pigments. Again, the spectra of the unknown match the spectra of the standard (not shown).

The appearance of orpiment on the manuscript is not surprising. It has been identified in Armenian, Arab and Persian manuscripts from the period in question (42).

Again, the laser desorption mass spectra clearly indicate that the compound is a sulfide, and that it is arsenic sulfide.

Black

Black inks are traditionally very difficult to chemically identify, since (prior to the introduction of modern pen inks) the colorants used were very complex mixtures of chemical species, not single compounds. One example is carbon black, a complex mixture of carbon and hydrocarbon particles. A second example is iron gallotannate ink, also a mixture of many compounds, since it is made from an extract of gall nuts, which are shown in Figure 4.19 (43). Galls are created by parasites (aphids, flies, wasps) to house their eggs, in various types of vegetation. They contain a high concentration of gallotannic acid (penta-gallolylglucose), which is extracted to make Fe-gall ink. Gallotannic acid is a glucose molecule (Figure 4.20a) with up to 5 gallic (3,4,5-trihydroxy-benzoic acid, 170 amu) (Figure 4.20c) and/or digallic acid groups (322 amu) (Figure 4.20b) attached. The gallotannic acid is dissolved in a solution of water and gum Arabic. Gum Arabic is a water soluble vegetable gum from the Acacia tree, which serves as suspension agent for insoluble pigment particles. Gum Arabic is also chosen to adjust the ink's viscosity (42).

Upon the addition of vitriol ($FeSO_4$) to the mixture, a water soluble ferrous tannate complex is formed. The solubility factor is crucial, since it allows the ink to penetrate the paper's surface. The initial ferrous tannate complex is colorless. Consequently, a natural or synthetic dye (logwood, indigo, aniline dye) may be included in the ink mixture in order to increase the visibility of a freshly prepared ink. Once the

ink is applied to paper, it is exposed to oxygen in the air. An insoluble ferric tannate pigment is precipitated, resulting in the dark blue/black permanent Fe-gallotannate ink (44).

There is some dispute over the true structure of the ferric tannate pigment. The chemical structure was investigated by C. H. Wünderlich and C. Krekel (45-47). They agree that the Fe II ions of the vitriol react with both gallic acid and gallotannic acid. However, Wünderlich believes Fe reacts with the 3 hydroxyl groups of gallic acid and with the carboxyl group, creating a three dimensional structure. Thus, the color formation in the ferric tannate complex is due to the benzene ring and oxygen/iron bonds (45,46). Krekel's research suggests that the black pigment is an iron pyrogallol complex instead of an iron gallic acid complex (47). The exact nature of the ferric tannate pigment has not been confirmed.

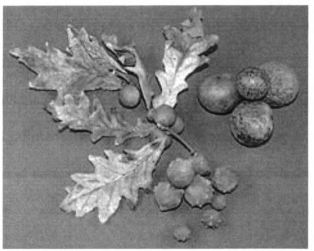

Figure 4.19: Gall nuts.

The ingredients for making iron gallotannate ink were obtained, and a batch of iron gallotannate ink was prepared in our laboratory. Positive and negative ion LD mass spectra (Figure 4.21) were obtained of the freshly prepared ink on paper. Table 4.4 lists all of the different possible combinations in which gallic and digallic acid molecules could attach to gallotannic acid. The tables provide the m/z values that we were expecting in the mass spectra. These values do not take into account that there may be Fe atoms attached, simply because the smallest possible ion formed would have a m/z value of 390 (336 amu + 54 amu), and peaks of significant intensity were not observed in either the positive or negative ion mass spectra.

Only a few peaks have been identified thus far, which are related to gallic acid. In the negative ion mass spectrum (Figure 4.21b), a peak is present at m/z 169, representing deprotonated gallic acid molecules. The peaks at m/z 152 and 124, represent neutral losses of a hydroxyl group and a carboxylic acid group from the deprotonated molecule, respectively. The negative ion mass spectrum (not shown) of gallic acid (Aldrich) suspended in gum Arabic and analyzed on a gold sample, coincided with these assignments. Additionally, there is a relatively small peak at m/z 321, which may represent deprotonated tannic acid molecules. The remainder of the peaks in the spectra of the homemade iron gallotannate ink remain unassigned. At this point, the spectra will be used as a fingerprint to compare with the spectra obtained of the black ink on the page of the Koran.

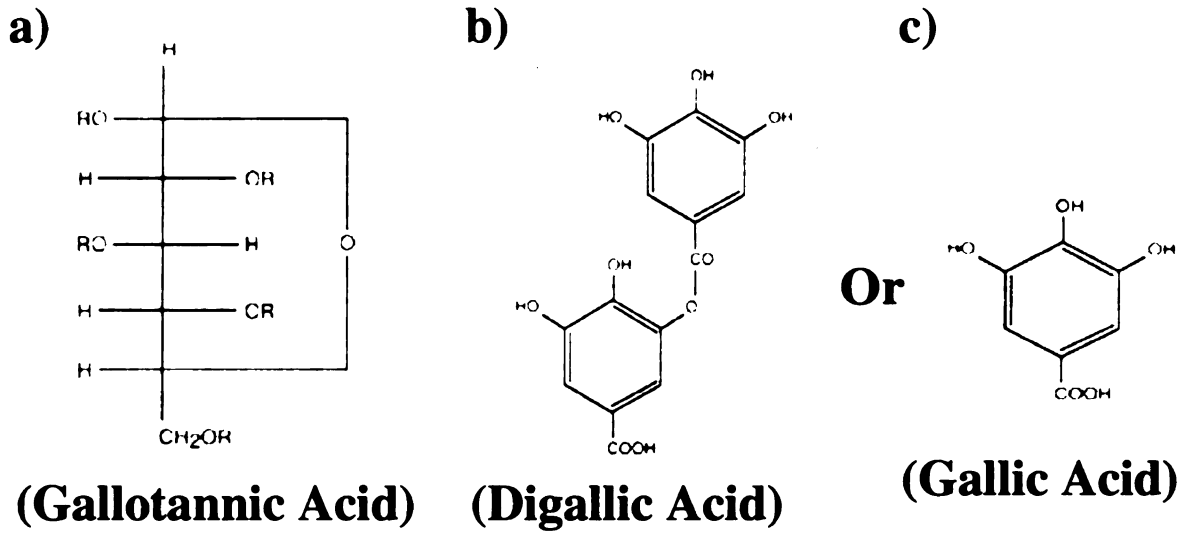

Figure 4.20: Structures of gall nut components.

R_1	R_2	R_3	R_4	R_5	MW (Da)
G	G	G	G	G	**940**
G	G	G	G	D	**1092**
G	G	G	D	D	**1244**
G	G	D	D	D	**1396**
G	G	D	D	D	**1548**
D	D	D	D	D	**1700**
G	G	G	G	H	**789**
G	G	G	H	H	**638**
G	G	H	H	H	**487**
G	H	H	H	H	**336**

G = Gallic Acid
D = Digallic Acid

R_1	R_2	R_3	R_4	R_5	MW (Da)
D	D	D	D	H	**1397**
D	D	D	H	H	**1112**
D	D	H	H	H	**827**
D	H	H	H	H	**542**
G	G	G	D	H	**941**
G	G	D	D	H	**1093**
G	D	D	D	H	**1245**
G	G	D	H	H	**790**
G	D	D	H	H	**942**
G	D	H	H	H	**639**

Table 4.4: A summary of possible molecular weights of the components of gallotannic acid.

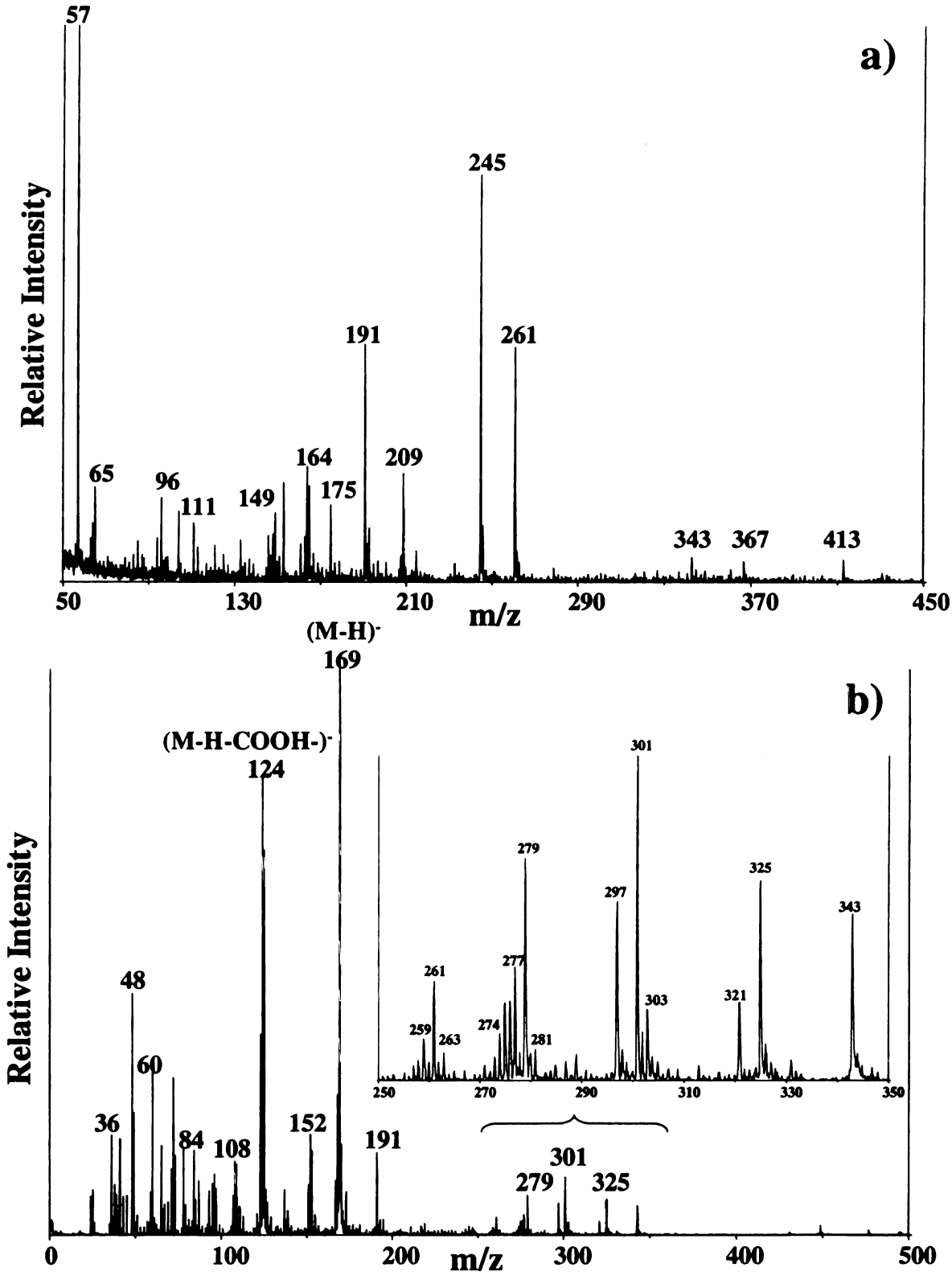

Figure 4.21: a) The partial positive ion and b) the negative ion LD mass spectra of homemade iron gallotannate ink on paper.

The positive and negative ion mass spectra of the black writing ink on the page of the Koran are shown in Figures 4.22a and 4.22b. No identifications have been made in the positive ion mass spectrum. Comparing the spectra in Figure 4.21 to the spectra in Figure 4.22, the ink does not appear to be iron gallotannate ink. In the negative ion mass spectrum, the lower mass range is dominated by anionic carbon cluster peaks such as C_4^- (m/z 48), C_5^- (m/z 60), C_6^- (m/z 72), etc., separated by 12 atomic mass units. While this may appear to be convincing evidence for the presence of carbon black, it is not necessarily the case. While infrequent, some aromatic organic compounds very easily char when exposed to high power UV light, forming essentially a C_n skeleton. This could be the case here. The carbon cluster anionic peaks may even evolve from a component of the paper itself. Peaks are present in the spectrum shown in Figure 4.22b which have been identified as $CuCl_2^-$, $Cu_2Cl_3^-$, and $Cu_3Cl_4^-$, based on the m/z values and isotopic distribution analysis. Returning to the negative ion mass spectrum of the gold pigment on the Koran (Figure 4.18b), the presence of Cu is also suggested by the peak at m/z 341. This peak cluster has been tentatively assigned as $CuAs_2S_4^-$. Copper is not a commonly used ink component. However, copper resinate has been cited as a pigment used on manuscripts during this time period (48-50). This observation has not been well-supported (51). Additionally, the incompatibility of orpiment with copper-containing pigments was well known by this time (52), which could mean that a copper salt may have simply been an impurity in the ink. The only conclusion which can be made for certain is that the ink is not modern.

As a side note, a visual examination is sometimes employed to help distinguish between carbon black and iron gallotannate ink. Carbon black ink is known to be

permanent and noncorrosive to the paper it is applied to. However, it is known to smudge easily before it is completely dry. Iron gallotannate ink, on the other hand, does not smudge, but is known to turn yellow along the edges. This is in fact due to the deterioration of paper caused by the ink. When examining the black used to create the manuscript, one might argue that both were used. When analyzing the text, there are no signs of the paper degrading or yellowing around the ink, which suggests the presence of carbon black. However, the black ink in the medallion of the page has caused serious deterioration of the paper, which is evident on the back side of the page (shown in Figure 4.12). This was the only area in which paper damage resulting from the ink was noted, which makes one wonder if a different type of ink was used to decorate the manuscript, and another used to write the document. It is not known to be a common practice, however it would explain the observation.

10
Relative Intensity

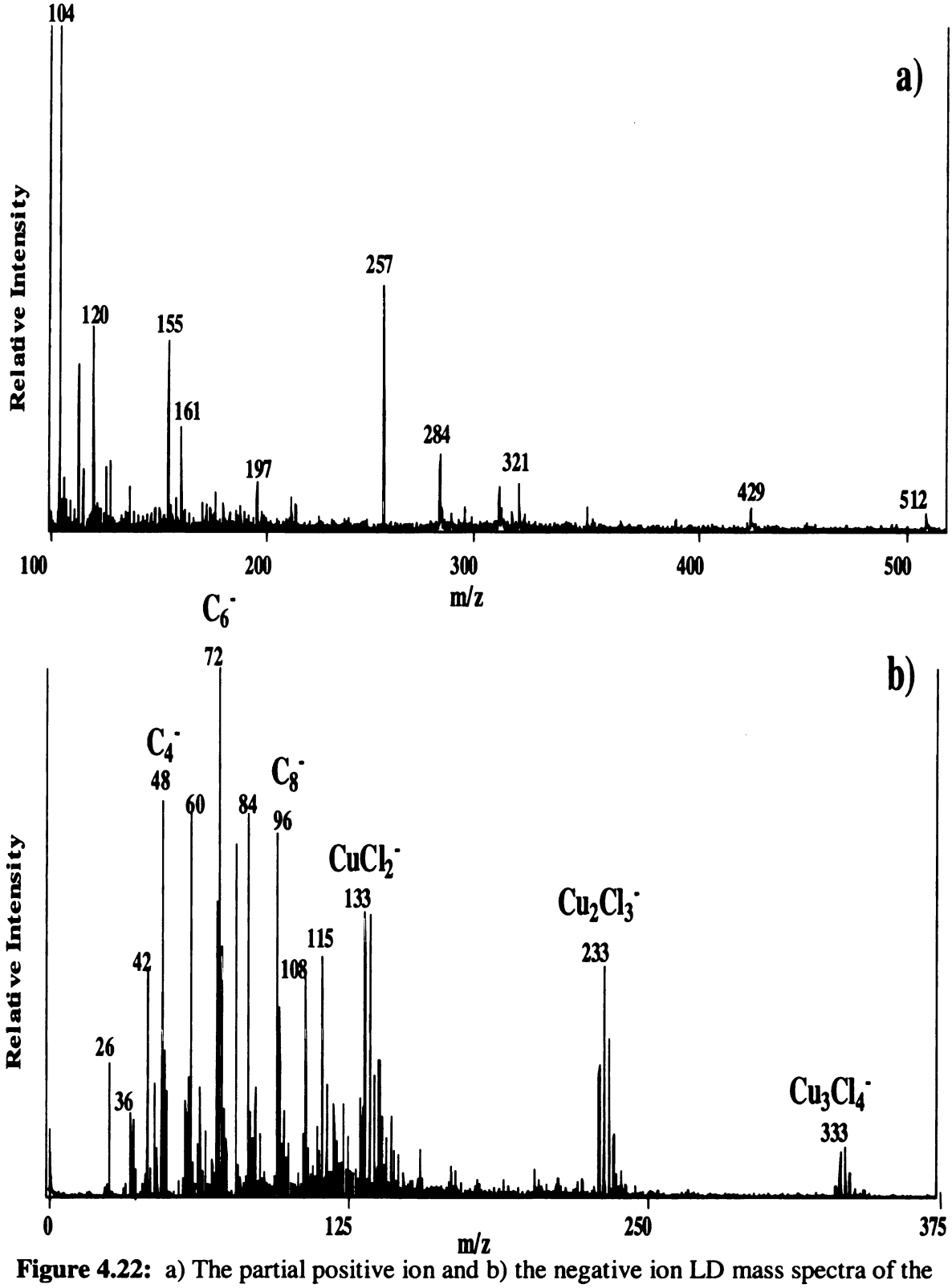

Figure 4.22: a) The partial positive ion and b) the negative ion LD mass spectra of the black ink of the Koran sample.

"Green"

Throughout the manuscript, there are several instances in which the character, as shown in the portion labeled "green" in Figure 4.16, appears. A vertical line is written in black ink and topped with a large dot of yellow ink. Sometimes the yellow dot appears to be outlined in black ink or was applied over black ink. Occasionally, the dot appears green. To determine if a fourth color was used, positive and negative ion LD mass spectra were obtained of these "green dots", beginning at the outer edge of the dot and working in towards the center of the dot. The negative ion results (shown in Figures 4.23 a –c) were informative and suggest several possibilities concerning their origin.

In Figure 4.23a, the negative ion mass spectrum of the outermost edge of the dot, peaks appearing at m/z 139, 171, 246, etc. strongly suggested the presence of the yellow pigment orpiment. What is interesting is that a few additional peaks (m/z 234, 309, and 373) are noted as containing both Cu and As. The peak at m/z 341 has been assigned as $CuAs_2S_4^-$, and was the only Cu-As containing peak which also appeared in the negative ion orpiment mass spectrum (Figure 4.23b). Moving the laser closer to the center of the dot, the spectrum in Figure 4.23b is obtained. The orpiment peaks have disappeared, and the spectrum contains peaks representing ions containing Cu and Cl atoms. Peaks representing $Cu_xCl_y^-$ ions (m/z 133, 231, and 331), which were also present in the black ink negative ion mass spectrum (Figure 4.22b), are noted. Additionally, dominant new peaks appear at m/z 115, 124, 147, and 204. These peaks have not been positively identified, however their isotopic patterns are consistent with the presence of Cu and Cl atoms. Finally, when the laser is focused directly on the center of the green dot, the spectrum in Figure 4.23c is generated. The pure $Cu_xCl_y^-$ peaks disappear. The isotopic

patterns of the peaks present in the mass spectrum clearly represent ions containing multiple Cu and Cl atoms, however the exact compound is not evident.

There are several green Cu-containing pigments, including copper resinate, verdigris ($Cu(CH_3COO)_2 \cdot [Cu(OH)_2]_3 \cdot 2H_2O$), malachite ($CuCO_3 \cdot Cu(OH)_2$), and emerald green ($3Cu(AsO_2)_2 \cdot Cu(CH_3COO)_2$). The pigment emerald green contains Cu and As, however the pigment was not discovered until the very late 18th century/early 19th century (53), and therefore would not have been available at the time this manuscript was created. One possibility is that the green dots were painted with a Cu-containing green pigment. The appearance of the orpiment peaks may suggest that a green pigment was painted over a yellow dot, however if this is so, it was not consistently done. Cu- and S-containing pigments should not be mixed. The darkened or discolored dots could have been due to the formation of black CuS. The green dots remaining may not have reacted at all or reacted to a lesser extent.

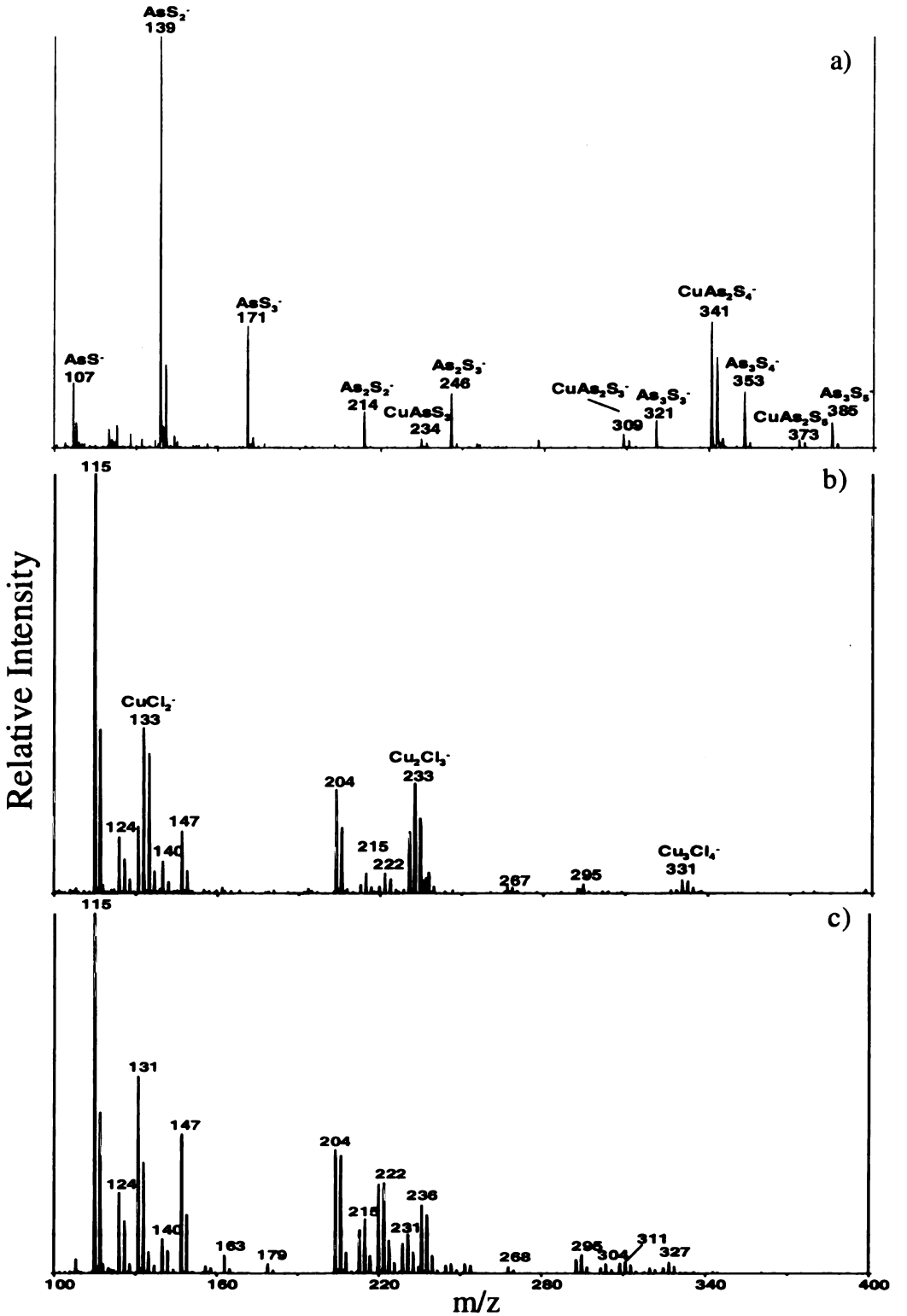

Figure 4.23: a-c) Negative ion LD mass spectra of the "green dot" taken from the outer edge of the dot, continuing to the center of the dot.

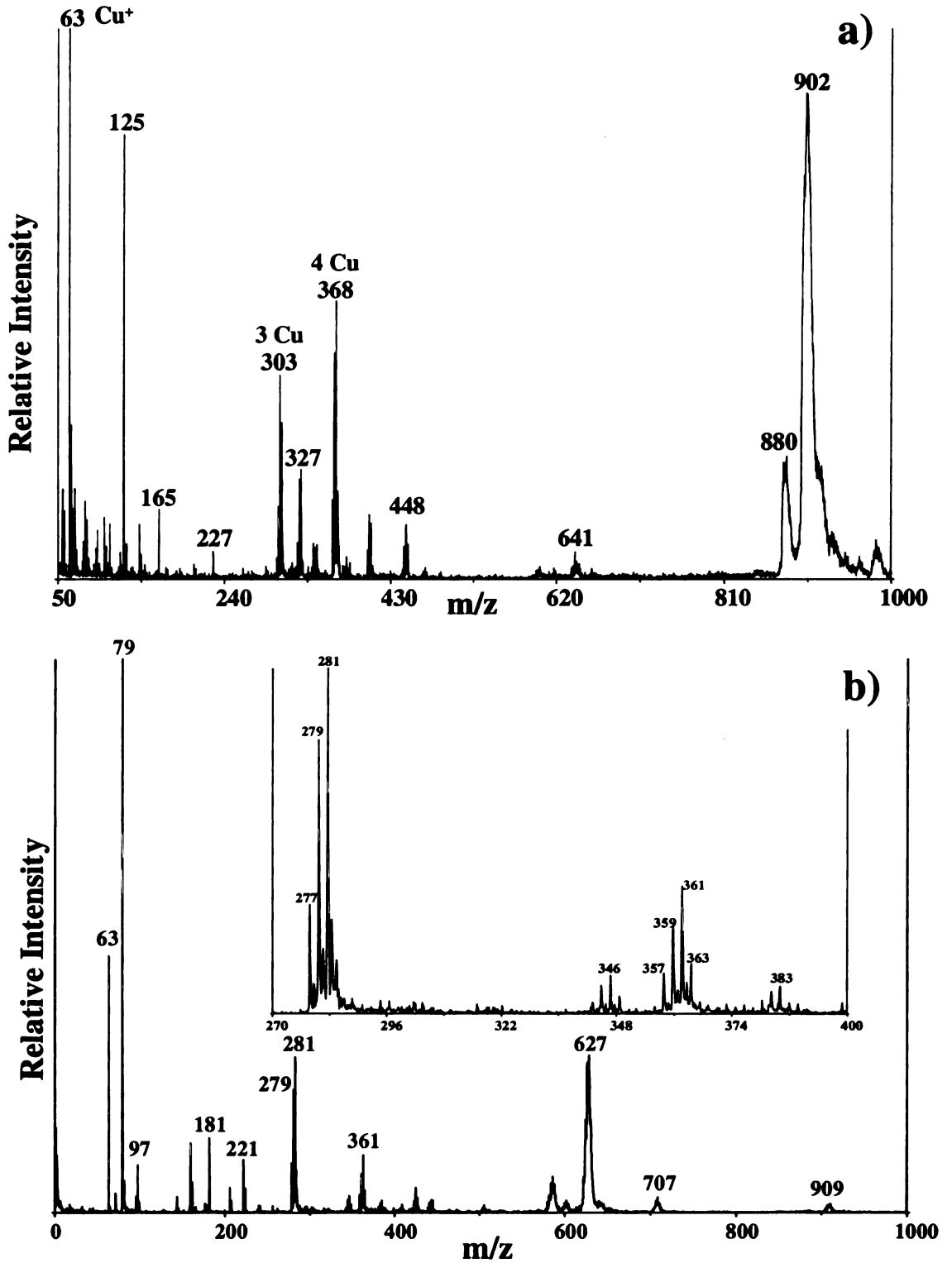

Figure 4.24: a) The partial positive ion and b) the negative ion LD mass spectra of malachite (Sinopia) suspended in linseed oil and applied to paper.

Based on the presence of $Cu_xCl_y^-$ ions in the black ink negative ion mass spectrum (Figure 4.22b), the discolored dots may have been the result of a reaction between the black and yellow ink. This is most likely because occasional green spots are only observed where both gold and black are in contact with each other. Positive and negative ion LD mass spectra were obtained of the Cu-containing green pigments, malachite (Figure 4.24) and verdigris (Figure 4.25) (Sinopia), suspended in linseed oil and applied to paper. Peak assignments were made, when possible. Except for Cu^+ ions, no peaks were identified in the malachite spectra. However, isotopic pattern analysis was used to determine the number of Cu atoms present in the ions represented at m/z 303 (3 Cu atoms) and m/z 368 (4 Cu atoms). The important point here is that the spectra do not match that of the green dot, lending further support to the latter explanation. Some questions will remain unanswered, however the sensitivity and versatility of the LDMS technique is demonstrated.

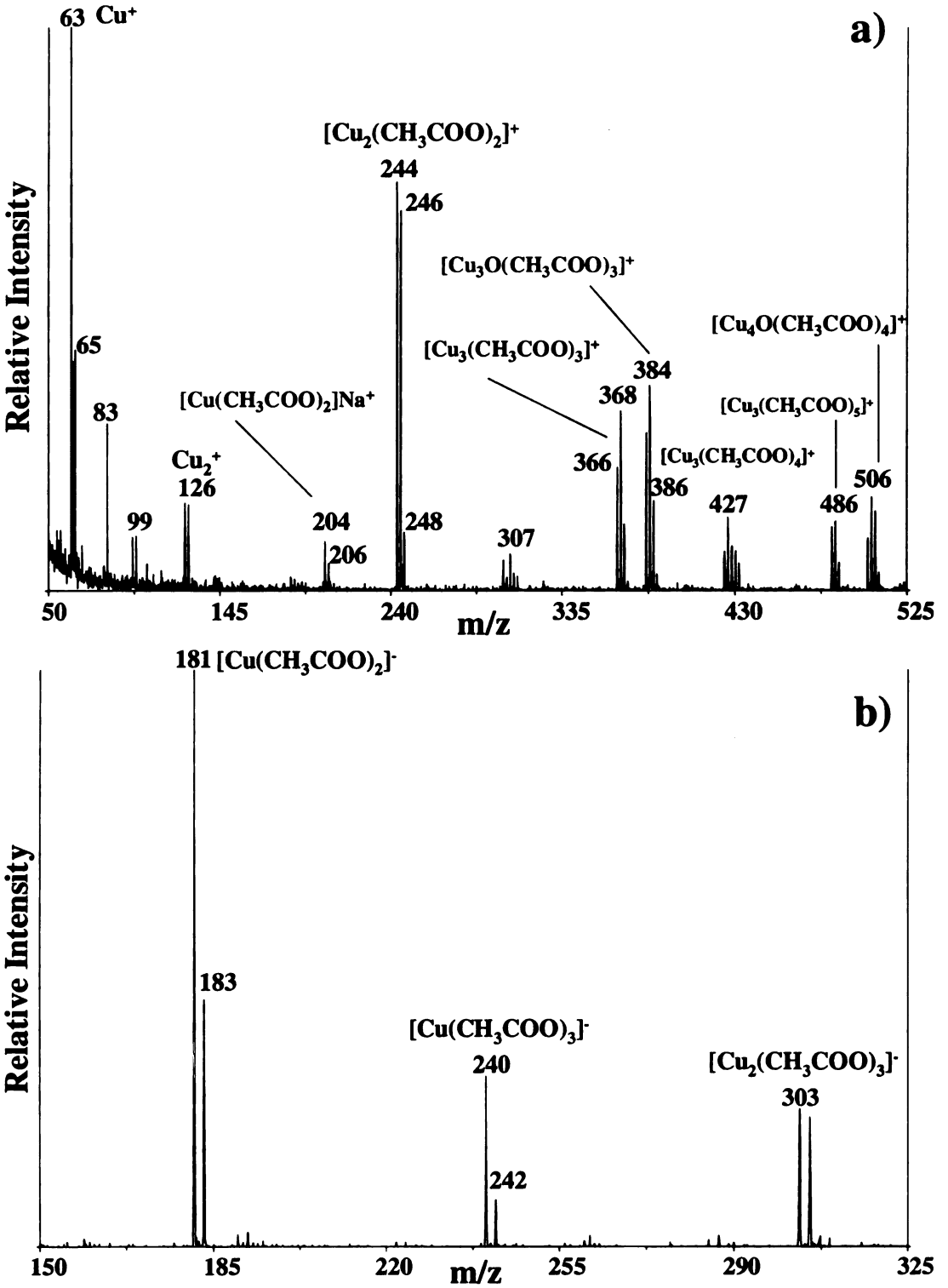

Figure 4.25: a) The partial positive ion and b) the partial negative ion LD mass spectra of verdigris (Sinopia) suspended in linseed oil and applied to paper.

Hebrew Manuscript

Figure 4.26 shows a portion of the illuminated page of the Hebrew manuscript from the 1800s that was analyzed. Our initial interest in this second example, a manuscript leaf reportedly from the 1800s, arose in part due to the claim that it was illuminated in gold. Our analyses indicated once again that "real gold" was not used on the document. However, unlike the Koran sample, many bright colors, including orange, blue, and green, were also used to decorate the miniature. The text is framed with four straight lines of different color: blue, orange, gold, and black. The authenticity of the manuscript was suspect because of the brightness of some of the colors, and the very different extent to which the various inks spread on the paper.

The analysis presented here focuses on the "framing lines". The positive ion mass spectrum of the blue line is shown in Figure 4.27a. The peak at m/z 372 has been identified in previous work as representing the cationic dye crystal violet (24,54). The structure is shown in Figure 4.27a. The positive ion LD mass spectrum of the black line is shown in Figure 4.27b. Again, the peak at m/z 372 is indicative of the dye crystal violet. Crystal violet is a very common component of modern blue and black pen inks. Should crystal violet be present at all? The information provided with the sample only indicated that it was from the 1800s. It has been reported that crystal violet was introduced in the 1860s (55), and was used to create manuscripts in the 1870s (56), so its presence alone is not inconsistent with its age. Of interest are the peaks at m/z values lower than m/z 372, separated by 14 amu - m/z 358, 344, 330, and 316. These represent degradation products of crystal violet, which have been extensively characterized (54,57,58) and discussed in Chapter 2. Crystal violet degrades over time, and its

degradation products can be detected using LDMS. There are very few degradation products present in Figure 4.27a, in contrast to Figure 4.27b, where they are abundant. This suggests that the blue line has only been on the page for a relatively short period of time, probably from a modern pen, while the black ink is much older. The different degrees of spreading of the two lines, and the straightness of the blue line may be consistent with it being added after the page was originally created.

Figure 4.26: Portion of the 1800s page of an Arabic manuscript that was evaluated.

Several spectra of the black writing ink were also obtained (not shown). The peaks representing crystal violet were present in the positive ion mass spectra at various stages of decomposition. The peaks at m/z 107 and 109, representing Ag^+ ions (also seen in Figure 4.27b) were also present. Silver has been documented as an ingredient in old ink recipes (44). Solutions of silver salts turn black upon contact with paper (reduction). Since a silver nitrate solution used would have been initially colorless, a dye was traditionally added to aid in writing.

There were many other aspects of the analysis of this document which suggested that, while it may have been created in the 1800s, it had subsequently been altered. For example, in a light blue "paint" used in the illustration, the dye copper phthalocyanine was positively identified (Figure 4.28). The copper phthalocyanine dye "Monastral Fast Blue" was developed by the chemical company ICI between 1935 and 1937. A green, chlorinated copper phthalocyanine was developed and became an important dye in the 1950s (27). These are still widely used in modern oil paints. Thus, many aspects of the second manuscript page support the proposal that the original work was "enhanced".

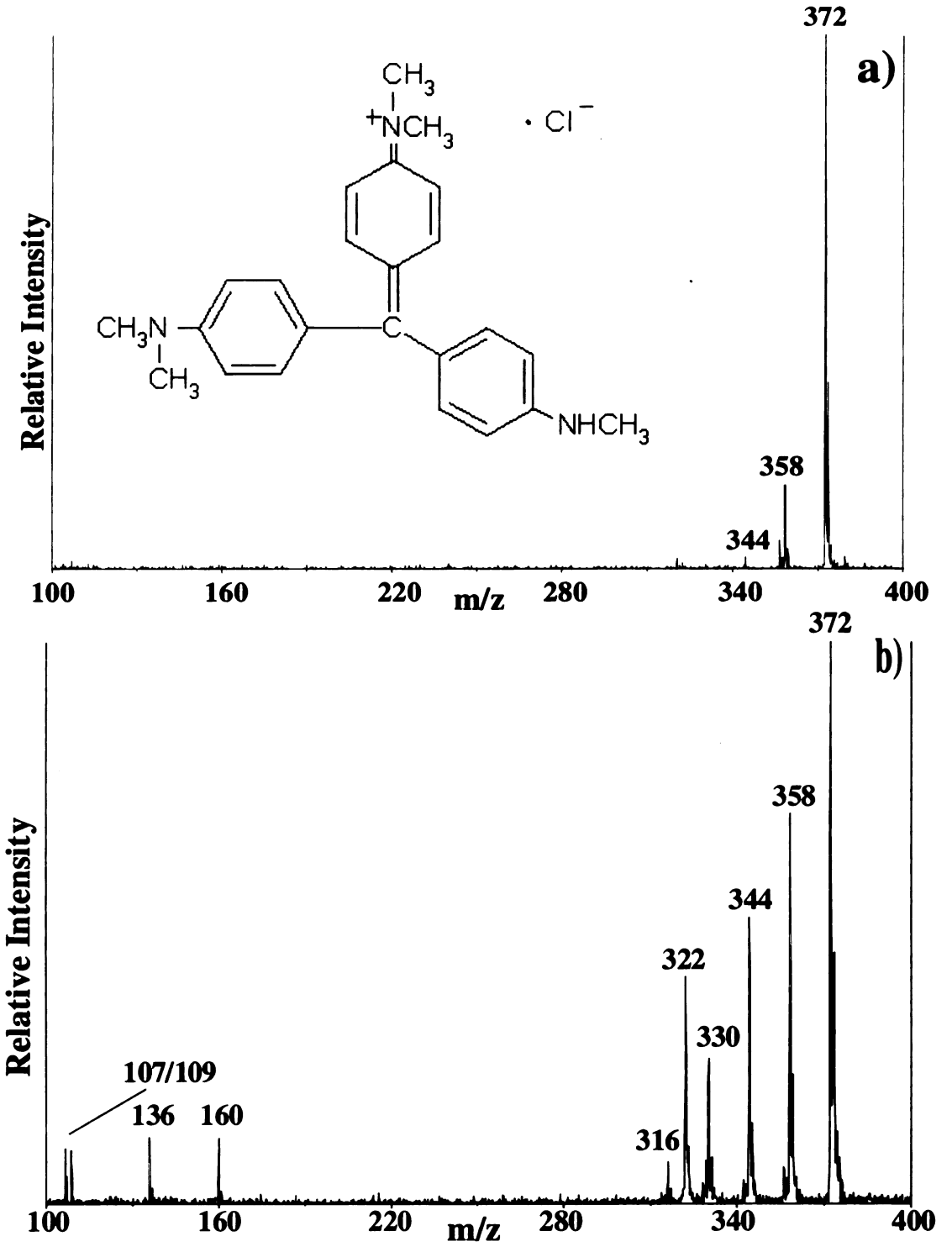

Figure 4.27: Positive ion spectra of a) the blue framing line, and b) the black framing line of the Hebrew manuscript page.

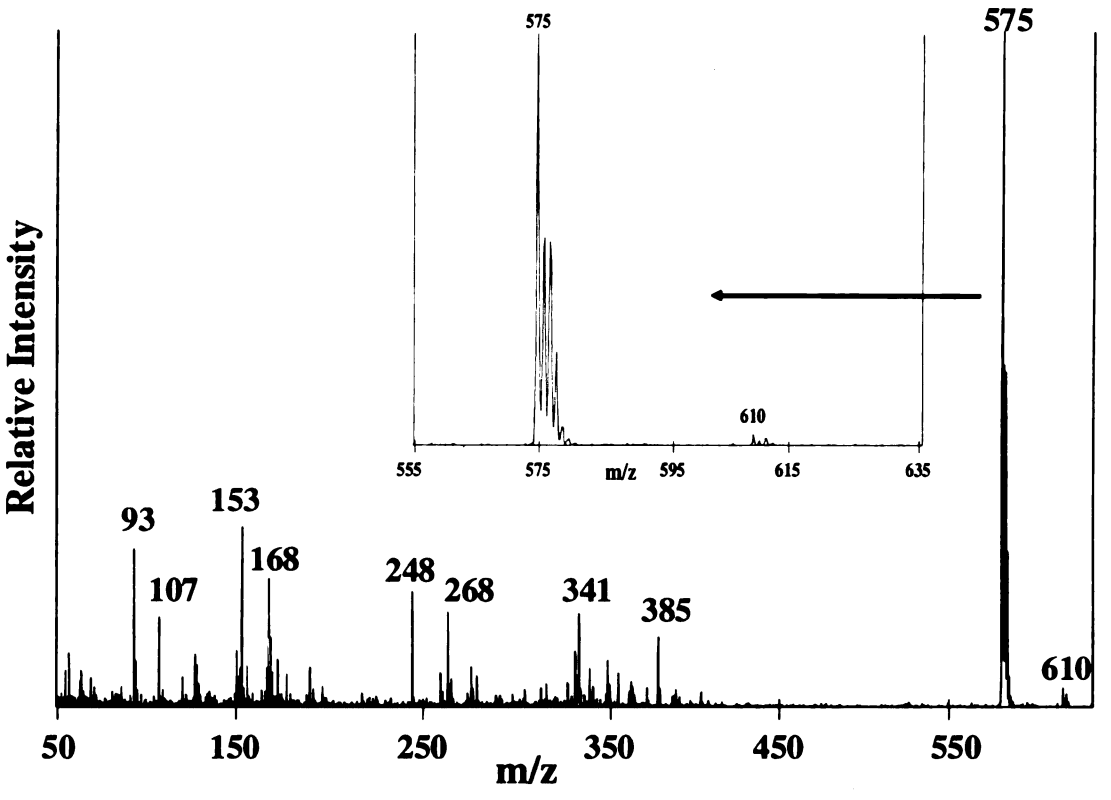

Figure 4.28: The partial positive ion LD mass spectrum of the blue paint on the Hebrew manuscript.

The positive and negative ion LD mass spectra of the orange colorant are shown in Figure 4.29. Identical spectra were obtained of the orange framing line and the orange paint in the picture. The exact pigment has not been identified, however we can use the information available in the mass spectrum to help characterize the colorants. The spectrum is similar to some of the red organic watercolor pigments discussed in Chapter 2. There are numerous peaks present in the spectra, indicating either the presence of multiple dyes (perhaps a red and yellow, to produce an orange shade) or the presence of an orange dye with multiple azo linkages. The azo linkages have proven to be relatively unstable, resulting in the formation of numerous fragment ions in a mass spectrum. There appears to be at least one neutral dye (M_1) present having a molecular weight of 370 amu. The characteristic overlap of the M_1^+ / $(M_1+H)^+$ peaks for a neutral dye is observed in the positive ion mass spectrum (Figure 4.29a). The peaks at m/z 393 $[(M_1+Na)^+]$ and m/z 409 $[(M_1+K)^+]$ lend support to this assignment. Additionally, a complimentary peak at m/z 369 representing $(M_1-H)^-$ ions is present in the negative ion mass spectrum (Figure 4.29b). A second neutral dye (M_2) may be present at m/z 340, with Na and K adducts present at m/z 363 and 379, respectively. The protonated molecule (m/z 341) is labeled in Figure 4.29a. However, it is unclear whether or not the dye represented at m/z 337 in the negative ion mass spectrum (Figure 4.29b) is related. Again, this is an indication that the document might be significantly newer than proposed, simply because modern day organic colorants were not as readily available in the 1800s as they are today. We may have expected to find peaks with unique isotopic patterns indicating the presence of an inorganic colorant.

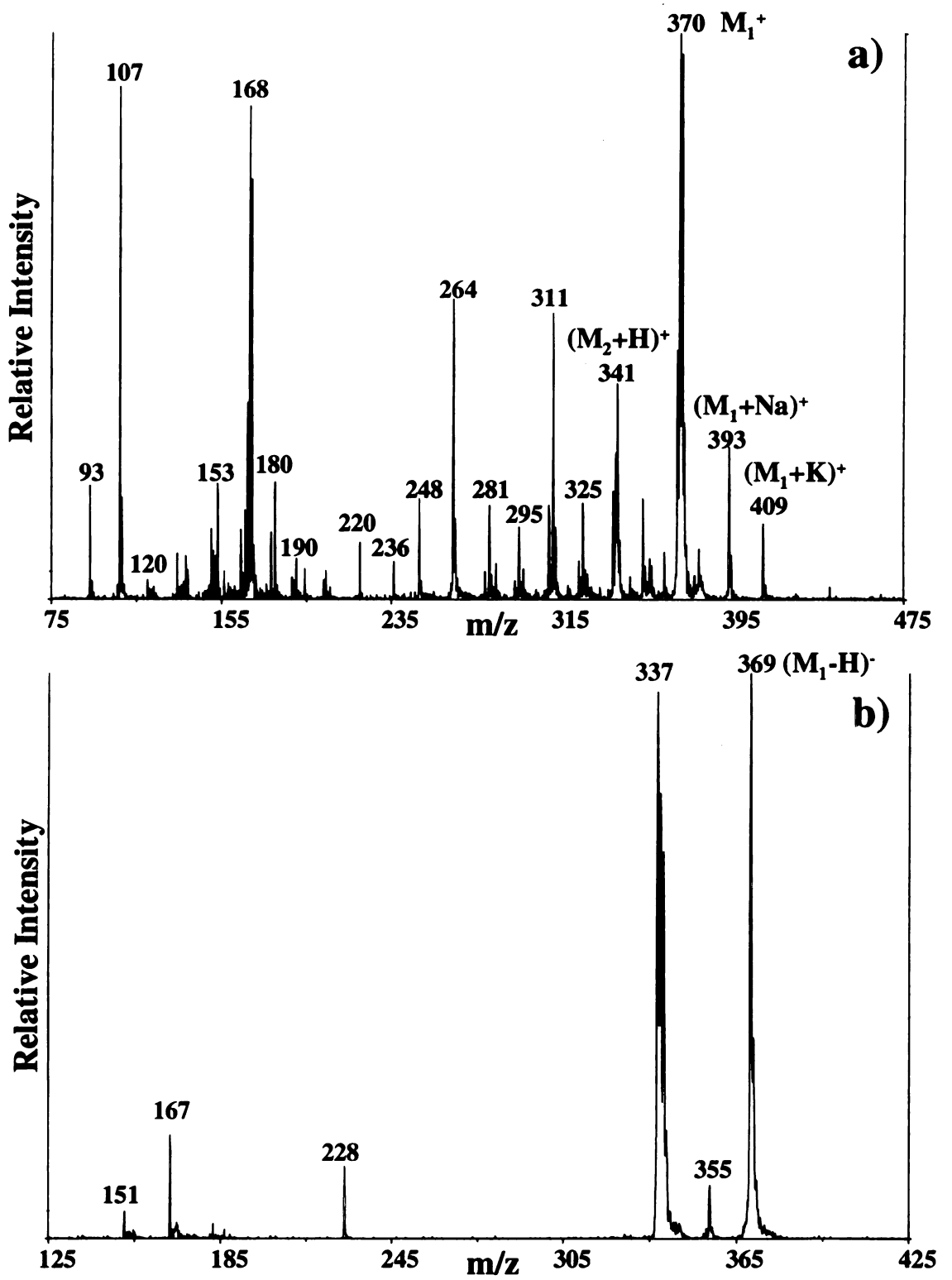

Figure 4.29: a) The partial positive ion and b) the partial negative ion LD mass spectra of the orange paint on the Hebrew manuscript.

The positive and negative ion LD mass spectra of the light green paint in the Hebrew manuscript are shown in Figure 4.30. Again the colorants have not been identified, however there appears to be at least two neutral dyes present (M_1 and M_2). M_1 has a molecular weight of 341 (M_1^+). The deprotonated molecule appears in the negative ion mass spectrum (Figure 4.30b) at m/z 340. The second dye (M_2) has a molecular weight of 395 amu, and has an isotopic pattern consistent with containing two Cl atoms. The deprotonated molecule appears in the negative ion mass spectrum at m/z 394. A fragment ion is noted at m/z 171 in Figure 4.30b, which has an isotopic pattern indicating the presence of only 1 Cl atom, most likely originating from M_2. In summary, the colorants are clearly organic modern day dyes, which sheds some doubt on the authenticity of the document.

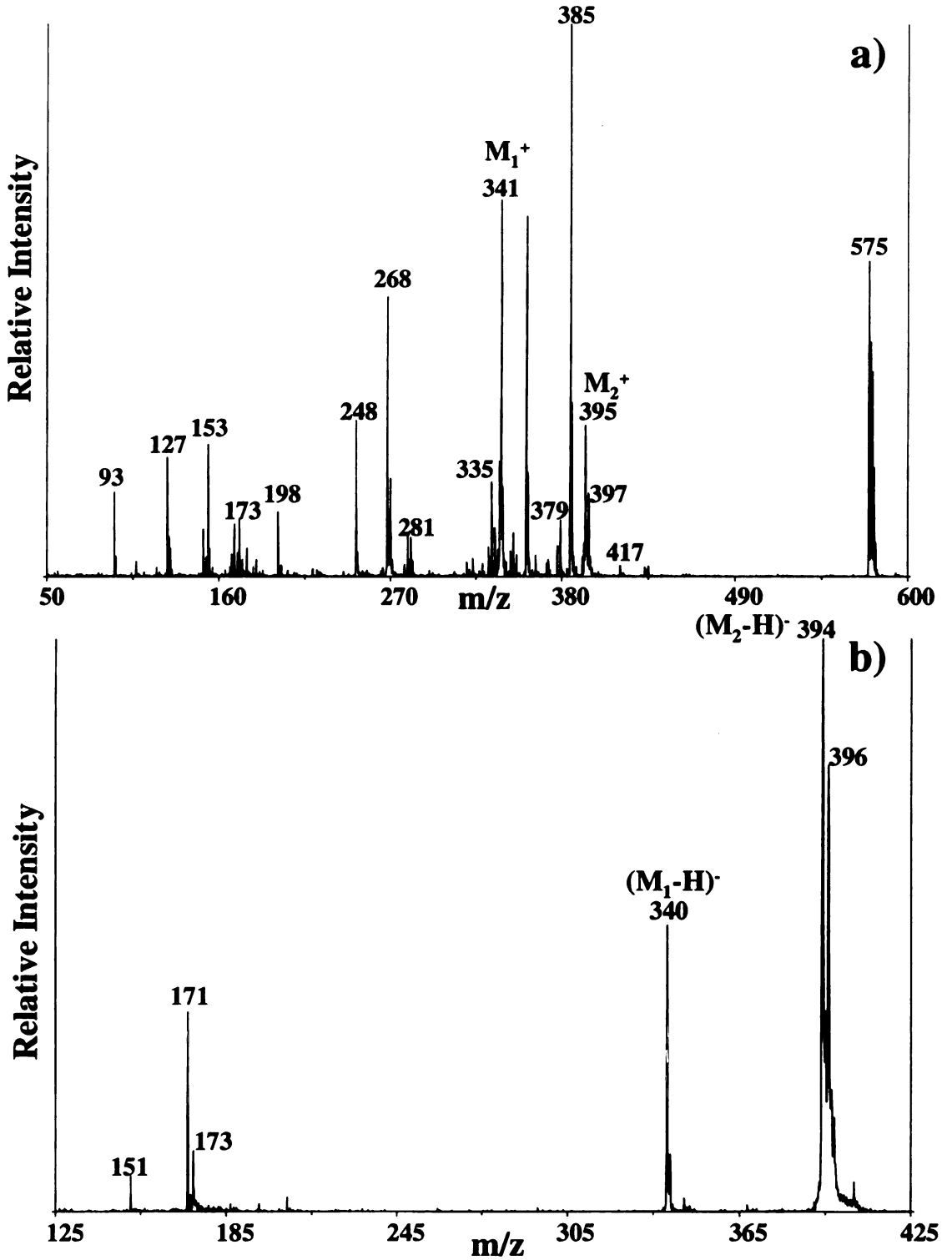

Figure 4.30: a) The partial positive ion and b) the partial negative ion LD mass spectra of the green paint on the Hebrew manuscript.

A New MALDI Matrix?

Currently, the most popular method for identifying colorants on illuminated manuscripts is Raman spectroscopy (59-62). Raman spectroscopy has the advantage of being a nondestructive analytical technique, which can perform the analysis directly on the document, without having to remove or extract a sample. However, organic compounds are not easily detected in this experiment. Consequently, Raman spectroscopy is limited to the analysis of inorganic colorants, for this application. A 16^{th} century Icelandic illuminated manuscript is shown in Figure 4.31 (59). Best and coworkers have been able to generate Raman spectra of several colorants, some of which have been presented here, including vermilion and orpiment. As with IR spectra, Raman spectra are typically used as fingerprints, and therefore require a library of standard spectra for comparison and identification of unknown samples. LDMS generates interpretable spectra, which do not require a library of reference spectra for comparison.

Let us consider a pigment, which has not been discussed yet, such as Fe_2O_3 (red ochre). Positive (not shown) and negative ion (Figure 4.32) LD mass spectra were obtained of Fe_2O_3 suspended in linseed oil and applied to paper. There was no evidence of iron or iron oxide ions in either of the spectra. However, the negative ion mass spectrum contains important information.

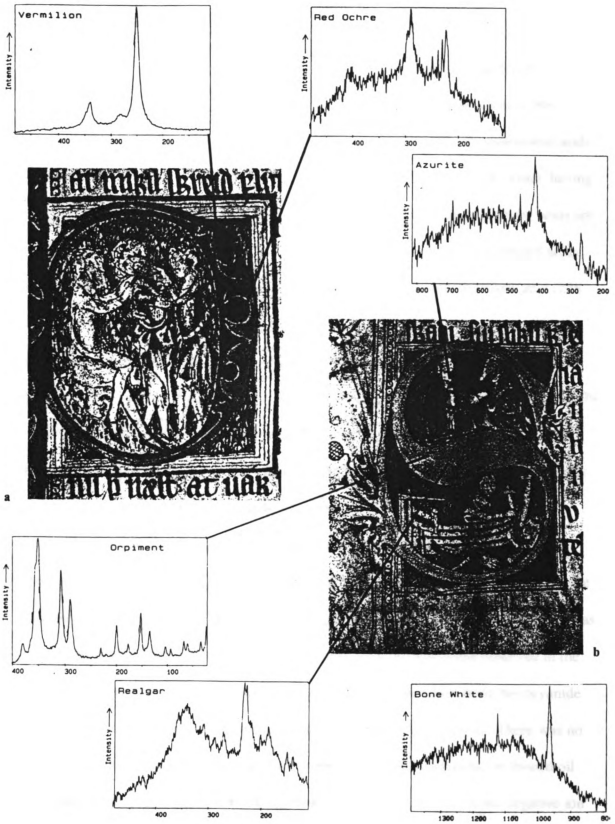

Figure 4.31: A 16th century Icelandic illuminated manuscript.

Up to this point, there has been no mention of the vehicle (linseed oil, in this case), simply because it never made its presence known in a LD mass spectrum. Additionally, we did not necessarily expect for it to be able to generate ions in this experiment. Linseed oil is transparent, and consists primarily of three unsaturated acids. These include linolenic (278 amu), linoleic (280 amu), and oleic acid (282 amu), having three, two, and one degrees of unsaturation, respectively. The structures of the acids are provided in Figure 4.33. The remainder of the mixture is composed of saturated acids, which include stearic acid (284 amu), palmitic acid (256 amu), and myrtistic acid (228 amu). Returning to the negative ion mass spectrum of Fe_2O_3, there is an interesting distribution of peaks around m/z 280. We believe that the peaks in the mass spectrum represent the deprotonated unsaturated acids of linseed oil (m/z 281 – oleic acid, m/z 279 – linoleic acid, m/z 277 – linolenic acid). The peaks in the higher mass region at m/z 896, may represent a polymerization product, since the m/z values are equivalent to the sum of approximately three of the unsaturated acids.

Let us now consider the two experiments which have been presented in this chapter involving Fe-containing pigments (ferric ferrocyanide and red ochre), which are illustrated in Figure 4.34. In the first experiment, Prussian blue (ferric ferrocyanide) was suspended in water and analyzed on paper. Several $Fe_xCN_y^-$ ions were observed in the negative ion mass spectrum. The same results were observed when ferric ferrocyanide was suspended in linseed oil and analyzed on paper (spectra not shown). There was no evidence of linseed oil. In the second experiment, Fe_2O_3 was suspended in linseed oil and analyzed on paper. Ions representing linseed oil were generated in the negative ion mass spectrum, however there was no evidence of the colorant. At this point in time, we

can not explain why we obtain such different results for these two experiments. Factors such as particle size, ionization potentials, and heats of formation values were considered, however there is no clear cut explanation why in one instance, colorant ions are generated, and in the other, vehicle ions are generated, but not both at the same time.

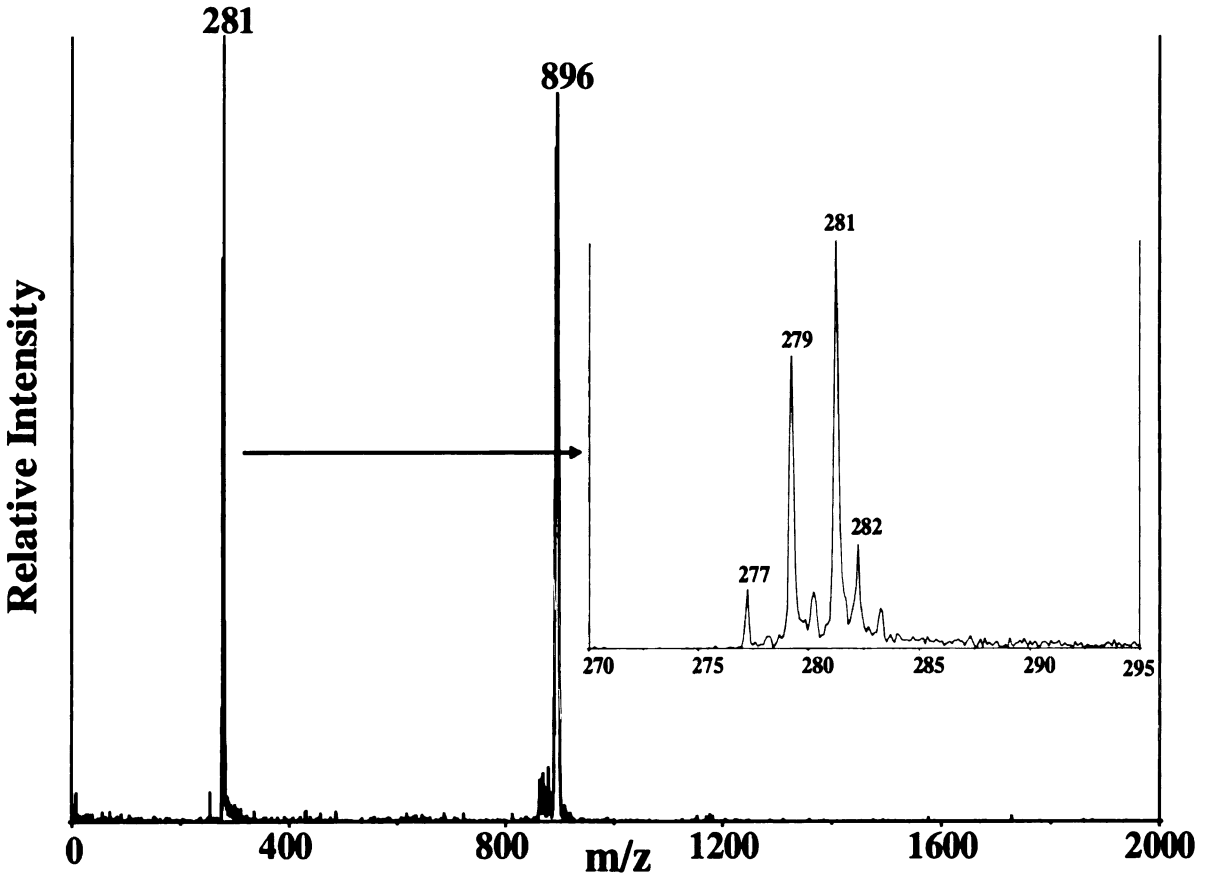

Figure 4.32: The negative ion LD mass spectrum of red ochre in linseed oil on paper.

Linseed Oil:

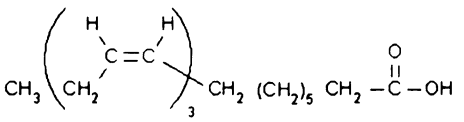

Linolenic Acid: 278 Da

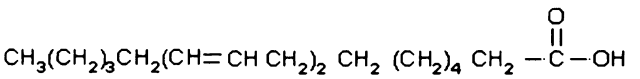

Linoleic Acid: 280 Da

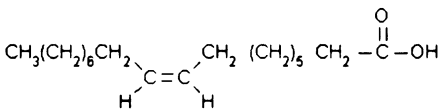

Oleic Acid: 282 Da

Figure 4.33: The structures of the primary unsaturated acids composing linseed oil.

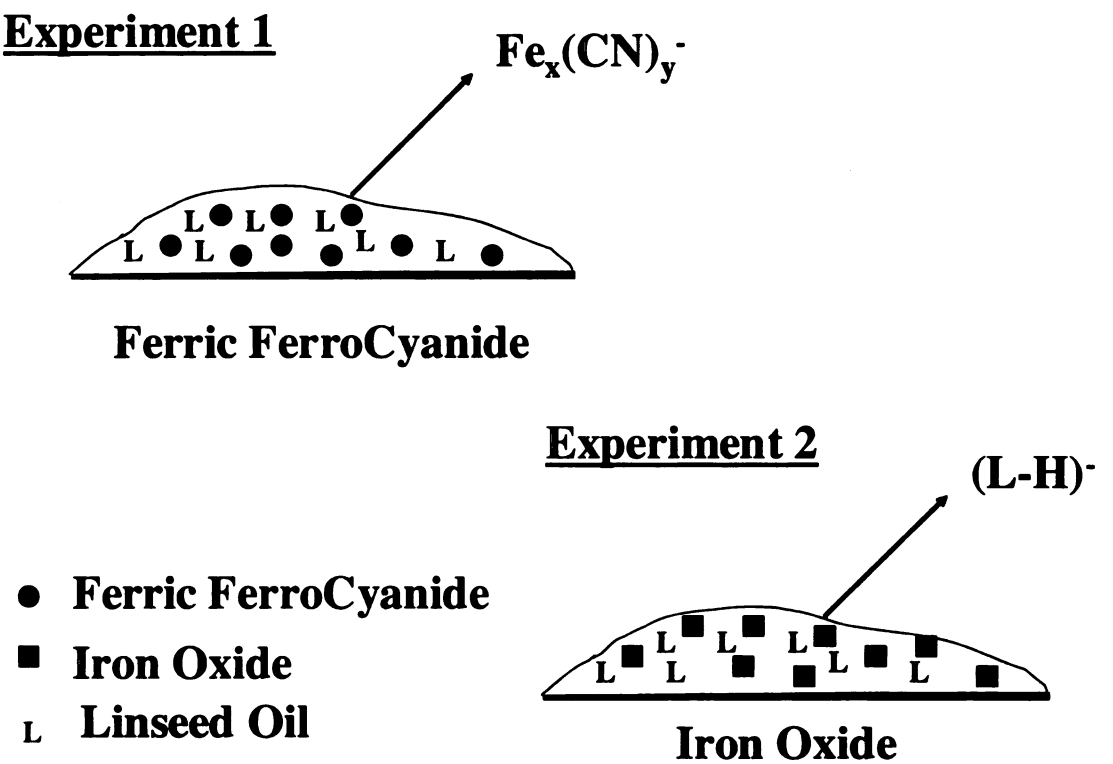

Figure 4.34: Summary of LDMS experiments involving Fe-containing pigments suspended in linseed oil.

Let us focus on the second experiment a little more closely. In this experiment, a fine particle solid (Fe_2O_3) which efficiently absorbs UV light is in a mixture with a nonabsorbing analyte (linseed oil). The experiment resembles traditional MALDI, which employs an organic matrix. In fact, in the early days of MALDI (1988), Tanaka and his research group first introduced the concept of using a matrix to assist in the LDMS experiment (63). In their experiment (illustrated in Figure 4.35), they suspended cobalt particles (30 nm diameter) and the analyte (protein) in glycerol and irradiated the sample using a pulsed N_2 laser (337nm, 15 ns pulse width). Ions formed were separated in a TOF mass analyzer. Monomeric and multimeric ions of the protein, lysozyme (~ 100,000 Da), were observed in the mass spectrum. Tanaka and coworkers characterized the cobalt nanoparticles as having a high photoabsorption, a low heat capacity, and a large surface area per particle. These physical properties were necessary for the experiment to be effective, meaning that the Co particles allow for a rapid heating to occur, which is necessary to desorb and ionize analyte molecules without thermal decomposition.

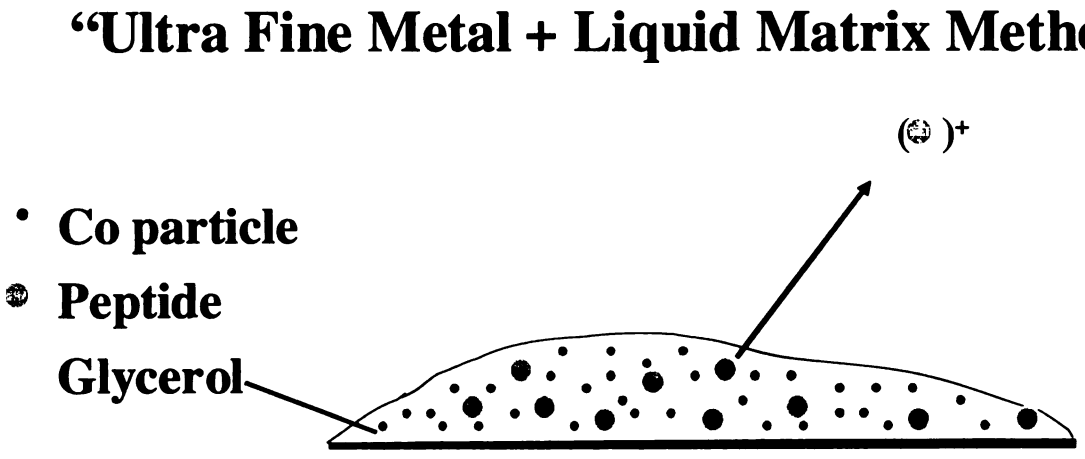

Figure 4.35: Illustration of Tanaka's *et al.* "ultra fine metal + liquid matrix method".

In contrast, Sunner *et al.* demonstrated that surface-assisted laser desorption/ionization (SALDI) using graphite particles and glycerol is useful for ionizing proteins and peptides (64). In their experiments, 10-150 μm diameter graphite particles and a 337 nm pulsed N_2 laser were used to ionize proteins and peptides. The particles were a thousand times larger in size than the 30 nm diameter Co particles that Tanaka and coworkers used. The results indicated that ionization might occur through a bulk desorption process like laser ablation. More recently (2000), Kinumi *et al.* performed an extensive study in which 11 metals and metal oxides (Al, Mn, Mo, Si, Sn, SnO_2, TiO_2, W, WO_3, Zn, and ZnO) were evaluated as potential inorganic matrix additives, for the detection of poly(ethylene glycol) 200 (PEG 200) and methyl stearate (65). As with traditional organic matrices used in MALDI experiments, the results varied according to the matrix used. Frequently, the experiment worked, meaning ions representative of the analyte were observed in the mass spectrum. Other times, matrix ions were formed. In some instances, both analyte and matrix ions were formed. In order to understand these differences, Kinumi and coworkers researched the ionization potentials and the standard heat of formation ($\Delta H_f°(g)$) for each inorganic matrix studied. Typically in MALDI experiments, heat of vaporation values for atoms or compounds are considered. Considering the relationship,

$$\Delta H_{vap}° = \Delta H_f°(g) - \Delta H_f°(s), \quad \text{where } \Delta H_f°(s) = 0,$$

$$\Delta H_{vap}° = \Delta H_f°(g).$$

No correlation was made concerning the performance of a matrix and either its ionization potential or energy required to sublime the matrix molecules. However, when analyzing the $\Delta H_f°(g)$ values, a trend appeared concerning whether or not matrix ions were formed.

They concluded that the matrix with the lower $\Delta H_f°(g)$ value will be easier to desorb and ionize in the MALDI experiment. Consequently, if one were analyzing a relatively low molecular weight analyte and wanted to suppress background peaks originating from the matrix, he should select a matrix additive, such as W, which has a large $\Delta H_f°(g)$ value (849 KJ/mol). However, this is only half of the story. The value Kinumi and coworkers should have been calculating and comparing is the sum of the ionization potential and $\Delta H_f°(g)$ value. For example, Ne requires a very small amount of energy to go from the solid to the gas phase. However, Ne would never be seen in an LD mass spectrum, simply because too much energy is required to ionize Ne atoms. The results are applicable to our experiments.

Unfortunately, Fe and Fe_2O_3 were not included in Kinumi and coworkers study, however their work helps to characterize our two experiments. When first trying to explain why in one experiment colorant ions were generated and in the second, linseed oil ions were formed, LD mass spectra of numerous Fe-containing compounds in linseed oil were obtained. The point in doing so, was to determine if a trend could be established with the type of ligand attached to the Fe and the peaks observed in the mass spectra. This was unsuccessful.

We next considered factors such as particle size, ionization potentials, and heats of formation values of ferric ferrocyanide and iron oxide. In terms of particle size, smaller particles have larger surface area-to-volume ratios, which may assist in the absorption process. The study of nanoparticle properties is a currently a well-researched, but poorly understood field of chemistry (66,67). Additionally, the work of Sunner *et al.* suggests that the performance of an inorganic matrix is not a function of its size (64).

Fe(s) has a relatively low ionization potential (7.8 eV), however the ionization potentials and heat of formation values for ferricferrocyanide and Fe_2O_3 are unavailable. We can conclude that ferric ferrocyanide should not be used as a matrix (at least for the analysis of artists' colorant vehicles).

It should be noted that the linseed oil peaks appeared in a few other pigment spectra. For example, linseed oil peaks also appeared in the negative ion mass spectrum of malachite (Figure 4.24b). An enlarged portion of the mass spectrum (m/z 270-400) is shown in the inset. It appears that there may be a related set of peaks at m/z 361. It is unclear whether or not they represent linseed oil-pigment complex ions or simply a linseed oil polymerization product. The fact that these ions do not appear in the Fe_2O_3 spectrum, suggests that the ions are unique to malachite.

To further investigate the utility of using Fe_2O_3 in terms of generating information on the vehicle component of a paint, Fe_2O_3 was suspended in other drying oils, which included walnut oil and poppy oil. Walnut oil and poppy oil contain the same unsaturated acids as linseed oil, but in different concentrations. Linseed oil "dries" through a cross-linking process at the sites of unsaturation (68). Consequently, the fastest drying oil will have the highest concentration of linolenic acid (three degrees of unsaturation). Walnut and poppy oils have a lower concentration of linolenic acid, compared to linseed oil, and therefore take longer to dry. The negative ion LD mass spectra of Fe_2O_3 suspended in walnut oil and poppy oil, and analyzed on paper, are shown in Figures 4.36 and 4.37, respectively. It is important to note that the relative intensities of the distribution of peaks representing the three unsaturated acids present in the oils has changed. The peak at m/z 279 is now the most intense peak. Based on the

compositions of the oils, it does not appear that their LD mass spectra may be used for quantitative analysis. However, they may be used to determine if linseed oil was used as the vehicle, as opposed to either walnut or poppy oil. Also, three examples were evaluated here. A more extensive study would be required. This is encouraging information, considering that even though we are not particularly interested in the vehicle component, there are certainly other research groups that are.

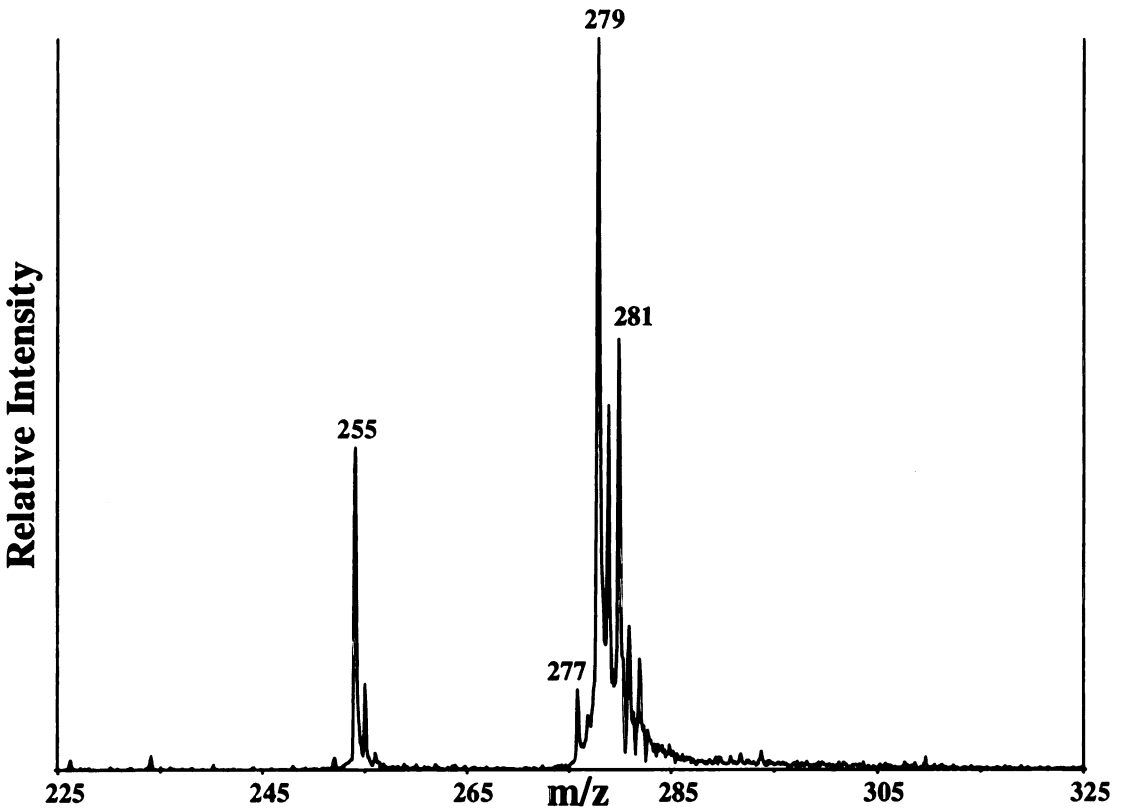

Figure 4.36: Partial negative ion LD mass spectrum of Fe_2O_3 suspended in walnut oil applied to paper.

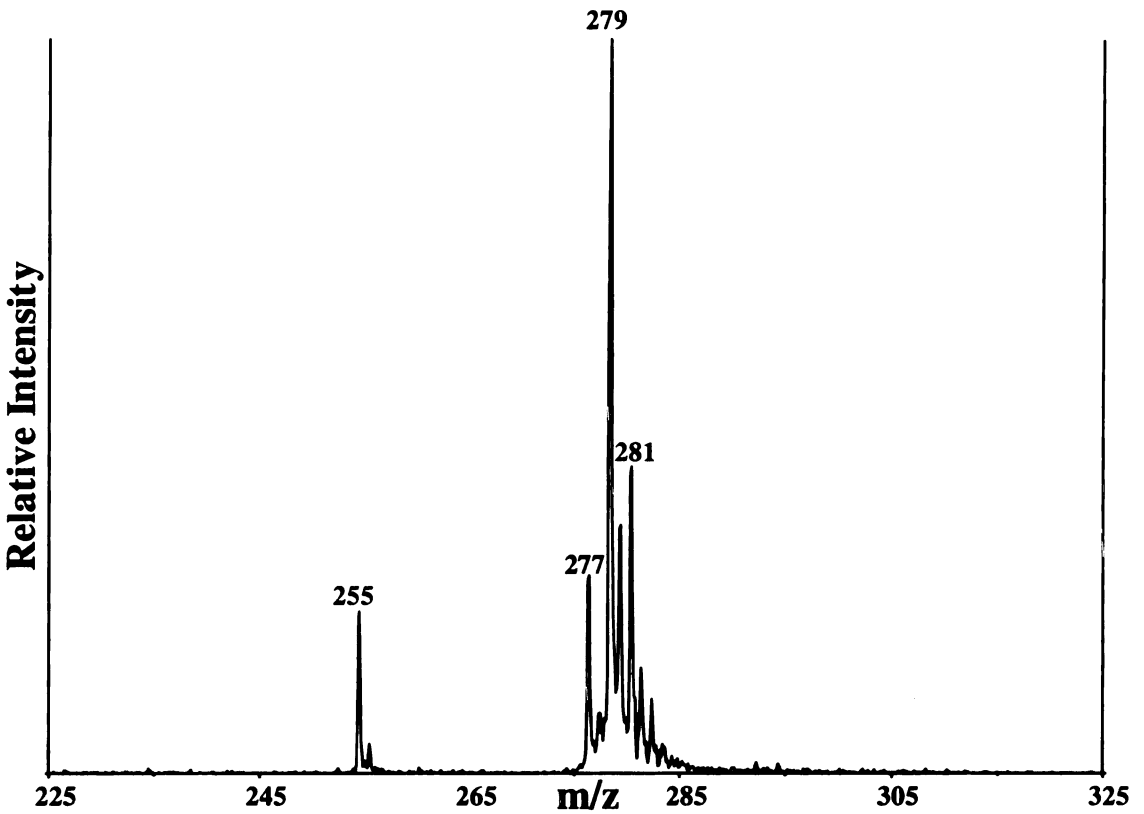

Figure 4.37: Partial negative ion LD mass spectrum of Fe_2O_3 suspended in poppy oil applied to paper.

References

1) Feller RL, editor. Artists' pigments: a handbook of their history and characteristics, vol. 1. New York: Cambridge University Press, 1986.

2) Roy A, editor. Artists' pigments: a handbook of their history and characteristics, vol. 2. New York: Oxford University Press, 1993.

3) Fitzhugh EW, editor. Artists' pigments: a handbook of their history and characteristics, vol. 3. New York: Oxford University Press, 1997.

4) Carlson JH, Krill J. Pigment analysis of early American watercolors and fraktur. J Am Institute for Conservation 1978;18:19-32.

5) Berrie BH. Prussian blue. In: Fitzhugh EW, editor. Artists' pigments: a handbook of their history and characteristics, vol. 3. New York: Oxford University Press,1997; 191-217.

6) Batcheler PH. Historic Structure Report, Old North Church, National Park Service, Denver Science Center;193-194.

7) Vitalis JB. Grundiss der Farberei 1842;239:242.

8) Brunello F. The art of dyeing in the history of mankind, trans. Hickey B, Vicenza, 1973;230.

9) Crawford W. The keepers of light. New York: Morgan & Morgan, 1979;67-68.

10) Latimer WM, Hildebrand JH. Reference book of inorganic chemistry, 3rd ed. New York: MacMillan Company, 1951;417.

11) Hurst GH. The painter's laboratory guide: a handbook on paints, colours, and varnishes for students. London, 1902;28-39.

12) Kühn H, Curran M. Chrome yellow and other chromate pigments. In: Feller RL, editor. Artists' pigments: a handbook of their history and characteristics, vol. 1. New York: Oxford University Press, 1986;187-218.

13) Fluck E, Kerler W, Neuwirth W. Angew Chem 1963;6:277-332.

14) Wertheim GK, Rosencwaig A. Characterization of inequivalent iron sites in Prussian blue by photoelectron spectroscopy. J Chem Phys 1971;54:3235.

15) Nakamoto K. Infrared spectra of inorganic and coordination compounds, 2nd ed. New York: Wiley-Interscience, 1970;178-186.

16) Newman R. Some applications of infrared spectroscopy in the examination of painting materials. J Am Institute for Conservation 1979;19:42-62.

17) Wilde RE, Ghosh SN, Marshall BJ. Prussian blues. Inorg Chem 1970;9:2512-2516.

18) Lechtman H. Thesis. New York City (NY): New York University, 1966.

19) Burgio L, Clark RJH. Library of FT-Raman spectra of pigments, minerals, pigment media and varnishes, and supplement to existing library of Raman spectra of pigments with visible excitation. Spectrochim Acta Part A 2001;57:1491-1521.

20) De Wild AM. The scientific examination of pictures. London, 1929.

21) Welsh FS. Particle characteristics of Prussian blue in a historical oil paint. J Am Institute for Conservation 1988;27:55-63.

22) Townsend JH. The materials of J.M.W. Turner: pigments. Studies in Conservation 1993;38:231-254.

23) Herbst W, Hunger K. Industrial Organic Pigments. Production, Properties, Applications, 2nd Ed., VCH, Weinheim, 1997.

24) Grim DM, Siegel J, Allison J. Evaluation of desorption/ionization mass spectrometric methods in the forensic applications of the analysis of inks on paper, J Forensic Sci 2001;46:1411-20.

25) Grim DM, Allison J. Identification of colorants as used in watercolor and oil paintings by uv laser desorption mass spectrometry. Int J Mass Spectrom 2003;222:85-99.

26) Lias S, Bartmess JE, Liebman JF, Holmes JL, Levin RD, Mallard G. Gas-phase ion and neutral thermochemistry. J Physical and Chemical Reference Data 1988;17:649,794-95.

27) Ball P. Bright earth. New York: Farrar, Strauss, and Giroux, 2001.

28) Burnin A, BelBruno JJ. $Zn_nS_m^+$ cluster production by laser ablation, Chemical Physical Letters 2002;362:341-48.

29) Benedetti-Pichler AA. Microchemical analysis of pigments used in the fossae of the incisions of Chinese oracle bones. Industrial and Engineering Chemistry, Analytical Edition 1937;9:149-52.

30) Feigl F. Qualitative analysis by spot tests. New York, 1946;227-228.

31) Gettens RJ, Feller RL, Chase WT. Vermilion and cinnabar. In: Roy A, editor. Artists' pigments: a handbook of their history and characteristics, vol. 2. New York: Oxford University Press, 1993;159-182.

32) Plesters J. Cross-sections and chemical analysis of paint samples. Studies in Conservation 1955-1956;2:110-57.

33) Aurivillius KL. On the crystal structure of cinnabar. Acta Chemica Scandinavica 1950;4:1413-16.

34) Swanson HE, Fuyat RK, Ugrinic GM.1955, Standard x-ray diffraction powder patterns in *National Bureau of Standards Circular* 539 Washington, DC.

35) Waring CL, Annell CS. Semiquantitative spectrographic method for analysis of minerals, rocks and ores. Analytical Chemistry 1953;25:1174-79.

36) Karr C, Kovach JJ. Far-infrared spectroscopy of minerals and inorganics. Applied Spectroscopy 1969;23:220-221.

37) van Asperen de Boer JRJ. Reflectography of paintings using an infrared Vidicon television system. Studies in Conservation 1969;14:96-118.

38) van Asperen de Boer JRJ. Infrared reflectography. Amsterdam, 1970.

39) Rees Jones S. Physics and painting. Bulletin of the Institute of Physics 1960;June: 157-65.

40) Bailey CK. The elder Pliny's chapters on chemical subjects, part 1. London, 1929.

41) Palache C, Berman H, Frondel C. Dana's system of mineralogy, vol. 1, 7th ed. New York, 1952;254.

42) Fitzhugh EW. In: Fitzhugh EW, editor. Artists' pigments: a handbook of their history and characteristics, vol. 3. New York: Oxford University Press,1997;47-79.

43) http://www.knaw.nl.ecpa/ink/html/ink.html

44) Lehner S. Manufacture of ink. London: Henry Carey Baird & Co, 1892.

45) Wunderlich CH. Über Eisengallustinte. Zeitung der Anorganischen Algemeinen Chemie 1991;598-599:371-76.

46) Wunderlich CH. Geschichte und chemie der eisengallustinte – rezepte, reaktionen und schadwirkungen. Restauro 1994;100:414-421.

47) Krekel C. Chemische untersuchungen an eisengallustinten und anwendung der ergebnisse bei der begutachtung mittelaltericherhandschrifte [thesis]. Institut für

Anorganische Chemie der Georg August Universitat Gottingen, 1990.

48) Flieder F. Mise au point des techniques d'identification des pigments et des liants inclus dans la couche picturale des enluminures de manuscripts. Studies in Conservation 1968;13:49-86.

49) Laurie AP. The pigments and mediums of the old masters. London: Macmillan, 1914.

50) Roosen-Runge H. Farbgebung und technik fruhmittelalterlicher buchmalerei, 2 vols. Berlin, 1967.

51) Kühn H.Verdigris and copper resinate. In: Roy A, editor. Artists' pigments: a handbook of their history and characteristics, vol. 2. New York: Oxford University Press, 1993;131-158.

52) Thompson DV, Jr. The materials and techniques of medieval painting, reprint of 1936 ed. New York, 1956;169.

53) Fielder I, Bayard M. Emerald green and scheele's green. In: Fitzhugh EW, editor. Artists' pigments: a handbook of their history and characteristics, vol. 3. New York: Oxford University Press,1997;219-271.

54) Grim DM, Siegel J, Allison J. Evaluation of laser desorption mass spectrometry and UV accelerated aging of dyes on paper as tools for the evaluation of a questioned document. J Forensic Sci 2002;47:1265-73.

55) Druding SC. Dye history from 2600 BC to the 20th century, http://www.straw.com/sig/dyehist.html

56) Dube L. The copying pencil: composition, history, and conservation implications, http://aic.stanford.edu/conspec/bpg/annual/v17/bp17-05.htm

57) Andrasko J. High pressure liquid chromatography analysis of ballpoint pen inks stored at different light conditions. J Forensic Sci 2001;46:21-30.

58) Grim DM, Siegel J, Allison J. Does ink age inside of a pen cartridge? J Forensic Sci 2002;47:1294-97.

59) Best SP, Clark RJH, Daniels MAM, Porter CA, Withnall R. Identification by Raman microscopy and visible reflectance spectroscopy of pigments on an Icelandic manuscript, Studies in Conservation 1995;40:31-40.

60) Burgio L, Ciomartan DA, Clark RJH. Pigment identification on medieval manuscripts, paintings and other artefacts by Raman microscopy: applications to the study of three German manuscripts. J Molecular Structure 1997;405:1-11.

61) Burgio L, Ciomartan DA, Clark RJH. Raman microscopy study of the pigments on three illuminated mediaeval Latin manuscripts. J Raman Spectroscopy 1997;28:79-83.

62) Clark RJH, Gibbs PJ, Seddon KR, Brovenko NM, Petrosyan YA. Non-destructive in situ identification of cinnabar on ancient Chinese manuscripts. J Raman Spectroscopy 1997;28:91-94.

63) Tanaka K, Waki H, Ido Y, Akita S, Yoshida Y, Yoshida T. Protein and polymer analyses up to m/z 100,000 by laser ionization time-of-flight mass spectrometry. Rapid Communications in Mass Spectrometry 1988;2:151-153.

64) Sunner J, Dratz E, Chen Y-C. Graphite surface-assisted laser desorption/ionization time-of-flight mass spectrometry of peptides and proteins from liquid solutions. Analytical Chemistry 1995;67:4335-4342.

65) Kinumi T, Saisu T, Takayama M, Niwa H. Matrix-assisted laser desorption/ionization time-of-flight mass spectrometry using an inorganic particle matrix for small molecule analysis. J Mass Spectrometry 2000;35:417-422.

66) Henglein A. Small-particle research: physicochemical properties of extremely small colloidal metal and semiconductor particles. Chem Rev 1989;89:1861-1873.

67) Alivisatos AP. Perspectives on the physical chemistry of semiconductor nanocrystals. J Phys Chem 1996;100:13226-13239.

68) Frankel EN. Lipid oxidation. Prog Lipid Res 1980;19:1-22.

Chapter Five: Stamps

Introduction

A postage stamp can mean many things to different people. For some, a stamp is merely an inconvenient tax required to send their correspondence. For others, a stamp is considered a work of art and an important part of history, which needs proper care and attention to preserve the stamp in its original form. Throughout history, stamps have honored famous people, places, and important events. Thus, philately, the collection and study of postage stamps, has developed into a big business, as well as a hobby for some. Consequently, forging and faking stamps has also become a big business. Experts can distinguish between an original and a fake stamp, by studying both its physical appearance and chemical composition.

The general composition of a postage stamp consists of a colorant (dyes or pigments), phosphors, paper, and an adhesive. Limited information is available in regards to colorants used, to maintain the security of the postage stamp ink formulations, for obvious reasons. The earliest stamps were limited to grayish shades, since only carbon black was used. Slowly, colors were introduced into the printing industry, and low chroma reds and browns appeared. These were produced using natural plant (indigo) and animal (cochineal) dyes. Nineteenth century postage stamps were characterized by the use of mineral pigments. These colorants included yellow lead nitrate ($Pb(NO_3)_2$), red and black iron oxide (Fe_2O_3), white lead (PbO), Prussian blue, green chromium oxide (Cr_2O_3), and ultramarine blue ($CaNa_7Al_6Si_6O_{24}S_3SO_4$) (1). Today, the colors available are substantial, due to the numerous synthetic organic dyes and pigments available. Table 5.1 lists some of the colorants recently used in postage stamp ink formulations (1).

The list is dated 1990. Typically, linseed oil or a refined petroleum oil is used as the colorant carrier.

Yellow Pigments	**Blue Pigments**
Diarylide yellow (dichlorobenzidene)	Copper phthalocyanine blue – GS and RS
Hansa yellow G	Alkali blue – RS and GS triphenylmethane type
Iron oxide yellow	Iron blue (Milori blue)
Orange Pigments	**Green Pigments**
Dinitroanaline orange	Phthalocyanine green
Dianisidine orange	Malachite green
Red Pigments	**Black Pigments**
Red lake "C" – calcium salt	Carbon blacks – oil and furnace blacks
Lithor rubine – calcium salt	Iron oxide black
Red 2B – calcium and barium salts	**White Pigments**
Violet Pigments	Titanium dioxide – opaque
Methyl violet	Calcium carbonate – transparent
Carbozole violet	Barite (barium sulfate) - transparent

Table 5.1: A list of colorants used in contemporary postage stamp ink formulations.

Phosphors are included in postage stamp ink formulations to serve as a tagging system. Post offices employ facer/canceller machines to locate and cancel stamps, by detecting the components which phosphoresce. A phosphorescent material is preferred over one which fluoresces, simply because the paper envelope typically contains a fluorescent material, which is added as a brightening agent. Tagging of airmail stamps was first achieved in 1963, using a calcium silicate compound ($CaSiO_3$), which glows an orange-red color when exposed to short-wavelength UV light. A zinc orthosilicate (Zn_2SiO_4) is used to tag first class stamps, and glows a green color (1).

An adhesive is applied to the back of the stamp, so that it may be affixed to an envelope. The earliest and most primitive adhesive used was gum Arabic, which comes

from the acacia tree found in tropical areas. Gum Arabic has a variety of uses. It is used as a stabilizing agent and viscosity adjuster in the food industry, in addition to the printing and adhesive industries. Gum Arabic is composed of a mixture of Ca, Mg and K salts of Arabic acid, which is a branched polysaccharide containing galactose, rhammose, glucuronic acid, and arabinose residues. The molecular weight of gum Arabic can range between 260,000 and 1,160,000 Da (1). Gum Arabic has the problem of drying-out, yellowing, and cracking. Consequently, a switch was made to dextrin.

Dextrin is derived from food grain corn starch and consists of a mixture of low molecular weight polysaccharides. As gum Arabic, dextrin is also used as a thickening agent in food and ink formulations (1). One drawback of the use of dextrin as an adhesive, is that it is known to deteriorate over time. Unfortunately, this devalues the stamp and alternatives needed to be considered.

The search for the ideal adhesive ended when polyvinyl alcohol (PVA) was tested. Besides its adhesive uses, PVA is also used as a sizing agent in the manufacture of textiles, paper, and plastics. It is a water-soluble resin with the formula $(\text{-}CH_2CHOH\text{-})_n$. The degradation processes noted with gum Arabic and dextrin are not observed when PVA is used, due to the inability of PVA to absorb moisture (1).

Additional ingredients are frequently included in the adhesive mixture to modify the adhesive's properties. These ingredients may include glycerin, corn syrup, glycols, urea, sodium silicate, and emulsified waxes. The addition of these ingredients affects properties such as flexibility, spreading quality, and ease of re-wetting. Sodium benzoate, quaternary ammonium salts, and phenol derivatives may also be found in the

mixture, as preservatives. Lastly, oils of wintergreen, lemon, grape, or anise are frequently added as scenting and flavoring components (1).

Overall, there is a lot of chemistry involved in the production of a postage stamp. As with all of our other studies, the focus of this project involves the colorant. Three separate cases will be presented. The first and most simple, is the analysis of a stamp whose color is claimed to be carmine. Having experience with the carmine lake colorant, we were interested in whether or not the colorant was truly carmine. The second case is an interesting story involving stamps which were used by French and British spys during WW II. A slight physical difference is noted between the original French stamp and the forged British spy stamp. However, we were interested in whether or not they could be distinguished chemically. The final case involves a "changeling". In the early history of stamps, stamps which were found to change color on exposure to light or gases in the environment were called "changelings" (2). The stamp studied here was printed using $PbCrO_4$, which is known to darken upon exposure to sulfur-containing gases in the atmosphere (1-5). This reaction was investigated.

Experimental

A mask was prepared, by cutting a 2 x 2 in^2 square from a manila folder. A 1 x 1 in^2 square was removed from the center of the larger square. A stamp was placed in the center of the modified sample plate and the mask was placed on top. The edges of the mask were taped to the sample introduction plate, so that the stamp was left completely unharmed. The user parameters of the MALDI instrument, as cited in Chapter One, were employed.

The Carmine Stamp

As was demonstrated in Chapter Two: Watercolors, the names of colorants may often times be misleading. Reds are frequently referred to as vermilion, cadium sulfide, or carmine, but are they chemically what these names imply? Let us consider a 2¢ carmine stamp. Red lakes were commonly used throughout history as colorants on postage stamps, therefore we were expecting to generate LD mass spectra indicative of carmine lake (Chapter Four). Red lakes were known to fade when exposed to light or water, so there was a phasing out of their use. Positive and negative ion LD mass spectra were obtained of the stamp. Only Na^+ and K^+ ion peaks were generated in the positive ion mass spectrum (not shown). The negative ion mass spectrum is shown in Figure 5.1.

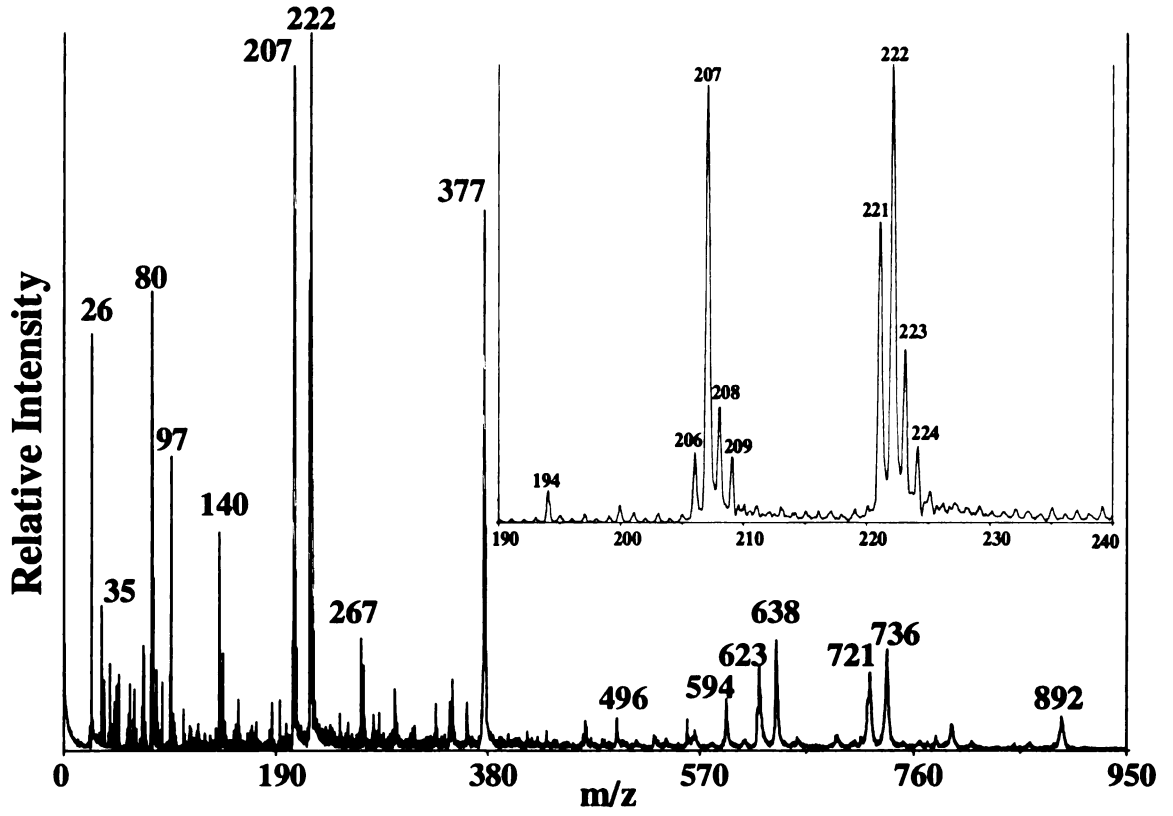

Figure 5.1: The negative ion LD mass spectrum of the 2¢ carmine stamp.

The mass spectrum is clearly not of carmine lake. A portion of the lower mass region is enlarged in the inset of Figure 5.1. It is difficult to determine whether or not the peaks at m/z 207 and 222 are related. The pattern of the peaks resemble that of a neutral dye, in which both the molecular ion (M^-) and deprotonated molecule $(M-H)^-$ are observed. However, one would expect to see a similar pattern in the positive ion mass spectrum, which was not observed. This suggests that the colorant is anionic. The pattern of peaks at m/z 222 does not resemble an isotopic pattern for a known element, which leads us in the direction of an organic colorant. The difference between m/z 207 and m/z 222 is 15 mass units. This could represent the loss of an O atom or an $-NH_2$ group, which would be replaced by a H atom, accounting for the 15 mass unit difference. Another possibility is that the peak at m/z 207 represents a fragment ion, resulting from the loss of a $-CH_3$ group. These are not typical losses observed in a mass spectrum, which suggests that the peaks represent separate colorants (components). The colorants remain unidentified, however the point here is that carmine lake was not used to color the stamp.

The French Spy Stamps

During WW II, communication between the French and the British was frequently intercepted by the Germans and plots were foiled. The French and British underground devised the brilliant idea of using stamps to mark important messages. Figure 5.2 shows two stamps. The stamp on the left is the original 1939 French stamp. The stamp on the right, is the British forgery, which has a slight physical defect, noticed only by those who were looking for the defect. The physical difference is indicated with arrows. Important messages were marked using the British forged stamp. Only a limited number of these valued stamps are available in mint condition. Currently, philatelists only relied on the slight physical difference to differentiate between the two stamps. We wanted to take it one step further and determine whether or not one could distinguish the two stamps by their chemical composition. The LD mass spectrometric analysis of the two stamps follows.

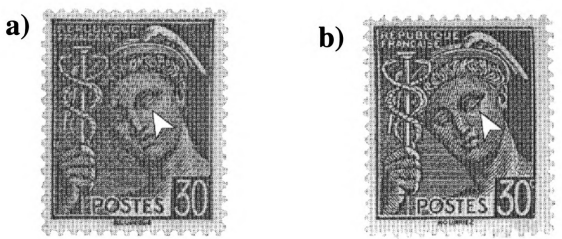

Figure 5.2: The spy stamps: a) the original French stamp; b) the forged British stamp.

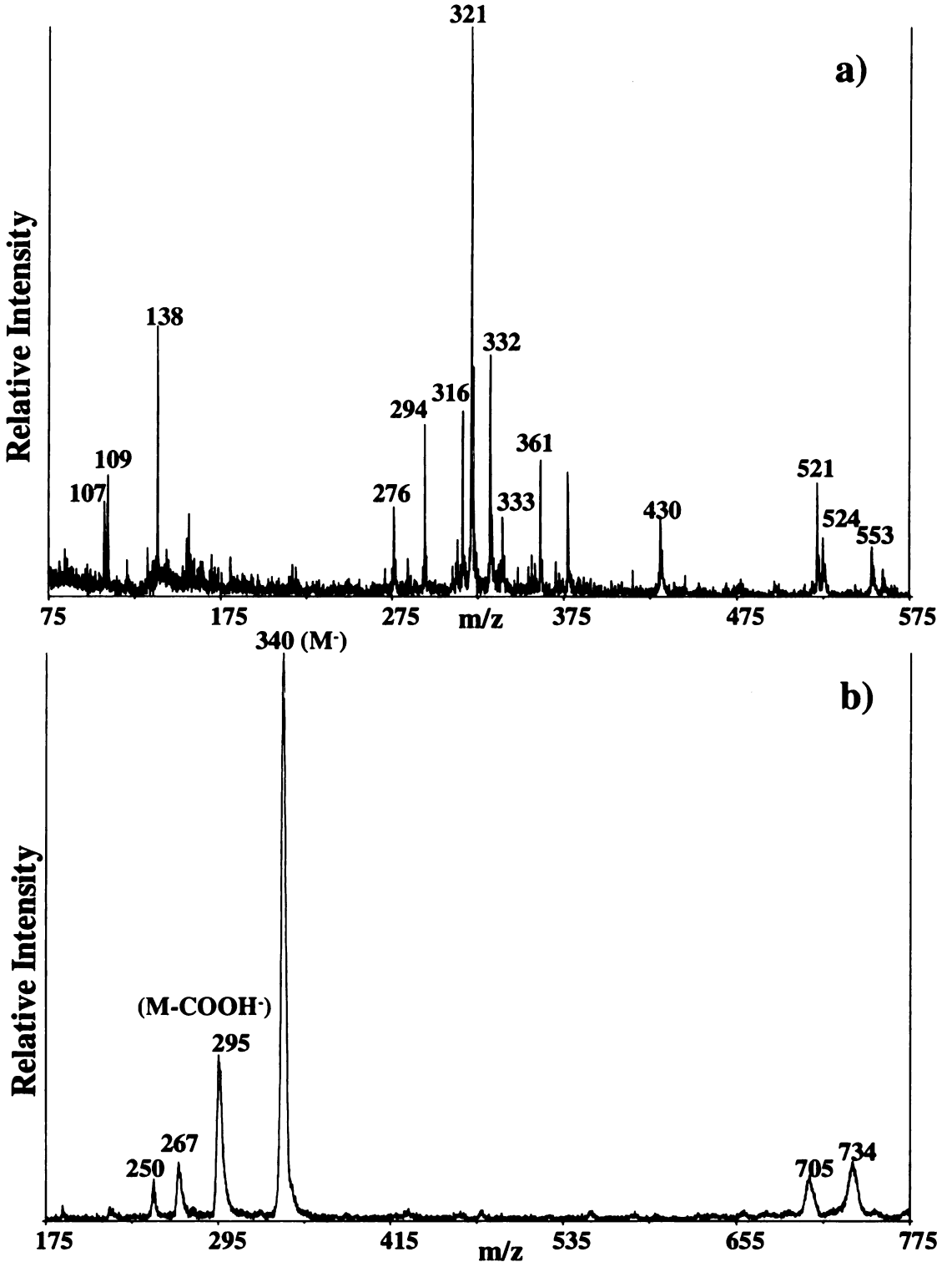

Figure 5.3: The LD mass spectra of the original French stamp: a) positive ions; b) negative ions.

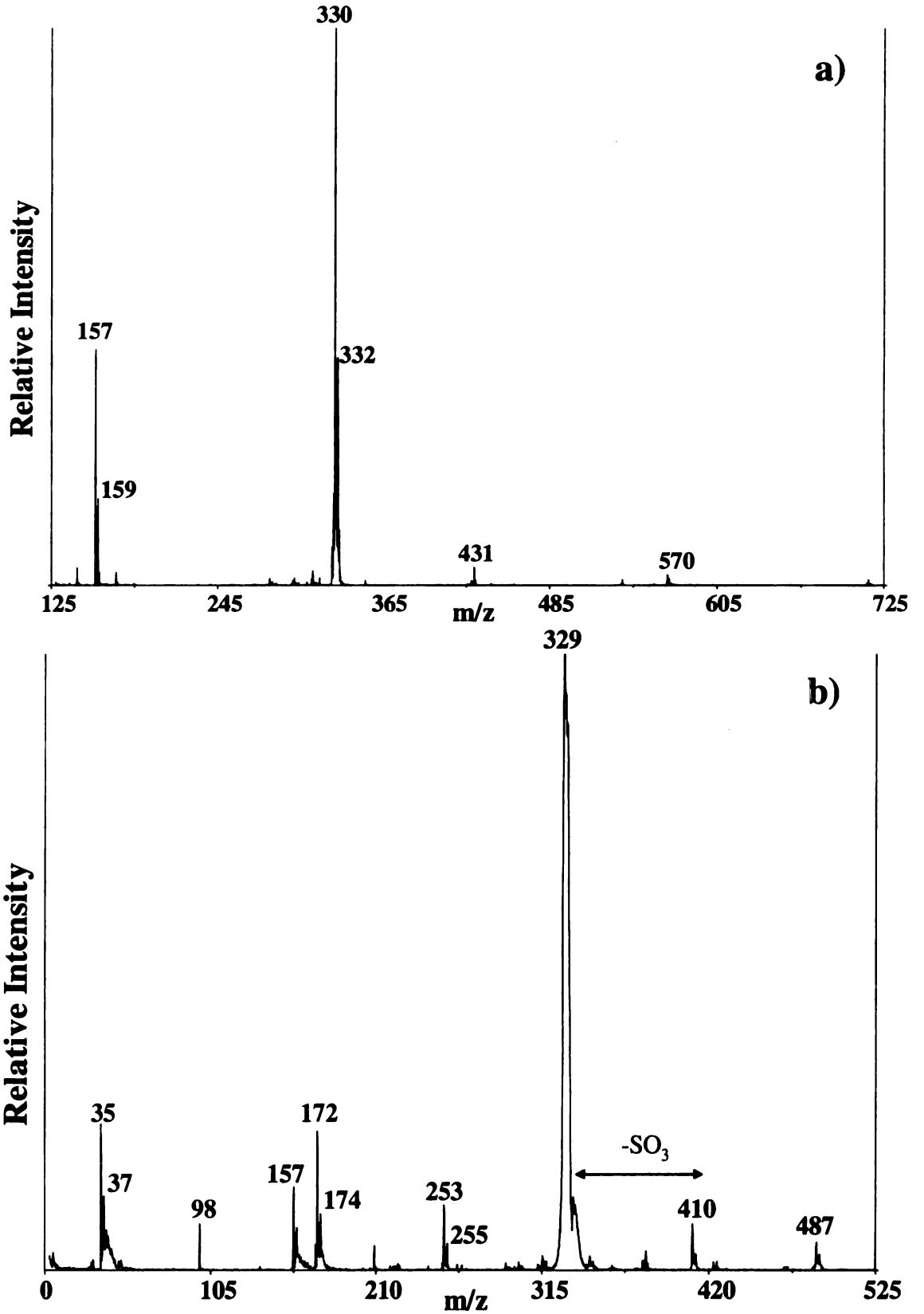

Figure 5.4: The LD mass spectra of the forged British stamp: a) positive ions; b) negative ions.

The positive and negative ion LD mass spectra of the original French stamp and the British forged stamp are shown in Figures 5.3 and 5.4, respectively. The stamps were clearly printed with inks containing different dye compositions. The identities of the dyes remain unknown, however we can characterize them. Three red colorants were cited in the introduction of this chapter, which were used to color postage stamps. These included Red Lake "C", Lithor rubine, and Red B. No information was found on Lithor rubine (calcium salt), however there was a Lithol Red discovered in 1899 by Julius (BASF). This colorant was considered the first of the azo pigment lakes. The colorant was prepared by an indirect diazotization method employing 2-napthylamine-1-sulfonic acid as a diazonium compound. The organic colorant was initially precipitated onto an inorganic support, which formed the lake. However, it was eventually determined that the inorganic material did not have much of an effect on the color or properties of the lake, thus the organic colorant was often times used alone. Lake Red C pigments were discovered shortly after the introduction of Lithol Red in 1902, by Meister Lucius & Brüning (now Hoechst AG) (6). The exact structures for these pigments were not found, however the general structure for these pigments is shown in Figure 5.5a. The pigments were classified as ß-naphthol pigments. The structure in Figure 5.5b is a related pigment classified as a napthol AS pigment. These structures will become important shortly. No information was found on "Red B".

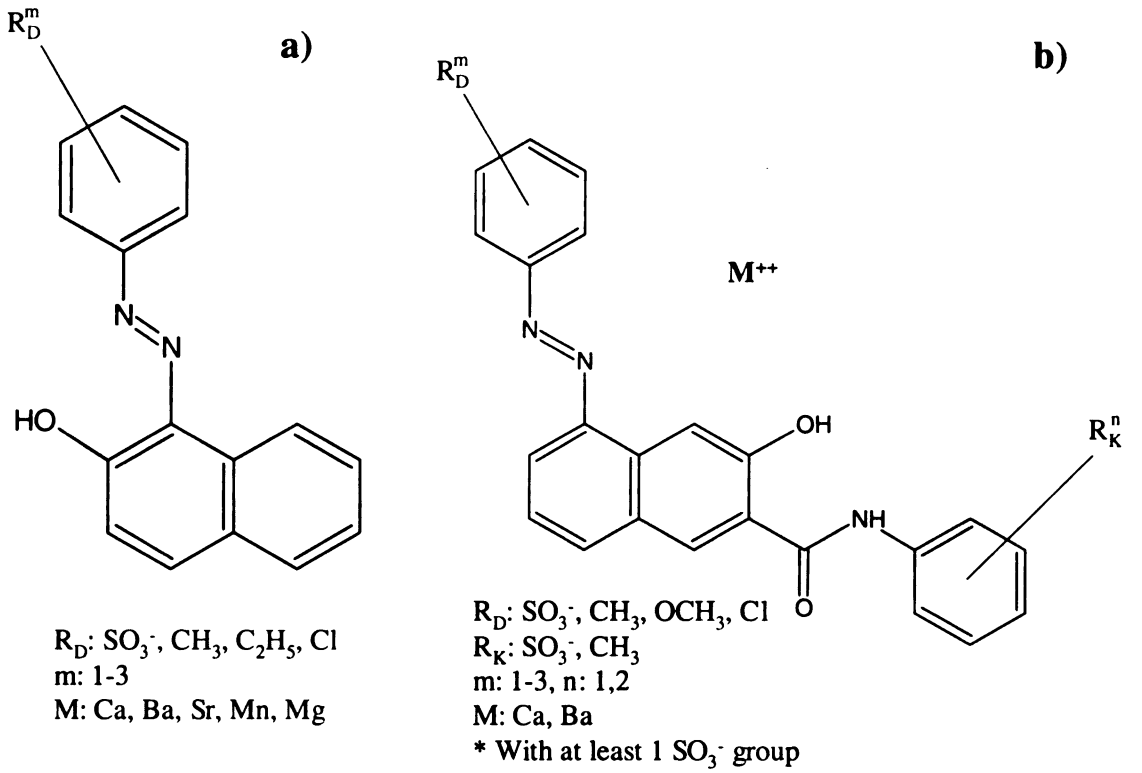

Figure 5.5: a) the general structure of a ß-naphthol pigment; b) the general structure of a naphthol AS pigment.

Focusing on the French stamp first (Figure 5.3), it appears as though a few dyes were used. The colorants are non-chlorinated. The negative ion mass spectrum suffers from poor resolution, however it appears that there is a set of related peaks stemming from the peak at m/z 340, which potentially represents a molecular ion (M^-). The peaks at m/z 295, 267, and 250 could represent the neutral consecutive losses of –COOH, -C_2H_5, and –OH, respectively.

The British spy stamp, on the other hand, appears to contain only one, chlorinated colorant. At first, it may seem as though the peak in the positive ion mass spectrum (Figure 5.4a) at m/z 330 represents the (M^+) ion and the peak in the negative ion mass

spectrum (Figure 5.4b) at m/z 329 represents the $(M-H)^-$ ion. However, if the structures in Figure 5.5 are considered, the peaks may actually represent fragment ions. Beginning with the smallest fragment ion at m/z 157, appearing in both the positive and negative ion mass spectra, what are the possibilities? In order to absorb in the UV, the intact structure probably contains an aromatic ring. The isotopic pattern also suggests that one Cl atom is present. Proposed structures for m/z 157 and m/z 172 are shown in Figure 5.6. The assignments were made based on the possible structures in Figure 5.5. Additional assignments were not made, however the remaining peaks are believed to represent fragments of the intact colorant molecule. The reason for this lies in the fact that all of the peaks maintain the isotopic pattern of one Cl atom, and there are mass differences between peaks which can be accounted for. For instance, the mass difference of 80 between m/z 329 and m/z 410, may be due to the loss of a sulfite group ($-SO_3$). These assignments have not been confirmed, however a variety of modern day red pigments were purchased and tested. The spectra did not match either of the spy stamps.

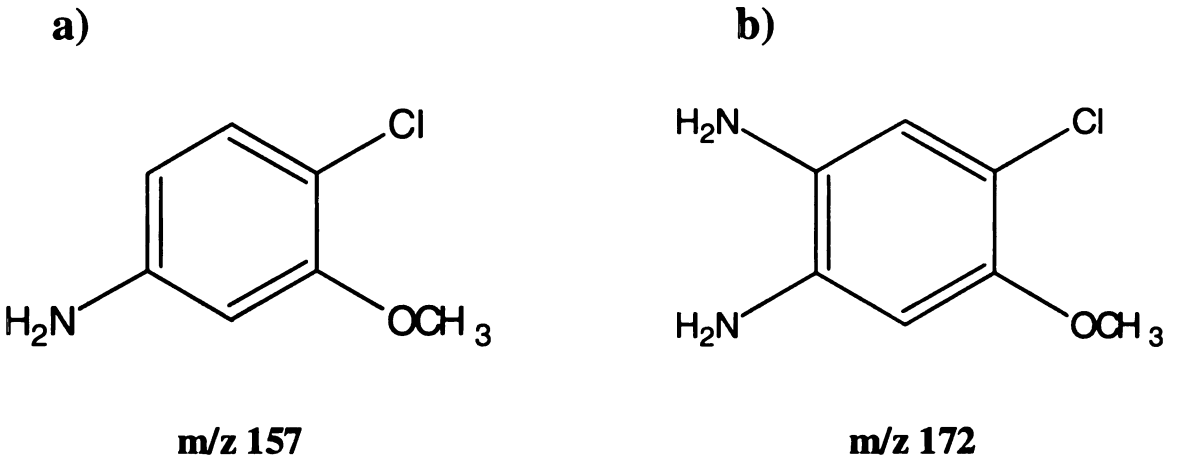

Figure 5.6: Proposed structures for a) m/z 157 and b) m/z 172.

Another approach is artificial aging. Modern day red rhodamine dyes have been studied extensively in our lab (7). It has been shown that one red ink containing rhodamine B and a second red ink containing rhodamine 6G produce the same positive ion mass spectrum, when the ink is freshly applied to paper. The reason for this is that both dyes have the same molecular weight, but differ structurally. When the inks age (degrade), they produce different degradation products, and unique peaks appear in the "aged" mass spectra. Thus, it has been demonstrated that UV light (among other light sources) can be used to artificially accelerate the age of the dye to obtain more structural information.

The French and British spy stamps studied here, are rare and highly valued. Therefore, the owner did not want them faded (aged). Numerous French and British stamps were purchased from a local stamp collector's shop. LD mass spectra were obtained of all of them in the hope to find a few samples with the same dyes as the spy stamps. One British stamp was found to have the same dye as the British spy stamp. This stamp was subjected to UV irradiation for several hours. Fading of the colorant was not observed, and the mass spectra remained the same. This approach was unsuccessful here.

Ideally, we had hoped to identify the exact dye composition used on the stamps, however the results are still interesting and useful. By completing this project, some important concepts were learned about philately. For example, it was learned that philatelists are more concerned with the physical appearance of stamps, rather than their chemical composition, in regards to the detection of forgeries. Perhaps, publishing these results in a philatelist journal (i.e. Linn's Stamp News), would peak the interest of avid

stamp collectors to seek more sophisticated analytical techniques to help characterize their stamps. LDMS is definitely an attractive option, considering it is a noninvasive technique, which leaves the stamp virtually unharmed. Until then, philatelists will be limited to microscopy techniques.

The $PbCrO_4$ Stamp

As was mentioned in the introduction, specific stamps have been known to change color throughout history (1,2). Initially, the color changes were thought to be the result of some sort of error in formulation. Eventually, it was determined that the colorants reacted in response to either light or gases in the environment. Red lakes were especially known to be fugitive and faded on exposure to light. Other metal containing pigments were known to darken in the presence of pollutant gases, such as H_2S. Fortunately, there are means to chemically reverse the color change. The focus of this study is on a yellow stamp (Gold Star Mothers) which contained the pigment $PbCrO_4$. Three samples were provided (shown in Figure 5.7): an original (c), one that was exposed to H_2S (g) and had blackened (b), and one that had been exposed to H_2S (g) followed by treatment with H_2O_2 (a). The stamps were analyzed using LDMS to detect and identify reaction products to characterize the reaction mechanism more effectively.

Figure 5.7: The Gold Star Mothers Stamps: a) Exposed to H_2S (g), followed by treatment with H_2O_2 (l); b) Exposed to H_2S (g); c) original (untreated).

The chemistry of this reaction is known (2-4). On exposure to H_2S (g), some black PbS(s) is formed. Following treatment with H_2O_2 (l), white $PbSO_4$ (s) forms and the original yellow color of unreacted $PbCrO_4$ returns. Is the reaction really this simple? It has been reported that Pb-containing pigments darken naturally on exposure to light, due to a change in crystal structure (8). Others have cited the formation of brown PbO_2(s) resulting from bacterial deterioration as the cause of the darkening (9). Additionally, there are two metals present: Pb and Cr. Does CrO_4^{2-} react with H_2S (g) to form Cr_2S_3 (a dark brown/black powder) or another product (10)? These are a few of the questions we were hoping to answer at the end of this study.

The positive ion LD mass spectra of all three stamp samples are shown in Figure 5.8, so that they may easily be compared. Likewise, the negative ion LD mass spectra of all three stamps are shown in Figure 5.9. Returning to the positive ion mass spectra, Figure 5.8a shows the mass spectrum of the stamp in its original form. Characteristic $PbCrO_4$ peaks are noted (appendix), which were discussed in Chapter 4. For example, the peaks at m/z 208 represent Pb^+ ions and the peaks at m/z 430 represent Pb_2O^+ ions.

Following exposure of the stamp to H_2S (g), the positive ion mass spectrum changed dramatically (Figure 5.8b). The colorants' vehicle is unknown. Therefore, positive and negative ion LD mass spectra were obtained of PbS in a variety of vehicles. The carriers included linseed oil, water and gum Arabic. The spectra (not shown, see Chapter Six) were not identical in every case. A few characteristic peaks were noted, which have not appeared in other Pb-containing pigment spectra. In the positive ion mode, a cluster of peaks at m/z 483 was noted and has been assigned Pb_2ClS^+. These peaks are not seen in Figure 5.8b. An observation which is consistent with the PbS spectra is the absence of the typical Pb-containing ions. This was noted in the spectra obtained of PbS in linseed oil and in gum Arabic. Unfortunately, the new ions formed, do not have unique isotopic patterns to aid in their identification. No peaks were observed having an isotopic pattern consistent with Cr, suggesting that Cr_2S_3 or -any other Cr-containing product was formed.

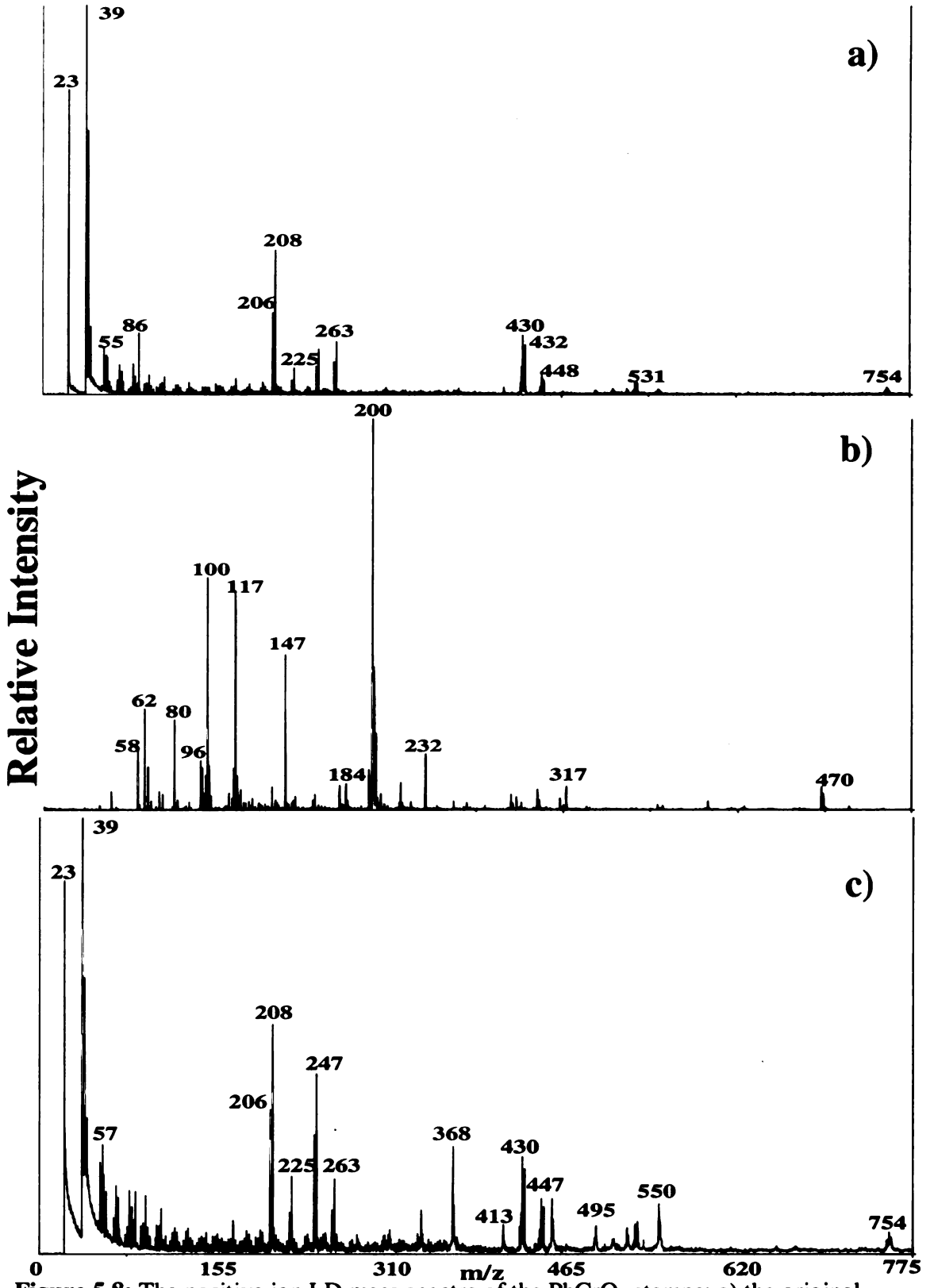

Figure 5.8: The positive ion LD mass spectra of the $PbCrO_4$ stamps: a) the original stamp; b) the stamp exposed to H_2S (g); c) the stamp exposes to H_2S (g) followed by treatment with H_2O_2 (l).

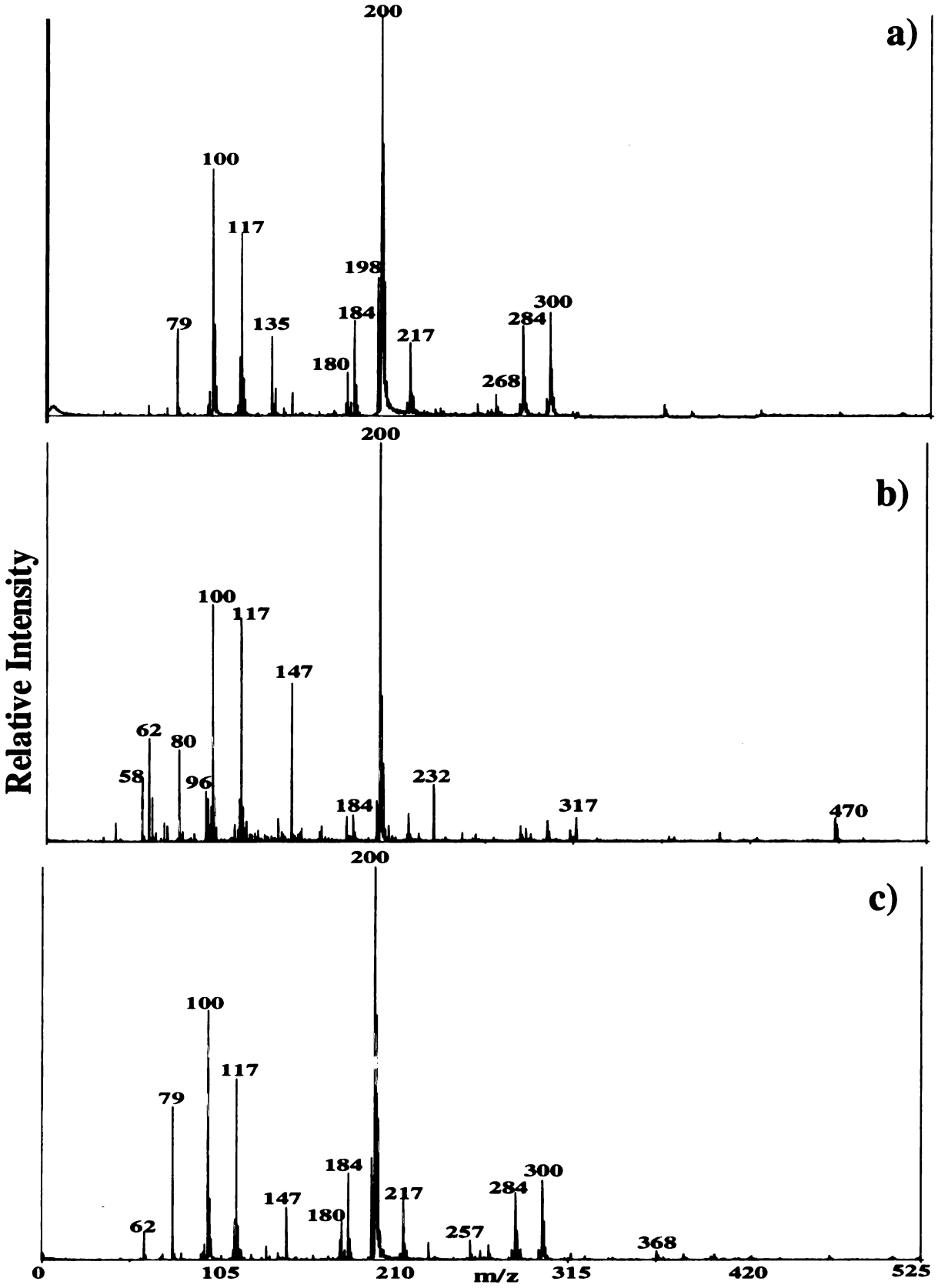

Figure 5.9: The negative ion LD mass spectra of the $PbCrO_4$ stamps: a) the original stamp; b) the stamp exposed to H_2S (g); c) the stamp exposes to H_2S (g) followed by treatment with H_2O_2 (l).

The sample was then treated with H_2O_2 (l) to restore the original yellow color. $PbCrO_4$ is not reformed. Rather, some of the PbS is converted into white PbO. This transformation gives the appearance that the yellow color has returned. In actuality, the color never left, it was simply masked by the inhomogeneous layer of black PbS formed on the surface. The positive ion LD mass spectrum of this sample is shown in Figure 5.8c. The spectrum has changed again. The characteristic Pb-containing ions (m/z 208, 247, 430, etc.) have returned. A new peak appeared at m/z 368, which again does not have any unique isotopes to help characterize the compound, indicating that it may simply be an impurity.

Switching to negative ion mode, the spectra (Figure 5.9) of the three samples remain relatively stable. In the mass spectrum of the original sample (Figure 5.9a), peaks representing characteristic $PbCrO_4$ ions (i.e. m/z 100, 200, and 300), as were discussed in chapter four, are observed. Once the stamp is exposed to H_2S (g), the spectrum (Figure 5.9b) changes slightly. The intensities of $Cr_xO_y^-$ ion peaks decrease in the m/z 300 region. Additionally, two new peaks are noted at m/z 232 and m/z 470. There was no evidence of any $Pb_xS_y^-$ or related ions formed

The sample was treated with H_2O_2 (l), and the negative ion mass spectrum of this sample is shown in Figure 5.9c. The intensities of the peaks at m/z 300 have increased, as compared to the H_2S (g) exposed sample. The peak at m/z 470 has disappeared.

Was this experiment successful? The sample studied had changed color in response to its environment. This was confirmed in both the positive and negative ion mass spectra. Unique PbS ions were not formed, however the absence of certain Pb-containing ions were noted, which is characteristic of the presence of PbS. Following

treatment with H_2O_2 (l), the spectra changed once again to resemble the original spectra. Peaks representing Cr_xS_y ions were not detected, which supports the accepted explanation for this reaction, in that only Pb and not Cr is reacting with the H_2S(g). The "new" peaks which appear sporadically in some of the spectra were not identified, however the conditions of the experiments preparing the stamps may not have been controlled, allowing for the presence of impurities. Overall, the experiment was successful in that we were able to map the chemical change of the stamp.

Summary

By completing this project, we have demonstrated the usefulness of LDMS in the area of philately. First, we showed how the color name of a stamp (carmine) may be misleading of its true composition. Next, we demonstrated how forged stamps may differ chemically, in addition to physically. We successfully used LDMS to determine that the famous French and British stamps were not chemically the same. Lastly, we used LDMS to detect and analyze the products formed from chemical reactions taking place on the stamps. The $PbCrO_4$ exposed to H_2S (g) reaction will be explored further in the following chapter.

References

1) Sharkey J. Chemistry of postage stamps: dyes, phosphors, adhesives. The United States Specialist 1990 August:469-482.

2) Cabeen RM. Standard handbook of stamp collecting. New York: Thomas Y. Crowell Company, 1965.

3) Clay HF, Watson V. Some important properties of chromes. Journal of the Oil and Colour Chemists' Association. 1944;27:3-18.

4) Torlaschi S, Caggiati L, Zorzella G. Chemical and physical effects of sulphur dioxide on inorganic pigments and paints. 207-215.

5) Erkens LJH, Hamers H, Hermans RJM, Claeys E, Bijnens M. Lead chromates: a review of the state of the art in 2000. Surface Coatings International Part B: Coatings Transactions 2001;84:169-176.

6) Herbst W, Hunger K. Industrial organic pigments: production, properties, applications, 2nd ed. Weinheim: VCH, 1997.

7) Dunn JD, Siegel J, Allison J. Photodegradation and laser desorption mass spectrometry for the characterization of dyes used in red pen inks. J Forensic Sci 2003;48:652-657.

8) Watson V, Clay HF. The light-fastness of lead chrome pigments. Journal of the Oil and Colour Chemists' Association 1955;38:167-177.

9) Petushkova JP, Lyalikova NN. Microbiological degradation of lead-containing pigments in mural paintings. Studies in Conservation 1986;31:65-69.

10) Saleh FY, Parkerton TF, Lewis RV, Huang JH, Dickson KL. Kinetics of chromium transformations in the environment. The Science of the Total Environment 1989;86:25-41.

Chapter Six: Studies of the Interactions of H_2S with Colorants

Introduction

Before the hazardous nature of lead compounds was established, Pb-containing pigments were frequently found in artists' palettes. Some of these pigments included chrome yellow ($PbCrO_4$), lead white ($PbCO_3 \cdot Pb(OH)_2$), and lead antimonate ($Pb_3(SbO_4)_2$). Throughout history, Pb-containing pigments were known to darken or change color over time in response to their environment. Researchers have cited several different mechanisms for these transformations, dependent on the type of Pb-pigment used and the environment it is in. The mechanisms of these reactions are at least partially understood and will be explained here.

In the 1950s, Watson and Clay investigated the crystal structures of lead chromes and how they affected the darkening of the lead chrome pigments in the presence of light (1-2). They proposed that a photochemical reduction was responsible for the blackening of $PbCrO_4$. Watson and Clay concluded that the polymorphic nature of lead chromate influenced the pigment's sensitivity to light, citing the monoclinic form to be more stable than the orthorhombic form. They were not able to detect any Pb-containing products formed or remaining, however they measured the pressure of gases released during the transformation. Watson and Clay explained that the darkening was caused by the formation of the greenish-black lead chromite.

Several research groups have investigated the darkening of lead white and proposed solutions to reverse the transformation (3-5). Petushkova and Lyalikova performed an interesting study involving bacterial deterioration of lead white, massicot

(PbO), and minium (Pb_3O_4) on mural paintings. Microorganisms frequently infest paintings resulting in detrimental effects on the pigments and the underlying material. Petushkova and Lyalikova discovered through X-ray examination that the darkened brown spots on the mural painting studied were due to the formation of PbO_2. They explained that heterotrophic bacteria generate H_2O_2, which resulted in the oxidation of bivalent lead. Equation (1) summarizes the overall reaction:

$$2PbCO_3 \cdot Pb(OH)_2 + 3H_2O_2 \rightarrow 3PbO_2 + 2H_2CO_3 + 2H_2O \quad (1)$$

Giovannoni and coworkers investigated a similar reaction involving the discoloration of the lead white pigment in wall paintings (4). They proposed a similar mechanism, but also noted that the alkalinity of the environment and moisture have a significant influence on the rate of transformation. A slightly acidic H_2O_2 solution was cited as a means to reverse the reaction (4,5). The following 3-step mechanism (equations 2-4) describes the reconversion to lead white.

$$PbO_2 + H_2O_2 + 2CH_3COOH \rightarrow Pb(CH_3COO)_2 + O_2 + 2H_2O \quad (2)$$

$$3Pb(CH_3COO)_2 + 2H_2O \rightarrow 2Pb(CH_3COO)_2 \cdot Pb(OH)_2 + 2CH_3COOH \quad (3)$$

$$2Pb(CH_3COO)_2 \cdot Pb(OH)_2 + 2CO_2 + 2H_2O \rightarrow 2PbCO_3 \cdot Pb(OH)_2 + 4CH_3COOH \quad (4)$$

Petushkova and Lyalikova also noted the transformation of the Pb-containing pigment to black PbS. When bacteria use S-containing amino acids, they generate H_2S. Again, H_2O_2 is cited as the appropriate treatment to use in order to reverse the reaction.

However, in this case, the product of the reconversion is $PbSO_4$, as opposed to lead white. The reaction between H_2S and Pb-containing pigments was noted in Chapter 5 and is investigated more in depth here.

In Chapter 5, the lead chromate stamps analyzed had been previously exposed to H_2S (g) and treated with H_2O_2, by another researcher. We wanted to recreate the experiment in our laboratory to learn more about the transformation and how LDMS could be used to help characterize the reaction. For instance, were there any additional products formed? Also, the transformation of $PbCrO_4$ to PbS is not complete, meaning that there is always yellow pigment remaining. Considering that PbS is not a commonly used black pigment by artists, as compared to the more commonly used carbon black pigments, the detection of PbS in a painting offers insight into the original pigments used and where the painting was stored (e.g. in a highly industrial area having a high concentration of S-containing gases). We also wanted to test whether or not the extent of deterioration could be determined by comparing the intensity of the peaks of the reactants ($PbCrO_4$) and the products (PbS) in the mass spectrum.

One other direction we were interested in pursuing is the treatment of H_2S-exposed samples with H_2O_2, to determine if reconversion products could be detected. Hypothetically, the reaction product is $PbSO_4$, however the samples analyzed are impure mixtures, and there may be additional products formed. This information could potentially be very useful to art conservatorss, since the detection of a reconversion product would reveal that a painting had previously been treated to cover up a discoloring reaction.

Experimental

Numerous Pb-containing pigments were obtained, including PbO, PbO_2, $PbCrO_4$, PbS, $Pb_3(SbO_4)_2$, $PbMoO_4$, and $PbSO_4$. All of the compounds were suspended in linseed oil and applied to paper. The samples were taped to the modified sample introduction plate and subjected to positive and negative ion LD mass spectral analysis.

The green G13 pigment from the pigment distributor's carrying case, discussed in Chapter 4, was used as the focus of this study. A second pigment, labeled Y12, was selected from the pigment set. Y12 is a yellow pigment composed of $PbCrO_4$. The second pigment was added to see if there was any difference in the results when $PbCrO_4$ was by itself (Y12) or in a mixture (G13, with Prussian blue). The pigments were suspended in linseed oil and applied to paper. Once the samples "dried", they were exposed to H_2S gas.

In the first experiments performed, H_2S (g) was made in our lab. Approximately 5 mL of HCl (l) was added to a beaker containing approximately 5 g Na_2S (s). A stick was taped across the top of the beaker, so that samples (~ 1 in^2 paint-on-paper) could hang freely in the center of the beaker. In the original experimental design, the samples were taped directly to the sides of the beaker. However, at the end of experiments, the samples were wet due to condensation on the walls of the beaker. To reduce condensation, the beakers were placed in an ice bath. The ice bath was also employed to reduce the HCl from vaporizing and reacting with the samples. The beaker was covered with a watch glass following the addition of HCl to the Na_2S in the beaker. The samples were exposed to H_2S (g) for varying time increments. The exposed samples were taped to a modified sample plate holder and subjected to LDMS analysis. The H_2S exposed

samples were then treated with H_2O_2 (l) until the darkened spots disappeared and the sample appeared to have returned to its original color. The samples were then taped to the LDMS plate and subjected to LDMS analysis once again.

The design is very primitive and not effectively controlled, however it provided us with data suggesting that it was possible to detect the chemical changes involved in the reaction, using LDMS. The results of these experiments led to a set of controlled experiments. A canister of H_2S (g) was purchased and connected to a vacuum manifold. Samples (G13 and pure $PbCrO_4$ in linseed oil on paper) were exposed to approximately 65 Torr H_2S (g) for a variety of time increments. Following H_2S exposure, the manifold and sample reaction chamber was flushed with air, and the samples were removed and analyzed using LDMS.

Preliminary Work

As a pigment, lead chromate is prepared in many ways. Other Pb-containing pigments, such as $PbSO_4$, $PbMoO_4$, and $Pb_3(SbO_4)_2$, are frequently precipitated with $PbCrO_4$ in order to alter its shade (6). Numerous Pb-containing compounds were obtained, which were cited in the literature as either possible impurities in lead chrome pigments or a reaction product resulting from exposure to H_2S gas. Positive and negative ion LDMS spectra were obtained of each of the samples, suspended in linseed oil and, applied to paper. The purpose in completing this task was to catalog all of the possible ions which might be observed in our H_2S exposure experiments involving lead chrome pigments. The results of these experiments are summarized in the Appendix. While there are some ions, which are generated from nearly every Pb-containing compound

(e.g. Pb^+, PbK^+, $Pb_2O_2H^+$), each compound usually produces at least one or two ions which help to distinguish it from others. The data in the Appendix will be referred to throughout this chapter.

Designing the H_2S Exposure Experiments

In the first experimental design, concentrated HCl was added to Na_2S in a beaker containing the sample, and the reaction proceeded at room temperature. Black spots appeared on both the G13 and Y12 samples during exposure, however the green G13 sample was turning an aqua, more bluish-color, while the yellow of the Y12 sample was disappearing. The G13 pigment is a mixture of blue ferric ferrocyanide and yellow $PbCrO_4$. The Y12 pigment is strictly $PbCrO_4$. The black spots were expected due to the formation of PbS. The $Cr_xO_y^-$ ions noted in the initial negative ion mass spectrum of the G13 sample (Figure 6.1b, Y12 spectrum not shown) also disappeared, supporting the hypothesis that the chromate chromophore was destroyed.

By cooling the reaction chamber, the black spots still formed upon exposure to H_2S (g), however the sample remained the appropriate color. This suggested that moisture played a role in the destruction of the chromate chromophore. Koller and coworkers had noted that moisture greatly accelerated the conversion of lead white to lead dioxide (5). Once the samples were removed from the cooled reaction chambers, the

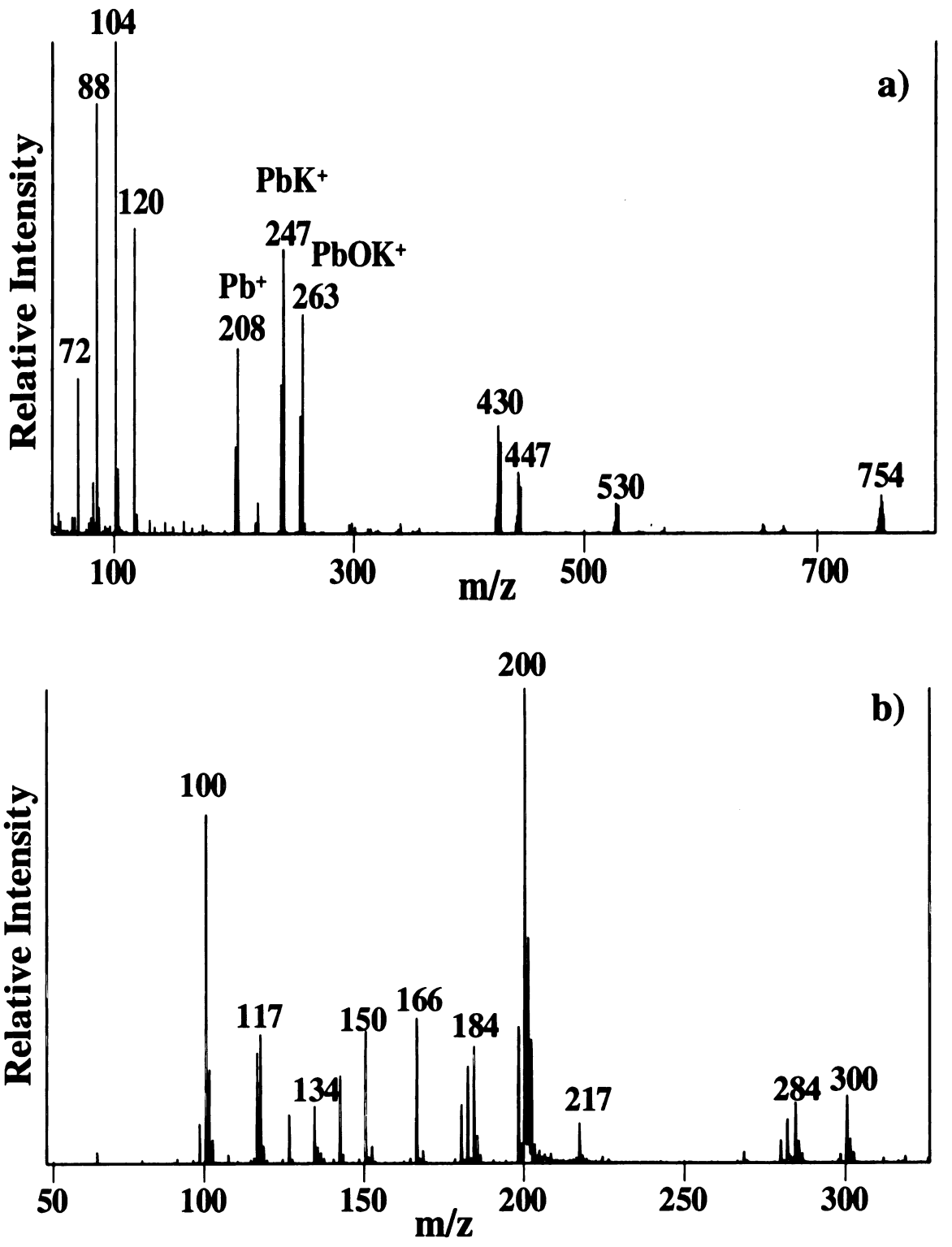

Figure 6.1: The LD mass spectra of G13 in linseed oil; a) the partial positive ion mass spectrum; b) the partial negative ion mass spectrum.

yellow $PbCrO_4$ pigment would gradually disappear and the aqua color of the G13 pigment returned. Thus, samples were analyzed immediately after exposure to H_2S (g) before any side reactions could take place.

What was causing the destruction of the chromate chromophore? It has previously been determined that oxygen can have detrimental effects on Pb-containing pigments (8). Specifically considering $PbCrO_4$, if left undisturbed, oxygen does not have any effect on the pigment. Pb has a high affinity for S. If a pollutant, such as H_2S (g), is introduced into the environment, Pb will bond with S to form PbS, leaving the chromate free to react. Linseed oil (and other drying oils) extracts O from CrO_4, ultimately destroying the chromophore (8). An oxygen rich environment accelerates this process. Lead may also react with linseed oil, forming Pb-linoleate (lead soap), which may be washed away by sulfurous acid (8).

What to Expect?

The proposed reaction between $PbCrO_4$ and H_2S (g) results in the formation of PbS. To return the pigment to its original color, the PbS product is treated with H_2O_2 (l) to form $PbSO_4$. Positive and negative ion LD mass spectra were obtained of PbS suspended in linseed oil and applied to paper. Two samples prepared at separate times produced different spectra. The spectra of the first sample are shown in Figure 6.2 and the spectra of the second sample are shown in Figure 6.3. In the positive ion mass spectrum of the first sample (Figure 6.2a) a small peak at m/z 208 is noted, representing Pb^+ ions. In the middle mass region, the peaks at m/z 240, 268, 304, 332, and 360 have not been identified, however they originate from the paper. In the higher mass region of

the mass spectrum, numerous peaks have been identified as representing $Pb_xS_yCl_z^+$ ions. The negative ion mass spectrum of the first sample (Figure 6.2b) is dominated by peaks representing $PbCl_3^-$ ions. This is an important observation. As will soon be revealed, $PbCl_3^-$ were detected in samples that were exposed to H_2S (g) created using HCl. Initially, we were concerned that our experiment was creating conditions which resulted in the formation of products that did form naturally. From these experiments, it appears as though, if Cl (even as an impurity) and PbS are present, $PbCl_3^-$ ions readily form. $PbCl_3^-$ ions have only been observed when PbS is present in the sample, and therefore appear to be and indicator that PbS is present.

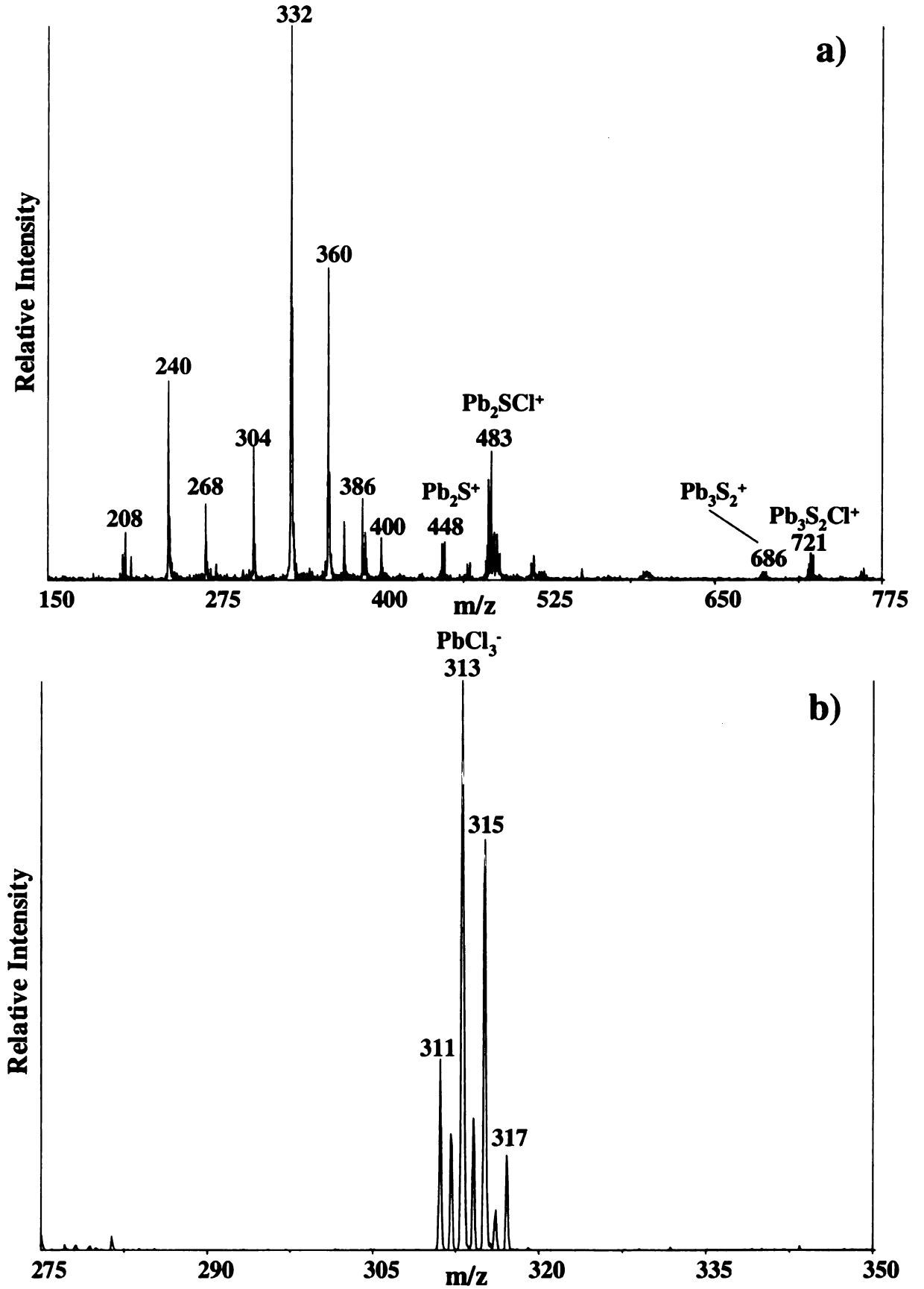

Figure 6.2: The LD mass spectra of PbS in linseed oil on paper (sample 1); a) the partial positive ion mass spectrum; b) the partial negative ion mass spectrum.

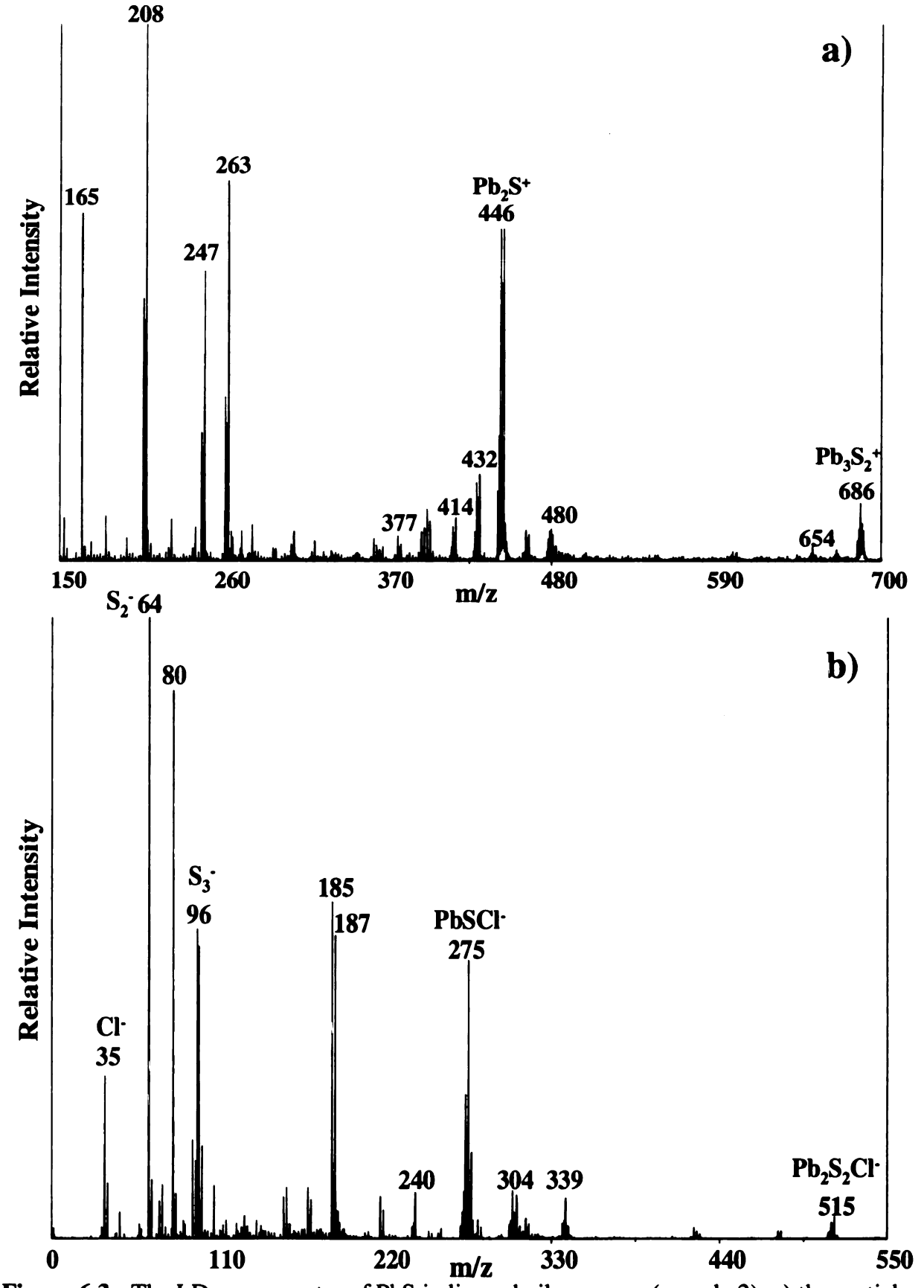

Figure 6.3: The LD mass spectra of PbS in linseed oil on paper (sample 2); a) the partial positive ion mass spectrum; b) the partial negative ion mass spectrum.

The mass spectra of the second PbS in linseed oil on paper sample (Figure 6.3) are very different. The positive ion mass spectrum (Figure 6.3a) is abundant with the Pb-containing peaks (m/z 208, 225, 247, 263, etc) characteristic of the positive ion mass spectrum of nearly every Pb-containing compound. It is important to point out the cluster of peaks at m/z 446, representing Pb_2S^+ ions. These peaks are indicative of PbS. Other Pb-containing pigments generate peaks at m/z 447, representing $Pb_2O_2H^+$ ions. It is also interesting to note that Cl^- ions are represented in the negative ion mass spectrum (Figure 6.3b) at m/z 35, but there were no $Pb_xS_yCl_z^+$ ions identified in the positive ion mass spectrum. Sulfur cluster ions (m/z 64, 96) are also noted in the negative ion mass spectrum, which do not consistently appear in every negative ion mass spectrum of PbS. The peaks at m/z 313, representing $PbCl_3^-$ ions, are not observed in Figure 6.3b, however there is a set of peaks at m/z 275 representing $PbSCl^-$ ions. In results to be discussed, the peaks at m/z 275 and 313 often times occur together. While it is discouraging that the mass spectra of PbS are not reproducible, variations could easily be due to differences in sample loading, for example. Both spectra provide unique peaks which may be potentially generated by the compound. These unique peaks have been identified in the spectra of H_2S exposed $PbCrO_4$ samples.

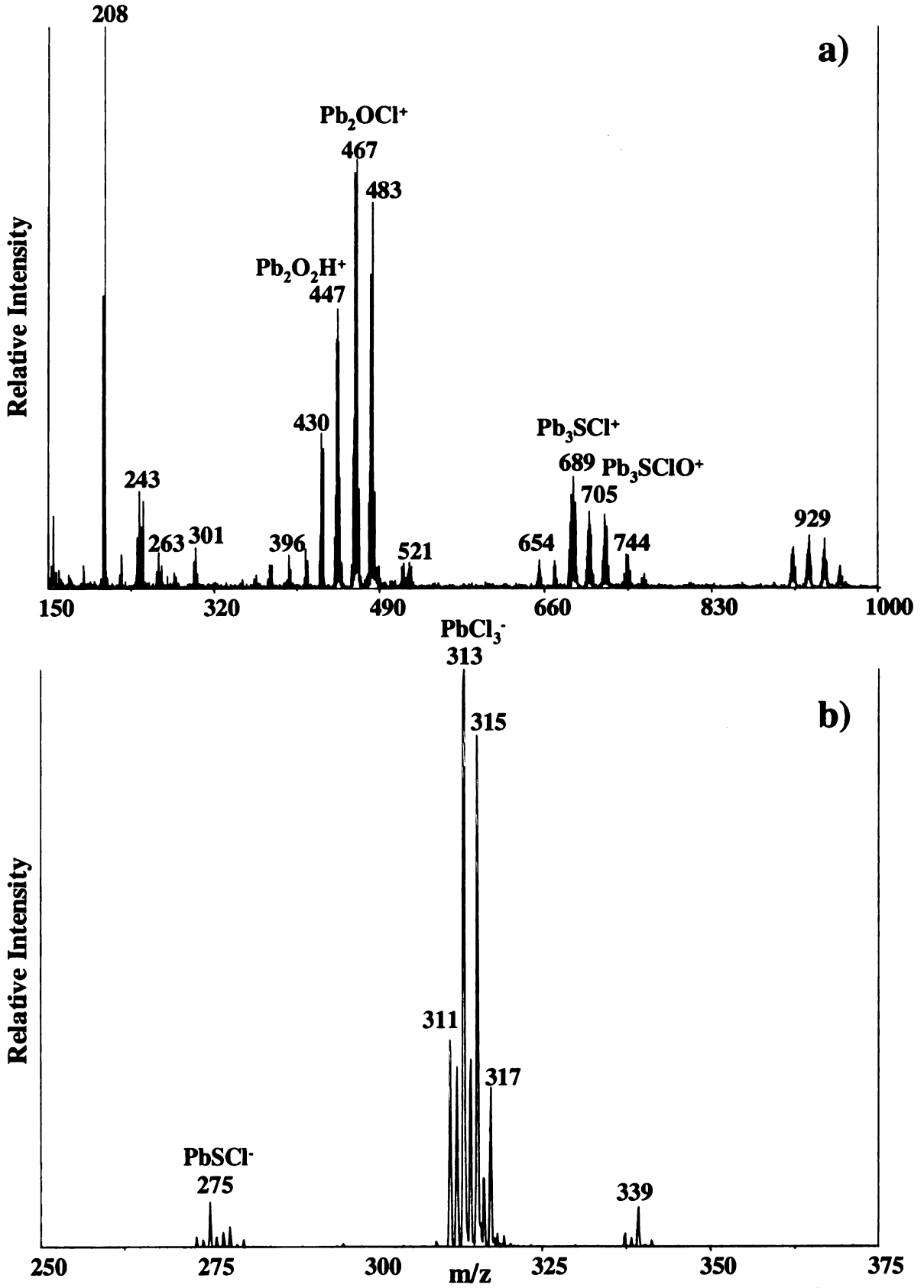

Figure 6.4: The LD mass spectra of PbS in linseed oil on paper treated with H_2O_2 (l); a) the partial positive ion mass spectrum; b) the partial negative ion mass spectrum.

The PbS in linseed oil on paper samples were then treated with enough H_2O_2 to give the samples a white "frosted" appearance. Theoretically, the spectra of this new sample would be that of $PbSO_4$. Positive and negative ion LD mass spectra (not shown) were obtained of $PbSO_4$ (Aldrich). Considering that $PbSO_4$ does not generate any unique peaks when compared to the other Pb-compounds, we will not be able to tell for certain if $PbSO_4$ is the product. Perhaps, the disappearance or a decrease in the intensities of PbS peaks will be observed.

The positive and negative ion LD mass spectra of the first PbS sample treated with H_2O_2 are shown in Figure 6.4. The positive ion mass spectrum (Figure 6.4a) changed dramatically. The results are summarized in Appendix B. Notably, the clusters of peaks at m/z 447 ($Pb_2O_2H^+$) have replaced the peaks at m/z 446 (Pb_2S^+). It should be noted that these experiments seem to be laser power dependent. A higher laser power allows for the ions with larger m/z values to be seen in the mass spectrum. The negative ion mass spectrum (Figure 6.4b) did not change dramatically. A new peak appeared at m/z 339, which has not been identified but contains Pb and Cl, based on its isotopic pattern. From this experiment, it appears as though we may expect for Pb^+ and PbO^+ ions to return.

Uncontrolled H_2S Studies

Preliminary experiments using the cooled reaction chambers and chemically generated H_2S (g) indicated that the spectra of the lead chrome pigments changed following H_2S (g) exposure, and PbS ions could be detected. Using this method, the reaction occurred very quickly (within seconds). As in the methyl violet degradation

study, we wanted to determine if we could effectively monitor this transformation. Several experiments were designed. One involved a timed study, in which samples were taken at half minute increments up to 2 minutes and then every two minutes there after up to 8 minutes. The reaction occurred too quickly. A second experiment was designed in which separate samples were exposed for 2 minute intervals to H_2S (g) created using a series of diluted HCl solutions. This approach appeared to be more effective and will be discussed here.

Approximately 5g Na_2S were placed in four beakers. A set of solutions was prepared, diluting the concentrated HCl 25%, 50%, and 75% with water. Approximately 5 mL of each solution was added to a separate beaker, with 5mL of the full strength HCl solution added to the fourth beaker. The purpose in doing so, was to vary the concentration of the H_2S (g) the samples were exposed to. Thus, Beaker 1 theoretically contained the least concentrated H_2S environment, since the least concentrated HCl solution was added. Four samples were prepared for each pigment (G13 and Y12). The samples were suspended in the beakers for 2 minutes. The samples were removed and analyzed immediately. We had hoped that exposing the samples for the same time period, to varying concentrations of H_2S (g), would result in a set of samples with a range of discoloration, resulting from the formation of PbS.

The results of the Y12 samples were comparable to the G13 samples. For simplicity sake, only the G13 results will be presented. The results of G13 were chosen, since the pigment was previously discussed in Chapter 4.

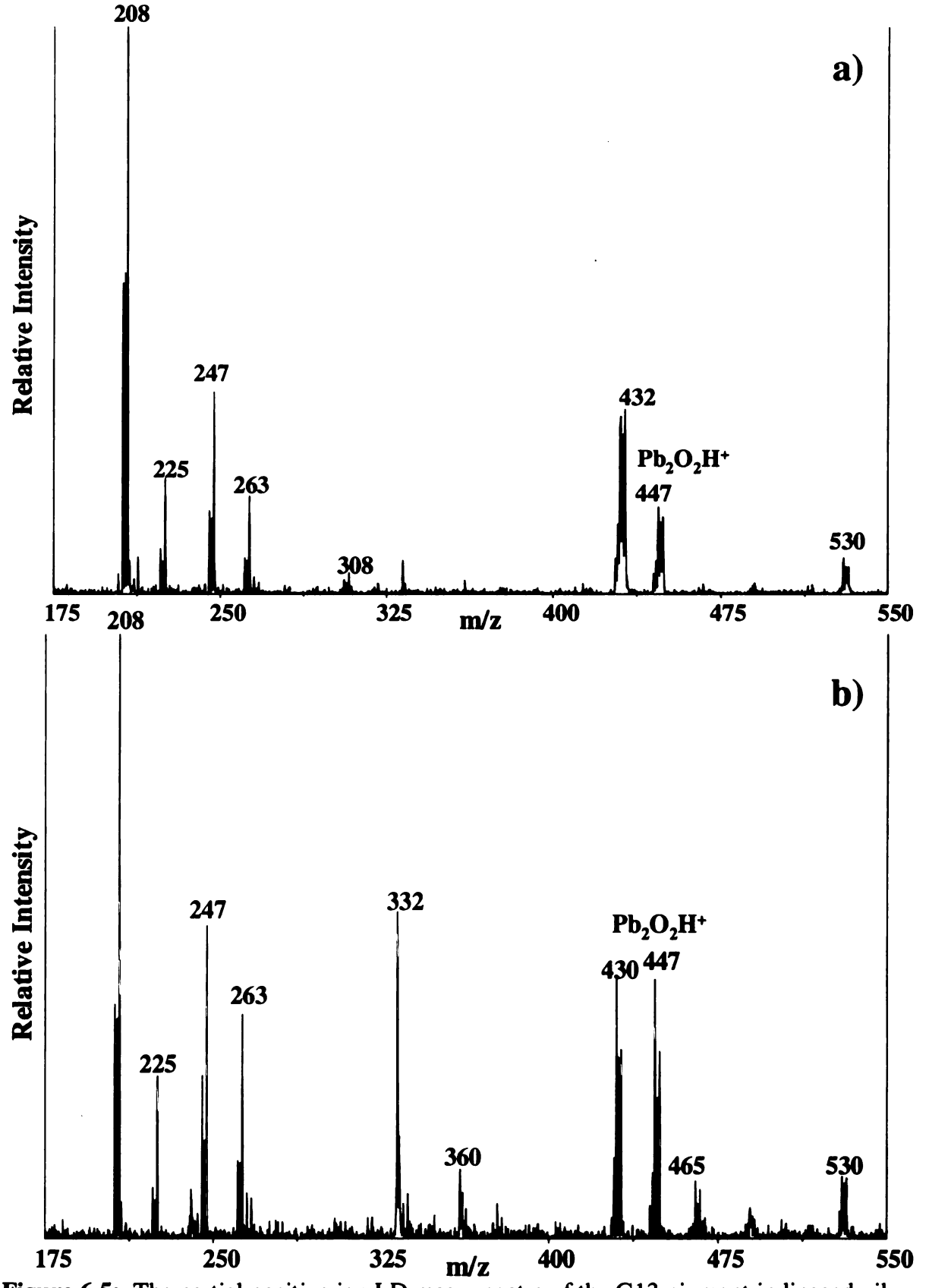

Figure 6.5: The partial positive ion LD mass spectra of the G13 pigment in linseed oil on paper samples exposed to 2 minutes H_2S (g) created using an HCl solution diluted; a) 75%; b) 50%.

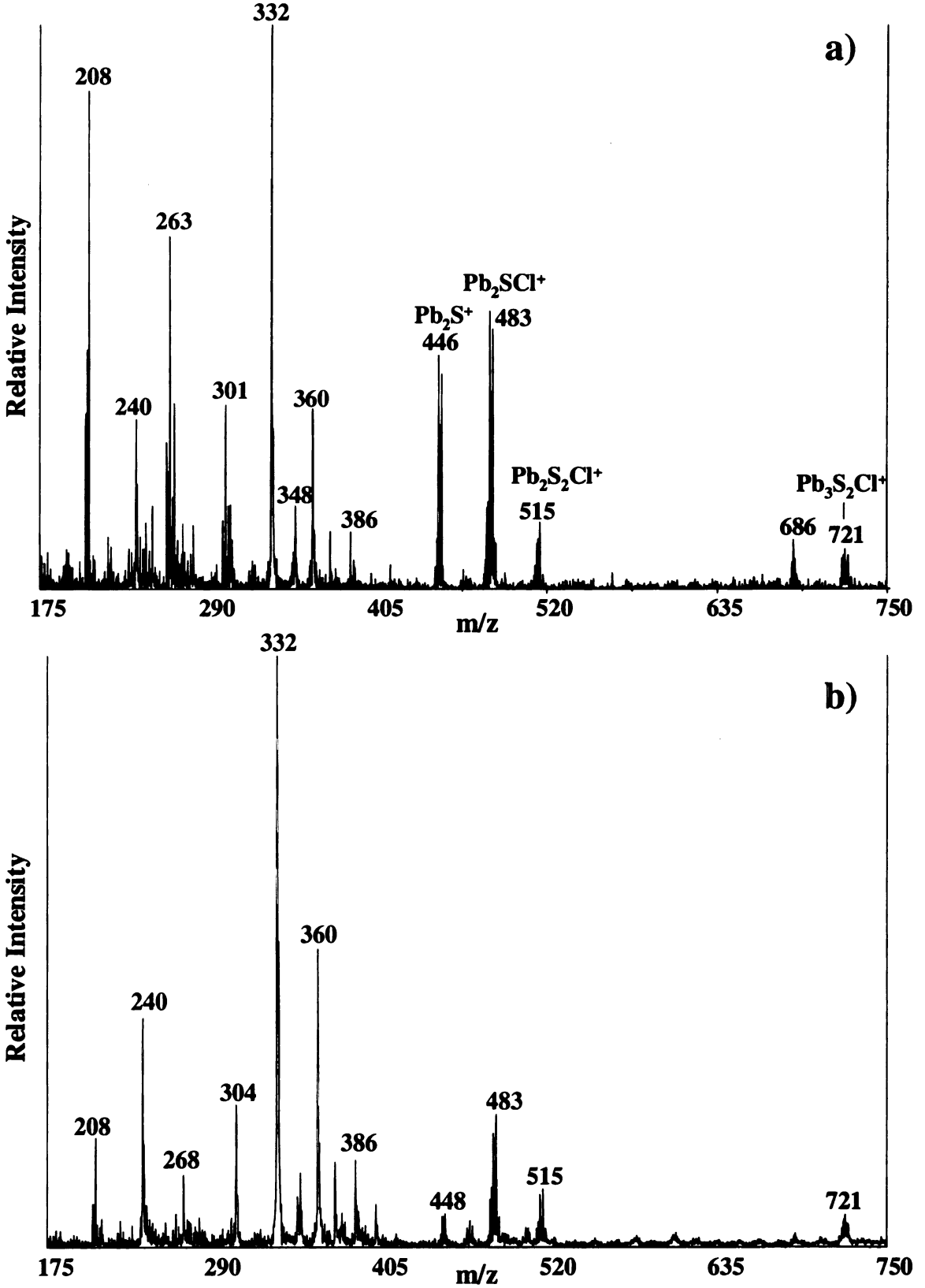

Figure 6.6: The partial positive ion LD mass spectra of the G13 pigment in linseed oil on paper samples exposed to 2 minutes H_2S (g) created using an HCl solution diluted; a) 25%; b) 0%.

The positive ion LD mass spectra of the G13 samples exposed to the less concentrated H_2S environments (Beakers 1 and 2) are shown in Figure 6.5. The LD mass spectra of the G13 samples exposed to the more concentrated H_2S environments (Beakers 3 and 4) are shown in Figure 6.6. The spectra in Figure 6.5 resemble the positive ion mass spectrum of the initial G13 sample in Figure 6.1a. No evidence of PbS is noted, however the paper peaks are becoming more evident. Evidence of PbS only appeared in the positive ion LD mass spectra of the G13 samples exposed to the more concentrated H_2S (g) environments. Peaks at m/z 446 representing Pb_2S^+ replaced the peaks at m/z 447 representing $Pb_2O_2H^+$ ions. Although it was not demonstrated in this example, in other studies, one may argue that there is an overlap of the two sets of peaks. This is more feasible. Additional evidence of PbS appeared at m/z 483, 515, and 721.

In the negative ion mass spectra of these samples, there appears to be a more gradual appearance of the ions representative of PbS. The negative ion LD mass spectra of the G13 samples exposed to the less concentrated H_2S (g) environment (Beakers 1 and 2) are shown in Figure 6.7 and the samples exposed to the more concentrated H_2S (g) environment (Beakers 3 and 4) are shown in Figure 6.8. The spectra in Figure 6.7 are similar to the negative ion mass spectrum of the nonexposed G13 sample in Figure 6.1b. The peaks representing $Cr_xO_y^-$ are the most abundant peaks in both of the mass spectra, however there is the appearance of a small peak at m/z 313, representing $PbCl_3^-$ ions in Figure 6.7a. The peak appears to be increasing in intensity in Figure 6.7b. As the concentration of H_2S (g) increases, the spectra change more dramatically, which is demonstrated in the negative ion mass spectra shown in Figure 6.8. The $Cr_xO_y^-$ ions are no longer generated by the sample, and the peaks representing $PbCl_3^-$ ions are the most

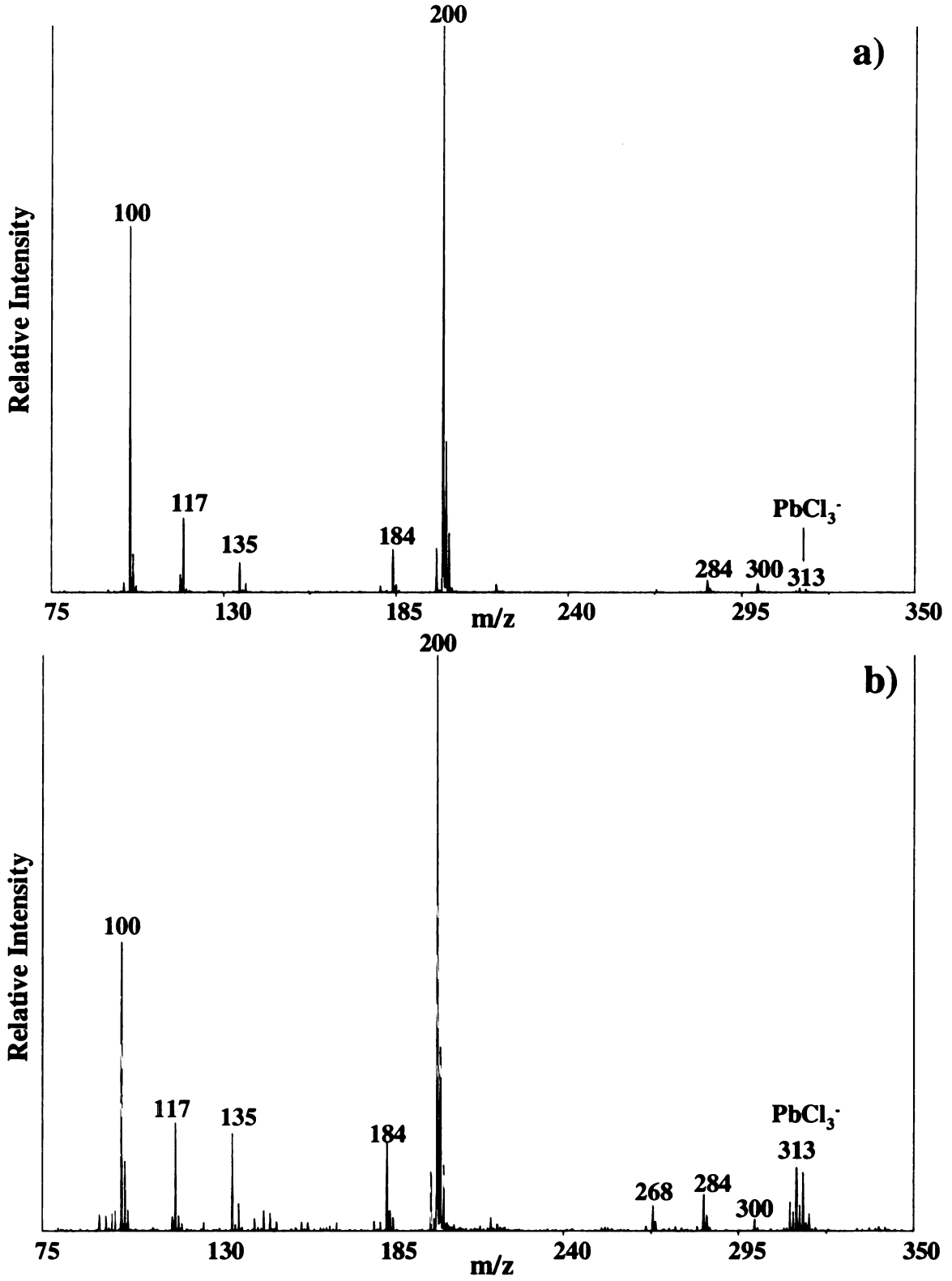

Figure 6.7: The partial negative ion LD mass spectra of the G13 pigment in linseed oil on paper samples exposed to 2 minutes H_2S (g) created using and HCl solution diluted; a) 75%; b) 50%.

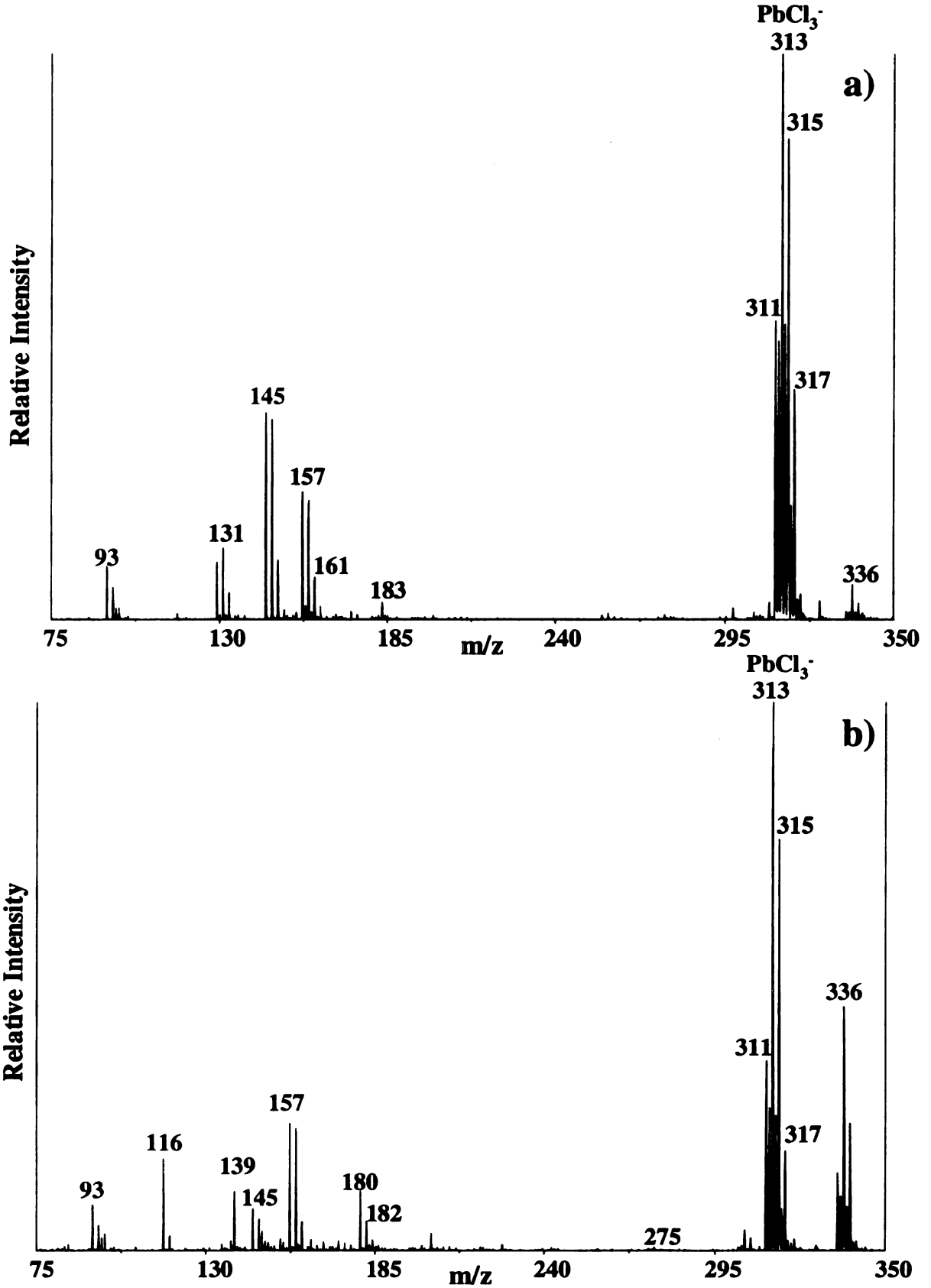

Figure 6.8: The partial negative ion LD mass spectra of the G13 pigment in linseed oil on paper samples exposed to 2 minutes H_2S (g) created using and HCl solution diluted; a) 25%; b) 0%.

intense peaks in the mass spectra. The peaks in the m/z 130-185 range have not been identified, but their isotopic patterns suggest that they are chlorinated products.

One more G13, suspended in linseed and applied to paper, sample was subjected to Beaker 4's conditions for 15 minutes. The darkened sample was then treated with enough H_2O_2 to return the sample to its original green color. Positve and negatitve ion LD mass spectra were obtained of the sample and are shown in Figure 6.9. In the positive ion mass spectrum (Figure 6.9a), peaks representing PbS ions have disappeared and the spectrum is abundant with peaks characteristic of a Pb-containing pigment not exposed to H_2S (g). The peaks at m/z 447, representative of $Pb_2O_2H^+$ ions, have replaced the peaks representative of Pb_2S^+ ions at m/z 446. This is one example in which the isotopic pattern is consistent with an overlap of the two sets of peaks. In the negative ion mass spectrum (Figure 6.9b), the $Cr_xO_y^-$ ions have returned, and the peaks representing $PbCl_3^-$ ions are still present, but have significantly decreased in intensity.

Like the uncontrolled H_2S study, in which the HCl solution was diluted to decrease the concentration of H_2S gas in the environment, an experiment was designed using diluted H_2O_2 solutions. Equal amounts of a range of diluted samples were applied to a set of G13 in linseed oil on paper samples, exposed to H_2S (g) for 15 minutes. The hope was to see a gradual transformation to the spectra in Figure 6.9. This was not successful.

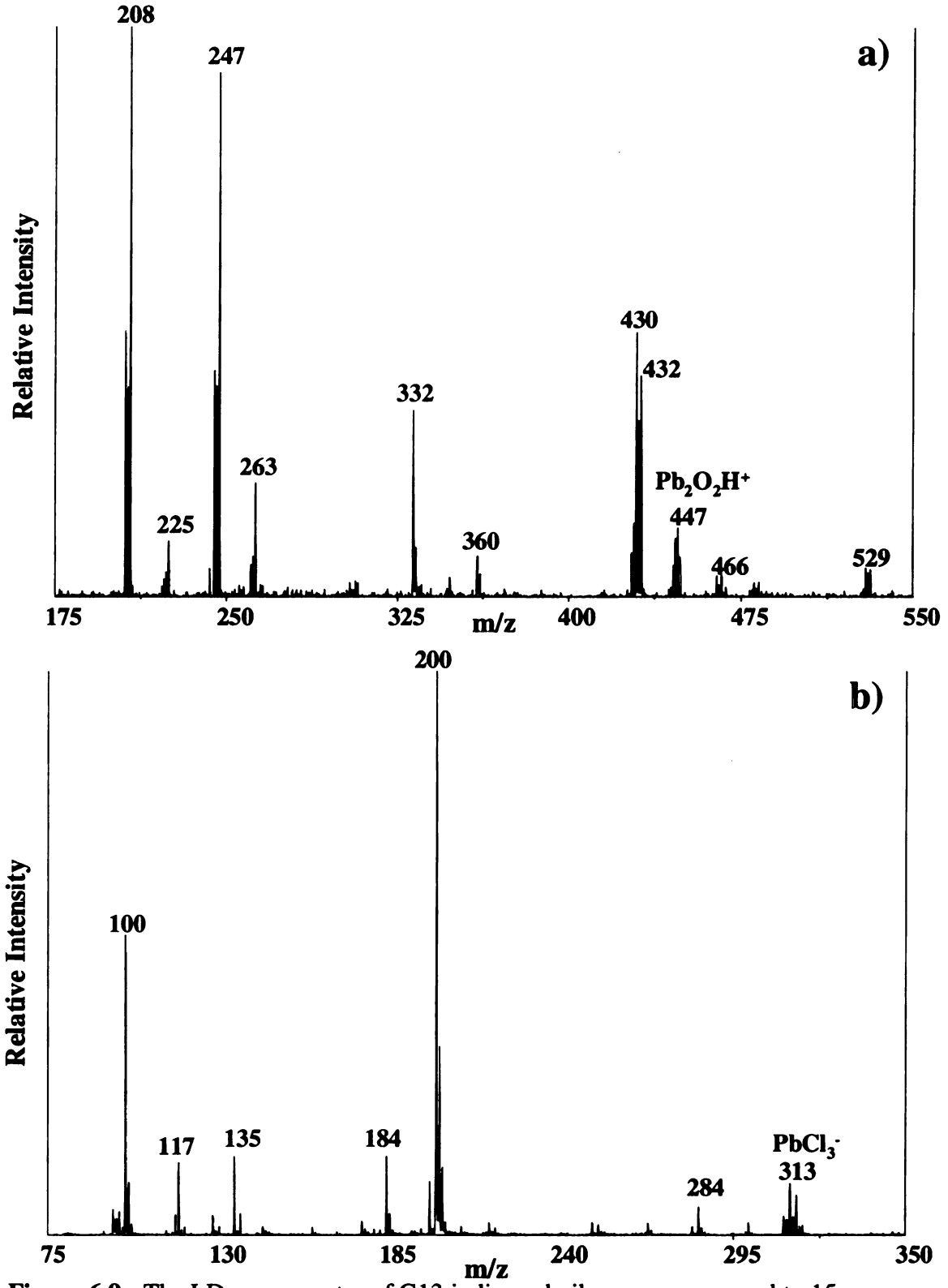

Figure 6.9: The LD mass spectra of G13 in linseed oil on paper exposed to 15 minutes H_2S (g) and treated with H_2O_2 (l); a) the partial positive ion mass spectrum; b) the partial negative ion mass spectrum.

By completing this experiment, it does not appear that we can effectively monitor the transformations using LDMS analysis. Additionally, without being able to obtain LD mass spectra of a real sample that has undergone this transformation, it is difficult to determine if we were effectively recreating the reaction. Part of the reason this experiment is referred to as the "uncontrolled H_2S study" is simply because there are too many variables involved. As will be demonstrated in the following section, the presence of some of the H_2S (g) reactants (HCl and H_2O) may have a greater influence on the rate and type of reaction occurring, beyond our understanding. For instance, did the increased HCl concentration have a greater effect on the increased intensities of the peaks representing $PbCl_3^-$ ions, than the increased concentration of H_2S (g)? For these reasons, a new controlled method was sought.

Controlled H_2S Exposure Studies

One way to eliminate the majority of the variables involved in the "uncontrolled H_2S studies" was to purchase H_2S (g), as opposed to making it in the lab. A lecture bottle of H_2S (g) (AGA) was connected to a vacuum manifold using tubing. A tank of compressed air was also attached. The vacuum manifold was connected to a rotary pump, which decreased the pressure in the manifold to approximately 300 mTorr. The samples were placed in a round flask, which was then attached to the manifold. The valve connected to the H_2S (g) was opened, allowing approximately 65 Torr H_2S (g) into the manifold. The valve connected to the flask holding the sample was then closed, and the manifold was flushed with air. Once the sample had reacted, the valve to the flask

was opened and flushed with air to halt the reaction. Samples were analyzed immediately using LDMS.

The G13 pigment and pure $PbCrO_4$ were used in this study. Contrary to the previous uncontrolled experiments, a significant amount of time was required for a visually-detectable reaction to occur. Approximately 40 hours elapsed before the $PbCrO_4$ sample acquired a darkened appearance. Black spots did not appear on the green G13 sample until about 65 hours had gone by. Both samples were analyzed following 65 hours exposure to H_2S (g), however only the $PbCrO_4$ results will be presented here.

Positive and negative in LD mass spectra were obtained of $PbCrO_4$ in linseed oil on paper, exposed to H_2S (g) for 65 hours, and are shown in Figure 6.10. There is very little evidence of PbS in both the positive and negative ion mass spectra. In positive ion mode (Figure 6.10a), an overlap of the peaks representing $Pb_2O_2H^+$ and Pb_2S^+ ions is noted. In the negative ion mass spectrum (Figure 6.10b), a very small set of peaks is noted at m/z 275, representing $PbSCl^-$ ions. Complications with the vacuum manifold set-up and the pressure gauge contributed to the end of this study.

Which set of conditions is more appropriate – the controlled or uncontrolled? Is it practical to consider the reaction taking place in the absence of O_2 or other contaminants (i.e. Cl)? Was the uncontrolled environment close to what occurs naturally? The equipment available in the laboratory was not sufficient to recreate natural conditions a painting may be subjected to.

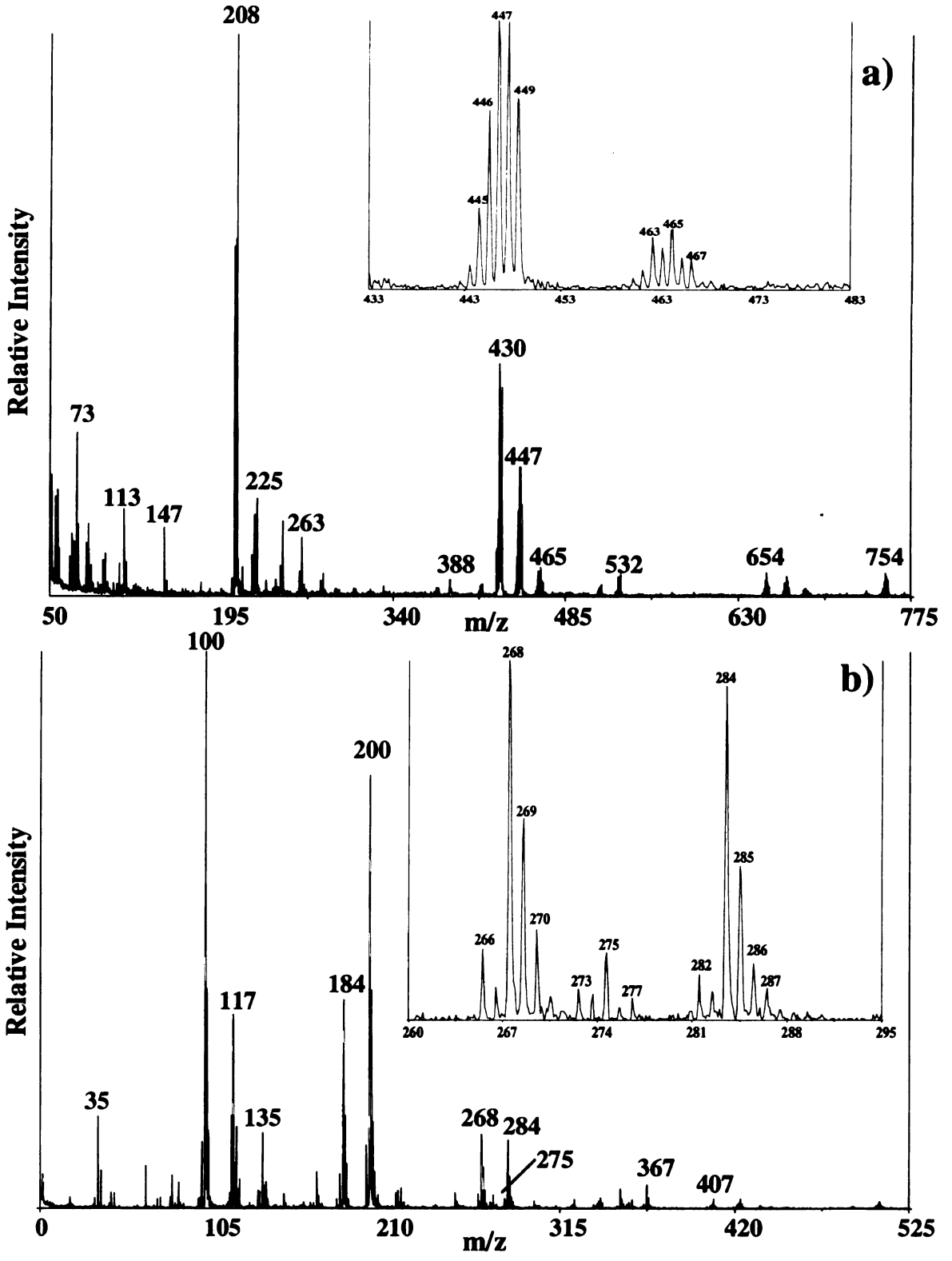

Figure 6.10: The LD mass spectra of $PbCrO_4$ in linseed oil on paper exposed to 65 hours H_2S (g); a) the partial positive ion mass spectrum; b) the partial negative ion mass spectrum.

Summary

The purpose in pursuing this project was to determine if LDMS could be used to characterize the products formed, when pigments in a paint mixture react with their environment (gases or other pigments). Was the project successful? We successfully produced darkened samples by exposing them to H_2S (g). Peaks were positively identified which are characteristic of PbS, the expected product. The darkened appearance was reversed upon the addition of H_2O_2. Again, the mass spectra changed, providing evidence that the unwanted PbS product had been converted to a white Pb pigment. So, the study was a success. The question is whether or not we recreated what occurs naturally in a painting exposed to H_2S (g). A donated sample from a painting which has suffered from H_2S (g) exposure over several years would answer this question. Ultimately, the H_2S studies were abandoned, since the focus of the project changed to using LDMS for the identification of pigments.

References

1) Clay HF, Watson V. The crystal structure of lead chromes. Journal of the Oil and Colour Chemist's Association 1948;31:418-422.

2) Watson V, Clay HF. The light-fastness of lead chrome pigments. Journal of the Oil and Colour Chemist's Association 1955;38:167-177.

3) Petushkova JP, Lyalikova NN. Microbiological degradation of lead-containing pigments in mural paintings. Studies in Conservation 1986;31:65-69.

4) Giovannoni S, Matteini M, Moles A. Studies and developments concerning the problem of altered lead pigments in wall painting. Studies in Conservation 1990;35:21-25.

5) Koller M, Leitner H, Paschinger H. Reconversion of altered lead pigments in alpine mural paintings. Studies in Conservation 1990;35:15-20.

6) Erkens LJH, Hamers H, Hermans RJM, Claeys E, Bijnens M. Lead chromates: a review of the state of the art in 2000. Surface Coatings International Part B; Coatings Transactions 2001;84:169-176.

7) Sharkey J. Chemistry of postage stamps: dyes, phosphors, adhesives. The United States Specialist 1990 August:469-482.

8) Standage HC. The artist's manual of pigments. Philadelphia: Janentzky & Weber 1886.

Chapter Seven: Newspaper Ink

History of the Printing Press

In early Egyptian, Greek, and Roman civilizations, handwritten copies of important manuscripts were extremely common. A number of factors escalated the need to develop a method to mass produce copies of written material in a timely manner. Religion was the main contributor for this need. The rise of the prosperous literate class during the Renaissance period, followed by the religious controversies resulting from Martin Luther's Reformation, placed a high demand on the printing press. Pamphleteering in particular was a key component in spreading religious propaganda during this time period (1).

The Chinese are credited for inventing the first printing press as early as 200 A.D. They employed a wooden block technique, using a movable type. Letters and pictures were cut in relief in wooden blocks and arranged in sequence. This method had been used previously for printing on textiles. Much of their success was based on the type of substrate available. The invention of paper by the Chinese in 195 A.D. proved to be a main contributing factor for their success. In the western world, writing substrates were limited to papyrus and vellum (animal skin), which were expensive and unsuitable for printing on. Early printing inks in the east were strictly aqueous (1).

By the 12th century, papermaking had found its way to the west and became popularized in the 13th and 14th centuries, paving the way for the development of the printing press in the west. Officially, Johann Gutenberg, of the German city of Mainz is considered the inventor of Western printing in 1450. A movable metal type cast was

employed and the design of the press modeled that of a winepress. Unlike the east, the west used oil-based inks from the start. Juan Pablos is given credit for bringing the printing press to the New World in 1539, when he established a printing press in Mexico City. Later, in 1628, Stephen Day assisted in the establishment of the Cambridge Press in Massachusetts Bay (1).

Improvements to the original design of the printing press have been made throughout the years leading to four main types of high speed printing techniques still used today. These include the letterpress and flexography, which employ a raised surface, and lithography and direct lithography, which employ a flat surface.

Printing Methods

The letterpress is a more simple and primitive technique which employs a rotary press with an elevated image area printing plate. Rollers transfer ink onto the raised surfaces and the image is transferred onto the newsprint using an impression cylinder. The cylinder consists of a hard rubber material, which is made to withstand numerous impressions. This method is simple and effective, however one disadvantage is that only one side can be printed at a time (1,2).

Flexography is another example of a raised surface printing technique, resembling the letterpress in many aspects. With this method a softer image plate is employed than that used in the letterpress. Consequently, an aqueous ink is used which is distributed uniformly and in the proper amount onto the printing plate using an anilox cylinder. The anilox cylinder is equipped with a scraper blade which cleans up excess ink applied to the plate, and recycles the ink back to the ink fountain. As in the letterpress, only one side of

the newsprint may be printed at a time, however the image is transferred directly from the printing plate to the newsprint, eliminating the need for an image cylinder (1,2).

With the phasing out of raised-surface mechanical printing techniques, lithography (offset) has surfaced as the most common type of printing press used today. Aloys Senefelder, a German map inspector, developed the underlying principles behind lithography printing, which he termed "chemical printing", in the late 18^{th} century. Modern day lithographic offset printing presses are much more technical, using computers to automate and generate the image process (1,2).

The design of a lithographic printing press employs a flat printing plate, with two chemically different areas. The non-printing area is hydrophilic, while the image area is hydrophobic. The printing plate is typically aluminum, with a thin surface coating of a photopolymer. The light sensitive material undergoes a solubility change when exposed to an intense source of blue or UV light. The image is transferred directly to the surface by exposing the plates directly, as in a graphic arts camera or by a computer controlled laser beam. During the printing process, an oil based ink and an aqueous fountain solution are applied to the plate. The ink is applied in a thin layer using rollers, and wets the image area. The fountain solution wets the non-image area. The solution may be sprayed directly onto the plate, transferred from a high speed brush, or by a molleton or sock roller (1,2).

The chemistry occurring on the plate is crucial to the quality of the completed copy. Oil and water do not mix, but here they must interact. Thus, the ink must possess specific properties which enable it to emulsify the fountain solution so it can wet the image area. This ensures uniform transfer of the ink. Additionally, the fountain solution

must possess detergent properties enabling it to wash away any ink deposited in the non-image area. Thus, formulating the ink and fountain solutions is an exact science (1).

Once the ink is properly applied to the printing plate, the ink is transferred to a blanket cylinder. The cylinder is covered with a compressible material, allowing it to conform to the printing surface. The image is then transferred to the newsprint. With this technique, double sided pages may be printed simultaneously (1).

Direct lithography is the same as lithography printing, except as the name implies, the blanket cylinder is missing, allowing for the direct transfer of the image from the printing plate to the newsprint. However, the absence of the blanket cylinder limits this method to strictly paper. The presence of the blanket extends the printing substrates to plastics and metals (1,2).

Newspaper Ink

In general, newspaper inks consist of pigments, resins, an oil or other carrier, and additives. The resin acts as both a dispersing agent and a binder for the pigment. The oil used is typically treated napthenic petroleum or poppyseed oil (3). These are non-drying oils, meaning that their purpose is strictly to carry the ink onto the paper. All printing methods, discussed thus far in this chapter, dry by absorption of the oil into the paper. No heat is applied and no other volatile components are added. Excluding flexography printing, the ink is not cleaned off of the press in between copies. Inclusion of volatiles in the ink formulations would result in the ink drying out directly on the rollers, ultimately causing printing problems. Other additives are included to control pigment wetting and dispersion, viscosity and flow characteristics, and provide proper ink/water

balance (3). It should be noted that in 1979 the board of directors of the American Newspaper Publishers Association ordered the development of a soy-based newspaper ink, since it has a lower VOC (volatile organic compound) count (4-6). Soy ink is composed of non-toxic soybean oil, extracted from soybeans produced domestically. Soybean oil is the same oil found in edible items, such as salad dressings and mayonnaise. However, the addition of petroleum-based pigments and resins creates a non-edible soy ink (4). The ink was not introduced until 1987. Approximately 90% of all U.S. daily newspapers are currently printed using soy-based ink, when printing in color.

Carbon black is commonly the primary pigment found in black newspaper ink. It is produced by cracking oil in a continuous furnace. The process is highly controlled in order to produce a specific grade of pigment, having a specific particle size and structure. When manufactured, carbon black is dry and packed together forming aggregates or agglomerates, resulting in the need for a dispersion agent, or resin, to form the appropriate pigment particles. The resin is the most expensive component of the ink, however it has the greatest effect on rub resistance of the ink on the final product. Thus, the manufacturer must find a balance between cost and quality, since rub resistance increases with increasing resin content, but so does cost. Other factors affecting rub resistance which can be used to offset the resin content include viscosity, ink film thickness, paper quality, humidity, and the time after printing (3).

Although only mass spectral data will be presented for black newspaper ink in this chapter, color appears in newspaper ink quite frequently. The three primary colors (cyan, magenta, and yellow) are used to produce all of the colors seen in a newspaper. The colors are synthetic organic pigments. Typical pigments used for each color include

phthalocyanine blue, Lithol Rubin, and Diarylide yellow (3). Black, cyan, magenta, and yellow colored newspaper inks were obtained from the Lansing State Journal. Positive and negative ion LD mass spectra were obtained of all four samples on paper, however the primary focus of this side project is black newspaper ink.

Experimental

Positive and negative LD mass spectra were obtained of the black ink on numerous newspapers dated between 1923 and 2002. This chapter will focus on the positive ion results of a current newspaper (2002), a 1986 newspaper, a 1963 Weekly Reader, and an issue of the Scientific American Journal, allegedly from the late 19th century. Spectra were obtained of the ink directly on the paper substrate, and of the paper by itself as a control. A 1 in^2 section was removed from each sample and taped to the modified sample plate. The user parameters as cited in the instrumental section were employed.

Results

A Current Newspaper

Beginning with the most recent sample, a current copy of the Michigan State University's State News was obtained and analyzed. The paper had been freshly printed the night before. The positive ion LD mass spectrum of the ink-on-paper sample is shown in Figure 7.1a. In the positive ion mass spectrum, there are notably two clusters of peaks present. The first cluster is extremely complex and is located between approximately m/z 240 to m/z 450. The most intense peaks in the cluster are separated

by 14 mass units, suggesting that the ions may be a homologous series. The complexity and distribution of peaks is characteristic of a mass spectrum of a polycyclic aromatic hyrdrocarbon (PAH), which one would expect to find in either a petroleum or soy-based product. For example, petroleum oil consists of three major types of hydrocarbons, which include paraffins, olefins, and aromatics (7). Several of these compounds, having varying vaporization and boiling points, constitute the oil, resulting in an array of peaks in a mass spectrum. Many of these compounds may only differ in chain length and according to the number of degrees of unsaturation, resulting in peak separations of 14 and 2 mass units, respectively.

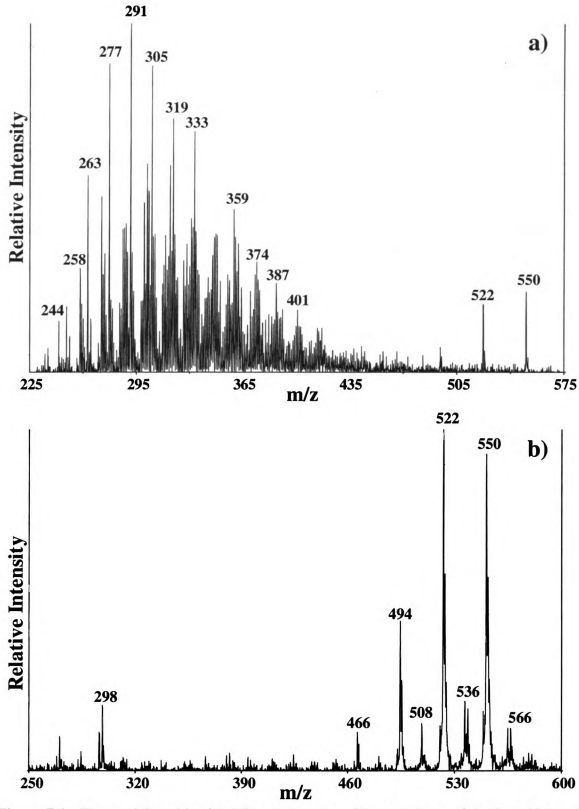

Figure 7.1: The partial positive ion LD mass spectra of a recent issue of the State News a) the black ink; b) the paper.

Nearly a decade ago, Zenobi and his research group investigated the used of LDMS for identifying polycyclic aromatic hydrocarbons (PAHs) in a petroleum pitch sample (8). A small percentage of the PAHs are volatile and may be detected in a GCMS experiment, which is a commonly employed technique for characterizing the volatile hydrocarbons of gasoline and other fuels. Here, Zenobi employed a two-step laser desorption technique to detect the nonvolatile, higher molecular weight species. In this technique, desorption of the PAHs was achieved using an IR (CO_2) laser, followed by ionization using a UV laser (308 nm). They designated this method as "L2MS".

Figure 7.2 shows the positive ion mass spectrum of the petroleum pitch sample generated using the L2MS method. The mass spectrum is similar to the mass spectra obtained of newspaper ink. In Figure 7.2, Zenobi and coworkers identified a PAH skeleton beginning at m/z 302. The peak at m/z 302 was identified as dibenzo[a,h] pyrene. The higher mass peaks in the mass spectrum were assigned, based on the simpler dibenzo[a,h] pyrene structure. The higher mass compounds were the result of alkylation ([M+14] for methylation, [M+28] for double methylation or ethylation), as well as the addition of ethylene bridges (M+24), ethyl bridges (M+26), or benzo groups (M+50). We will apply their method of assigning peaks to our own results.

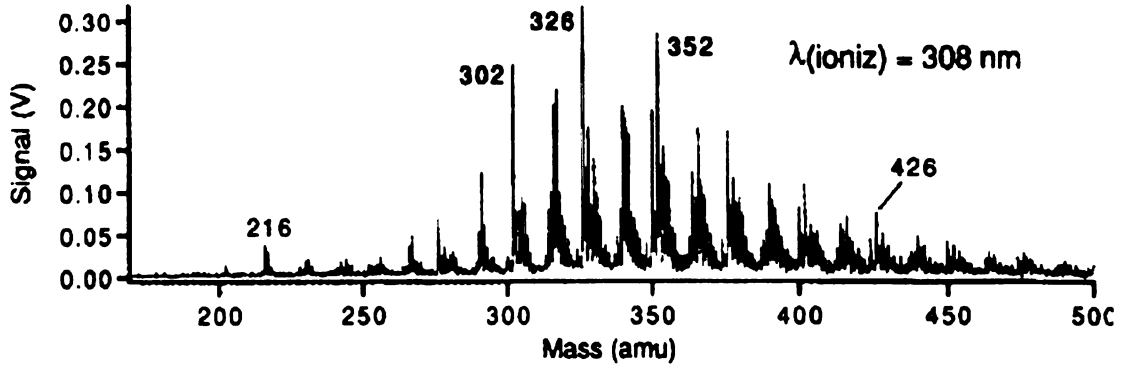

Figure 7.2: L2MS spectrum from a petroleum pitch sample.

A second notable set of peaks separated by 28 mass units occurs at m/z 494, 522, and 550. While these peaks remain unassigned, they were initially suspected to represent a component(s) of the paper. The positive ion LD mass spectrum of the paper is shown in Figure 7.1b. The same cluster of peaks at m/z 494, 522, and 550 are noted, lending support to the hypothesis that the ions are generated from the paper. It is also important to note here that the peaks in the lower mass region of the spectrum, believed to represent the petroleum oil carrier, are significantly more intense than the peaks in the higher mass region of the spectrum, at this point believed to represent components of the paper.

Aged Newspaper Ink

Having had experience with aged modern ballpoint pen ink samples (9-11), we wanted to investigate if the mass spectra of newspaper ink changed over time. To do so, a newspaper dated 1986 and a "Weekly Reader" dated 1963 were analyzed. The positive ion LD mass spectra of the black ink on the two documents are shown in Figures 7.3a and 7.3b, respectively. Again, two distinct clusters of peaks are observed in both spectra. The lower mass clusters appear to have shifted to a higher mass, and the distribution of peaks has become more narrow and less intense as compared to the higher mass cluster of peaks around m/z 550. The effect is most obvious in the mass spectrum of the 1963 newspaper ink (Figure 7.3b) and will be discussed shortly.

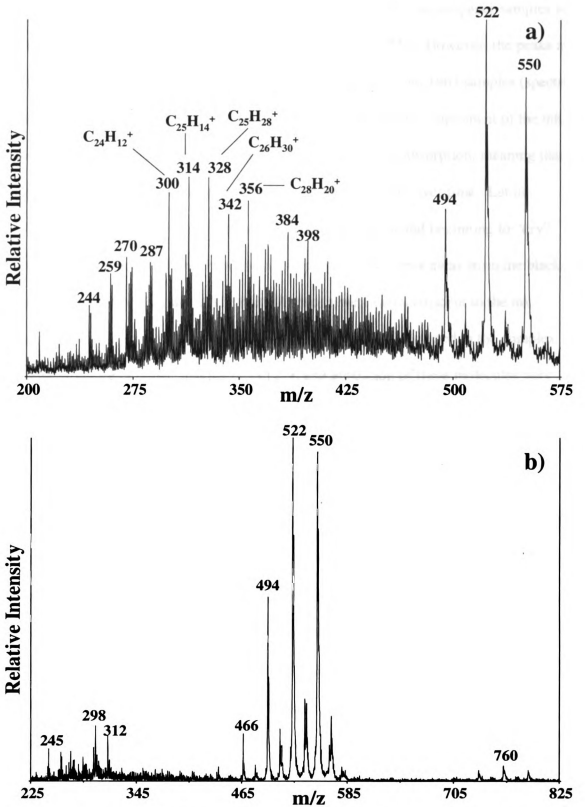

Figure 7.3: The partial positive ion LD mass spectra of black newspaper ink a) a 1986 sample; b) a 1963 sample.

The positive ion LD mass spectra of all three newspaper ink-on-paper samples all contain the higher mass group of peaks at m/z 494, 522, and 550. However, the peaks are absent in the positive ion control LD mass spectra of the 1986 and 1963 samples (spectra not shown). This suggests that these peaks may represent another component of the ink, such as the resin. Newspaper ink "dries" by the mechanism of absorption, meaning that components of the ink are continuously migrating into the paper over time. Let us consider the current newspaper ink sample. The ink was fresh and beginning to "dry". The carrier component (oil and resin) began seeping into the paper away from the black pigment deposited on the paper. The control spectra were taken adjacent to the ink samples. In the older samples, the resin may harden or become trapped in the complex cellulose structure of paper, making desorption and ionization of these molecules very difficult. In the case of the current newspaper sample, the ink is still "wet", perhaps making it possible to observe other components of the ink, such as the resin.

Another important, and somewhat unexpected observation is that the m/z values of the most intense peaks in the positive ion mass spectrum of the current newspaper ink are odd and those of the 1986 sample are even. Aromatic hydrocarbons have the ability to generate either molecular ions ($M^{+\bullet}$) or protonated molecules $(M+H)^+$. If the m/z value of a peak is even, it represents the $M^{+\bullet}$. If the value is odd, there exists a couple of possibilities. The first is that the peak represents the protonated molecule. The second is that the compound is not a pure PAH, but actually contains an odd number of nitrogen atoms. Assuming that there are only PAHs present, potential peak assignments can be made.

Peak Assignments

In regards to assigning peaks, let us focus on Figure 7.3a. Looking at the wide distribution of peaks in the positive ion mass spectrum of the 1986 newspaper ink, there appears to be a series of related peaks separated by 14 mass units, beginning at m/z 300. If the compound was a saturated alkane, it would have the formula $C_{22}H_{36}$. Considering that alkanes do not absorb in the UV, this assignment is improbable. Aromatic compounds tend to absorb efficiently in the UV region. For m/z 300, one possibility would be $C_{24}H_{12}$. A proposed structure, illustrated in Figure 7.4, represents coronene. The next possible compound would be $C_{25}H_0$. Considering compounds containing a lower number of C atoms, the next possible compound would be $C_{23}H_{24}$, followed by $C_{22}H_{36}$ (the alkane).

Figure 7.5 shows an enlarged section of Figure 7.3a in the m/z 300 region. The structure in Figure 7.4 can not lose any additional H atoms. The peaks greater than m/z 300 can be accounted for by saturating some of the double bonds of coronene. For example, the peak at m/z 302 would represent $C_{24}H_{14}$. Odd m/z values are difficult to assign. In this case, m/z 301 could represent either the protonated coronene molecule or a fragment ion, if the ion's composition is limited to only C and H atoms. The other possibility is that the ion contains an odd number of N atoms ($C_{23}NH_{11}$).

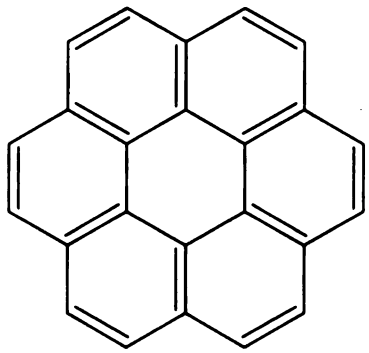

Figure 7.4: The structure of coronene.

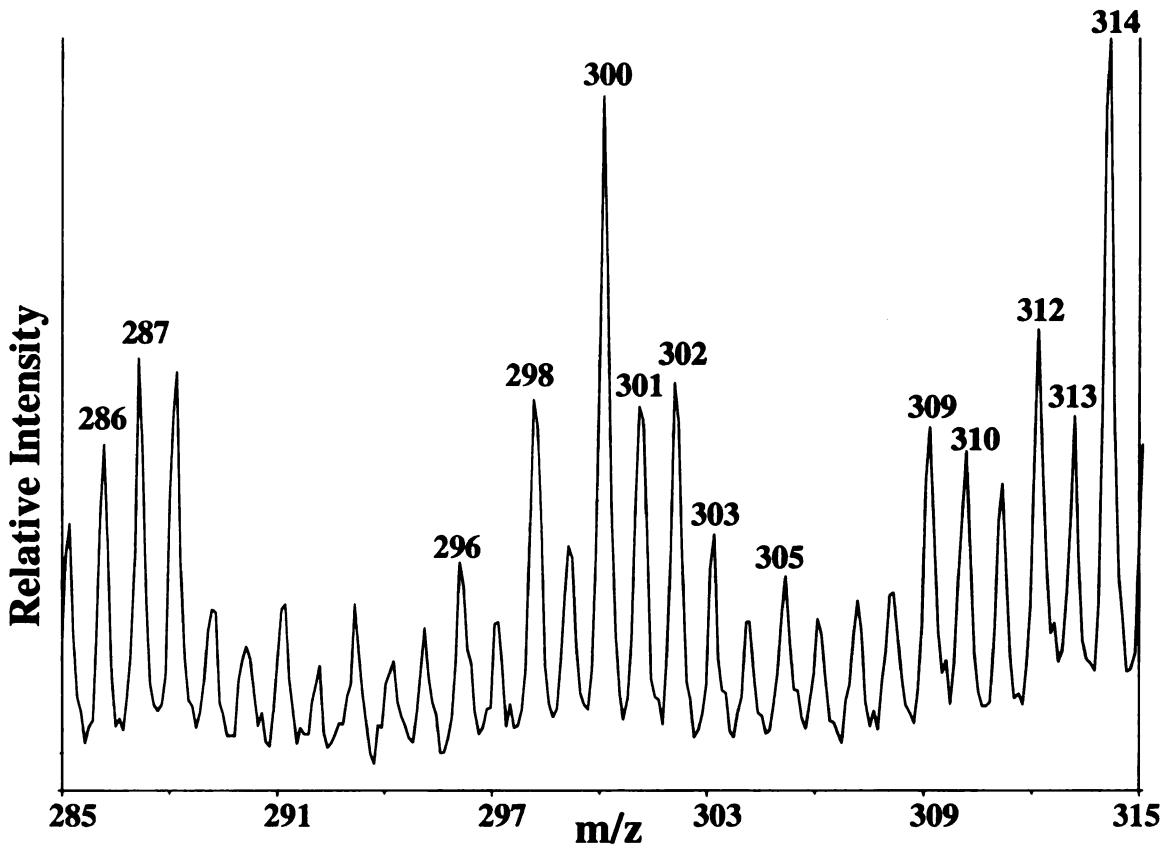

Figure 7.5: An enlarged portion of the positive ion LD mass spectrum of the 1986 ink sample.

Additional assignments were made in Figure 7.3a, however they have not been confirmed. It is also difficult to propose a structure for these compounds, considering the possibilities are large. Consulting the literature, the m/z values in the newspaper ink spectra we generated do not match any of the previously observed gas phase PAH ions documented (12). Identifying PAHs in petroleum based products has proven to be a difficult task by other research groups as well (13-15). In fact, the complexity of the petroleum mixtures has prompted one research group to identify the field as "Petroleomics", in comparison to the more well-known field of Proteomics (16).

Weathering

Returning to the observation noted earlier concerning the relative intensities of the peaks in the lower and higher mass clusters, we propose an explanation. It appeared as though, as a newspaper ink "aged", the distribution of peaks shifted to a higher mass, became more narrow, and decreased in intensity relative to the "paper peaks". There is a phenomenon associated with drying oils, termed "weathering". Weathering is used to describe the processes which alter an oil's characteristic fingerprint. These processes include, evaporation, dissolution, photochemical oxidation, and biodegradation, to name a few (17). Evaporation and dissolution are the main contributors to the weathering process (18). Although the two processes are in direct competition with each other, the initial rate of weathering is proportional to the concentration of smaller, more volatile saturated or aromatic hydrocarbons present, and results from evaporation. Larger components are less volatile, but also less soluble, resulting in dissolution. These components are not absorbed in the paper, and are "washed" away by physical processes.

Consequently, in a mass spectrum, the fingerprint distribution of peaks shift to higher masses and become more narrow, resulting from the evaporation and dissolution processes. The peak intensities would also become less intense, since the concentration of the carrier would decrease as a result of evaporation, dissolution, and absorption into the paper (19).

Initially, it appeared as though the spectra of the three newspaper inks supported the weathering theory. However, more samples needed to be analyzed to test this theory. The spectra of these samples (not shown) did not always follow the same trend. The possible PAH distribution was present in each spectrum, however a pattern could not be established, which is not all that surprising. As with writing inks, each manufacturer has its own formula, so we would not expect the mass spectrum of every newspaper ink freshly applied to paper (never mind aged ink) to be identical. We also need to keep in mind the switch to a soy-based ink in the late 1980s, early 1990s. A more extensive study could be performed to first determine if LD mass spectral data could provide a "fingerprint" of the different types of newspaper inks. If so, then other factors, such as the type of paper the ink is printed on and storage conditions, can be considered to determine if the aging of newspaper ink can be characterized.

Scientific American Journal

In the initial stages of the newspaper ink project, it appeared as though the weathering process of complex drying oils, such as petroleum oil, could be illustrated using LD mass spectral analysis. The assumption was based on the results of the 2002, 1986, and 1963 samples discussed in greater detail in a previous section. To test this

aging picture, an issue of the American Scientific Journal, dated 1886, was analyzed. The authenticity of the document was immediately suspect, based on the perfect condition of the document. The document was folded, therefore different portions of the ink-on-paper were analyzed. The spectra of the different sections sampled were predominantly the same, therefore a representative positive ion mass spectrum was chosen and shown in Figure 7.6. The spectrum reflects significant differences in the newsprint ink formula encountered thus far in the study.

In the positive ion mass spectrum, the absence of the standard PAH peaks is noted. Rather, the spectrum shows evidence of the cationic dye, methyl violet, at m/z 372. Methyl violet is documented as a commonly used toner in modern day ballpoint pen and ink jet printer inks. Additional peaks, at m/z 250 and 275, indicate that more than one colorant has been included in the ink mixture. This sample was not the first time these peaks (m/z 250 and 275) appeared in the positive ion mass spectrum, with a complimentary peak in negative ion mode at m/z 250 (spectrum not shown). The peaks frequently appeared in yellow colored samples. In fact, the peaks appear to represent the yellow colorant in the soy-based yellow ink used to print the Lansing State Journal (Figure 7.7).

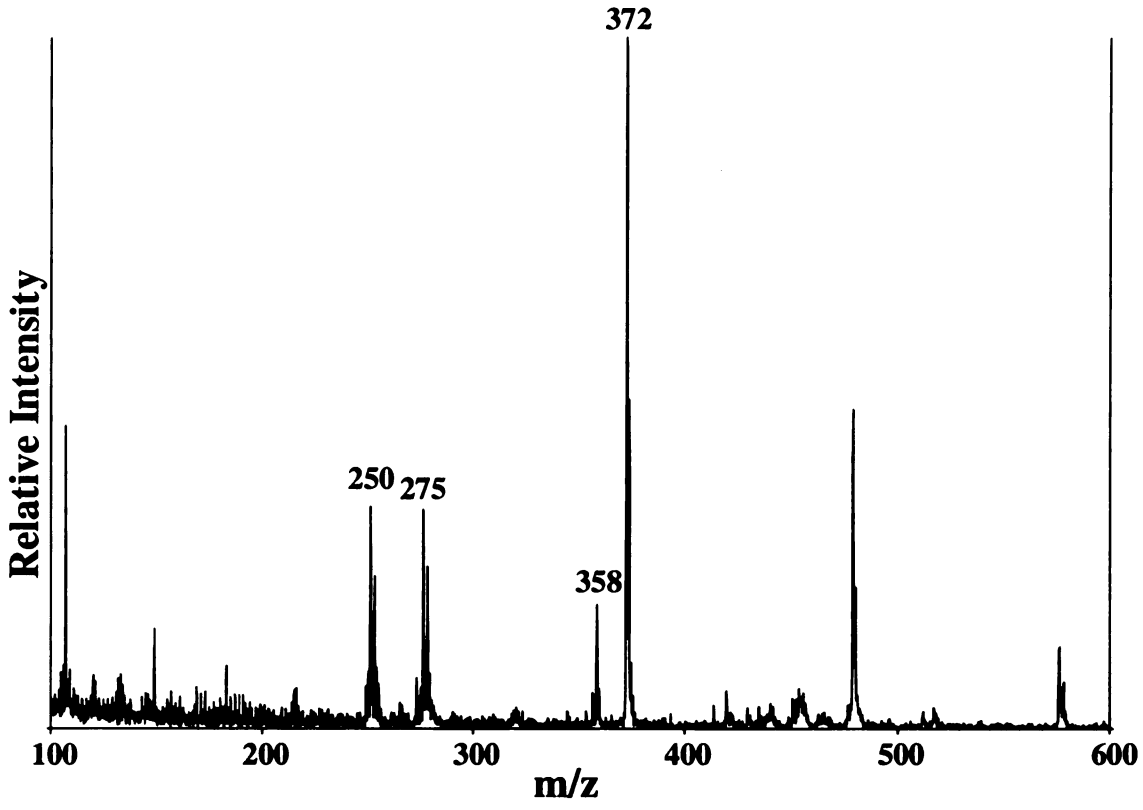

Figure 7.6: The positive ion LD mass spectrum of the Scientific American Journal.

Figure 7.7 shows the positive ion mass spectrum of the yellow ink applied to paper, which was supplied by the Lansing State Journal. Much time and effort has been devoted to determining the identity of this colorant. A structure has been proposed (Figure 7.8), based on the m/z value of the ion, as well as its isotopic pattern. However, this compound is categorized as a rare chemical in the Aldrich catalog. It is doubtful that a rare chemical would be employed in this application. The isotopic distribution is consistent with the compound containing either 2 Cl atoms or 1 Cu atom. The colorant remains unidentified, however the important point here is that it is most likely a modern day yellow pigment. In contemporary ink jet printer inks, it is common to have a mixture of yellow and violet dyes to produce black ink. The chemical analysis of the document

using LD mass spectral data confirmed our suspicions that the document is a modern day copy and not made from carbon black newsprint ink.

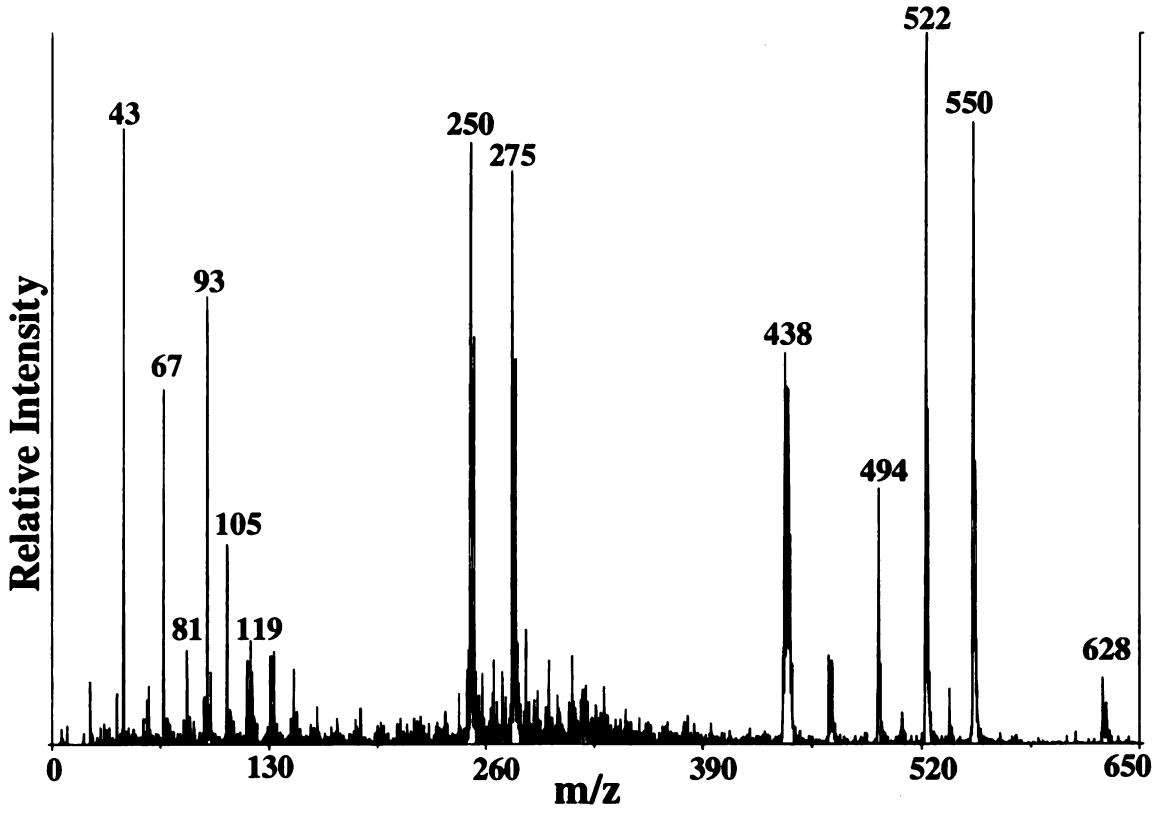

Figure 7.7: The positive ion LD mass spectrum of yellow newspaper ink on paper.

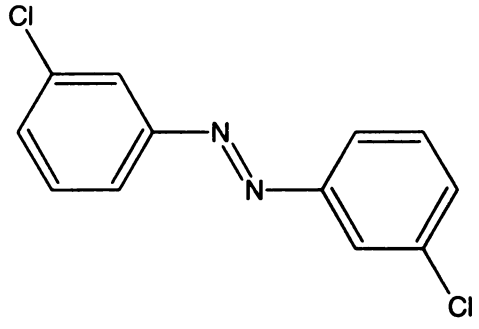

Figure 7.8: A proposed structure for the compound represented at m/z 250.

References

1) The history of printing. http://www.usink.com/history_printing.html

2) How is a newspaper printed, vol XXIV. US Ink, 1998, 1-5.

3) What is ink? http://www.usink.com/what_is_ink.html

4) Soy ink talking points. http://www.soyink.com/inktalking.html

5) For printers. Kohler's corner – soy ink article.
http://www.ippaper.com/gettips_kc_soy.html

6) Brown MS. Printers shift to environmentally friendly soybean ink. Memphis Business Journal 1999.

7) Wigger JW, Torkelson BE. Petroleum hydrocarbon fingerprinting – numerical interpretation developments.
http://www.bioremediationgroup.org/Bioreferences/Tier1Papers/petroleum.htm

8) Zenobi R. Advances in surface analysis and mass spectrometry using laser desorption methods. Chimia 1994;48:64-71.

9) Grim DM, Siegel J, Allison J. Evaluation of desorption/ionization mass spectrometric methods in the forensic applications of the analysis of inks on paper. J Forensic Sci 2001;46:1411-1419.

10) Grim DM, Siegel J, Allison J. Does ink age inside of a pen cartridge? J Forensic Sci 2002;47:1294-1297.

11) Grim DM, Siegel J, Allison J. Evaluation of laser desorption mass spectrometry and UV accelerated aging of dyes on paper as tools for the evaluation of a questioned document. J Forensic Sci 2002;47:1265-1273.

12) Lias S, Bartmess JE, Liebman JF, Holmes JL, Levin RD, Mallard G. Gas-phase ion and neutral thermochemistry. J Physical and Chemical Reference Data 1988;17:649,794-95.

13) Balasanmugam K, Viswanadham SK, Hercules DM. Characterization of polycyclic aromatic hydrocarbons by laser mass spectrometry. Anal Chem 1986;58:1102-1108.

14) Rodgers RP, Lazar AC, Reilly PTA, Whitten WB, Ramsey JM. Direct determination of soil surface-bound polycyclic aromatic hydrocarbons in petroleum-contaminated soils by real-time aerosol mass spectrometry. Anal Chem 2000;72:5040-5046.

15) Herod AA, Stokes BJ, Hancock P, Kandiyoti R, Parker JE, Johnson CAF, John P, Smith G. Laser-desorption mass spectrometry of standard polynuclear aromatic hydrocarbons and fullerenes. J Chem Soc Perkin Trans 1994;2:499-506.

16) Rodgers RP, Klein GC, Hendrickson CL, Marshall AG. Petroleomics: environmental forensic applications of high resolution FT-ICR mass spectrometry. In: Proceedings of the 55th American Academy of Forensic Sciences Annual Meeting. Chicago, IL February 17-22, 2003.

17) Forensic oil analysis (fingerprinting). http://www.rdc.uscg.gov/mslpages/method.html#source.ptr

18) Smith CL, MacIntyre WG. Initial aging of fuel oil films on sea water. In: Proceedings of Joint Conference on Prevention and Control of Oil Spills. Sheraton Park Hotel, Washington, D.C. June15-17, 1971.

19) Rodgers R, Blumer EN, Freitas MA, Marshall AG. Complete compositional monitoring of the weathering of transportation fuels based on elemental compositions from fourier transform ion cyclotron resonance mass spectrometry. Environ Sci Technol 2000;34:1671-1678.

The Problem

The usefulness of LDMS for the identification and characterization of colorants found in inks and paints, has been well demonstrated thus far. However, what use is the technique if it is not practical for art conservators and forensic scientists? One major problem we encounter is sample size. The problem is illustrated in Figure 8.1.

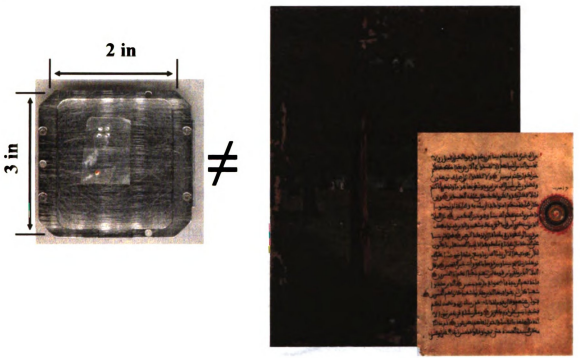

Figure 8.1: Illustration of the sample size problem. Samples which can be analyzed using LDMS are limited to a 6 in^2 sample plate.

The figure shows the modified sample plate, which was machined to hold polyacrylamide gels. Unless the piece of art or questioned document is a stamp or a post-it-note, we can not introduce the sample into the instrument. There are a couple of

solutions to this problem. These include "going big' and "going small". The two solutions will be dealt with separately.

"Go Big"

A MALDI mass spectrometer similar to the instrument in our lab, is shown in Figure 8.2 (1). One option is to physically increase the size of the ion source housing to accommodate a large painting. This design is illustrated in Figure 8.3. There are no limitations in doing so, it simply has rarely been done before. The design could be modified to hold a wide range of art objects, including pottery and vases. There are some concerns with this solution. The LDMS experiment is performed at an extremely low pressure (10^{-6} Torr). Art objects contain volatile components, and are not made to withstand vacuum conditions. We are concerned that placing an art object in a high vacuum system could have detrimental effects on the object. These effects include dehydration and eruption of the samples.

Figure 8.2: A MALDI MS similar to the instrument in our laboratory.

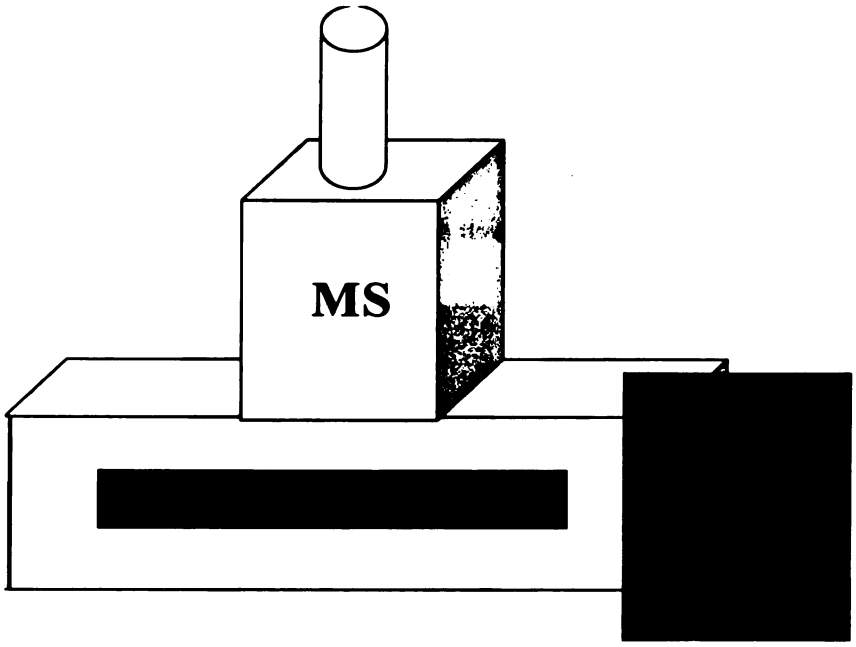

Figure 8.3: A cartoon of a MALDI instrument with an enlarged ion source housing to accommodate large samples, such as a painting.

Dehydration is a concept which deals with items such as pottery and vases, in which water plays an integral structural role. In a specific example, Barbara Berrie, an inorganic chemist at the National Gallery of Art, Washington, D.C., was analyzing a 14th century Spanish ciborium (a container for the Holy wafer during communion services) shown in Figure 8.4. The ciborium is made of gilded copper and champléve enamel. Specific areas of the ciborium, which contained a turquoise glass enamel, were corroded. Analysis of the turquoise glass enamel revealed a high lead content. Berrie explained that potassium glass is not stable, and is susceptible to slight fluctuations in the relative humidity of the surrounding atmosphere. The ciborium was drying out (as would occur in a high vacuum system). As water from the ciborium evaporated, the remaining potassium became potassium hydroxide. The hydroxide reacted with CO_2 in the air, and potassium carbonate was formed. The environment around the copper metal became

alkaline. Consequently, copper carbonate corrosion resulted. Once the corrosion was removed, the ciborium was placed in an environment of constant relative humidity, which was not permitted to fall below 40% (2). The case of the Spanish ciborium is just one example, which would pose a great risk to analyze using LDMS.

Figure 8.4: A 14th century Spanish ciborium.

Eruption is a concept which deals moreso with paintings. When a painting is created, air, moisture, and volatile components become trapped under the protective varnish layer. Chemical changes in the underlying paint layer may result in the mechanical expansion and protrusions at the surface of the painting. Over time, these protrusions naturally erupt (3,4). We are concerned that subjecting a painting to high vacuum conditions, will ultimately accelerate the inevitable eruption process. The goal of the project is to develop a technique which provides useful data, without harming the sample. An alternative direction would be to "go small".

"Go Small"

The Analysis of Questioned Documents

In the field of forensic science, questioned document examiners are asked to analyze the ink on a document, to provide data on either its source or its age. The document in question is often times admitted in a court of law, and therefore maintaining the integrity of the document in its original form is essential. In the field of questioned document examination, a method for removing ink samples from a document, resulting in minimal damage to the document, has been approved. Figure 8.5 shows a couple of tools, which are used by questioned document examiners to remove small punches from a sample. The tool in the top portion of Figure 8.5 is actually used at a local questioned document laboratory (Speckin Forensic Laboratories). The tool in the bottom portion of the figure is a more primitive model. We experimented with the Speckin tool, and removed several punches from a black ballpoint pen ink-on-paper sample, and also from the red ink on the Koran discussed in Chapter 4. The experiment is illustrated in Figure 8.6. The appropriate mass spectrum was generated in both cases, as when a much larger sample was employed.

One drawback is that resolution tends to suffer as the sample size decreases. Often times, this problem may be rectified by tweeking the user parameters slightly. The important point here is that the removal of small punches is an acceptable sampling method in the field of questioned document examination, and we have shown that it is possible to generate an informative mass spectrum from a single punch. It should be noted that the most commonly used methods by document examiners to analyze ink, such

as HPLC, require the removal of 10 to 15 punches to perform one analysis (5,6). With LDMS, we only need one.

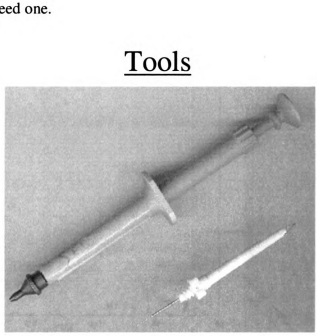

Figure 8.5: Examples of two punches used by questioned document examiners to remove microplug samples from documents in questions.

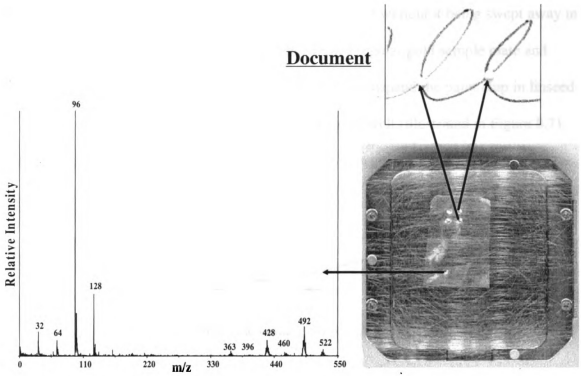

Figure 8.6: Illustration of the microplug experiment. The negative ion mass spectrum of the red ink on the 17th century Koran presented in Chapter 4.

The Analysis of Paintings

In the area of painting analysis, we could "go small" in a couple of ways. At the Walter McCrone Institute in Chicago, IL, it is common to remove microplug samples from a painting and analyze the cross-sections using microcopy (7,8). It is stated that if the diameter of the microplug is less than 0.01 mm, the "damage" to the painting can not be seen by the naked eye. The other possibility is to remove small paint chips from the painting.

Dr. Karen Trentelman from the Detroit Institute of Arts, Detroit, MI, was kind enough to supply us with two paint chips from a painting at the Institute. The sample we analyzed had the dimensions of approximately 75 x 30 μm. The challenge became, how

we were going to introduce the sample into the instrument without it being swept away in the vacuum system. We could not simply place it on a regular gold sample plate and double stick tape seemed too risky. The solution was to suspend the paint chip in linseed oil, and deposited the mixture in a standard sample plate well (illustrated in Figure 8.7). Positive and negative ion LD mass spectra (Figure 8.8) were successfully obtained of the sample.

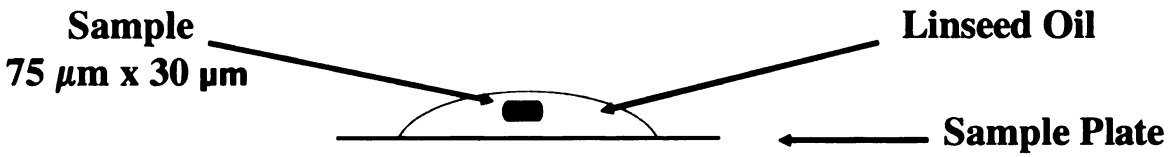

Figure 8.7: A cartoon of the paint chip in linseed oil experiment.

In the positive ion mass spectrum (Figure 8.8a), numerous peaks have been identified containing the element Pb. Due to the absence of any unique Pb-containing peaks, such as $PbCrO_4^+$ in the mass spectrum of the lead chromate pigment, we can not positively identify the pigment present. Again, note the decrease in resolution as the sample size decreases.

Switching to the negative ion mass spectrum (Figure 8.8b), linseed oil peaks, as discussed in Chapter 4, are noted. This could suggest a couple of possibilities. The first is that the paint mixture contains a pigment, such as red ochre, which does not appear in the mass spectrum itself, but has a "matrix" quality, which allows us to see the vehicle component. The other explanation is that the ability to generate linseed oil peaks in the LDMS experiment is a function of particle size. This observation surfaces again, very shortly. Overall, we were not discouraged by the fact that we could not identify the pigments present. Our goal here was to overcome the sampling size problem.

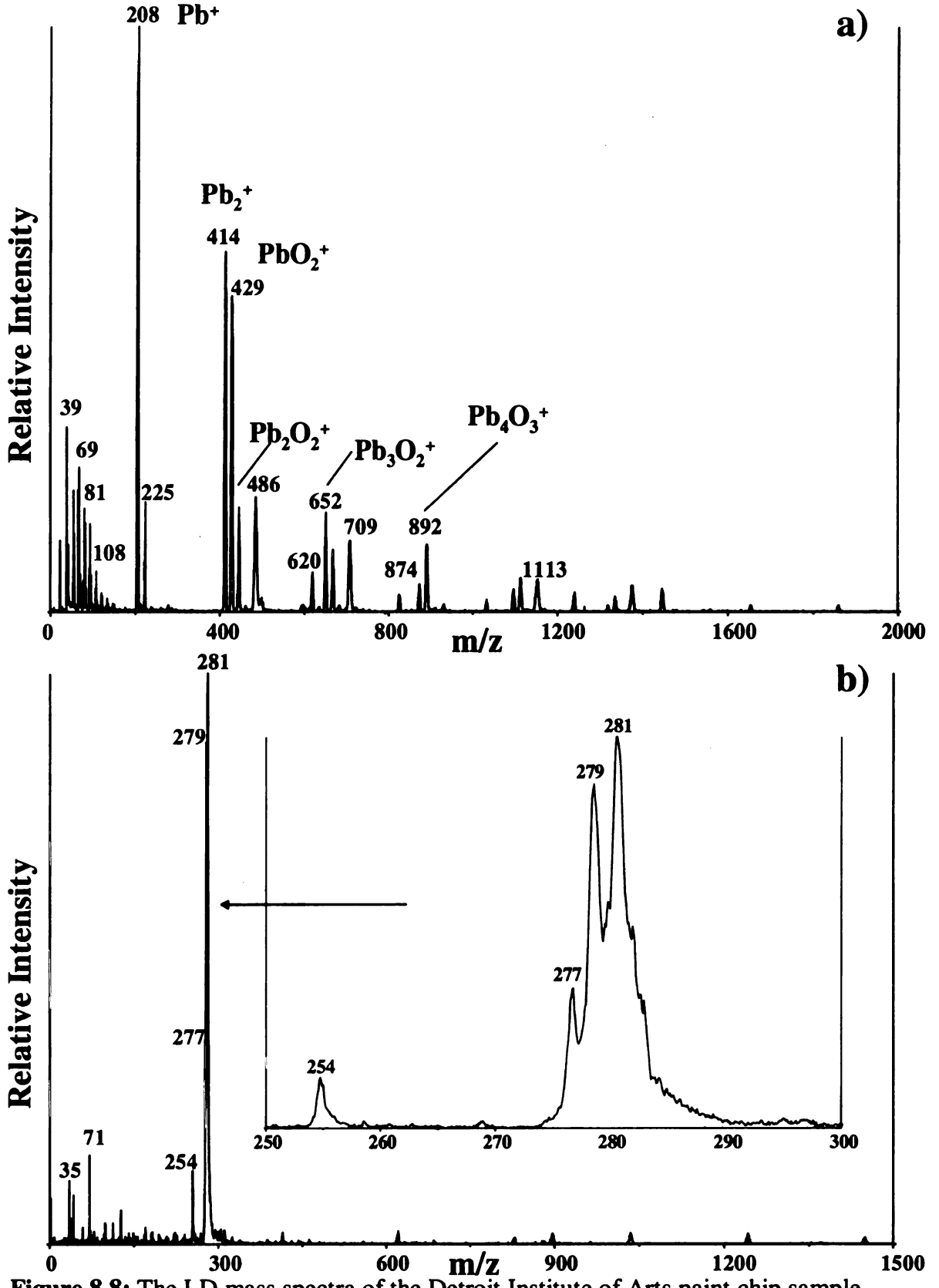

Figure 8.8: The LD mass spectra of the Detroit Institute of Arts paint chip sample suspended in linseed oil on a gold sample plate a) the positive ion mass spectrum; b) the negative ion mass spectrum.

To explore the paint-chip in linseed oil method a little more in depth, a second painting was provided, from which we were able to obtain our own paint chip samples. The painting was created in the early 1900s. White, green and red paint chips were removed from the painting. Positive and negative ion LD mass spectra were obtained of the samples. All three paint chips produced the same spectra, as can be seen in Figure 8.9 a-c, which shows the positive ion mass spectra. What is happening here? There are a few possibilities.

The first explanation is simply the colorants do not absorb at this wavelength. A solution to this problem, is to revert to traditional MALDI MS and add a matrix. Several matrices were tested, including alpha hydroxyl cinnaminic acid and dihydroxy benzoic acid, however the matrix did not improve the spectra. The second possibility may have been that the painting was protected by a varnish layer, which was trapping the colorants underneath. Varnish removal treatments were researched and attempted. Specifically the Pettenkofer's process was employed (9). The technique was rather simple. The paint chips were exposed to ethanol vapors in an enclosed container, and then brushed with distilled water. Spectra of the paint chips following the varnish removal process were the same as for the pretreated samples.

The last possibility involved the vehicle. Linseed and other drying oils dry by a crosslinking mechanism (3,10). Hence, it is quite plausible that over 100 years time (the estimated age of the painting), the drying oil present in the painting formed a protective polymer layer, trapping the colorants underneath. The solution to this problem was to grind up the pigment and suspend the particles in linseed oil on a gold sample plate. In a sense, we were creating a "fresh" paint.

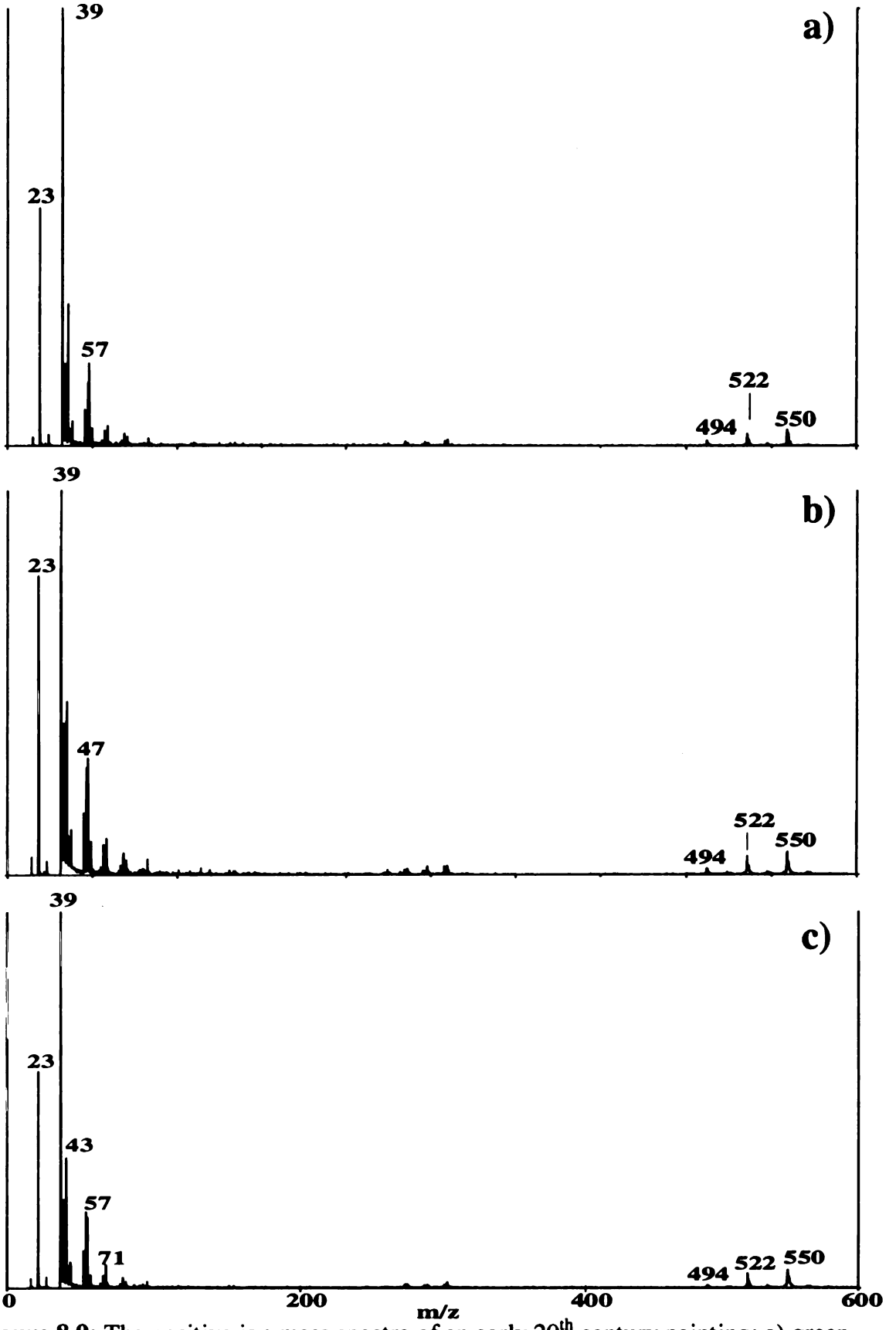

Figure 8.9: The positive ion mass spectra of an early 20th century painting; a) green paint chip; b) white paint chip; c) red paint chip.

The solution was successful and unique positive and negative ion LD mass spectra of the three different color paint chips were obtained. Focusing on the red paint chip, the positive ion mass spectrum is shown in Figure 8.10. Numerous lead and lead oxide ions were identified based on their isotopic patterns. Considering these ions are common to many lead-containing pigments, the identity of the red colorant can not be confirmed. However, there are two likely possibilities. The first is, the pigment is red lead, which has the formula Pb_3O_4. The second possibility is that the peaks represent the pigment lead white ($Pb(OH)_2 \cdot 2PbCO_3$). In the painting, there is clearly a layer of white paint underneath the red layer.

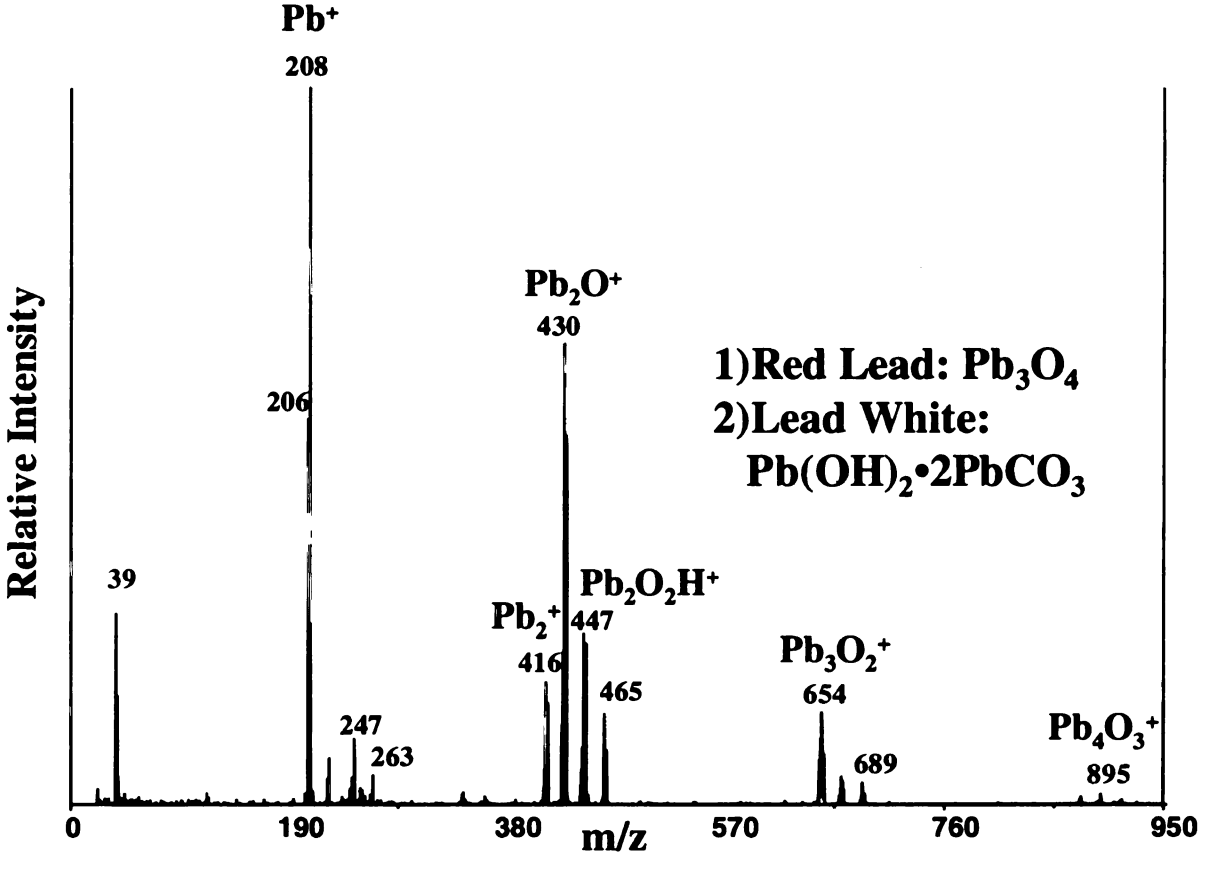

Figure 8.10: The positive ion LD mass spectrum of the red paint ground up, in linseed oil, and analyzed on a gold sample plate.

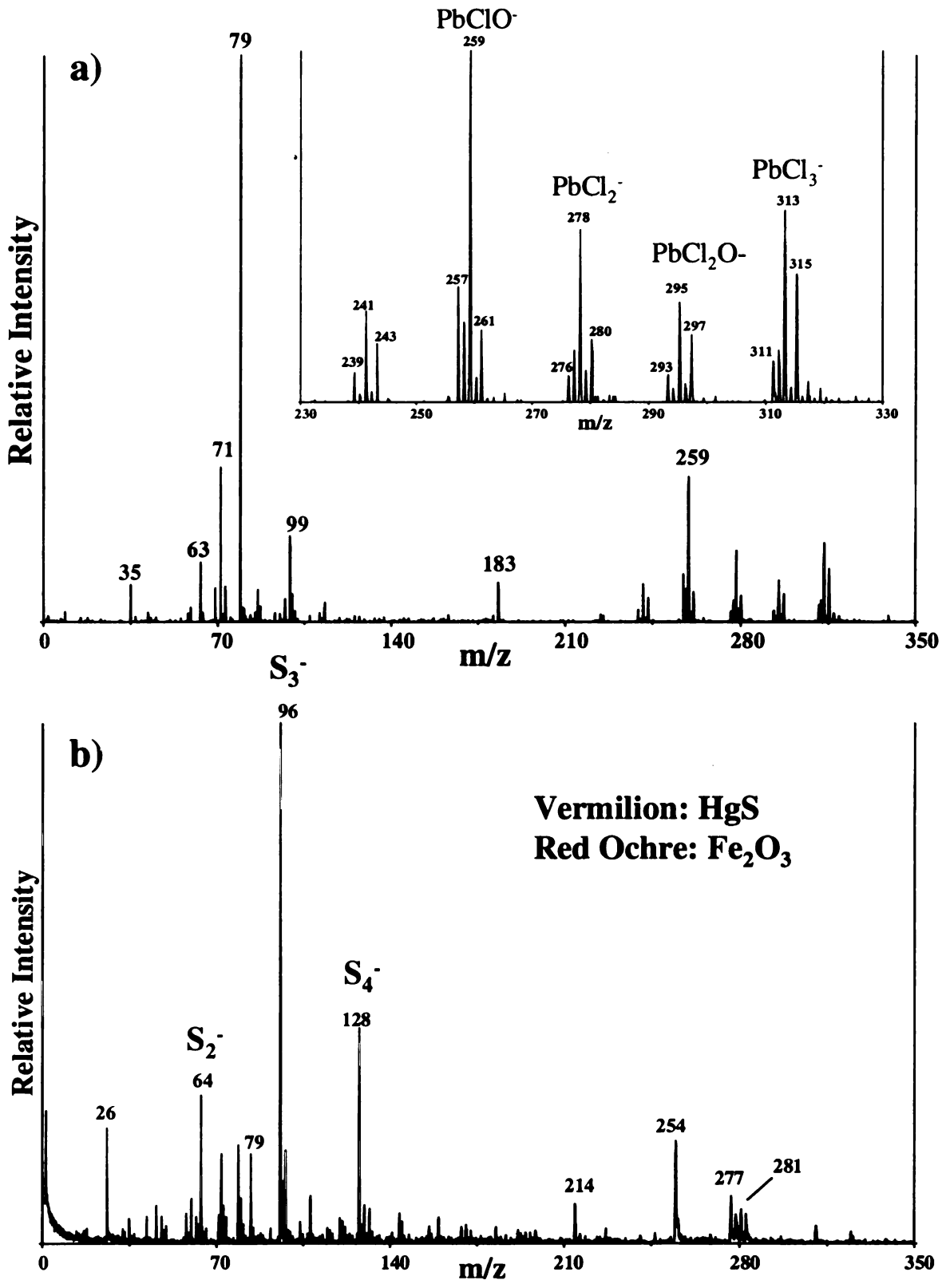

Figure 8.11: The negative ion mass spectra of the red paint ground up in linseed oil and analyzed on a gold sample plate; a) the first spot irradiated; b) the second spot irradiated.

The negative ion mass spectrum of the red paint chips (Figure 8.11a), also supports the presence of a lead-containing pigment in the paint mixture. Various lead chloride ions were identified, which have only appeared thus far in aging studies (Chapter 5). Considering that the paint mixture was an inhomogeneous mixture, different spectra were generated as the sample was moved so that the laser could irradiate new spots. Figure 8.11b shows another negative ion mass spectrum of the ground-up red paint chip sample. Sulfide ions are noted in the lower mass region of the spectrum. This is encouraging, since there are red sulfur-containing pigments, such as vermilion. In the higher mass region, a set of peaks is noted of relatively low intensity around m/z 281, resembling the linseed oil peaks discussed in Chapter 4. If these are linseed oil peaks, the red pigment may actually be red ochre. Again, the identity of the pigments remain unknown for certain, however we have shown that it is possible to obtain mass spectra from extremely small samples.

References

1) http://chemistry.caltech.edu/resources/massspec.html

2) Ember LR. Chemistry and art: helping to conserve the nation's treasure. Chemical and Engineering News 2001; July 31: 51-59.

3) The drying of oils and oil paint. Smithsonian Center for Materials Research and Education. http://www.si.edu/scmre/takingcare/paint_cracking.htm

4) Boon JJ. Analytical mass spectrometry: MOLART painting studies. http://amolf.nl/publications/annual.

5) Andrasko J. HPLC analysis of ballpoint pen inks stored at different light conditions. J Forensic Sci 2001;46:21-30.

6) Brunelle RL, Cantu AA. A critical evaluation of current ink dating techniques. J Forensic Sci 1987;32:1522-1536.

7) McCrone WC. Authenticity study of a possible Manet painting. The Microscope 1987;35:173-195.

8) McCrone WC. Microscopial examination of art and archaeological objects. Proceedings of the IS&T/SPIE Conference on Scientific Detection of Fakery in Art;1998 Jan;San Jose, California.

9) Schmitt S. Effects of regeneration methods on paintlayers – with special reference to the effects of solvent vapour and copaiba balsam. http://www.amolf.nl/research/biomacromolecule/Pettenkofer.htm

10) Turner GPA. Introduction to paint chemistry and principles of paint technology. 3rd ed. New York: Chapman and Hall.

Chapter Nine: Conclusions and Future Directions

Laser desorption mass spectrometry was evaluated as an analytical tool for the analysis of colorants on art objects. The results of this project can be used by scientists in the fields of art conservation and forensic science. The ability of LDMS to provide molecular level information for both organic and inorganic components of a paint mixture, simultaneously, makes the technique a more attractive choice over some currently used methods. Additionally, the sensitivity of the LDMS instrument was demonstrated.

Completing this project has provided a survey of the various forms of artwork, which can be analyzed using LDMS. For example, the technique is well-suited for the analysis of both watercolor and oil paints on a variety of substrates. Other pieces of "art", including ancient Chinese coins and an old cross allegedly from the Crusades were analyzed. The results of these experiments were not presented, however the experiments were quite challenging. Standard samples in our studies included either ink-on-paper or paint-on-paper samples. In other words, they were flat. In the cases of the Chinese coins and the cross, the samples were three-dimensional. Using a special sample plate holder, with the disposable sample plate removed, we were able to introduce the samples into mass spectrometer and generate mass spectra.

Practical aspects of the LDMS experiment in regards to sample size were also addressed. It was shown that even though increasing the size of the ion source housing to accommodate larger, three-dimensional samples is feasible, it may not be best (safest) solution. Currently, there are acceptable sample removal procedures in the fields of art

conservation and questioned document examination. We have shown that the sensitivity of the LDMS experiment can accommodate these small sample sizes, making this option more appealing.

One other solution, which was not discussed previously, is atmospheric pressure laser desorption mass spectrometry (AP LDMS). AP MALDI and AP LD are not novel techniques (1,2). In this technique, analyte molecules are desorbed and ionized at atmospheric conditions outside of the mass spectrometer. A stream of N_2 (g) transports the formed ions into the mass spectrometer for analysis. This is not an efficient method. Consequently, AP MALDI requires a larger quantity of sample. Considering the typical sample sizes encountered in the fields of art conservation and forensic science, there may not be enough sample to perform the experiment. However, the design of the instrument could be manufactured to accommodate a document or a large painting, so that the laser could be moved to irradiate different portions of the sample directly, negating the need for an extraction of a sample. The development of an AP LDMS method for this type of application would, of course, fall under the category of future work.

In conclusion, laser desorption mass spectrometry has considerable potential in the analysis of colorants used in various works of art. If funds are limited to purchase an LD mass spectrometer, which is often the case for art museums and especially forensic laboratories, there are numerous mass spectrometry facilities nationwide, such as the one here at Michigan State University, to which samples could be submitted. Of course, paint chips would not qualify as traditional samples submitted, however accommodations could be made. The point is that our work has demonstrated the benefits of LDMS in the

analysis of colorants, compared with traditional instrumentation currently used. The technique is worth developing further.

References

1) Laiko VV, Baldwin MA, Burlingame AL. Atmospheric pressure matrix-assisted laser desorption/ionization mass spectrometry. Analytical Chemistry 2000;72:652-657.

2) Laiko VV, Taranenko NI, Berkout VD, Musselman BD, Doroshenko VM. Atmospheric pressure laser desorption/ionization on porous silicon. Rapid Communications in Mass Spectrometry 2002;16:1737-1742.

APPENDIX

Ion	m/z	PbO	PbO_2	$PbMoO_4$	$Pb_3(SbO_4)_2$	$PbSO_4$	PbS	$PbCrO_4$
Pb^+	208	*	*	*	*		*	*
$PbOH^+$	225	*	*	*				*
PbK^+	247	*	*		*		*	*
$PbOK^+$	263						*	
$PbCrO_2^+$	293							*
$PbCrO_3^+$	308							*
$PbSbO_2^+$	361				*			
Pb_2^+	414						*	*
Pb_2O^+	430	*	*	*	*		*	*
Pb_2S^+	446						*	
$Pb_2O_2H^+$	447	*	*	*				*
Pb_2SCl^+	483						*	
$Pb_2CrO_3^+$	514							*
$Pb_2CrO_4^+$	530							*
$Pb_2SbO_3^+$	585				*			
$Pb_3O_2^+$	654	*	*					*
$Pb_3O_3H^+$	671	*	*					
$Pb_3S_2^+$	686						*	
$Pb_3S_2Cl^+$	721						*	
$Pb_3CrO_5^+$	754							*
$Pb_3SbO_4^+$	807				*			
$Pb_4O_3^+$	878	*	*					
$Pb_4O_4H^+$	895	*	*					
$Pb_5O_4^+$	1102	*	*					
$Pb_5O_5H^+$	1119	*	*					

Table 1: Summary of Positive Ions Generated by Pb-compounds in the LDMS Experiment.

Ion	m/z	PbO	PbO_2	$PbMoO_4$	$Pb_3(SbO_4)_2$	$PbSO_4$	PbS	$PbCrO_4$
CrO_3^-	100							*
MoO_4^-	162			*				
$Cr_2O_5^-$	184							*
$Cr_2O_6^-$	200							*
PbO^-	224	*	*					
PbO_2H^-	241	*	*					
$Cr_3O_7^-$	268							*
$PbClS^-$	275						*	
$Cr_3O_8^-$	284							*
$Mo_2O_6^-$	288			*				
$Cr_3O_9^-$	300							*
$Mo_2O_7^-$	304							
$PbCl_3^-$	313						*	
$Cr_4O_9^-$	352							*
$Cr4O_{10}^-$	368							*
Pb_2^-	414	*						
$Mo_3O_9^-$	432			*				
$Pb_2O_2^-$	446	*						
$Pb_2O_3H^-$	463	*	*					
$Pb_2S_2^-$	480						*	
$Pb_2S_2Cl^-$	515						*	
Pb_3^-	622	*						
$Pb_3O_3^-$	670	*						
$Pb_3O_4H^-$	687	*	*					
$Pb_4O_5^-$	910	*						
$Pb_5O_6^-$	1134	*						
$Pb_6O_6^-$	1340	*						
$Pb_6O_7H^-$	1357	*						

Table 2: Summary of Negative Ions Generated by Pb-compounds in the LDMS Experiment.

Ion	m/z	PbS	Sample 1 (25% HCl)	Sample 2 (50% HCl)	Sample 3 (75% HCl)	Sample 4 (100% HCl)
Pb^+	208	*	*	*	*	*
$PbOH^+$	225		*	*		
PbK^+	247	*	*	*		
$PbOK^+$	263	*	*	*	*	
Pb_2^+	414	*				
Pb_2O^+	430	*	*	*		
PbS^+	446	*			*	*
$Pb_2O_2H^+$	447		*	*		
Pb_2SCl^+	483	*			*	*
$Pb_2S_2Cl^+$	515				*	*
$Pb_2CrO_4^+$	530		*	*		
$Pb_3S_2^+$	686	*			*	
$Pb_3S_2Cl^+$	721	*			*	*
CrO_3^-	100		*	*		
$Cr_2O_5^-$	184		*	*		
$Cr_2O_6^-$	200		*	*		
$Cr_3O_7^-$	268					
$PbClS^-$	275	*				*
$Cr_3O_8^-$	284		*	*		
$Cr_3O_9^-$	300		*	*		
$PbCl_3^-$	313	*	*	*	*	*
?	336				*	*
$Cr_4O_9^-$	352					
$Cr_4O_{10}^-$	368					
$Pb_2S_2^-$	480	*				
$Pb_2S_2Cl^-$	515	*				

Table 3: Summary of Positive and Negative Ions Generated in the Uncontrolled H_2S (g) Exposure Experiments.

Ion	m/z	PbS/H_2O_2	Sample 4 (exposed 15minutes)
Pb^+	208	*	*
$PbOH^+$	225	*	*
PbO_2H^+	241	*	
$PbCl^+$	243	*	
PbK^+	247	*	*
$PbOK^+$	263	*	*
$PbCl_2H^+$	279	*	
Pb_2^+	414	*	
Pb_2O^+	430	*	*
$Pb_2O_2H^+$	447	*	*
Pb_2OCl^+	465	*	*
Pb_2SCl^+	483	*	
$Pb_2CrO_4^+$	530		*
$Pb_3O_2^+$	654	*	*
Pb_3SO^+	670	*	
$Pb_3S_2^+$	686	*	*
Pb_3SCl^+	689	*	
Pb_3SClO^+	705	*	
$Pb_3S_2Cl^+$	721	*	
$Pb_3CrO_5^+$	754		*
Pb_4SClO^+	913	*	
$Pb_4SClO_2^+$	929	*	
$Pb_4SClO_3^+$	961	*	
CrO_3^-	100		*
$Cr_2O_5^-$	184		*
$Cr_2O_6^-$	200		*
$Cr_3O_7^-$	268		*
$PbSCl^-$	275	*	*
$Cr_3O_8^-$	284	*	*
$PbCl_3^-$	313		

Table 4: Summary of Positive and Negative Ions Generated in the Uncontrolled H_2S (g) Exposure Experiments Followed by Treatment with H_2O_2.